

# Virus-host interaction during persistent foot-and-mouth disease virus infection

Von Benedikt Litz

Inaugural-Dissertation zur Erlangung der Doktorwürde

der Tierärztlichen Fakultät der

Ludwig-Maximilians-Universität München

Virus-host interaction during persistent foot-and-mouth disease virus  
infection

Von Benedikt Litz

aus Weingarten

München 2025



Aus dem Veterinärwissenschaftlichen Department der Tierärztlichen Fakultät  
der Ludwig-Maximilians-Universität München  
Lehrstuhl für Experimentelle Parasitologie

Arbeit angefertigt unter der Leitung von Univ.- Prof. Dr. Markus Meissner

Angefertigt am Institut für Virusdiagnostik  
des Friedrich-Loeffler-Instituts,  
Bundesforschungsinstitut für Tiergesundheit, Insel Riems

Mentor: Prof. Dr. Martin Beer



Gedruckt mit Genehmigung der Tierärztlichen Fakultät  
der Ludwig-Maximilians-Universität München

**Dekan:** Univ.-Prof. Dr. Reinhard K. Straubinger, Ph.D.

**Berichterstatter:** Univ.- Prof. Dr. Markus Meissner

**Korreferent/en:** Priv.-Doz. Dr. Susanne Zöls  
Univ.-Prof. Dr. Laurent Frantz  
Univ.-Prof. Dr. Dusan Palic  
Univ.-Prof. Dr. Wolfram Petzl

Tag der Promotion: 8. Februar 2025



*Meiner Familie*



Die vorliegende Arbeit wurde gemäß § 6 Abs. 2 der Promotionsordnung für die Tierärztliche Fakultät der Ludwig-Maximilians-Universität München in kumulativer Form verfasst.

**Die folgenden wissenschaftlichen Arbeiten sind in dieser Dissertationsschrift enthalten:**

1. Publication I: Litz B, Sehl-Ewert J, Breithaupt A, Landmesser A, Pfaff F, Romey A, Blaise-Boisseau S, Beer M, Eschbaumer M: „**Leaderless foot-and-mouth disease virus serotype O did not cause clinical disease and failed to establish a persistent infection in cattle**“, erschienen in Emerging Microbes & Infections, 2024, online verfügbar unter doi: 10.1080/22221751.2024.2348526
2. Publication II Litz B, Pfaff F, Forth L, Hägglund S, Valarcher JF, Beer M, Eschbaumer M: „**Persistent foot-and-mouth disease virus infection in the bovine nasopharynx is associated with suppression of innate and cellular immunity**“, eingereicht bei PLOS ONE
3. Publication III Litz B, Forth L, Pfaff F, Beer M, Eschbaumer M: „**Distinct mutations emerge in the genome of serotype O foot-and-mouth disease virus during persistence in cattle**“, erschienen in Journal of Virology, 2025,

**Weitere wissenschaftliche Arbeiten, die nicht Teil dieser Dissertationsschrift sind**

Keck H, Litz B, Hoffmann B, Eschbaumer M, Beer M: „**Full-Length Genomic RNA of Foot-and-Mouth Disease Virus is Infectious for Cattle by Injection.**“, erschienen in Viruses, 2022, online verfügbar unter doi: 10.3390/v14091924.

Matiasek K, Pfaff F, Weissenböck H, Wylezich C, Kolodziejek J, Tengstrand S, Ecke F, Nippert S, Starcky P, Litz B, Nessler J, Wohlsein P, Baumbach C, Mundhenk L, Aebischer A, Reiche S, Weidinger P, Olofsson KM, Rohdin C, Weissenbacher-Lang C, Matt J, Rosati M, Flegel T, Hörnfeldt B, Höper D, Ulrich RG, Nowotny N, Beer M, Ley C, Rubbenstroth D: “**Mystery of fatal**

**'staggering disease' unravelled: novel rustrela virus causes severe meningoencephalomyelitis in domestic cats**” erschienen in Nature Communications, 2023, online verfügbar unter doi: 10.1038/s41467-023-36204-w

Haring VC, Litz B, Jacob J, Brecht M, Bauswein M, Sehl-Ewert J, Heroldova M, Wylezich C, Hoffmann D, Ulrich RG, Beer M, Pfaff F: „**Detection of novel orthoparamyxoviruses, orthonairoviruses and an orthohepevirus in European white-toothed shrews**“ erschienen in Microbial Genomics, 2024, online verfügbar unter doi: 10.1099/mgen.0.001275

# Contents

I. Introduction.....	5
II. Review of literature .....	9
1. Foot-and-mouth disease virus .....	9
i. Structural proteins.....	9
ii. Non-structural Proteins .....	10
iii. Genome characteristics, replication and translation.....	14
2. Epidemiology.....	16
3. Pathogenesis and clinical presentation.....	18
4. Viral Persistence.....	19
i. Persistence versus Latency .....	19
ii. Persistent FMDV infection .....	21
5. Immune response and vaccination .....	25
III. Objectives.....	31
IV. Results .....	35
V. Discussion .....	125
VI. Summary .....	139
VII. Zusammenfassung.....	141
IX. Appendix.....	169
1. List of Figures .....	169
2. Legal Permissions .....	169
3. List of abbreviations.....	170
X. Acknowledgements .....	175



## CHAPTER I: INTRODUCTION



# I. Introduction

Pictures of apocalyptic landscapes with piles of farm animals being incinerated in the fields during the foot-and-mouth disease (FMD) outbreak in the United Kingdom in 2001 have shaped the public perception of this highly contagious notifiable disease. During the 2001 epizootic, millions of animals were killed to prevent further spread of FMD across the UK and Europe, but emergency vaccination was not performed.

Inactivated vaccines against foot-and-mouth disease virus (FMDV) are commercially available, reliably prevent clinical disease and reduce transmission. On the other hand, vaccine production requires the growth of large amounts of virus posing a risk for a breach of containment like in the FMDV outbreak of 2007 in the UK. Furthermore, current vaccines are not able to induce a sterile immunity and vaccinated animals can be subclinically infected, leading to possible persistence of infection in ruminants. Virus can be recovered from subclinically infected as well as from persistently infected cattle, and they are indistinguishable by clinical examination. In contrast to persistently infected cattle, during subclinical infection FMD virus is excreted in nasal fluid and saliva and poses a high risk of transmission. Even though transmission from persistently infected animals has only been documented in the African buffalo (*Syncerus caffer*) and not in cattle (*Bos taurus*), every infected animal has to be culled to regain FMD-free status under the rules of the World Organization for Animal Health (WOAH).

Since the first description of persistent FMDV infection in cattle, the so-called carrier state, by Jaap van Bakkum in 1959, the infection of the epithelia of the upper respiratory tract in cattle by FMDV has been described in detail. But efforts for a prevention or disruption of the carrier state have been in vain. The fundamental mechanism of establishment of persistent infection as well as answers to the crucial questions of which animals become carriers and why remain elusive. To shed a light on these key points of understanding FMDV, this work presents studies which aim to decipher the virus-host interaction during the persistent phase by (i) characterizing the influence of FMDV and especially its L<sup>pro</sup> protein on persistently infected tissues in vivo and (ii) documenting the genomic evolution of virus during infection under selective pressure from the host immune system.



## CHAPTER II: REVIEW OF LITERATURE



## II. Review of literature

### 1. Foot-and-mouth disease virus

In 1898 Friedrich Loeffler and Paul Frosch demonstrated that FMD is caused by an agent which could pass through bacteria-proof filter, but not through a Kitasato-filter for very small particles, and concluded for the first time that its infectious agents are particles smaller than bacteria, but not homogeneous fluids as hypothesized before by Beijerinck (Witz 1998).

The etiological agent of FMD we know now as foot-and-mouth disease virus (FMDV) is a single-stranded RNA virus of positive polarity. It belongs to the genus *Aphthovirus* and the family *Picornaviridae*. FMDV and other species of the genus *Aphthovirus* such as equine rhinitis virus and bovine rhinitis virus differ from other *Picornaviridae* in their acid lability (Mahy 2005). In contrast to acid-stable picornaviruses like poliovirus in the genus *Enterovirus*, which can pass the stomach and infect the gastrointestinal epithelium, FMDV infects primarily epithelia of the upper respiratory tract and causes a highly infectious disease with characteristic vesicular lesions on hairless epithelia.

#### i. Structural proteins

The virion of FMDV consists of four structural proteins VP1, VP2, VP3 and VP4 as depicted in *Figure 1*. The four structural proteins of FMDV form a protomer as the smallest structural unit and five of those make a pentamer with the VP1 units centrally located around the fivefold axis of symmetry. Overall, 60 protomers form the icosahedral capsid of FMDV. VP1, VP2 and VP3 are exposed on the outer surface of the capsid and mediate receptor binding and antigenicity. The general structure of these three structural proteins is similarly constructed from 8-stranded  $\beta$ -sandwiches connected by loops (Mateu 1995). An exception to this universal blueprint is the G-H loop of VP1, which is motile and prominently exposed on the surface. With its highly conserved RGD-motif formed by amino acid residues 145-147 it facilitates the binding of receptors for cellular adhesion and entry (Logan et al. 1993). By changing its conformation between the 'up' and 'down' position, the G-H loop can avoid a recognition by antibodies (Parry et al. 1990). The G-H loop of VP1 comprises an important antigenic site, called "site 1", and has been traditionally a target of experimental vaccines (Bittle et al. 1982).

The antigenic sites 3 and 5 are located on the surface of VP1 as well, while site 2 is situated on the surface of VP2 and site 4 on VP3. Site 1 has historically been considered to be immunodominant, but after vaccination more antibodies are directed against site 2 on VP2 (Mahapatra et al. 2012). The distribution of the antigenic sites over the surface resembles among all serotypes and amino acid substitutions here determine the serotype and cross-reactivity within serotypes (Mateu et al. 1994).

VP4 on the other hand, which constitutes the inner surface of the capsid, is no target of neutralizing antibodies, supporting the highly conserved structure of VP4 among all serotypes (van Lierop et al. 1995). VP4 is further myristylated on its N-terminus, enhancing capsid stability and cell entry (Chow et al. 1987).

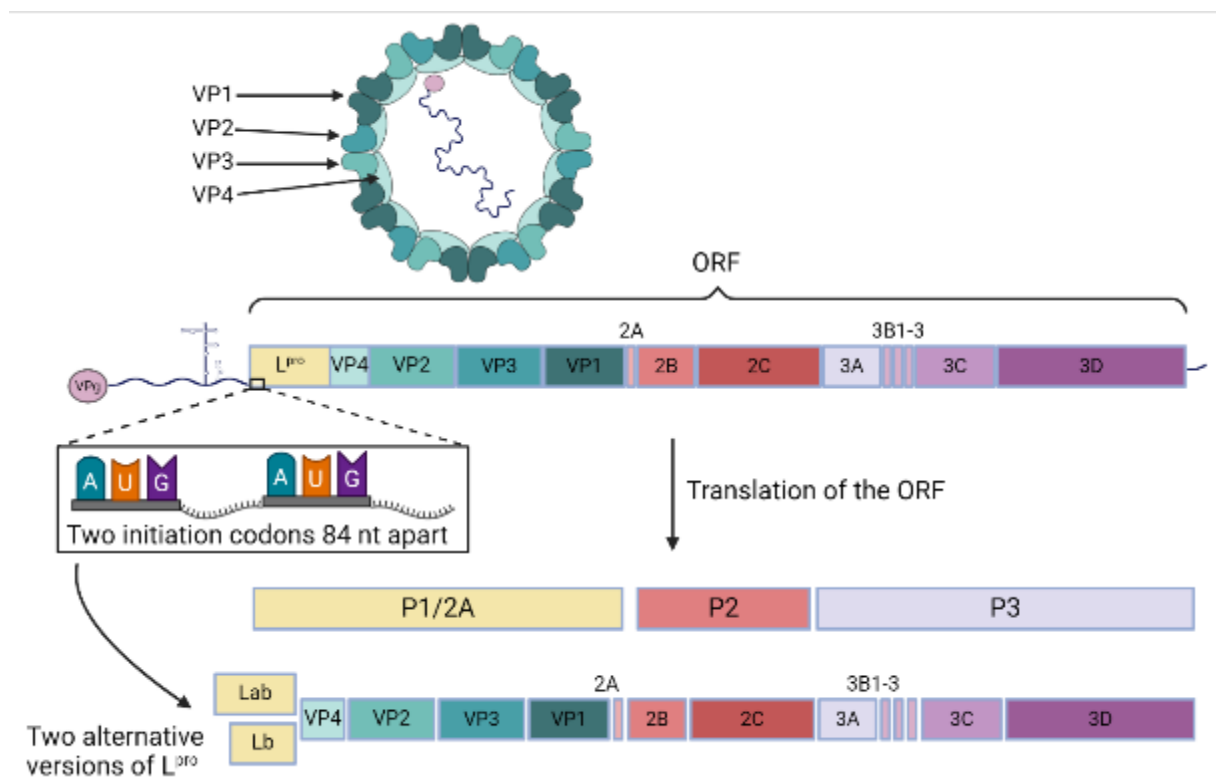


Figure 1. Structure of the virion and genome organization of FMDV (created with BioRender)

## ii. Non-structural Proteins

The Leader protein L<sup>pro</sup> is the first protein to be translated in the polyprotein of FMDV. The papain-like cysteine proteinase autocatalytically cleaves itself from the polyprotein. The sequence coding for L<sup>pro</sup> contains two separate initiation codons 84 nucleotides apart, termed

Lab and Lb, as depicted in Figure 1. The second codon is preferentially used for translation initiation, producing a 28 amino acid smaller L<sup>pro</sup> more often, but there is no functional difference observed between the alternate versions of the Leader protein (Medina et al. 1993). L<sup>pro</sup> inhibits cap-dependent mRNA translation in the host cells by cleaving the eukaryotic translation initiation factor 4 gamma (eIF4G) using a conserved SAP domain (Los Santos et al. 2009; Devaney et al. 1988). Therefore, it is promoting the cap-independent translation of FMDV RNA which requires the cleaved product of eIF4G (López de Quinto et al. 2001). Similarly, eIF3 subunits a and b are cleaved by L<sup>pro</sup> as well, contributing to the host translation shutdown (Rodríguez Pulido et al. 2007). L<sup>pro</sup> plays another important role in the inhibition of the innate immune response. Degradation of the p65 subunit of NF-κB by L<sup>pro</sup> after its translocation into the nucleus prevents the transcription of NF-κB dependent genes TNFα and RANTES (Los Santos et al. 2007). The type I interferon (IFN) antiviral response is antagonized by L<sup>pro</sup>, resulting in a strong attenuation of genetically modified FMDV strains lacking a functional Leader protein (Los Santos et al. 2006). Recent discoveries have elucidated the manifold ways in which L<sup>pro</sup> disrupts the induction of an IFN type I response, beginning with the cleavage of important cytosolic receptors detecting viral RNAs like RIG-I, MDA5, and MAVS (Visser et al. 2020), as well as LGP2, which acts as a positive regulator for these receptors in the presence of viral RNA (Rodríguez Pulido et al. 2018). Downstream in the IFN signalling pathway, the expression of type I IFNs is inhibited by L<sup>pro</sup> cleaving the IFN regulation factors 3 and 7 (IRF-3,-7) and as a result IRF-responsive genes are downregulated in their expression (Wang et al. 2010). Another mechanism of L<sup>pro</sup> to antagonize the IFN response is its role as a viral deubiquitinase. Inhibiting the ubiquitination of several signalling molecules in the IFN-signalling cascade like RIG-I, TBK1, TRAF6 and TRAF3 prevents their activation and suppresses the downstream signalling (Wang et al. 2011). The importance of L<sup>pro</sup> functions in inhibiting the IFN response is demonstrated by the deletion of the Leader coding sequence, which results in a very strong attenuation in vivo (Belsham 2013). It is not suitable as a live-attenuated vaccine, since sufficient replication has to take place to elicit an antibody response, but it could be used for the production of inactivated virus with a lower biological risk (Uddowla et al. 2012).

The short protein 2A, which is only 18 amino acids long, has only one function in the processing of the polyprotein. It is released from the following 2B co-translationally by ribosomal skipping

mediated by a C-terminal motif of 2A, but remains linked to the polyprotein P1 until final release by 3C cleavage (Donnelly et al. 2001).

The viroporin 2B can interact with the hydrophobic membrane of the host cell promoting the destruction of the cell and release of the viral particles (Da Ao et al. 2014). In other picornaviruses it has been shown that 2B is able to remodel membranes of the cell organelles forming an immunoprivileged viral production compartment (Li et al. 2019). The calcium influx caused by the viroporins was documented to trigger the innate immune response via the NLRP3 inflammasome after encephalomyocarditis virus infection (Ito et al. 2012). But this immune activation is counteracted by 2B itself by reducing the expression of the viral-sensing receptors RIG-I and MDA5 (Li et al. 2018) and targeting cyclophilin-A, an enhancer of these receptors (Liu et al. 2018).

Among many species of the family *Picornaviridae* and across FMDV serotypes, the coding sequence for protein 2C is highly conserved, implicating an essential function in viral replication (Chen et al. 2021). 2C is less studied in FMDV but conclusions can be drawn in analogy from related picornaviruses. Similar to 2B, 2C is membrane-associated and can induce a conformational change in membranes forming the viral replication complex (Gosert et al. 2000). Similar to other picornaviruses, 2C of FMDV has ATPase activity and is able to bind RNA, which are both essential functions for viral replication (Sweeney et al. 2010). Additionally, 2C promotes apoptosis and a IFN type I response via recruitment of Nmi and the IFN-induced protein IFP35 (Zheng et al. 2014). But on the other hand, 2C can inhibit the IFN response by downregulating the expression of the receptor NOD2 and preventing the recognition of viral ssRNA (Liu et al. 2019).

The polyprotein P3 consists of the non-structural proteins 3A, 3B1-3, 3C and 3D. 3A is membrane-associated like 2B and 2C, but in contrast to them it cannot induce a conformational change in the membranes (García-Briones et al. 2006). It further inhibits the IFN- $\beta$  signalling by downregulation of the expression of the viral-sensing receptors RIG-I, MDA5 and MAVS (Li et al. 2016a). Alterations in the amino acid sequence of 3A can cause significant changes in virulence or even a shift of host tropism, such as the amino acid substitution Q44R which adapted the FMDV strain in question to guinea pigs (Núñez et al. 2001) or the deletion of

amino acids 93-102 in the naturally occurring FMDV strain O/TAW/97 which causes severe disease in swine but cannot productively infect cattle (Beard and Mason 2000).

Different from other members of the *Picornaviridae* family, the ORF of FMDV encodes three copies of the 3B protein (3B1, 3B2 and 3B3) also known as VPg (“viral protein, genome-linked”). The three proteins are highly homologous and interchangeable without a loss of function, but not identical (Forss and Schaller 1982). An insertion of another copy of VPg as well as a deletion in the genome is tolerated by FMDV and produces infectious virus (Falk et al. 1992). But FMDV strains carrying only a single copy of VPg are attenuated in swine in vivo (Pacheco et al. 2003). As the name VPg implies it is covalently bound to the 5' end of the viral RNA and serves as a replication primer after uridylation (Paul and Wimmer 2015). VPg can inhibit the ubiquitination of RIG-I and by that prevents binding to MAVS, suppressing the downstream activation of the IFN response (Zhang et al. 2020b).

3C<sup>pro</sup> is a chymotrypsin-like cysteine protease, which is responsible for almost all cleavages occurring during the processing of the FMDV polyprotein, except the autocatalytic cleavage of L<sup>pro</sup>, the ribosomal skipping at the C-terminus of 2A and the maturational cleavage of VP0 (Birtley et al. 2005; Bablanian and Grubman 1993). Like the other major protease of FMDV, L<sup>pro</sup>, 3C<sup>pro</sup> contributes to the host cell shut-off promoting viral replication and translation. By cleaving the transcription initiation factors eIF4G and eIF4A, the cap-dependent translation of host mRNA is suppressed while the cap-independent translation of viral RNA can utilise all the resources of the cell. This cleavage occurs later in infection than the one by L<sup>pro</sup> (Belsham et al. 2000). Host cell transcription is also inhibited by 3C<sup>pro</sup> cleaving the histone H3 at its N terminus. Truncated H3 remains chromatin-associated, thereby rendering the host cell DNA inaccessible for transcription (Falk et al. 1990). The IFN type I response signalling is targeted by 3C<sup>pro</sup> as well. Like L<sup>pro</sup>, it can downregulate the expression of LGP2 reducing the activation of the RNA sensing receptors RIG-I and MDA5 (Zhu et al. 2017) and it targets the receptor NOD2 preventing detection of viral RNA. Additionally, 3C<sup>pro</sup> affects the JAK-STAT pathway, which is activated by IFN type I, by blocking the translocation of STAT1 and STAT2 into the nucleus preventing the transcription of IFN stimulated genes (ISGs) (Du et al. 2014).

3D<sup>pol</sup> is the largest protein encoded by FMDV and the last to be translated. Its essential main function is that of an RNA-dependent RNA polymerase, replicating the positive-sense single-stranded genomic RNA of FMDV through a negative-sense intermediary. Since this is a critical task for viral survival, the sequence of 3D<sup>pol</sup> is highly conserved among serotypes and their subtypes (George et al. 2001). Unlike the replication apparatus of other positive-sense single-stranded RNA viruses such as SARS-CoV 2, which possesses an exonuclease for correcting erroneously incorporated nucleotides and thereby reducing the error rate during replication (Denison et al. 2011), the FMDV 3D polymerase has no error correction. This comparatively low fidelity of the viral protease results in a high mutational rate in picornaviruses (Ma et al. 2013). Apart from its major replicative function only interactions with two other proteins have been described (Sarry et al. 2022).

### **iii. Genome characteristics, replication and translation**

The genome of FMDV is roughly 8300 nucleotides in length. It includes one large open reading frame (ORF) coding for a polyprotein containing all proteins of FMDV. This ORF is framed by two untranslated regions (UTR), with a long 5' UTR of 1300 nt and a shorter 3' UTR of 100 nt which ends in a poly(A) tail. At the 5' end, the small VPg protein encoded by 3B is covalently attached to the RNA. The 5' UTR contains several secondary structures, among them the cis-acting replication element (cre) and the internal ribosome entry site (IRES), which are essential for replication and translation. In the ORF, the sequence of the four structural proteins (VP1-4) is flanked by sequences coding for the eight non-structural proteins, with the Leader proteinase L<sup>pro</sup> at the 5' end and the remaining non-structural proteins on the 3' end, beginning with 2A as depicted in *Figure 1* (Belsham 2005).

The replicative cycle of FMDV in cells begins by binding to superficial integrins consisting of the  $\alpha$ V subunit in connection with  $\beta$  subunits  $\beta$ 1,  $\beta$ 3,  $\beta$ 6 or  $\beta$ 8. Preferentially targeted by FMDV is  $\alpha$ V $\beta$ 6 integrin, which is expressed especially in hairless epithelia (O'Donnell et al. 2009). The receptor binding is facilitated by the highly conserved RGD domain in the GH-loop of VP1. In vitro, FMDV can evolve a receptor binding capacity independently from integrins and the RGD motif, developing an affinity to heparan sulphate caused by amino acid changes in the superficial layer of VP3 (Wang et al. 2015). Endocytosis of FMDV takes place in a clathrin-dependent

manner after binding to integrin  $\alpha V\beta 6$  (Berryman et al. 2005). In order to release the viral RNA from the endosome into the cytoplasm, where it can finally be translated, it has been hypothesized for picornaviruses that VP1 is piercing through the endosomal membrane forming a channel for the RNA which is guided by VP4 (Tuthill et al. 2009; Hogle 2002). Once the RNA has reached the cytoplasm, translation is initiated in a cap-independent manner. A secondary RNA structure in the 5'-UTR, the so-called internal ribosome entry site (IRES), is recruiting the translational initiation complex to the viral genome. FMDV requires all eukaryotic initiation factors (eIFs) except eIF4E, which binds to the cap structure of host cell mRNA (Belsham 2005). The binding of the translation initiation complex to eIF4E is prevented by cleavage of eIF4E by the FMDV Leader proteinase L<sup>pro</sup> (Devaney et al. 1988). Following 450 nucleotides downstream of the beginning of the IRES, the first AUG initiation codon is conserved in the sequence but poorly recognized by the ribosomal translation apparatus, resulting in the initiation of translation more often at the second initiation codon another 84 nucleotides downstream, as depicted in Figure 1 (Belsham 1992). Translation of the viral ORF of FMDV produces a polyprotein which is successively cleaved into its constituent proteins via the three intermediates P1, P2 and P3. P1 includes L<sup>pro</sup>, VP0, VP1, VP3 and 2A, P2 includes 2B, 2C and P3 includes 3A, 3B1-3, 3C and 3D. VP0 is further cleaved into VP4 and VP2 during maturation of the viral capsid. Cleavage of these proteins is performed by the two viral proteases 3C<sup>pro</sup> and L<sup>pro</sup>, which releases itself by autocleavage from the P1 polyprotein (Bablanian and Grubman 1993).

Since the FMDV genome is a positive-sense single-stranded RNA, it can be directly used as an mRNA for translation of its proteins. For FMDV replication, on the other hand, at first a negative-stranded template has to be transcribed which can then be transcribed into the genomic positive-stranded RNA again. This is performed by the viral RNA-dependent RNA polymerase (RdRp) 3D (Gamarnik and Andino 1998). To avoid the recognition of double-stranded viral RNA, which is produced during replication, by the host's innate immune response, viral RNA and proteins colocalize in segregated compartments in the vicinity of the nucleus and the Golgi apparatus (Monaghan et al. 2004). As a precursor to the viral capsid, the structural proteins VP1-4 are folded into a protomer. At the beginning, this smallest unit of the capsid still contains the predecessor protein of VP4 and VP2, termed VP0, which is probably autocatalytically cleaved in presence of the viral RNA, further stabilizing the protomer and the superordinate pentamer structure of the capsid assembled from 5 protomers (Fry et al. 2005). FMDV as an

unenveloped virus does not require any further maturation and is finally released by cell lysis after accumulation of virus particles in the host cell.

## **2. Epidemiology**

FMDV has ravaged farm animal populations worldwide for centuries and, as a consequence of its high mutational rate, seven serotypes have emerged. These are O, A, C, Asia1 and Southern African Territories (SAT) 1, 2 and 3. The serotypes with the widest distribution around the globe are O and A. The topotype PanAsia of Serotype O, originally named after the French department Oise (Vallée and Carré 1922), was the cause of a severe panzootic beginning in the 1990 and reaching its climax in the early 2000s with the FMDV outbreak in the United Kingdom in 2001 (Knowles and Samuel 2003). Serotype A, named after Allemagne (French for “Germany”) (Vallée and Carré 1922), shows the highest antigenic difference among the seven serotypes (Knowles and Samuel 2003). Shortly after the definition of these first two serotypes, serotype C was discovered through complement fixation tests by Otto Waldmann and Karl Trautwein on the isle of Riems (Waldmann and Trautwein 1926). Serotype C has circulated worldwide across Europe, Asia, Africa and South America, but to a lesser extent than O and A. Since the last reports of an outbreak of serotype C in Kenya and the Amazon region of Brazil in 2004, no further cases have been detected worldwide and it is assumed that serotype C is extinct in the wild (Paton et al. 2021). Serotype Asia 1 was first documented in samples from Pakistan in 1954 (Brooksby and Rogers J. 1957). The SAT 1-3 serotypes were historically confined to sub-Saharan Africa (Thomson 1995), but in the last years SAT2 has made its way towards Europe via Saudi Arabia, Iraq and Turkey, where it was reported in 2023 for the first time (WRLFMD 2023). The clade of serotypes O, A, C and Asia1 is genetically distinct from the SAT serotypes, with a divergent evolution estimated to have begun in the early middle ages in the Mediterranean region (Aiewsakun et al. 2020). FMDV is distributed globally but only serotypes O and A occur on every continent. Different serotypes can simultaneously be present in affected regions and according to Paton et al. (2009) seven endemic pools can be distinguished with individual sets of topotypes circulating therein. The countries mainly affected by FMD are located in central Africa, the Middle East and central and southern Asia as illustrated in Figure

2. This is of great concern since these areas are densely populated by susceptible livestock as well (Knight-Jones and Rushton 2013).

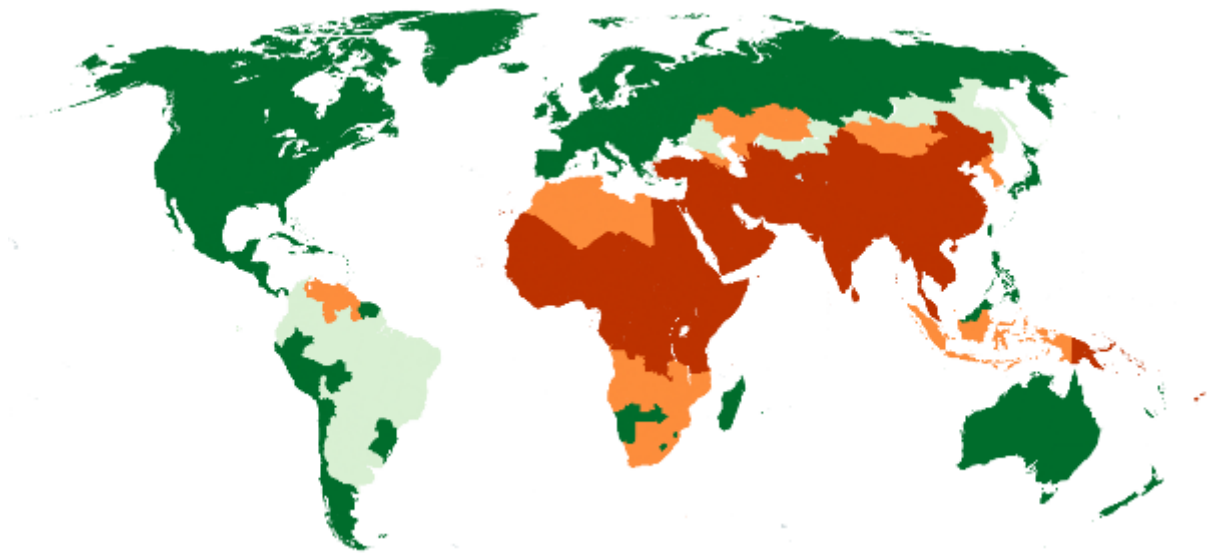


Figure 2. Global FMDV distribution, adapted from (Freimanis et al. 2016) using the official FMD status recognized by WOAHA as of February 2024 (WOAHA 2024). Green: free from FMDV without vaccination, light green: free from FMDV with vaccination, orange: sporadic FMDV, red: endemic FMDV. Created with mapchart.net

The host range of FMDV is mainly comprised of species belonging to the order of Artiodactyla. The presumed natural host of FMDV is the African buffalo (*Syncerus caffer*) which shows very limited signs of disease but is able to transmit virus in the acute and persistent phases of infection (Dawe et al. 1994b; Anderson et al. 1979). Besides many undomesticated species of cloven-hoofed animals like wild ruminants (Brown and Bevins 2019), wild suidae (Breithaupt et al. 2012) and camelidae (Wernery and Kaaden 2004), the economically most important species which can be infected by FMDV are cattle (*Bos taurus*), domesticated pigs (*Sus scrofa*) as well as sheep (*Ovis aries*) and goats (*Capra hircus*) (Knight-Jones and Rushton 2013). Experimentally, mice and guinea pigs can be infected with adapted strains (Vleeschauwer et al. 2016; Borca et al. 1986). FMDV used to be considered a zoonosis, but compared to the frequent exposure of farm workers and veterinarians in past FMD epizootics, only very few human cases have been described (Bauer 1997) and none have been confirmed with modern diagnostic methods.

### 3. Pathogenesis and clinical presentation

Generally, the progression of infection in cattle can be divided into 4 phases: the first phase after infection is the incubation phase, when the virus is already replicating within the host but clinical signs are not yet present. During the incubation, infected animals can already be infectious. The acute phase starts with the occurrence of the first clinical signs of infection which is usually fever, followed by vesicular lesions. During this period, the animal is highly infectious and transmits virus easily. As soon as the lesions are healing and the general condition of the animal improves, the phase of transition begins. In this phase, ruminants either clear the infection or become persistently infected. The persistent phase is the last phase of infection, when virus is present in small amounts in epithelia of the nasopharynx with only limited replication (Stenfeldt and Arzt 2020).

As mentioned above, cattle are highly susceptible to infection via aerosols, in contrast to pigs which are more susceptible to an infection via the oral route (Alexandersen et al. 2003; Sellers and Gloster 2008). In both species, initial viral replication depends on lymphoid epithelium: in cattle, the localization for primary replication is the follicle-associated epithelium (FAE) overlying the mucosa-associated epithelium (MALT) (Stenfeldt et al. 2015), in swine the preferred localization are the epithelial crypts of the oropharyngeal and laryngopharyngeal tonsils (Stenfeldt et al. 2014b). Epithelial cells are the first cells to be infected and shortly thereafter FMDV can be detected in the adjacent MALT, in which it colocalizes with endothelial cells. From here on, viremia is established (Arzt et al. 2010). The onset of viremia defines the end of the incubation and the beginning of the clinical phase (Yadav et al. 2019). Hematogenous spread causes systemic infection and distributes virus to the sites of secondary lesions, which usually appear one day after the onset of viremia (Eschbaumer et al. 2016a). The locations of vesicular lesions are determined by the distribution of the preferred binding receptors of FMDV,  $\alpha V\beta 3$  and  $\alpha V\beta 6$  (O'Donnell et al. 2009). During the clinical phase, typical signs of FMDV infection can be observed, i.e. fever, vesicular lesions on the tongue, the dental plate, the gingiva, the muzzle and in the nares as well as in the interdigital cleft and on the coronary bands. Vesicles rupture after 1-2 days, leaving behind sensitive erosions in the epithelium, which subsequently heal with fibrin overlaying the wounds. The emergence and rupture of vesicles in the mouth of cattle is commonly accompanied by excessive drooling. Due to the reduced general

condition, a loss of production in infected herds can appear (Alexandersen and Mowat 2005). Overall mortality is low but can rise in young immunologically naïve animals, in which FMDV causes fatal myocarditis — the so-called ‘tiger heart’ (Sahoo et al. 2023; Stenfeldt et al. 2014a; Ryan et al. 2008).

Clearance of the infection begins with a fast immune response 4-7 days after infection, producing antibody IgM and IgG which can end viremia within days of onset (Eschbaumer et al. 2016a). A detectable amount of virus can remain in peripheral lesions up to 14 days (Zhang and Alexandersen 2004). While ruminants now enter the transitional phase, in which the virus is either completely cleared or establishes a persistent infection, swine cannot be persistently infected, as no virus can be recovered from them later than the 28<sup>th</sup> day of infection (Stenfeldt et al. 2016b).

## **4. Viral Persistence**

### **i. Persistence versus Latency**

Retreating from an activated immune response into a niche with limited exposure to the immune system allows many different viruses to remain in an infected host and guarantees survival within the affected population. The underlying basic principles of such a prolonged infection can be differentiated between a persistent infection and a latent infection. During the persistent phase, infectious virus is continuously or intermittently produced and the viral genome can still be present after clearance of infectious virus. During latency, on the other hand, the viral genome is not replicated or only at very low levels, and latently infected cells are poorly recognized by the immune system. The latent state can be interrupted by phases of recurrence during which productive viral replication occurs (Flint et al. 2020). Mainly large DNA viruses meet the complex requirements for a latent infection, such as the herpesviruses varicella zoster virus (Varicellovirus humanalpha3), herpes simplex virus (Simplexvirus human-alpha1), pseudorabies virus (Varicellovirus suidalpha1) and the bovine herpesvirus 1 (Varicellovirus bovinealpha1). Among them, the herpes simplex virus (HSV) represents the prototype of a latent infection. Two thirds of humanity are seropositive for HSV-1 which causes orolabial or genital lesions during the acute phase (James et al. 2020). After the primary infection of mucosal epithelia, which is productive and cytolytic, HSV spreads retrograde along the

neuronal axons to the nucleus located in the ganglion where it establishes the latent infection (Zhu and Viejo-Borbolla 2021). An important driver for the initiation of the latent state could be the quick onset of the innate immune response mainly through IFN $\alpha$  (Regge et al. 2010). During the latent phase, the viral DNA is coated by nucleosomes and is not replicated, while distinct sections of viral mRNA are transcribed, the so-called latency-associated transcripts, which inhibit further viral transcription (Zhu and Viejo-Borbolla 2021). Reactivation of the latent virus, which can be caused by stress, fever or UV light, leads to translation of the viral proteins and nascent viral particles spread anterograde back to the mucosal epithelia (Roizman and Whitley 2013). CD8<sup>+</sup> cytotoxic T cells prevent this reactivation but ultimately cannot clear the latently infected cells which remain infected for the lifetime of the host (St Leger and Hendricks 2011).

A persistent infection with productive viral replication, on the other hand, is often caused by RNA viruses including Ebola virus (Orthoebolavirus), human immunodeficiency virus (HIV), bovine viral diarrhoea virus (Pestivirus bovis; BVDV) and several others. As diverse as these group of RNA viruses are phylogenetically as diverse are the strategies, they use for establishing a persistent infection.

As one of the most fearsome infectious diseases of our time, Ebola virus can cause a persistent infection after the acute hemorrhagic phase. Male survivors, persistently infected, can shed virus in the semen and can transmit virus via sexual contact. This reservoir of persistent virus poses a significant risk for public health (Jacob et al. 2020). Late in the acute infection, Ebola virus tends to infect immunoprivileged tissues, such as the eyes, the brain and the testes, which are shielded from immune cells in the blood by a blood-tissue barrier. Ultimately, the virus is cleared from these sites, but this can take months or years and during that time, virus can be shed through the semen or, if the fine balance between viral persistence and immune response is disturbed, a relapse to acute infection can occur (Schindell et al. 2018). BVDV in comparison infects cattle and in a gravid cow BVDV can spread transplacentally to the foetus. If a foetus is infected by a non-cytopathic strain of BVDV before the 110<sup>th</sup> day of gestation, it is in most cases born as a persistently infected calf, which is clinically inconspicuous but sheds large amounts of virus. This is possible through an immunotolerance against BVDV, facilitated by an immune evasion of the adaptive immune system which is not fully established at the

time of infection and an inhibition of the IFN response (Lanyon et al. 2014; Peterhans and Schweizer 2010). Another mechanism is the occurrence of mutations in the viral genome which change the viral phenotype, like it is observed in panencephalitis induced by measles virus (Mathieu et al. 2021) or in Theiler's virus, where a single amino acid change can establish the persistent infection (Jarousse et al. 1994). Targeting the immune response directly is also a method used by several viruses to establish a persistent infection. The flavivirus hepatitis C virus (Hepacivirus hominis), for example, degrades TRIF, an essential adaptor protein for the toll-like receptor 3, suppressing the recognition of viral RNA and can chronically infect the host (Kar et al. 2017; Liang et al. 2018). HIV infects various immune cells and by that is transported throughout the body. Infected immune cells are less susceptible to antibody-dependent cytotoxicity (Astorga-Gamaza et al. 2022).

For the persistent FMDV infection in ruminants the mechanisms are still elusive.

## **ii. Persistent FMDV infection**

Persistently infected animals, the so-called carriers, have first been described in 1959 by van Bakkum et al. (1959). Since then, our knowledge concerning this phase of infection has grown constantly. Currently, carriers are defined as animals from which virus can be recovered later than the 28<sup>th</sup> day of infection. The carrier incidence after acute FMD infection varies vastly but usually lies around 50% under experimental conditions after 28 dpi. The incidence of carriers slowly declines over time, but individual animals can remain persistent for months (Moonen and Schrijver 2000).

A carrier animal does not exhibit any clinical signs of infection and therefore cannot be distinguished from subclinically infected or convalescent animals. From subclinically infected animals and carriers virus can be recovered. In subclinical animals, shedding of virus is reduced compared to the acutely infected, but in carriers the only way to recover virus is by sampling the oropharyngeal region with a probang cup, as established by van Bakkum et al. (1959). The probang cup is a round metal cup on the end of a flexible rod or chain which collects saliva and superficial tissue from the oropharyngeal region, the so-called oropharyngeal fluid, as pictured in Figure 3. From this sample, virus can be directly isolated in cell culture, but a treatment with 1,1,2-trichloro-1,2,2-trifluoroethane (TTE) enhances the probability of a positive

virus isolation(Sutmoller and Cottral 1967). It is thought that TTE treatment releases antibody-complexed virus (Brown and Cartwright 1960). If the unprocessed oropharyngeal fluid is transferred directly into another naïve animal by intranasopharyngeal inoculation, the inoculated animals develops FMD as well (Arzt et al. 2018).



*Figure 3. (Left) Sampling of cattle with a probang cup in the BSL4vet facility on the Isle of Riems, (Right) OPF collected in the probang cup.*

This special sampling technique is required because replicative FMDV is only present in a limited localization during the persistent phase in cattle: the epithelia of the nasopharynx. Among these epithelia, the preferential site of infection are the dorsal nasopharynx and the dorsal soft palate, which are opposing epithelia in the nasopharyngeal region (Pacheco et al. 2015). Immunofluorescence and PCR from laser-capture micro-dissected tissue were used to further define the microanatomical localization of persistence, which is the FAE covering the MALT (Stenfeldt et al. 2016a). The distribution of this specialized lymphoid epithelium in the pharynx coincides with the preferential tissue of persistent FMDV (Meek et al. 2022) and is of special interest since this is also the site of primary replication for FMDV as described above.

Even though the OPF recovered from carriers is infectious for cattle, no convincing evidence has been found that transmission of FMDV from carrier cattle is possible (Stenfeldt and Arzt 2020). Carriers have been historically hypothesized to be the source of an outbreak where other routes of introduction had been excluded, but in several co-housing trials only one transmission event has been documented under experimental conditions (Tenzin et al. 2008; Suttmoller et al. 1968). Doubts have been raised concerning the biosecurity measures during the trial reported by Suttmoller et al., which could have led to an infection of the contact animal via a different route. Neither the induction of stress in carriers by transport or steroid treatment nor scarification of contact animals enhances viral transmission (Suttmoller et al. 1968).

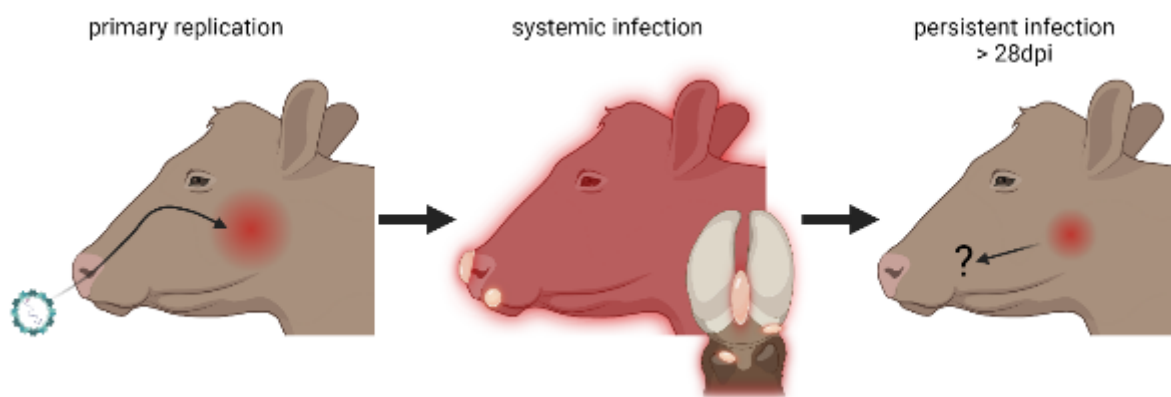


*Figure 4. Progression of FMDV infection in naive cattle from primary infection in the nasopharynx, to a systemic infection with lesions on hairless epithelia and shedding of virus, to the persistent infection with limited replication in the nasopharynx and disputed potential of shedding (Created with BioRender.com)*

In contrast to the disputed contagiousity of carrier cattle, in the wildlife reservoir of FMDV, the African buffalo (*Syncerus caffer*), carrier animals are indeed infectious. Infection of these animals with FMDV is causing only mild clinical signs with minor vesicular lesions (Dawe et al. 1994a), but results in a high proportion of persistently infected animals (Jolles et al. 2021). These persistently infected animals have been demonstrated to transmit FMDV to cattle (Dawe et al. 1994b; Vosloo et al. 1996). Recent investigations of carrier buffalo have shown that FMDV requires the persistent infection with onward transmission to maintain endemicity in buffalo populations (Jolles et al. 2021). This different epidemiologic aspect of persistent FMDV in buffalo compared to cattle may be due to an altered preferential location of infection

in the nasopharynx. The palatine tonsil seems to be infected to a higher proportion for a longer time than comparable tissues in the pharyngeal region and sampling with a tonsil brush collects virus more reliably than using a probang cup (Maree et al. 2016). This shift of the preferred persistently infected tissue from the upper region of the nasopharynx in cattle to the lower region in close vicinity to the oral cavity in buffalo may be one of the crucial factors for active shedding of virus and transmission by carriers.

The high mutation rate of FMDV leads to a hypothesis connecting viral persistence with distinct genomic traits. Even though viral replication seems to be slower during persistence (Horsington and Zhang 2007a), the substitution rate is maintained at a high level (Arzt et al. 2019). Traditional Sanger sequencing of FMDV focused mainly on VP1 for serotyping. With its exposed antigenic sites, VP1 was of high interest for the hypothesized antigenic escape by mutation. In consensus sequences of VP1 from probang samples, Gebauer et al. (1988) demonstrated a similar number of mutations acquired within days of persistence compared to years of viral evolution during the acute phase. Pauszek et al. (2016) found an amino acid change at VP1 114 of O/ME-SA/PanAsia to be correlated with persistent infection. By expanding the range of sequencing to other regions of the ORF, other mutational changes were identified and connected with persistence, e.g. by Horsington and Zhang (2007b), who found such an amino acid substitution at position 79 in the B-C loop of VP2. However not every investigation found a distinct correlation between the persistent phase and the viral genome (Cortey et al. 2019). Using more advanced deep sequencing techniques, the simultaneous presence of different viral populations caused by the high mutational rate could be addressed. In this viral super swarm, several haplotypes are present in the inoculum as well as during the acute phase, but with progression of infection into the persistent phase one haplogroup becomes dominant (Fish et al. 2020). Within the same study, Fish et al. (2020) could prove that distinct regions of the capsid surface of serotype A are subjected to a positive selection pressure during persistence. The still replicating persistent virus might be the source for interserotypic recombination after an acute superinfection with a heterologous serotype as Arzt et al. (2021) showed. The natural release of such interserotypic recombinants from persistently infected animals has not been documented yet, while many interserotypic strains have been isolated from field outbreaks and pose a significant risk to the efficacy of vaccines (Jamal et al. 2020).

## 5. Immune response and vaccination

The establishment and eventual clearance of FMDV infection is an ever-evolving battle arms race between the host 's immune response and viral immune evasion mechanisms. The duration of the acute phase in naïve cattle represents the time span the adaptive immune system requires to elicit an efficient response following the first contact with an unknown pathogen. The clearance of viremia in acutely infected cattle, which signifies the end of the acute phase, is largely facilitated by the fast onset of neutralizing antibodies, IgM followed by IgG (Eschbaumer et al. 2016a). This rapid and efficient humoral response is independent of T lymphocytes as it has been demonstrated by the depletion of CD4<sup>+</sup>, CD8<sup>+</sup> and  $\gamma/\delta$  T cells which had no effect on the generation of neutralizing antibodies and isotype switching (Juleff et al. 2009). An immunosuppression accompanied by a transient lymphopenia during the acute phase of FMDV infection in swine (Díaz-San Segundo et al. 2009) could not be corroborated in cattle by Windsor et al. (2011). But more recent investigations did indeed observe a short lymphopenic phase in cattle during peak viremia accompanied by a downregulation of antigen-presenting MHC II in dendritic cells and monocytes (Sei et al. 2016). Evidence for a deficiency of natural killer (NK) cells in swine during the acute phase has been brought up (Toka et al. 2009), but this could not be shown in cattle (Patch et al. 2014). A difference in the immunological response between pigs and cattle can be observed considering the IFN and cytokine response as well. In pigs, high levels of type I IFN and interleukin (IL) 10 can be detected (Nfon et al. 2010; Díaz-San Segundo et al. 2009) and inoculation with a type I IFN expressing vector even protects swine from challenge (Dias et al. 2011), suggesting an important function in the clearance of FMDV in swine for these cytokines. Cattle on the other hand show comparably low levels of IFN type I and IL-10 pointing to a different role of these cytokines in cattle (Windsor et al. 2011).

Type I IFNs are part of the innate immune response and act as a first-line defense by exerting proinflammatory signaling and promoting the antiviral response by activating cells of the innate and adaptive immunity (Snell et al. 2017). FMDV on the other hand as developed several mechanisms to counteract the innate immune response (reviewed in Sarry et al. 2022). In the initial phase of IFN signaling, viral RNA in the infected cells is detected by toll-like receptors (TLRs) or retinoic acid-inducible gene-I (RIG-I) like receptors (RLRs). This recognition evokes a

downstream cascade involving the recruitment of several signaling adapters resulting in the phosphorylation of interferon regulatory factors (IRFs). These IRFs translocate into the nucleus in combination with NF $\kappa$ B, where they stimulate the expression of proinflammatory cytokines and the interferons type I, II and III (Negishi et al. 2018). These IFNs then further activate the JAK-STAT-pathway resulting in the expression of interferon-stimulated genes (ISGs), which exert antiviral functions targeting important steps of the viral replicative cycle (Schoggins 2019). Diverse steps of the IFN signaling pathway are targeted by FMDV. The main proteins exerting inhibitory functions are the viral proteinases L<sup>pro</sup> and 3C, by cleavage of a plethora of signaling proteins (Sarry et al. 2022). In addition to its proteinase function, L<sup>pro</sup> can deubiquitinate signaling proteins, thereby deactivating them (Wang et al. 2011). Other proteins of FMDV inhibit interferon signaling by regulatory binding and reducing the mRNA expression level of signaling peptides as it was demonstrated for 3A, which downregulates the expression of RIG-I and MDA5 (Li et al. 2016a). The innate immune response is not only counteracted by non-structural proteins. Also structural proteins such as VP1 and VP3 have been shown to promote viral replication by interacting with receptors and signaling transmitters, blocking the downstream signaling (Li et al. 2016b). This diverse set of mechanisms to counteract the innate immune response orchestrated mainly by IFN type I allows FMDV to replicate efficiently.

During persistent infection, the fine balance between viral replication and the immune response is skewed, because replicative virus is still present in an otherwise immune host. The strong antibody response which terminates acute infection is not capable of clearing FMDV from the epithelia of the nasopharynx (Alexandersen et al. 2002), even though carrier animals show elevated levels of IgA in nasal fluid and saliva which can be used as a diagnostic parameter for the identification of carrier animals on a herd level (Biswal et al. 2021). This prolonged stimulation of mucosal antibodies might be due to the presence of virus in the lymphoid mucosa, where IgA is mainly synthesized (Suzuki et al. 2010). Immune evasion of the virus by antigenic variation is still discussed, while testing the neutralizing efficiency of serum from early phase against virus isolation the persistent phase and vice versa showed no difference in cattle (Horsington and Zhang 2007b) or in buffalos (Cortey et al. 2019). On the other hand, (Gebauer et al. 1988) demonstrated that isolates from carriers did differ from their parental strain when tested against a panel of monoclonal antibodies. *In vivo* clearance of virus from the nasopharynx during the transitional phase was associated with a higher abundance of

CD3<sup>+</sup> and CD8<sup>+</sup> T cells whose cytotoxic response likely contributed significantly to the clearance of virus after the acute phase. The same study used microarray analysis of laser-capture microdissected tissue to quantify the differential expression between carriers and animals which could clear the infection. The results indicated an enhanced activation of the cell-mediated, cytotoxic immune response (Stenfeldt et al. 2017). Further microarray studies from the same laboratory carried out with tissues from persistently infected animals showed that in carrier animals the chemotactic activity for the recruitment of immunocompetent cells is reduced, the activity of cytotoxic NK cells and macrophages is inhibited, the apoptosis of cells is suppressed and the Th17 activity is downregulated (Zhu et al. 2020, 2022). These studies suggest an inability of the local immune system of the mucosa to clear infected cells.

The currently used vaccines against FMDV, which are made from BEI-inactivated FMDV antigen cultured on BHK-21 cells, protect against homologous challenge infection but provide protective immunity only for about 6 months (Parida 2009). In contrast to recovered animals, vaccination does not prevent primary replication in the nasopharynx and during subclinical infection of vaccinated cattle virus can be shed (McVicar and Suttmoller 1976). Neither do current vaccine options prevent cattle from becoming persistently infected after subclinical FMDV infection, from which they are clinically indistinguishable. In vaccinated cattle, no systemic spread is observed and the virus remains at the location of primary replication throughout the infection and, in some animals, until the persistent phase. Viral loads in the oropharyngeal fluid however can be reduced by an increased vaccine dose (Stenfeldt et al. 2016a). The current tests of vaccination efficacy do not consider the potential of vaccines in preventing persistent infection. The standard intraepidermolingual challenge is unable to reproduce the natural infection to the extent which is required for persistent infection (Stenfeldt and Arzt 2020).

Whether vaccination has an influence on the carrier state and several other immunological aspects of the persistent FMDV infection will be furthermore discussed in the next chapter in consideration of our findings.



## CHAPTER III: OBJECTIVES



### III. Objectives

Since the first description of persistently FMDV-infected animals by Jaap van Bakkum in the 1950s scientists have tried to elucidate the pathogenesis and localization of the persistent infection in ruminants. But fundamental questions such as what determines whether an animal will remain persistently infected and how the virus is able to maintain active replication in an immune host are still unanswered. The present work focuses on improving the understanding of the interplay between the virus and its host that allows FMDV to persist in pharyngeal epithelia.

#### **Objective I:** Influence of FMDV on the host

##### Publication I & II

In vitro studies have demonstrated that FMDVs viral proteins exert a plethora of functions aiming to inhibit the innate immune response. Documentation of the effects of these proteins *in vivo* is scarce, especially in context of the persistent infection. We characterized the influences of FMDV on persistently infected tissue on the level of gene and protein expression, with a special focus on the leader protein L<sup>pro</sup>. Additionally, the ability of L<sup>pro</sup> to establish a persistent infection in cattle of a FMDV strain lacking coding sequence L<sup>pro</sup> was tested.

#### **Objective II:** Influence of the host on the viral evolution

##### Publication III

A connection between the occurrence of persistently infected animals and the factors in the viral genome was suggested by several studies. By sequencing viral RNA from oropharyngeal fluid of persistently infected animals the mutational pattern was observed over the period from acute to persistent phase of infection. A functional analysis was performed with individual emerging mutations to characterize the advantages conferred by these variants and if these changes were induced by the host immune response.



## CHAPTER IV: RESULTS



## **IV. Results**

Publications are presented in an order, as mentioned in the related “study objectives” -section. Figure and table numbering refer to the original paper and references are presented in the respective journal style and do not appear in the reference section of this document.



1. Publication I: Leaderless foot-and-mouth disease virus serotype O is fully attenuated and unable to establish persistent infection in cattle

Publication I

**Leaderless foot-and-mouth disease virus serotype O is fully attenuated and unable to establish persistent infection in cattle**

Benedikt Litz, Julia Sehl-Ewert, Angele Breithaupt, Anja Landmesser, Florian Pfaff, Aurore Romey, Sandra Blaise-Boisseau, Martin Beer, Michael Eschbaumer

Emerging Microbes & Infections

2024

doi: 10.1080/22221751.2024.2348526

## Leaderless foot-and-mouth disease virus serotype O did not cause clinical disease and failed to establish a persistent infection in cattle

Benedikt Litz<sup>a</sup>, Julia Sehl-Ewert<sup>b</sup>, Angele Breithaupt<sup>b</sup>, Anja Landmesser<sup>a</sup>, Florian Pfaff<sup>a</sup>, Aurore Romey<sup>c</sup>, Sandra Blaise-Boisseau<sup>c</sup>, Martin Beer<sup>a</sup> and Michael Eschbaumer<sup>a</sup>

<sup>a</sup>Institute of Diagnostic Virology, Friedrich-Loeffler-Institut, Greifswald-Insel Riems, Germany; <sup>b</sup>Department of Experimental Animal Facilities and Biorisk Management, Friedrich-Loeffler-Institut, Greifswald-Insel Riems, Germany; <sup>c</sup>Animal Health Laboratory, Foot-and-Mouth Disease Reference Laboratory, Virology JRU, ANSES, INRAE, ENVA, Paris-Est University, Maisons-Alfort, France

### ABSTRACT

The foot-and-mouth disease virus (FMDV) Leader proteinase L<sup>Pro</sup> inhibits host mRNA translation and blocks the interferon response which promotes viral survival. L<sup>Pro</sup> is not required for viral replication in vitro but serotype A FMDV lacking L<sup>Pro</sup> has been shown to be attenuated in cattle and pigs. However, it is not known, whether leaderless viruses can cause persistent infection in vivo after simulated natural infection and whether the attenuated phenotype is the same in other serotypes. We have generated an FMDV O/FRA/1/2001 variant lacking most of the L<sup>Pro</sup> coding region ( $\Delta$ Lb). Cattle were inoculated intranasopharyngeally and observed for 35 days to determine if O FRA/1/2001  $\Delta$ Lb is attenuated during the acute phase of infection and whether it can maintain a persistent infection in the upper respiratory tract. We found that although this leaderless virus can replicate in vitro in different cell lines, it is unable to establish an acute infection with vesicular lesions and viral shedding nor is it able to persistently infect bovine pharyngeal tissues.

**ARTICLE HISTORY** Received 22 January 2024; Revised 26 March 2024; Accepted 23 April 2024

**KEYWORDS** Foot-and-mouth disease virus; FMDV; persistence; carrier; leader proteinase

### Introduction

The single-stranded (+)RNA foot-and-mouth disease virus (FMDV) belongs to the genus *Aphthovirus* of the family *Picornaviridae*. It causes vesicular lesions in the mouth, on the tongue, muzzle and in the interdental cleft in cloven hoofed animals including pigs. The acute phase with its clinical lesions is accompanied by fever, shedding of high viral loads and a decline in productivity [1]. Vaccination and rigorous culling have successfully eradicated FMDV in Europe [2] but the reintroduction of FMDV into free countries poses a severe risk and causes dramatic economic losses as seen in the United Kingdom in 2001 [3]. The acute phase of FMDV infection is followed by a persistent phase in more than 50% of infected cattle, the so-called carriers [4–7], whereas pigs do not become persistently infected [8]. The persistent infection is characterized by an absence of clinical lesions but infectious virus can be recovered from the animal after the 28th day of infection [9]. In contrast to a generalized subclinical infection, the persistent infection in cattle is strictly limited to epithelia of the upper respiratory tract, mainly the dorsal nasopharynx and the dorsal soft palate [10].

Microanatomically, the follicle-associated epithelium (FAE) overlying the mucosa-associated lymphoid tissue (MALT) has been described as the preferential location [4]. As this site is not easily accessible for sampling, special probang cups are used for the collection of oropharyngeal fluid (OPF) from the oesophagus. Although live virus can be recovered from persistently infected animals, the contagiousity of persistently infected cattle is still debated as no convincing evidence for onward transmission has been found [8,11]. However, in the natural host for FMDV, the African buffalo (*Synceus caffer* [Sparrman, 1779]), persistently infected animals have been observed to transmit virus to naïve buffalo and cattle under experimental conditions [12,13]. A transmission model informed by the experimental data suggested that carrier buffalo are important for the maintenance of FMDV endemicity in buffalo populations [12].

The single open reading frame (ORF) of the FMDV genome encodes 4 structural proteins and 10 non-structural proteins, of which the Leader proteinase L<sup>Pro</sup> is the first to be translated and forms the N-terminus of the polyprotein. The coding sequence of L<sup>Pro</sup> contains two start codons as alternative translation

**CONTACT** Michael Eschbaumer  michael.eschbaumer@fli.de  Institute of Diagnostic Virology, Friedrich-Loeffler-Institut, 17493 Greifswald-Insel Riems, Germany

© 2024 The Author(s). Published by Informa UK Limited, trading as Taylor & Francis Group, on behalf of Shanghai Shangyibun Cultural Communication Co., Ltd. This is an Open Access article distributed under the terms of the Creative Commons Attribution License (<http://creativecommons.org/licenses/by/4.0/>), which permits unrestricted use, distribution, and reproduction in any medium, provided the original work is properly cited. The terms on which this article has been published allow the posting of the Accepted Manuscript in a repository by the author(s) or with their consent.

initiation sites, termed Lab and Lb, 84 nucleotides apart [14]. A functional difference between the two proteins has not been observed [15]. The deletion of the L<sup>Pro</sup> coding region after the second start codon Lb allows the rescue of viable virus, but complete deletion of the entire L<sup>Pro</sup> does not. The inter-AUG region between the start codons has therefore been demonstrated to be necessary for viral replication. The Lab start codon can be mutated as long as the inter-AUG region and the Lb start codon remain intact, whereas the mutation of the Lb start codon does not produce viable virus [16].

Post-translational release of the papain-like protease L<sup>Pro</sup> from the structural protein VP4 in the FMDV polyprotein takes place by self-cleavage [17]. An important function of L<sup>Pro</sup> is the inhibition of the host cell translation by cleaving the initiation factor eIF4G [18], resulting in the shutdown of the cap-dependent mRNA translation. Translation of the viral RNA of FMDV is not affected due to the internal ribosome entry site (IRES) in the 5'UTR which mimics the cellular translation initiation complex by its three-dimensional RNA secondary structure. In addition to an enhancing viral replication at the expense of the host, L<sup>Pro</sup> inhibits the interferon (IFN) response by either cleaving or deubiquitinating important transcriptional factors such as IRF3, IRF7, TRAF3 or RIG-I, as has been demonstrated *in vitro* [19,20]. *In vivo*, this may be less effective, as strong viral replication tends to induce rather than suppress the interferon response [21].

Some FMDV variants have been constructed that lack the Leader proteinase. Piccone et al. [22] produced a variant based on FMDV A<sub>12</sub>, by removing the L<sup>Pro</sup> coding sequence following the second start codon Lb. It grew more slowly in BHK-21 cells and was slightly attenuated in suckling mice compared to wildtype FMDV. After aerosol inoculation of cattle with the A<sub>12</sub> mutant, the animals showed no clinical signs at 72 h post infection (hpi) and only focal virus replication, primarily in the lung [23]. Following this initial *in vivo* characterization, a further challenge experiment was carried out using intradermal or intramuscular inoculation of the leaderless A<sub>12</sub>, which induced protective immunity against a homologous challenge. Oropharyngeal fluid was collected in this animal study, but no virus could be isolated prior to challenge infection at 35 days post infection (dpi) [24]. Uddowla et al. [25] used FMDV A<sub>24</sub> Cruzeiro with the same deletion to inject animals intradermally. No clinical signs or viral shedding were observed but the inoculated cattle did develop neutralizing antibodies. In the same study, animals were vaccinated with a chemically inactivated leaderless A<sub>24</sub> Cruzeiro formulated with adjuvant and were protected from clinical FMD after homologous challenge.

The O1K ΔLb mutant constructed by Belsham et al. has the same deletion of the Lb coding sequence in the backbone of FMDV O<sub>1</sub> Kaufbeuren and showed similar growth kinetics in BHK-21 cells as wildtype O1 K, but it was unable to infect primary bovine thyroid cells [16]. Another method that achieved attenuation in cattle with unimpeded replication *in vitro* was a 54-nt in-frame insertion in the inter-AUG region, maintaining the functionality of L<sup>Pro</sup> [26].

When evaluating the safety of leaderless viruses, recombination of a leaderless virus with a Leader proteinase from a closely related virus such as bovine rhinitis B virus (BRBV), which is ubiquitous in cattle [27], should be considered. Picornaviruses having a high recombination rate [28], with breakpoints for recombination in the FMDV genome following L<sup>Pro</sup> [29]. Uddowla et al. have addressed this issue by showing that such a chimeric virus is also fully attenuated in cattle and of low virulence in swine [30].

Long-term persistence of leaderless virus in infected animals could constitute a reservoir for potential recombination. The aim of this study was therefore to create an FMDV variant from a more recent virulent FMDV isolate (O/FRA/1/2001), to characterize its early infection dynamics after simulated natural infection via the intranasopharyngeal route and to determine whether it is capable of persistently infecting cattle and remaining in the epithelia of the upper nasopharynx.

## Material and methods

### Generation of leaderless FMDV

A plaque-purified isolate of FMDV O/FRA/1/2001 was provided by the Animal Health Laboratory, ANSES, Maisons-Alfort, France, and a cow was experimentally infected with this clone at the BSL4vet facility of the FLI in Riems. Vesicular material from this cow was sequenced on an Ion Torrent platform as previously described [31] (Genbank accession no. OV121130.1). The entire genome including both UTRs (with a 13-mer poly-C region in the 5'UTR) was synthesized by GeneArt (Regensburg, Germany). The cDNA was inserted into the original pT7S3 plasmid [32] by restriction-free cloning [33], replacing the entire O1 K genome. Clones with the correct insertion were selected after a restriction enzyme digestion and the insertion was verified by Sanger sequencing using the universal FMDV primer set of Dill et al. [34]. Confirmed clones were linearized by *HpaI* digestion and transfected into BSR-T7 cells, a BHK-21 cell line expressing T7 RNA polymerase [35], using 1 µl of Lipofectamine 3000 and 500 ng of linearized DNA in a 12-well plate.

The deletion of the Lb coding sequence from the O/FRA/1/2001 infectious clone was performed with the

Q5 site-directed mutagenesis kit (New England BioLabs) using primers 5'-GGCGCCGGGCAATC-CAGC-3' and 5'-CATCTTTCCTTGCTCGTGAT AAGAACAGTGTTTTAATCTC-3'. Transformation, selection and sequencing of correct clones were carried out as described above. For transfection 1.5 µl lipofectamine was used with 500 ng of linearized DNA and the cell culture plates were centrifuged for 1 h at 800×g after transfection to increase efficiency [36].

### Growth kinetics

Viral growth kinetics were examined in a comparison between the parental strain O/FRA/1/2001 wildtype (WT) and its leaderless derivative O/FRA/1/2001 ΔLb at a multiplicity of infection (MOI) of 0.1 on BHK-21 cells (CCLV-RIE 0164, Collection of Cell Lines in Veterinary Medicine, FLI, Greifswald-Insel Riems, Germany), porcine kidney cells expressing bovine αVβ6 integrin (LFBK-αVβ6, CCLV-RIE 1419) [37], IB-RS-2 porcine kidney cells (CCLV-RIE 103) [38] and ZZ-R goat tongue cells (CCLV-RIE 127) [39]. Samples were taken on time points 0, 4, 8, 16, 24 and 42 hpi and titrated on BHK-21 cells. The data were collected from three biological replicates.

### Animal trial

The animal experiment was carried out under BSL4vet conditions at the Riems site of the FLI. Sixteen Holstein-Friesian heifers of around 4 months of age and with an average body weight of 110 kg were obtained from the same breeder and randomly assigned to two groups of eight animals. The groups were housed in separate rooms and observers were not blinded to treatment group assignment. After 1 week of acclimatization to the containment facility, the animals were inoculated via intranasopharyngeal instillation, which closely simulates natural infection [40]. One group was inoculated with O/FRA/1/2001 ΔLb and the other was inoculated with the recombinantly produced parental strain O/FRA/1/2001 WT. Both viruses had been passaged twice on BHK-21 cells. The cultures were frozen and thawed and the supernatants were clarified by centrifugation. Virus titres were determined by end-point titration on BHK-21 cells. For inoculation, the virus preparations were diluted in cell culture medium (minimum essential medium with Hanks' and Earle's salts and non-essential amino acids) to adjust the virus concentration and applied in a single dose of  $0.8 \times 10^7$  TCID<sub>50</sub> in 2 ml medium. We used the highest dose possible based on the available volumes and titres of the virus preparations to demonstrate the safety of the leaderless virus even when applied at a high dose.

For inoculation as well as for clinical examinations on days 2, 4, 6, 8 and 10 pi, the animals were sedated

with 0.3 mg/kg xylazine. The sedation was reversed by atipamezole at a dose of 0.025 mg/kg. Rectal body temperatures were recorded daily. To avoid the potentially confounding use of anti-inflammatory drugs for analgetic treatment [6], buprenorphine at 0.01 mg/kg was given daily to animals with vesicular lesions during the acute phase. Animals which showed signs of bronchopneumonia were treated with 750 mg of enrofloxacin per animal.

Out of each group, two animals were euthanized 24 hpi, the remaining animals were euthanized on day 35 or 36 pi. For euthanasia, animals were lightly sedated with xylazine at 0.05 mg/kg and led to the necropsy room. There they were deeply sedated with xylazine at 0.3 mg/kg and euthanized by intravenous administration of 90 mg/kg pentobarbital. Once pain reflexes had ceased, the animals were exsanguinated.

The protocol for the animal trial (file no. 7221.3-1-052/21) has been approved by the State Office for Agriculture, Food and Fisheries of Mecklenburg-Vorpommern (LALLF M-V).

### Ante and post mortem sample collection

As a negative control, serum, nasal fluid, saliva and OPF were collected from each animal before infection. Immediately after inoculation, an additional sample of nasal fluid was collected. From 1 to 10 dpi, serum, nasal fluid and saliva were collected each day, thereafter samples were taken on days 14, 17, 21, 24, 28, and 31 pi. The collection of OPF with a special probang cup was started on 7 dpi in the ΔLb group. In the WT group, the first OPF sample was taken on 10 dpi to avoid contamination by recently ruptured vesicles in the oral cavity. The collection of OPF was carried out on the same days as listed above with an additional sampling on 35/36 dpi before euthanasia. During necropsy, a set of tissue samples was collected representing different epithelial surfaces in the pharynx, the lungs, and their draining lymph nodes (see Table 1). Tissue samples from the lungs were only collected from animals euthanized 24 hpi. From each tissue, one specimen was archived for histopathological

**Table 1.** Summary of tissue samples collected at necropsies 24 hpi and 35/36 dpi.

	24 hpi	35 dpi
Ventral soft palate (VSP)	X	X
Dorsal soft palate (DSP)	X	X
Dorsal nasopharynx (DNP)	X	X
Pharyngeal tonsil	X	X
Laryngeal epithelium at the base of epiglottis	X	X
Lung, right proximal cranial lobe	X	
Lung, right proximal distal lobe	X	
Lung, right medial lobe	X	
Lung, right caudal lobe	X	
Retropharyngeal lymph node	X	X
Submandibular lymph node	X	X
Tracheobronchial lymph node	X	

examination, while the remainder was used for genome detection and virus isolation. Tissues from the dorsal soft palate (DSP) and the dorsal nasopharynx (DNP) were split into five biological replicates per region to address the focal nature of persistent infection. Tissue samples for RT-qPCR and virus isolation were frozen over liquid nitrogen immediately after collection and then stored at  $-80^{\circ}\text{C}$ .

#### RNA extraction from samples and tissues

RNA was extracted from 100  $\mu\text{l}$  of serum, nasal fluid, saliva and OPF using the NucleoMag Vet kit (Macherey-Nagel) with a King Fisher Flex (Thermo Scientific) magnetic particle processor. As an internal control, 10  $\mu\text{l}$  of IC2 RNA were added during the extraction [41]. Tissue samples collected during necropsy were disintegrated in 750  $\mu\text{l}$  of PBS using a 5-mm steel ball in a TissueLyser II (Qiagen) for 2 minutes at 30 Hz. Supernatants were collected after centrifugation and used for RNA extraction and virus isolation.

#### Genome detection

FMDV genome was detected and quantified by RT-qPCR using AgPath-ID One-Step RT-PCR reagents (Thermo Fisher Scientific) with a primer/probe set targeting the 3D-coding region [42]. To detect concurrent infection with BRBV, a possible donor for the reacquisition of a leader protease through recombination, all animals were tested by RT-qPCR using primers and a probe published by Xie et al. [43].

#### Virus isolation from collected samples

Sampling with the probang cup was performed to determine if animals were persistently infected [44]. Recovered OPF was mixed with 4 ml of cell culture medium. The liquid was then homogenized by repeated aspiration with a 16G blunt cannula before half of the sample was mixed with an equal amount of 1,1,2-trichloro-1,2,2-trifluoroethane (TTE) [45]. This mixture was vigorously shaken for 5 min and afterwards centrifuged at  $1000\times g$  for 10 min at  $4^{\circ}\text{C}$ . The supernatant was removed and aliquoted. A 90% confluent LFBK- $\alpha\text{V}\beta 6$  monolayer in 25  $\text{cm}^2$  culture flasks was inoculated with 250  $\mu\text{l}$  of the TTE-treated OPF. For the  $\Delta\text{Lb}$  group, this was repeated with BHK-21 cells. Positive virus isolation (i.e. cytopathic effect) was confirmed by FMDV RT-qPCR as described above. Two passages were performed to confirm negative results.

For virus isolation from tissues, the supernatants were mixed with an equal amount of TTE and then vigorously shaken for 5 min, afterwards the mixture was centrifuged at  $900\times g$  for 20 min at  $4^{\circ}\text{C}$  [46]. A volume of 50  $\mu\text{l}$

supernatant were used for virus isolation on LFBK- $\alpha\text{V}\beta 6$  cells. Only samples with a positive FMDV RT-qPCR result were selected for virus isolation.

#### Serology

Antibodies against non-structural proteins (NSP) of FMDV were detected with the PrioCHECK FMDV NS ELISA (Thermo Fisher Scientific) using the overnight protocol.

#### Histopathology

Collected tissue samples (see Table 1) were fixed in 10% neutral-buffered formalin for at least 3 weeks and processed for paraffin-embedding. Embedded tissues were cut at 2–3  $\mu\text{m}$  thick sections, mounted on glass slides, dewaxed in xylene, and rehydrated in descending graded alcohols. For morphological evaluation, sections were stained with haematoxylin–eosin (HE) following standard procedures.

To detect viral RNA, RNA *in situ* hybridization was performed on selected tissues (DSP, DNP) obtained from animals which were tested virus positive at the end of the experiment. RNAScope probes were custom-designed against the highly conserved FMDV NSP 3D (ACD, Advanced Cell Diagnostics, Newark, CA, USA) and used with the corresponding RNAScope 2–5 HD Reagent Kit-Red according to manufacturer's instructions. As technical assay controls, a positive control probe for the housekeeping gene peptidylprolyl isomerase B (cyclophilin B, *PP1B*) and a negative control probe for dihydrodipicolinate reductase (*DapB*) were included.

#### Statistical analysis

The binomial proportion confidence interval for the incidence of persistent FMDV infection in the wild-type group was calculated by the Wilson method [47] using R (<https://www.r-project.org/>).

## Results

#### Virus replication in vitro

An infectious clone of FMDV O/FRA/1/2001 was created by inserting commercially synthesized cDNA in the pT7S3 plasmid. Cytopathic effect (CPE) was observed after the transfection of BSR-T7 cells with the plasmid containing the O/FRA/1/2001 WT sequence. After two passages on BHK-21 cells, the titre of the recombinantly produced WT virus was  $1.21 \times 10^7$  TCID<sub>50</sub>/ml.

Its leaderless derivative O/FRA/1/2001  $\Delta\text{Lb}$  was also passaged twice on BHK-21 cells and then titrated on the same cell line. Its titre was  $1.00 \times 10^7$  TCID<sub>50</sub>/ml.

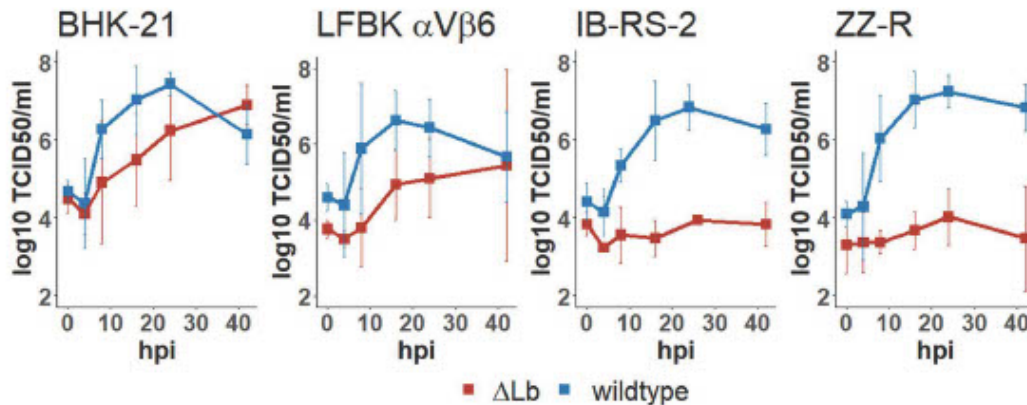


**Figure 1.** *In vitro* replication of O/FRA/1/2001 wildtype versus leaderless ( $\Delta$ Lb) FMDV over 42 h on four cell lines (BHK-21, LFBK  $\alpha$ V $\beta$ 6, IB-RS-2, and ZZ-R) infected at an MOI of 0.1. Supernatant was collected at 0, 4, 8, 16, 24, and 42 hpi and titrated on BHK-21 cells.

In BHK-21 cells, growth kinetics and final titre were similar between the leaderless mutant O/FRA/1/2001  $\Delta$ Lb and the parental virus as shown in Figure 1. In LFBK- $\alpha$ V $\beta$ 6 cells, growth of the mutant was delayed and did not reach titres as high as the wildtype. In IB-RS-2 as well as in ZZ-R cells, on the other hand, the mutant was strongly inhibited in its growth.

#### ***In vivo* attenuation of leaderless FMDV without virus shedding**

In the animal trial, two groups of eight cattle were inoculated with WT FMDV O/FRA/1/2001 or its leaderless derivative and two animals of each group were euthanized 24 hpi. Clinical signs consistent with FMD were only observed in the animals of the WT group. All remaining animals in this group developed vesicular lesions beginning on 4 dpi. Prominent vesicular lesions were seen on the tongue, dental plate, gingiva, muzzle and in the nostrils. Five of six animals also had lesions on all four extremities; animal 770 only had lesions in three of four interdigital clefts on 14 dpi. No lameness or recumbency was observed in any of the heifers.

$\Delta$ Lb infected cattle did not develop any vesicular lesions or any other clinical signs of FMD.

Figure 2 shows the results of the FMDV RT-qPCR for the WT (Figure 2A) and the  $\Delta$ Lb group (Figure 2B), respectively. All animals were positive for FMDV RNA in the nasal fluid sample taken immediately after intranasopharyngeal instillation of the WT or  $\Delta$ Lb virus, confirming the successful inoculation. In the  $\Delta$ Lb group, no viral RNA was detected in any other sample over the course of the experiment.

In the WT group, FMDV RNA detection in nasal fluid, saliva and serum peaked between 4 and 6 dpi. Viraemia was cleared in all animals before 10 dpi with animal 770 having detectable viraemia only at 2 dpi.

#### ***Incidence of persistently infected carrier animals***

According to the World Organisation for Animal Health, an animal is considered persistently infected with FMDV when virus can be recovered later than 28 days after infection [48]. This threshold is arbitrarily chosen and FMDV carriers can be already diagnosed at earlier time points [8]. However, we decided to use the standard definition for this study. TTE-treated OPF samples from two animals (758 and 773) in the WT group were consistently positive in the virus isolation from 10 dpi to the end of the experiment, resulting in an incidence of persistent infection of 33% (95% confidence interval 10–70%). In two other animals, 764 and 770, virus isolation was positive on 10 dpi only.

No virus was isolated from TTE-treated OPF from any animal in the  $\Delta$ Lb group on either LFBK- $\alpha$ V $\beta$ 6 or BHK-21 cells, corresponding to an incidence of persistent infection of 0% (95% confidence interval 0–39%).

#### ***Leaderless FMDV does not induce an antibody response***

In the WT group, NSP antibody levels started to rise around day nine after infection, except for animal 770 which had a detectable antibody response only after 17 dpi. In the  $\Delta$ Lb group, no animal developed detectable anti-NSP antibodies over the course of the experiment (not shown).

#### ***Viral RNA in tissues at 24 hpi versus 35 dpi***

Of each infected group, two animals were euthanized 24 hpi, while the remaining six animals were euthanized on 35 dpi. From each animal, a set of tissue

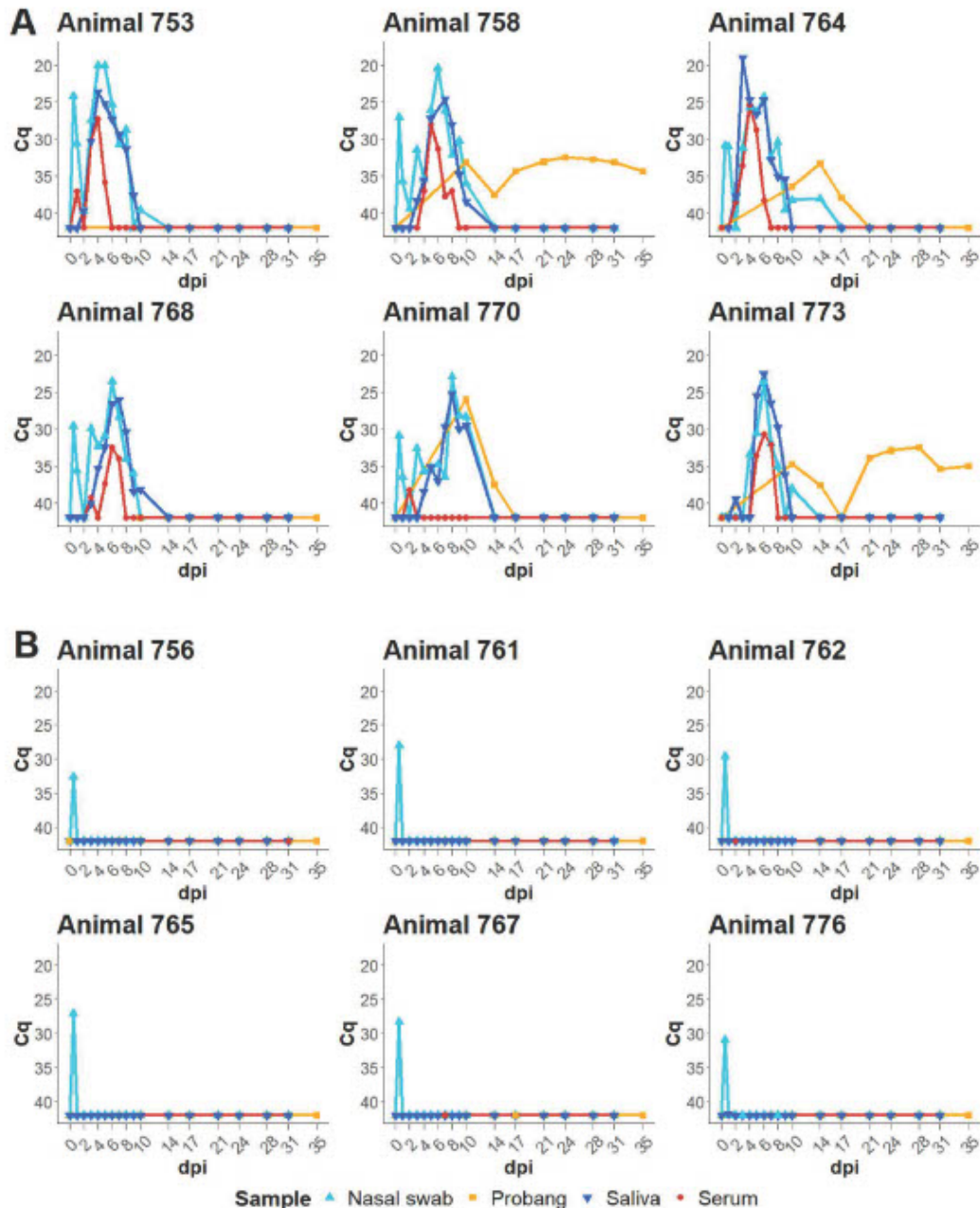


**Figure 2.** Ante-mortem infection dynamics of cattle infected with (A) wildtype FMDV or (B) FMDV  $\Delta$ Lb. The  $C_q$  values of the FMDV RT-qPCR for samples collected during the animal trial, including serum, nasal fluid, saliva, and OPF (probang) are shown on a reversed y-axis over the course of the experiment, from immediately before and immediately after inoculation on 0 dpi until the end of the trial on 35 dpi.

samples was collected at necropsy and tested for FMDV RNA by RT-qPCR. All tissue samples with a positive FMDV RT-qPCR were used for virus isolation. The sample set included epithelia of the pharynx and the draining lymph nodes. In the animals euthanized 24 hpi, the tracheobronchial lymph node and four samples from different regions of the lung were collected in addition.

In the two animals from the WT group that were euthanized at 24 hpi, FMDV RNA was detected in several tissues, with the highest viral load in the distal mid lobe of the lung followed by the pharyngeal tonsil as shown in Supplemental Table S1.

At the end of the experiment, several tissues of WT cattle were positive in the FMDV RT-qPCR as depicted in Figure 3. Irrespective of the animal's

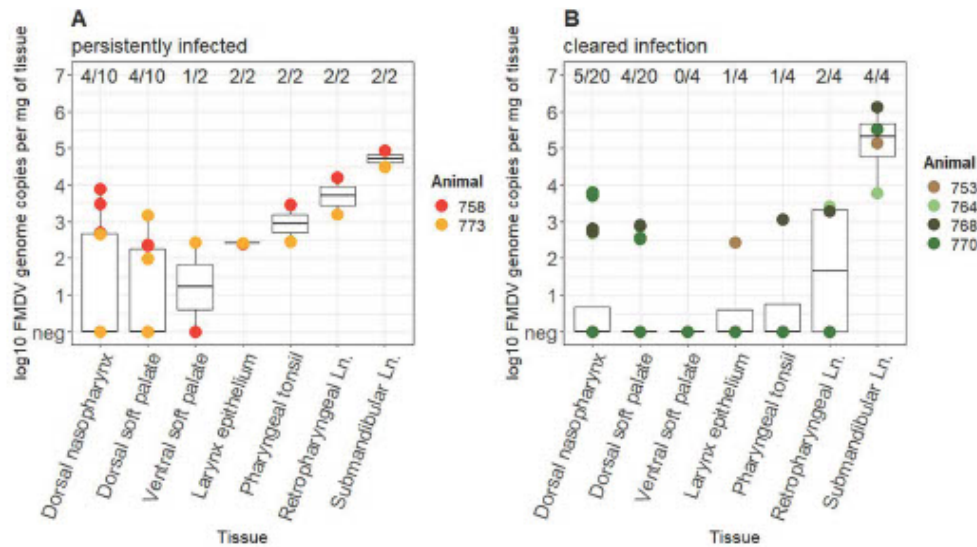


**Figure 3.** Tissue distribution of FMDV RNA in samples collected at necropsy on 36 dpi, compared between the two persistently infected animals 758 and 773 (i.e. animals from whose OPF virus was isolated after 28 dpi) (A) and the four animals 753, 764, 768, and 770 that had cleared the infection (i.e. had no detectable virus in OPF) at the time of euthanasia (B). The following tissues were collected from each animal: dorsal nasopharynx ( $n = 5$ ), dorsal soft palate ( $n = 5$ ), ventral soft palate ( $n = 1$ ), larynx epithelium ( $n = 1$ ), pharyngeal tonsil ( $n = 1$ ), retropharyngeal lymph node ( $n = 1$ ), and submandibular lymph node ( $n = 1$ ). Their FMDV RNA content was quantified by RT-qPCR and is presented as  $\log_{10}$  genome copy numbers per mg of tissue. The boxplots represent the distribution of FMDV content in each tissue including negative samples. The proportion of positive samples for each tissue is indicated by the fraction at the upper edge of the panels. Neg, negative; Ln, lymph node.

carrier status, the highest viral genome loads in animals euthanized on day 35 or 36 pi were detected in the lymph nodes, particularly in the submandibular lymph node, followed by the retropharyngeal lymph node and the samples taken from the dorsal nasopharynx. Several epithelial tissues as well as the majority of lymph nodes of animals in the WT group contained detectable FMDV RNA. Overall, the four animals that successfully cleared the infection had similar amounts of FMDV RNA in the same tissues as the two carrier animals, but a lower proportion of positive samples overall (17/60 or 28% vs. 17/30 or 57%, as shown in Figure 3).

Virus isolation with tissue samples from 36 dpi was only successful in one (animal ID: 758) of the two carrier animals, whose carrier status had been previously defined by the virus isolation from OPF. The positive tissue samples from this animal were DNP ( $n = 2$ ), DSP and larynx (both  $n = 1$ ) as described in Supplemental Table S1. Despite the high viral genome loads in the sampled lymph nodes of WT-infected animals, it was not possible to recover live virus from these tissues.

No tissue collected at 24 hpi or 35 dpi from animals infected with  $\Delta$ Lb contained any detectable FMDV RNA.

#### Localization of viral RNA in tissues of persistently infected animals

On the basis of positive virus isolation at 36 dpi, the DSP and DNP of the two carrier animals (animal

IDs: 758 and 773) were investigated with RNA *in situ* hybridization. While in animal 758 NSP 3D RNA was detectable in both tissue samples, in 773 only the DSP revealed positive signals (for comparison of staining in acutely infected tissue, see Figure S1). Viral RNA was mainly found in the ciliated pseudostratified columnar epithelium and less often in the submucosal lymphoid follicles and stromal cells of the DSP. Positive signals were identified throughout the epithelium within basal cells as well as within and on the apical surface of columnar epithelial cells (Figure 4A). In contrast, only single epithelial and submucosal stromal cells of the DNP were positive for viral RNA (Figure 4B).

#### Discussion

Any work with FMDV has to be carried out under the highest biosecurity conditions. Even though containment restrictions have become very sophisticated, vaccine production involving large amounts of infectious virus carries a significant risk of inadvertent release of FMDV. Producing inactivated vaccines using a strongly attenuated virus with the same capsid proteins offers a considerable safety advantage. *In vivo* attenuation of leaderless FMD viruses was successful with serotypes O and A [16,22], while protection afforded by inactivated vaccines prepared from a leaderless virus has been described only for serotype A [25,49]. Mason et al. [24] also evaluated the carrier

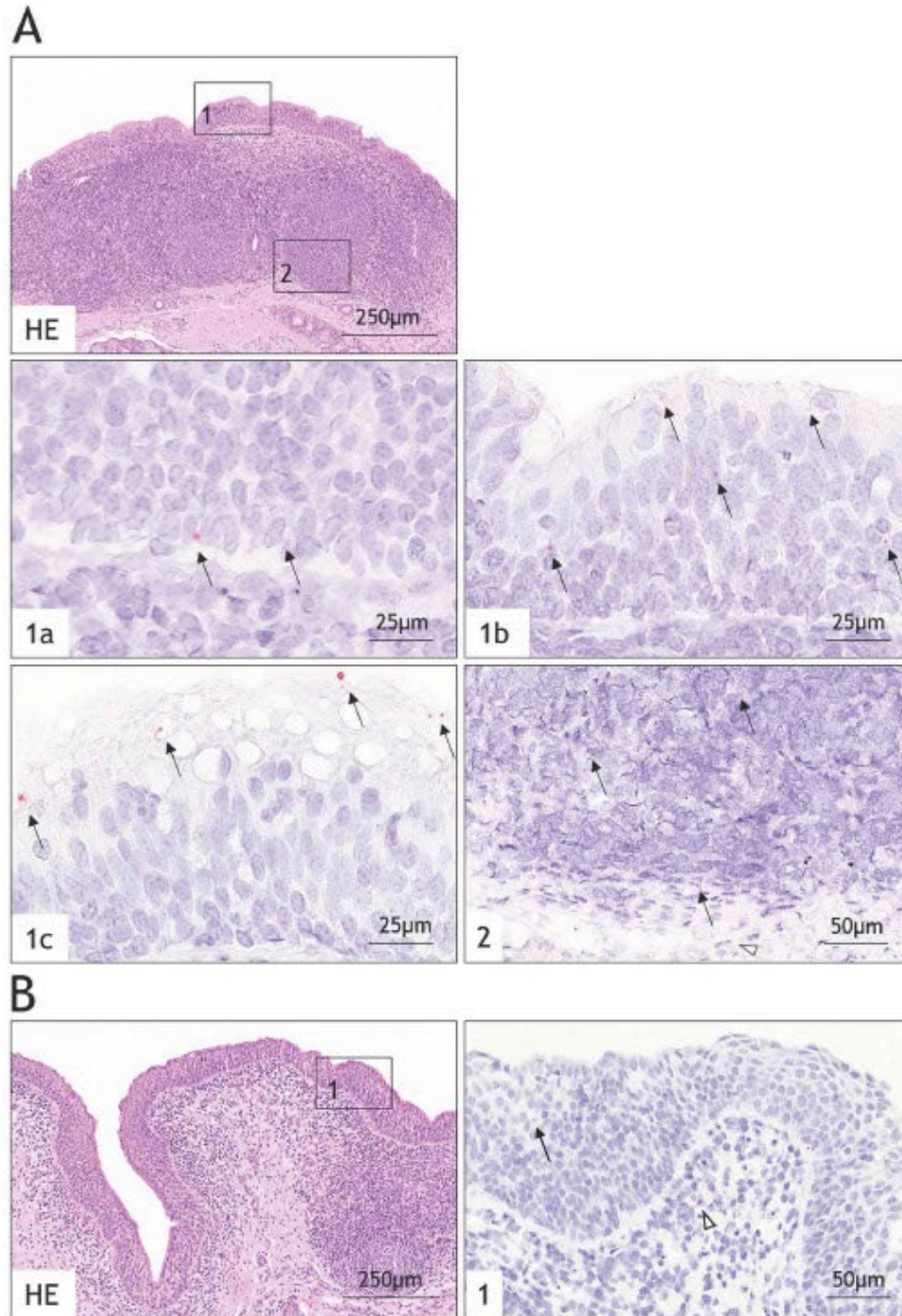


**Figure 4.** Histopathological findings using RNA *in situ* hybridization for tissues of carrier animal 758 infected with wildtype FMDV strain O/FRA/1/2001. HE stains are shown for morphological orientation in the tissues only. Consecutive sections were used for the *in situ* hybridization. (A) HE-stained overview of the dorsal soft palate (DSP) showing the approximate location of positive FMDV NSP 3D-specific RNA signals in the ciliated pseudostratified columnar epithelium (box 1) and submucosal lymphoid tissue (box 2). On consecutive sections, arrows indicate viral RNA within basal cells (1a), within columnar cells (1b), on the apical surface of columnar cells (1c) and within submucosal lymphoid follicles (2), stained by *in situ* hybridization. (B) Overview of the dorsal nasopharynx (DNP) indicating the approximate location of positive RNA signals (box 1), HE stain. On consecutive sections, compared to the DSP, viral RNA was found in fewer cells in the epithelium (arrow) and submucosa (arrowhead) by *in situ* hybridization.

status of animals inoculated with leaderless FMDV O but did not find any. However, in their study the leaderless virus had been injected subcutaneously, which is a highly artificial route of delivery for live FMDV and may not be able to cause persistent infections at all.

For our animal trial, the intranasopharyngeal instillation method was used, simulating the natural route of infection in the best possible way without requiring additional animals for contact exposure [40]. Contact exposure was not considered appropriate due to the expected strong attenuation of leaderless viruses. Our results support the previous finding of a strong attenuation of leaderless FMDV *in vivo* and we did not find any evidence that leaderless FMDV can persist in epithelia of the upper nasopharynx.

We compared an FMDV mutant lacking the Leader protease L<sup>P<sup>ro</sup></sup> to its parental wildtype strain, genetically identical to a FMDV field isolate from the 2001 outbreak in France, but rescued by reverse genetics.

Both viruses were characterized *in vitro* by growth kinetics in four different cell lines. The similar growth of the leaderless  $\Delta$ Lb FMDV in BHK-21 cells is most likely due to the interferon deficiency of this cell line [50], removing any advantage given to the wildtype virus by the inhibition of the interferon response by L<sup>P<sup>ro</sup></sup>. Similarly, FMDV  $\Delta$ Lb grew well in our LFBK- $\alpha$ V $\beta$ 6 cells, which are contaminated with a non-cytopathic strain of bovine viral diarrhoea virus (BVDV) known to inhibit the interferon response [51,52]. However, a comparison of the leaderless FMDV and its parental strain on BVDV-free LFBK- $\alpha$ V $\beta$ 6 cells [42] would be interesting. In interferon-competent cell lines (IB-RS-2 and ZZ-R), leaderless FMDV grew to much lower titre than the wildtype. This is in line with previous reports about leaderless FMDV in primary cells [16]. Even in an air-liquid interface model of bovine dorsal soft palate, as a highly susceptible tissue *in vivo*, our O/FRA/1/2001  $\Delta$ Lb strain was unable to replicate (Michaud et al., manuscript in preparation).

*In vivo*, the wildtype FMDV O/FRA/1/2001 caused clinical FMD. Every exposed animal became infected, developed vesicular lesions on hairless epithelia and shed virus in nasal fluid and saliva for up to 10 days. Viraemia lasted for several days, reaching its peak around days 4–6 post infection, except in animal 768, which was viraemic for only one day with a low viral genome load.

Of six animals in our study that remained in the experiment until day 35, two (animal IDs: 758 and 773) could be defined as carrier animals with several positive virus isolations from TTE-treated OPF after the 28th day of infection which was confirmed by the presence of FMDV NSP 3D-specific RNA in selected tissues. Due to the small number of animals, the confidence interval for the incidence of

persistent infection in our study (9.7–70.0%) overlaps with findings of earlier studies, which reported varying incidences around 50% due to small animal numbers [8]. In detail, for serotype A the carrier incidence ranged from 62% to 94% [4–6,53], while for serotype O incidences between 25% and 100% have been documented using smaller animal numbers than for serotype A [7,54–56]. Two other animals with relatively high viral loads in OPF after the acute phase (764 and 768) may be of interest for identifying factors which lead to the clearance of persistent FMDV.

Overall, the recombinant O/FRA/1/2001 wildtype virus was highly infectious and caused clinical signs comparable to the original outbreak strain. In contrast to this, the leaderless derivative O/FRA/1/2001  $\Delta$ Lb was neither able to cause acute disease nor did it persist in tissues of the nasopharynx. Although viral RNA was present in nasal fluid sampled right after the inoculation from every animal, none was detected later on, neither in body fluids nor in tissue samples. The absence of seroconversion in this group also supports the conclusion that no infection has occurred in the  $\Delta$ Lb group.

Our examination of the tissue distribution of wildtype FMDV in animals euthanized 24 hpi showed high viral genome loads in lung tissue, as reported by Brown et al. [23] who unlike us have used aerosol inoculation. The prominent replication of wildtype FMDV in the region of the nasopharynx in one heifer after 24 h was not observed by Brown et al. [23]. This differing tissue distribution could indicate a substantial difference between the inoculation methods used herein.

In samples taken at the end of the experiment, high amounts of viral RNA were detected in the lymph nodes of animals infected with the wildtype virus, especially in the submandibular lymph node. This is in accordance with the findings of Juleff et al. [57]. Despite the high viral genome loads, it was not possible to recover live virus from these tissues, which may be explained by only RNA remaining in the lymph nodes after clearance of virus by the cellular immune response [4]. The high viral genome loads found especially in the submandibular lymph node may be due to drainage from mucosa of the rostral skull, e.g. on the muzzle, nostrils, gingiva, and tongue [58], which are the main localization for vesicular lesions. The high viral RNA loads in lymph nodes in infected animals may be a result of clinical disease during the acute phase rather than the persistent infection.

The absence of detectable viral RNA in the lymph nodes of the animals in the  $\Delta$ Lb group, on the other hand, suggests that there was virtually no replication of this virus in the nasopharynx at any time. As seen by the high loads in submandibular lymph nodes of

animals in the wildtype group, viral RNA remains detectable for 5 weeks after acute infection.

Viral RNA was detectable in different tissues of all WT-infected animals at the end of the trial, and we were able to recover virus from one carrier animal (758). The localization of the viral RNA was consistent with previous immunohistochemical studies of persistent FMDV infection. Immunofluorescence targeting structural protein VP1 found it mostly in the superficial layer of the epithelium [4,59,60]. Pacheco et al. [10] detected non-structural protein 3D preferentially in the basal layer and viral RNA was stained by *in situ* hybridization in the basal layer as well [61–63]. The detection of viral RNA in basal and columnar cells of the dorsal soft palate in the present study could indicate that, similar to papillomaviruses [64], FMDV targets the basal cell layer for initial persistent infection. In the basal cells, the viral genome is maintained in the absence of a productive viral life-cycle. Structural proteins and viral progeny are only produced upon differentiation of the epithelial cells into the more superficial columnar cells.

In at least one animal in our trial, the closely related BRBV was detected at the time of infection with leaderless FMDV. This is likely due to the generally high prevalence of BRBV in cattle herds [27]. This simultaneous occurrence can lead to recombination by template switching of the RNA polymerase. One of the breakpoints for recombination is in close vicinity to the L<sup>pro</sup> coding region [29]. This is not of great concern, since Uddowla et al. [30] have shown that a chimeric FMDV with a BRBV L<sup>pro</sup> is still attenuated.

## Conclusion

The BSL4vet conditions under which FMD infection trials have to be conducted limit the number, age and size of animals used and the statistical significance that can be obtained. Based on our results alone, it cannot be ruled out that leaderless virus is able to establish persistence in a small proportion of exposed animals. Nevertheless, our results demonstrate the essential role of L<sup>pro</sup> for a productive FMDV infection. Without a functioning Leader proteinase, in our hands FMDV could neither establish an acute infection nor was it able to persist in the bovine nasopharynx. This strongly attenuated phenotype, which prevents clinical disease while retaining the full capsid-coding sequence, makes leaderless viruses a much safer alternative to wildtype FMDV for research, diagnostics (e.g. neutralization tests) and production of inactivated vaccines at lower biosafety levels.

## Acknowledgements

We thank Anja Schulz, Doreen Schulz and Silvia Schuparis for their excellent technical assistance, Christian Loth, Ralf

Henkel and Andreas Bath for their valuable support during necropsies and Matthias Jahn, Steffen Brenz, Dominique Lux and Patrice Mary for their diligent animal care.

## Disclosure statement

No potential conflict of interest was reported by the author(s).

## Funding

This work was funded by the Federal Office for Agriculture and Food (Bundesanstalt für Landwirtschaft und Ernährung, Germany) through the ICRAD ERA-Net project FMDV\_PersistOmics, grant number 2821ERA28D.

## References

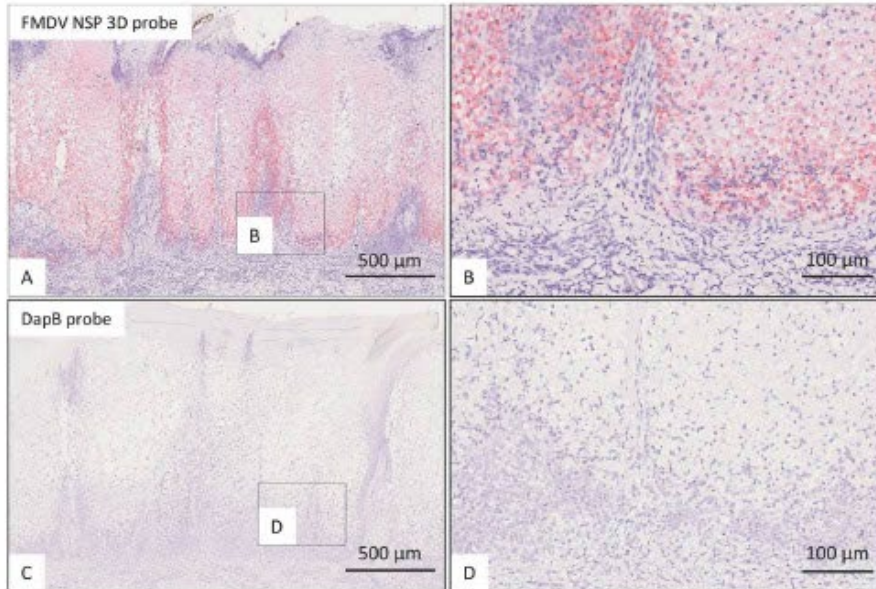
- [1] Grubman MJ, Baxt B. Foot-and-mouth disease. *Clin Microbiol Rev.* 2004;17:465–493. doi:10.1128/CMR.17.2.465-493.2004
- [2] Barnett PV, Geale DW, Clarke G, et al. A review of OIE country status recovery using vaccinate-to-live versus vaccinate-to-die foot-and-mouth disease response policies I: benefits of higher potency vaccines and associated NSP DIVA test systems in post-outbreak surveillance. *Transbound Emerg Dis.* 2015;62:367–387. doi:10.1111/tbed.12166
- [3] Thompson D, Muriel P, Russell D, et al. Economic costs of the foot and mouth disease outbreak in the United Kingdom in 2001. *Rev Sci Tech.* 2002;21:675–687. doi:10.20506/rst.21.3.1353
- [4] Stenfeldt C, Eschbaumer M, Rekant SI, et al. The foot-and-mouth disease carrier state divergence in cattle. *J Virol.* 2016;90:6344–6364. doi:10.1128/JVI.00388-16
- [5] Suttmoller P, McVicar JW, Cottral GE. The epizootiological importance of foot-and-mouth disease carriers. I. Experimentally produced foot-and-mouth disease carriers in susceptible and immune cattle. *Arch Gesamte Virusforsch.* 1968;23:227–235. doi:10.1007/BF01241895
- [6] Ilott MC, Salt JS, Gaskell RM, et al. Dexamethasone inhibits virus production and the secretory IgA response in oesophageal-pharyngeal fluid in cattle persistently infected with foot-and-mouth disease virus. *Epidemiol Infect.* 1997;118:181–187. doi:10.1017/S0950268896007376
- [7] Cox SJ, Joyce C, Parida S, et al. Protection against direct-contact challenge following emergency FMD vaccination of cattle and the effect on virus excretion from the oropharynx. *Vaccine.* 2005;23:1106–1113. doi:10.1016/j.vaccine.2004.08.034
- [8] Stenfeldt C, Arzt J. The carrier conundrum: a review of recent advances and persistent gaps regarding the carrier state of foot-and-mouth disease virus. *Pathogens.* 2020;9. doi:10.3390/pathogens9030167
- [9] Burrows R. Studies on the carrier state of cattle exposed to foot-and-mouth disease virus. *J Hyg (Lond.)* 1966;64:81–90. doi:10.1017/S0022172400040365
- [10] Pacheco JM, Smoliga GR, O'Donnell V, et al. Persistent foot-and-mouth disease virus infection in the nasopharynx of cattle: tissue-specific distribution and local cytokine expression. *PLoS One.* 2015;10:e0125698.

- [11] Arzt J, Belsham GJ, Lohse L, et al. Transmission of foot-and-mouth disease from persistently infected carrier cattle to naive cattle via transfer of oropharyngeal fluid. *mSphere*. 2018;3. doi:10.1128/mSphere.00365-18
- [12] Jolles A, Gorsich E, Gubbins S, et al. Endemic persistence of a highly contagious pathogen: foot-and-mouth disease in its wildlife host. *Science*. 2021;374:104–109. doi:10.1126/science.abd2475
- [13] Dawe PS, Sorensen K, Ferris NP, et al. Experimental transmission of foot-and-mouth disease virus from carrier African buffalo (*Syncerus caffer*) to cattle in Zimbabwe. *Vet Rec*. 1994;134:211–215. doi:10.1136/vr.134.9.211
- [14] Gao Y, Sun S-Q, Guo H-C. Biological function of foot-and-mouth disease virus non-structural proteins and non-coding elements. *Virology*. 2016;13. doi:10.1186/s12985-016-0561-z
- [15] Medina M, Domingo E, Brangwyn JK, et al. The two species of the foot-and-mouth disease virus leader protein, expressed individually, exhibit the same activities. *Virology*. 1993;194:355–359. doi:10.1006/viro.1993.1267
- [16] Belsham GJ. Influence of the Leader protein coding region of foot-and-mouth disease virus on virus replication. *J Gen Virol*. 2013;94:1486–1495. doi:10.1099/vir.0.052126-0
- [17] Strelbel K, Beck E. A second protease of foot-and-mouth disease virus. *J Virol*. 1986;58:893–899. doi:10.1128/jvi.58.3.893-899.1986
- [18] Devaney MA, Vakharia VN, Lloyd RE, et al. Leader protein of foot-and-mouth disease virus is required for cleavage of the p220 component of the cap-binding protein complex. *J Virol*. 1988;62:4407–4409. doi:10.1128/jvi.62.11.4407-4409.1988
- [19] Wang D, Fang L, Li P, et al. The leader proteinase of foot-and-mouth disease virus negatively regulates the type I interferon pathway by acting as a viral deubiquitinase. *J Virol*. 2011;85:3758–3766. doi:10.1128/JVI.02589-10
- [20] Wang D, Fang L, Luo R, et al. Foot-and-mouth disease virus leader proteinase inhibits dsRNA-induced type I interferon transcription by decreasing interferon regulatory factor 3/7 in protein levels. *Biochem Biophys Res Commun*. 2010;399:72–78. doi:10.1016/j.bbrc.2010.07.044
- [21] Arzt J, Pacheco JM, Smoliga GR, et al. Foot-and-mouth disease virus virulence in cattle is co-determined by viral replication dynamics and route of infection. *Virology*. 2014;452–453:12–22. doi:10.1016/j.virol.2014.01.001
- [22] Piccone ME, Rieder E, Mason PW, et al. The foot-and-mouth disease virus leader proteinase gene is not required for viral replication. *J Virol*. 1995;69:5376–5382. doi:10.1128/jvi.69.9.5376-5382.1995
- [23] Brown CC, Piccone ME, Mason PW, et al. Pathogenesis of wild-type and leaderless foot-and-mouth disease virus in cattle. *J Virol*. 1996;70:5638–5641. doi:10.1128/jvi.70.8.5638-5641.1996
- [24] Mason PW, Piccone ME, McKenna TS, et al. Evaluation of a live-attenuated foot-and-mouth disease virus as a vaccine candidate. *Virology*. 1997;227:96–102. doi:10.1006/viro.1996.8309
- [25] Uddowla S, Hollister J, Pacheco JM, et al. A safe foot-and-mouth disease vaccine platform with two negative markers for differentiating infected from vaccinated animals. *J Virol*. 2012;86:11675–11685. doi:10.1128/JVI.01254-12
- [26] Piccone ME, Pacheco JM, Pauszek SJ, et al. The region between the two polyprotein initiation codons of foot-and-mouth disease virus is critical for virulence in cattle. *Virology*. 2010;396:152–159. doi:10.1016/j.virol.2009.10.020
- [27] Zhang M, Hill JE, Alexander TW, et al. The nasal viromes of cattle on arrival at western Canadian feedlots and their relationship to development of bovine respiratory disease. *Transbound Emerg Dis*. 2021;68:2209–2218. doi:10.1111/tbed.13873
- [28] Simon-Lorieri E, Holmes EC. Why do RNA viruses recombine? *Nat Rev Microbiol*. 2011;9:617–626. doi:10.1038/nrmicro2614
- [29] Heath L, van der Walt E, Varsani A, et al. Recombination patterns in aphthoviruses mirror those found in other picornaviruses. *J Virol*. 2006;80:11827–11832. doi:10.1128/JVI.01100-06
- [30] Uddowla S, Pacheco JM, Larson C, et al. Characterization of a chimeric foot-and-mouth disease virus bearing a bovine rhinitis B virus leader proteinase. *Virology*. 2013;447:172–180. doi:10.1016/j.virol.2013.08.035
- [31] Forth LE, Höper D, Beer M, et al. High-resolution composition analysis of an inactivated polyvalent foot-and-mouth disease vaccine. *Pathogens*. 2020;9. doi:10.3390/pathogens9010063
- [32] Ellard FM, Drew J, Blakemore WE, et al. Evidence for the role of His-142 of protein 1C in the acid-induced disassembly of foot-and-mouth disease virus capsids. *J Gen Virol*. 1999;80(Pt 8):1911–1918. doi:10.1099/0022-1317-80-8-1911
- [33] Bond SR, Naus CC. RF-Cloning.org: an online tool for the design of restriction-free cloning projects. *Nucleic Acids Res*. 2012;40:W209–W213. doi:10.1093/nar/gks396
- [34] Dill V, Beer M, Hoffmann B. Simple, quick and cost-efficient: a universal RT-PCR and sequencing strategy for genomic characterisation of foot-and-mouth disease viruses. *J Virol Methods*. 2017;246:58–64. doi:10.1016/j.jviromet.2017.04.007
- [35] Buchholz UJ, Finke S, Conzelmann KK. Generation of bovine respiratory syncytial virus (BRSV) from cDNA: BRSV NS2 is not essential for virus replication in tissue culture, and the human RSV leader region acts as a functional BRSV genome promoter. *J Virol*. 1999;73:251–259. doi:10.1128/JVI.73.1.251-259.1999
- [36] Keil GM, Klopffleisch C, Giesow K, et al. Novel vectors for simultaneous high-level dual protein expression in vertebrate and insect cells by recombinant baculoviruses. *J Virol Methods*. 2009;160:132–137. doi:10.1016/j.jviromet.2009.05.001
- [37] Larocco M, Krug PW, Kramer E, et al. A continuous bovine kidney cell line constitutively expressing bovine  $\alpha\beta 6$  integrin has increased susceptibility to foot-and-mouth disease virus. *J Clin Microbiol*. 2013;51:1714–1720. doi:10.1128/JCM.03370-12
- [38] de Castro MP. Comportamento do vírus aftoso em cultura de células: susceptibilidade da linhagem de células suínas IB-RS-2. *Archiv Instit Biológ São Paulo*. 1964;31:63–78.
- [39] Brehm KE, Ferris NP, Lenk M, et al. Highly sensitive fetal goat tongue cell line for detection and isolation of foot-and-mouth disease virus. *J Clin Microbiol*. 2009;47:3156–3160. doi:10.1128/JCM.00510-09

- [40] Pacheco JM, Stenfeldt C, Rodriguez LL, et al. Infection dynamics of foot-and-mouth disease virus in cattle following intranasopharyngeal inoculation or contact exposure. *J Comp Pathol.* 2016;155:314–325. doi:10.1016/j.jcpa.2016.08.005
- [41] Hoffmann B, Depner K, Schirrmeier H, et al. A universal heterologous internal control system for duplex real-time RT-PCR assays used in a detection system for pestiviruses. *J Virol Methods.* 2006;136:200–209. doi:10.1016/j.jviromet.2006.05.020
- [42] Callahan JD, Brown F, Osorio FA, et al. Use of a portable real-time reverse transcriptase-polymerase chain reaction assay for rapid detection of foot-and-mouth disease virus. *J Am Vet Med Assoc.* 2002;220:1636–1642. doi:10.2460/javma.2002.220.1636
- [43] Xie Y-L, Lv D-H, Wen X-H, et al. Development of a real-time quantitative RT-PCR assay for detection of bovine rhinitis B virus. *Front Vet Sci.* 2021;8:680707. doi:10.3389/fvets.2021.680707
- [44] Suttmoller and Gaggero. (1965). FMD carriers\_Probang.
- [45] Suttmoller P, Cottral GE. Improved techniques for the detection of foot-and-mouth disease virus in carrier cattle. *Arch Gesamte Virusforsch.* 1967;21:170–177. doi:10.1007/BF01241441
- [46] Mayr KB A. The Chloroform resistance test in the isolation and characterization of enteroviruses. *Zentral Veter.* 1961;8:908–922.
- [47] Wilson EB. Probable inference, the law of succession, and statistical inference. *J Am Stat Assoc.* 1927;22:209–212. doi:10.1080/01621459.1927.10502953
- [48] Bonbon E, Funes GM, Hammami S, et al. WOAHP manual 2022: Chapter 3.1.8. Foot and Mouth Disease (Infection with Foot and Mouth Disease Virus) [cited 2024 Mar 22].
- [49] Hardham JM, Krug P, Pacheco JM, et al. Novel foot-and-mouth disease vaccine platform: formulations for safe and DIVA-compatible FMD vaccines with improved potency. *Front Vet Sci.* 2020;7:554305. doi:10.3389/fvets.2020.554305
- [50] Kraatz F, Wernike K, Hechinger S, et al. Deletion mutants of Schmallenberg virus are avirulent and protect from virus challenge. *J Virol.* 2015;89:1825–1837. doi:10.1128/JVI.02729-14
- [51] Holinka-Patterson LG, Fish IH, Bertram MR, et al. Genome of bovine viral diarrhoea virus (BVDV) contaminating a continuous LFBK- $\alpha$ V $\beta$ 6 cell line. *Microbiol Resour Announc.* 2022;11:e0116721. doi:10.1128/mra.01167-21
- [52] Schweizer M, Peterhans E. Noncytopathic bovine viral diarrhoea virus inhibits double-stranded RNA-induced apoptosis and interferon synthesis. *J Virol.* 2001;75:4692–4698. doi:10.1128/JVI.75.10.4692-4698.2001
- [53] Moonen P, Jacobs L, Crienen A, et al. Detection of carriers of foot-and-mouth disease virus among vaccinated cattle. *Vet Microbiol.* 2004;103:151–160. doi:10.1016/j.vetmic.2004.07.005
- [54] Stenfeldt C, Heegaard PMH, Stockmarr A, et al. Analysis of the acute phase responses of serum amyloid a, haptoglobin and type 1 interferon in cattle experimentally infected with foot-and-mouth disease virus serotype O. *Vet Res.* 2011;42(1):66. See <https://www.ncbi.nlm.nih.gov/pmc/articles/PMC3123197/>
- [55] Horsington J, Zhang Z. Consistent change in the B-C loop of VP2 observed in foot-and-mouth disease virus from persistently infected cattle: implications for association with persistence. *Virus Res.* 2007;125:114–118. doi:10.1016/j.virusres.2006.12.008
- [56] Malirat V, de Mello PA, Tiraboschi B, et al. Genetic variation of foot-and-mouth disease virus during persistent infection in cattle. *Virus Res.* 1994;34:31–48. doi:10.1016/0168-1702(94)90117-1
- [57] Juleff N, Windsor M, Reid E, et al. Foot-and-mouth disease virus persists in the light zone of germinal centres. *PLoS One.* 2008;3:e3434. doi:10.1371/journal.pone.0003434
- [58] Nickel R, Schummer A, Seiferle E. *Lehrbuch der Anatomie der Haustiere. Band III.: Kreislaufsystem, Haut und Hautorgane.* 4th edn. Berlin/Hamburg: Paul Parey Vlg; 1976.
- [59] Stenfeldt C, Hartwig EJ, Smoliga GR, et al. Contact challenge of cattle with foot-and-mouth disease virus validates the role of the nasopharyngeal epithelium as the site of primary and persistent infection. *mSphere.* 2018;3. doi:10.1128/mSphere.00493-18
- [60] Stenfeldt C, Eschbaumer M, Smoliga GR, et al. Clearance of a persistent picornavirus infection is associated with enhanced pro-apoptotic and cellular immune responses. *Sci Rep.* 2017;7:17800. doi:10.1038/s41598-017-18112-4
- [61] Murphy ML P, Forsyth MA, Belsham GJ, et al. Localization of foot-and-mouth disease virus RNA by in situ hybridization within bovine tissues. *Virus Res.* 1999;62:67–76. doi:10.1016/S0168-1702(99)00050-7
- [62] Alexandersen S, Zhang Z, Donaldson AI. Aspects of the persistence of foot-and-mouth disease virus in animals—the carrier problem. *Microbes Infect.* 2002;4:1099–1110. doi:10.1016/S1286-4579(02)01634-9
- [63] Zhang ZD, Kitching RP. The localization of persistent foot and mouth disease virus in the epithelial cells of the soft palate and pharynx. *J Comp Pathol.* 2001;124:89–94. doi:10.1053/jcpa.2000.0431
- [64] Kajitani N, Satsuka A, Kawate A, et al. Productive life-cycle of human papillomaviruses that depends upon squamous epithelial differentiation. *Front Microbiol.* 2012;3:152. doi:10.3389/fmicb.2012.00152

## Appendix

**Figure S1.** RNA *in situ* hybridization with the tongue of an acutely FMDV-infected heifer collected 2 dpi. (A–B) Treatment with the FMDV NSP 3D probe results in a high number of positive signals (=positive control), (B) shows a magnification of (A). (C–D) Incubation of a consecutive section of (A) with the negative control probe DapB shows no signal (=technical control), (D) shows a magnification of (C).



**Supplemental Table S1.** Numbers in the table represent log<sub>10</sub> FMDV viral genome copies per mg of tissue collected at necropsy either at 24 hpi or 36 dpi in the WT group. Underlined numbers indicate positive virus isolation. neg, negative RT qPCR; –, sample was not collected; DSP, dorsal soft palate; DNP, dorsal nasopharynx; VSP, ventral soft palate; PHT, pharyngeal tonsil; LYX, epithelium of the larynx; lung 1/4, proximal cranial lobe; lung 2/4, distal cranial lobe; lung 3/4, distal mid lobe; lung 4/4, distal caudal lobe; RPLN, medial retropharyngeal lymph node; SMLN, submandibular lymph node; HLN, hilar lymph node.

Euthanasia Animal	24 hpi				36 dpi				
	755	769	758 Carrier	773 Carrier	753	764	768	770	
DSP 1/5	neg	neg	<u>2.4</u>	3.2	neg	neg	neg	2.6	
DSP 2/5	<u>2.7</u>	neg	neg	neg	neg	neg	2.9	neg	
DSP 3/5	neg	neg	neg	2.0	neg	neg	2.9	neg	
DSP 4/5	<u>3.5</u>	neg	neg	neg	neg	neg	neg	2.5	
DSP 5/5	neg	neg	2.3	neg	neg	neg	neg	neg	
DNP 1/5	neg	1.9	neg	2.7	neg	neg	2.7	3.8	
DNP 2/5	neg	neg	neg	neg	neg	neg	2.8	3.7	
DNP 3/5	neg	neg	3.5	neg	neg	2.7	neg	neg	
DNP 4/5	neg	neg	3.9	neg	neg	neg	neg	neg	
DNP 5/5	neg	neg	<u>2.7</u>	neg	neg	neg	neg	neg	
VSP	neg	neg	neg	2.4	neg	neg	neg	neg	
PHT	4.7	neg	3.5	2.5	neg	neg	3.1	neg	
LYX	<u>1.7</u>	neg	<u>2.4</u>	2.4	2.4	neg	neg	neg	
Lung 1/4	neg	neg	–	–	–	–	–	–	
Lung 2/4	neg	neg	–	–	–	–	–	–	
Lung 3/4	6.1	neg	–	–	–	–	–	–	
Lung 4/4	1.9	neg	–	–	–	–	–	–	
RPLN	1.3	1.9	4.2	3.2	–	3.4	3.3	–	
SMLN	neg	neg	4.9	4.5	5.1	3.8	6.1	5.5	
HLN	neg	neg	–	–	–	–	–	–	

2. Publication II: Persistent foot-and-mouth disease virus infection in the bovine nasopharynx is associated with suppression of innate and cellular immunity

Publication II

**Persistent foot-and-mouth disease virus infection in the bovine nasopharynx is associated with suppression of innate and cellular immunity**

Benedikt Litz, Florian Pfaff, Leonie Forth, Sara Hägglund, Jean François Valarcher, Martin Beer, Michael Eschbaumer

Eingereicht bei  
PLOS ONE

1 **Persistent foot-and-mouth disease virus infection in the**  
2 **bovine nasopharynx is associated with suppression of innate**  
3 **and cellular immunity**

4 Benedikt Litz<sup>1</sup>, Florian Pfaff<sup>1</sup>, Leonie Forth<sup>1,#</sup>, Sara Hägglund<sup>2</sup>, Jean François Valarcher<sup>2</sup>, Martin  
5 Beer<sup>1</sup> and Michael Eschbaumer<sup>1,\*</sup>

6

7 **Affiliations**

8 1 Institute of Diagnostic Virology, Friedrich-Loeffler-Institut, 17493 Greifswald-Insel Riems, Germany.

9 2 Host Pathogen Interaction Group, Unit of Ruminant Medicine, Department of Clinical Sciences,  
10 Swedish University of Agricultural Sciences (SLU), 751 56 Uppsala, Sweden.

11 # current address: German Federal Institute for Risk Assessment, 10589 Berlin, Germany.

12

13 **Corresponding author**

14 Michael Eschbaumer

15 Friedrich-Loeffler-Institut

16 Südufer 10

17 17493 Greifswald - Insel Riems

18 Tel: +49 38351 7 1211

19 Michael.Eschbaumer@fli.de

20

21 **Keywords**

22 FMDV, Persistence, Transcriptomics, Proteomics, DSP, Pharynx, follicle-associated epithelium  
23 (FAE)

## 24 **Abstract**

25 Foot-and-mouth disease is a devastating disease of cattle that is caused by foot-and-mouth  
26 disease virus (FMDV). After acute infection, FMDV persists in the upper respiratory tract of  
27 about 50% of infected cattle. The persistent infection is characterized by very localized viral  
28 replication in the absence of clinical signs, but the underlying mechanisms are still not clear. In  
29 our study, we investigated tissue samples collected from 20 cattle which had been  
30 experimentally infected with FMDV O/FRA/1/2001. In 18 animals, the infection persisted for  
31 longer than 28 days. Epithelial tissue from the dorsal nasopharynx and the dorsal soft palate  
32 (DSP), the two main locations for persistent infection, was collected at necropsy. Five biological  
33 replicates from each animal and location were screened by FMDV specific RT-qPCR, and  
34 subsets of the samples were selected for transcriptome sequencing (n=52) and protein mass  
35 spectrometry (n=18). There was a good correlation between the expression patterns identified  
36 by the transcriptomic and proteomic analysis.

37 Higher loads of viral genome were detected in DSP samples. Overexpression of cellular  
38 markers for follicle-associated epithelium (FAE) and downregulated genes of epithelial integrity  
39 and keratinization correlated with viral genome loads, confirming the microanatomic  
40 localization of persistent FMDV infection in follicle-associated epithelium (FAE) in lymphoid  
41 tissue of the nasopharynx. An upregulation of genes which negatively influence T-cell  
42 responses indicates a T-cell exhaustion, most likely caused by prolonged immune stimulation.  
43 Moreover, decreased expression levels of RIG-I and TRAF6 probably resulted in inhibited  
44 detection of viral RNA by the innate immune system and ultimately an impeded type I interferon  
45 response. These observations are in line with the hypothesis that FMDV actively suppresses  
46 the local immunity in FAE to maintain a persistent infection in the bovine nasopharynx.

## 47 Introduction

48 Foot-and-mouth disease virus (FMDV; species *Aphthovirus vesiculæ*, genus *Aphthovirus*,  
49 family *Picornaviridae*) infects mammals of the order *Artiodactyla* and causes severe outbreaks  
50 of vesicular disease in agriculturally important species such as cattle and pigs. Persistent FMDV  
51 infection follows the acute infection in roughly 50% of infected cattle. In contrast to fulminant  
52 foot-and-mouth disease (FMD) in the acute phase, no clinical signs are observed during  
53 persistent infection and onward transmission from persistently infected cattle is unlikely [1]. On  
54 the other hand, in persistently infected African buffalo (*Syncerus caffer*), which are the natural  
55 host of FMDV, transmission is common and probably contributes to maintain endemicity in  
56 buffalo populations in the wild [2]. To detect persistently infected animals, so-called “carriers”,  
57 oropharyngeal fluid (OPF) is collected using a probang cup. Probang sampling collects  
58 epithelial scrapings from the caudal nasopharynx, since persistent FMDV infection is restricted  
59 to epithelial surfaces in this otherwise inaccessible location [3].

60 The epithelial tissues of the dorsal nasopharynx (DNP) and the dorsal soft palate (DSP) have  
61 been identified as the main sites of persistent infection in cattle [4]. By using  
62 immunofluorescence and laser-capture microdissection (LCM), its microanatomical location  
63 was determined to be the follicle-associated epithelium (FAE) in this region [5]. The FAE is a  
64 specialized epithelial structure overlying the mucosa-associated lymphatic tissue (MALT),  
65 which is important for the induction of mucosal immunity. Sampling of antigens from the lumen  
66 and their transport to the subepithelial MALT is carried out by microfold cells (M-cells) [6].  
67 These cells are found in similar epithelia overlying lymphoid follicles throughout the body, such  
68 as in the Peyer’s patches or the bronchial associated lymphoid tissue (BALT) [7]. Histologically,  
69 the FAE of the MALT in the nasopharynx of cattle differs from the surrounding epithelium by  
70 an incomplete base membrane and disorganized cuboidal epithelial cells interspersed with  
71 mixed mononuclear cells. Overall, FAE appears rarefied and disorganized [8].

72 The FAE has been the subject of a previous study to analyze the gene expression in specific  
73 epithelia of the nasopharynx using LCM, which found an inhibition of T-cell mediated immunity  
74 [5]. In other studies, a bovine whole-transcriptome microarray was used for the analysis of gene  
75 expression using tissue samples collected from persistently infected animals [9–11]. RNA  
76 sequencing (RNA-seq) as a method for comprehensive unbiased transcriptomic analysis has  
77 been applied to persistently infected cell lines from non-bovine species [12], to primary cultures  
78 of bovine tissue other than pharyngeal epithelium [12,13] and in an air–liquid interphase cell  
79 culture model prepared from bovine epithelial tissue from the DSP [14]. In this study, we used  
80 RNA-seq and mass spectrometry for the first time to investigate tissue samples collected from

81 the DNP and the DSP of 18 persistently FMDV-infected cattle. The transcriptomic and  
82 proteomic analysis from the same samples showed high congruency between gene expression  
83 and protein abundance, mutually corroborating the results of each method.

84 The findings improve our understanding of the virus-host dynamics occurring during persistent  
85 infection and how the virus may be able to suppress innate immunity to maintain active  
86 replication in the epithelia of the nasopharynx despite a strong systemic immune response.

## 87 **Material and methods**

### 88 **Animal trial**

89 A vaccination trial was carried out under BSL4vet conditions at the Friedrich-Loeffler-Institut  
90 on the Isle of Riems. Twenty Holstein-Frisian heifers (6-12 months) were split into four groups:  
91 six animals were vaccinated twice intramuscularly (i.m.) at an interval of three weeks with a  
92 commercially available FMDV O<sub>1</sub> Manisa vaccine, six animals were vaccinated three times  
93 intranasally with an experimental vector vaccine 21 and 52 days after the first vaccination, four  
94 animals were vaccinated three times i.m. with the same vector vaccine and one control group  
95 of four animals was injected i.m. with sterile PBS. The animals were challenged by  
96 intranasopharyngeal instillation [15] two weeks after the third vaccination (seven weeks after  
97 the second) with a twice plaque-purified isolate of FMDV O/FRA/1/2001 which had been  
98 passaged once in cattle after intraepidermolingual inoculation. The full genome sequence of  
99 the challenge virus is available in GenBank (accession no. OV121130.1). Clinical examination  
100 under xylazine sedation (0.3 mg/kg estimated body weight i.m.; reversed with 0.05 mg/kg  
101 atipamezole) was performed every day from 2 to 8 days post-challenge (dpc). The animals  
102 were euthanized in groups of four per day beginning on 35 dpc. The protocol of the animal trial  
103 was approved by the State Office for Agriculture, Food and Fisheries of Mecklenburg-  
104 Vorpommern (LALLF M-V) under the file no. 7221.3-1-019/18.

### 105 **Sample collection**

106 Serum and nasal fluid were collected every day from 0-8 dpc and on 10, 14, 17, 21, 24, 28, 31,  
107 and 35 dpc. Probang samples were collected on 0, 14, 17, 21, 24, 28, and 35 dpc. Tissue  
108 samples from the nasopharyngeal region were collected at necropsy. To reflect the focal  
109 distribution of persistent FMDV infection in this region, five biological replicates were collected  
110 from each DNP and DSP epithelium. To avoid any degeneration of mRNA, these samples were  
111 immediately frozen in liquid nitrogen and stored at -80°C.

112 **Probang virus isolation**

113 Sampling of OPF using a probang cup was performed to determine if animals were persistently  
114 infected with FMDV. The collected OPF was mixed with 4 ml of cell culture medium and  
115 homogenized by repeated aspiration using a 1.6 mm blunt cannula. Then, half of the sample  
116 was mixed with an equal amount of 1,1,2-trichloro-1,2,2-trifluoroethane (TTE) [3] to dissociate  
117 any bound antibody. Following vigorous shaking for 5 minutes and subsequent centrifugation  
118 at 1000 × g for 10 minutes at 4°C, the supernatant was removed and aliquoted. A 25 cm<sup>2</sup> culture  
119 flask of 90% confluent LFBK- $\alpha$ V $\beta$ 6 cells (porcine kidney cells expressing bovine  $\alpha$ V $\beta$ 6 integrin  
120 monolayer, CCLV-RIE 1419) [16] was then inoculated with 250  $\mu$ l of the TTE-treated OPF  
121 solution. The remainder was stored at -80°C.

122 **RNA extraction**

123 Disintegration of the samples was performed with a CP02 cryoPREP (Covaris). The pulverized  
124 tissue was mixed with 250  $\mu$ l AL buffer (Qiagen) and 750  $\mu$ l TRIzol LS (Invitrogen). After removal  
125 from biocontainment, the samples were mixed with 200  $\mu$ l trichloromethane and separated by  
126 centrifugation. Approximately 400  $\mu$ l of the upper aqueous phase containing the RNA were  
127 removed and total RNA was extracted using the Agencourt RNAdvance Tissue Kit (Beckman  
128 Coulter) with a KingFisher Flex magnetic particle processor (Thermo Fisher Scientific). The  
129 quantity and quality of extracted total RNA were measured using a NanoDrop 1000  
130 spectrophotometer (Thermo Fisher Scientific).

131 **FMDV genome detection**

132 FMDV RNA was detected with an RT-qPCR using AgPath-ID One-Step RT-PCR Reagents  
133 (Thermo Fisher Scientific) and a primer/probe set targeting the highly conserved 3D coding  
134 region [16].

135 **Library preparation and sequencing**

136 For transcriptomic analysis, 52 samples were selected for sequencing. These included 25 DNP  
137 and 23 DSP samples from 14 persistently infected animals and from two animals which cleared  
138 the infection before 21 dpc (Table S1). From the extracted total RNA, mRNA was isolated using  
139 the Dynabeads mRNA DIRECT Micro Purification Kit (Invitrogen) and the Colibri Stranded RNA  
140 Library Prep Kit for Illumina (Invitrogen) was used for library preparation. ERCC internal control  
141 (Invitrogen) was used before mRNA extraction as recommended by the manufacturer. In detail,  
142 isolated mRNA was fragmented by RNase III to an approximate length of 150 nucleotides.

143 Adapters were hybridized and then ligated to the fragmented RNA. Adapter-ligated RNA was  
144 transcribed into cDNA using 10× SuperScript IV Enzyme Mix and purified. Finally, cDNA was  
145 amplified in 12 or 13 cycles (depending on the input) using appropriate index primers for the  
146 generation of barcoded Illumina libraries. Length and quality of the libraries was assessed on  
147 an Agilent 4150 TapeStation (Agilent Technologies). The libraries were quantified using a Qubit  
148 2.0 (Invitrogen) and the Qubit dsDNA HS Assay Kit (Invitrogen) and pooled at an equimolar  
149 ratio. For sequencing, a NovaSeq machine (Illumina) running in 100 bp single-end mode was  
150 used.

### 151 **Mass spectrometry**

152 For proteomics analysis, 18 samples, which had also been used for RNAseq, were sent to  
153 Proteome Sciences (Frankfurt, Germany). Protein was extracted from the organic TRIzol  
154 phase, tryptic peptides were produced, labelled with 18 isobaric TMTpro reagents (Thermo  
155 Fisher Scientific) and combined to generate one TMTpro 18-plex sample. The 18-plex was  
156 fractionated into 24 fractions using basic reversed-phase chromatography. All fractions were  
157 analyzed by tandem mass spectrometry using a data-dependent acquisition method combined  
158 with an inclusion list for peptides expected to derive from FMDV. Peptide quantification was  
159 based on TMTpro reporter ion intensities, and a proprietary statistical pipeline was used to  
160 determine regulated peptides and proteins.

### 161 **Statistical analysis of gene expression data**

162 Raw reads were initially trimmed by removing low quality regions and adapter contamination  
163 using TrimGalore (v0.6.6) together with cutadapt (v1.18) running in automated adapter  
164 detection mode. A genome and transcriptome reference for cattle was received from NCBI  
165 (ARS-UCD1.2; GCA\_002263795.2) and combined with reference sequences for ERCC internal  
166 controls and the FMDV O/FRA/1/2001 inoculum sequence. The RNA transcriptome and DNA  
167 genome references were concatenated into a single file and a decoy-aware index was created  
168 using the “index” function of Salmon (v1.9.0). The index was then used to quantify the  
169 transcript abundancies within each sample using the “quant” function of Salmon. Corrections  
170 for sequence-specific bias, fragment-level GC bias and position-specific fragment bias were  
171 activated and 10 bootstraps were applied in order to compute abundance estimates. The  
172 resulting transcript abundancies were further analyzed using R (v4.2.1) and imported into a  
173 DESeq2 (v1.40.2) compatible format using the package tximport (v1.28.0). The transcripts in  
174 the dataset were filtered based on their abundance, so that only transcripts that scored a  
175 relative abundance of at least 10 transcripts per million (TPM) observed within at least 2

176 independent samples were further analyzed. Before principal component analysis (PCA), the  
177 filtered abundance data was transformed using the “rlog” function from the DESeq2 package  
178 that applies a regularized log transformation. PCA was done using the “prcomp” function from  
179 the stats package based on the transformed abundancies of 1000 transcripts that showed the  
180 highest variance within the dataset.

181 In order to find differentially expressed genes (DEG), we applied the main “DESeq” function  
182 from DESeq2 package using different designs in order to reflect the underlying contrast. The  
183 resulting log<sub>2</sub> fold changes (log<sub>2</sub>FC) were further adjusted using the function “lfcShrink”  
184 function from the DESeq2 package. The final dataset was filtered using a cutoff *p-value* of <0.05  
185 and a cutoff log<sub>2</sub>FC of >|1|.

### 186 **Pathway analysis**

187 DE gene sets were analyzed for their biological function using the “enrichPathway” function in  
188 the reactomePA package (version 1.46.0) [17]. An overview of enriched pathways was  
189 conducted using the g:Profiler webservice (<https://biit.cs.ut.ee/gprofiler/gost>) [18]. Predicted  
190 networks and Canonical Pathways were generated using Quiagen Ingenuity Pathway Analysis  
191 (IPA) software (version 90348151, 2023 QIAGEN) [19].

192

### 193 **Statistics**

194 The binomial proportion confidence interval for the incidence of persistent infection was  
195 calculated by the Wilson method using R (<https://www.r-project.org/>) [20].

## 196 **Results and discussion**

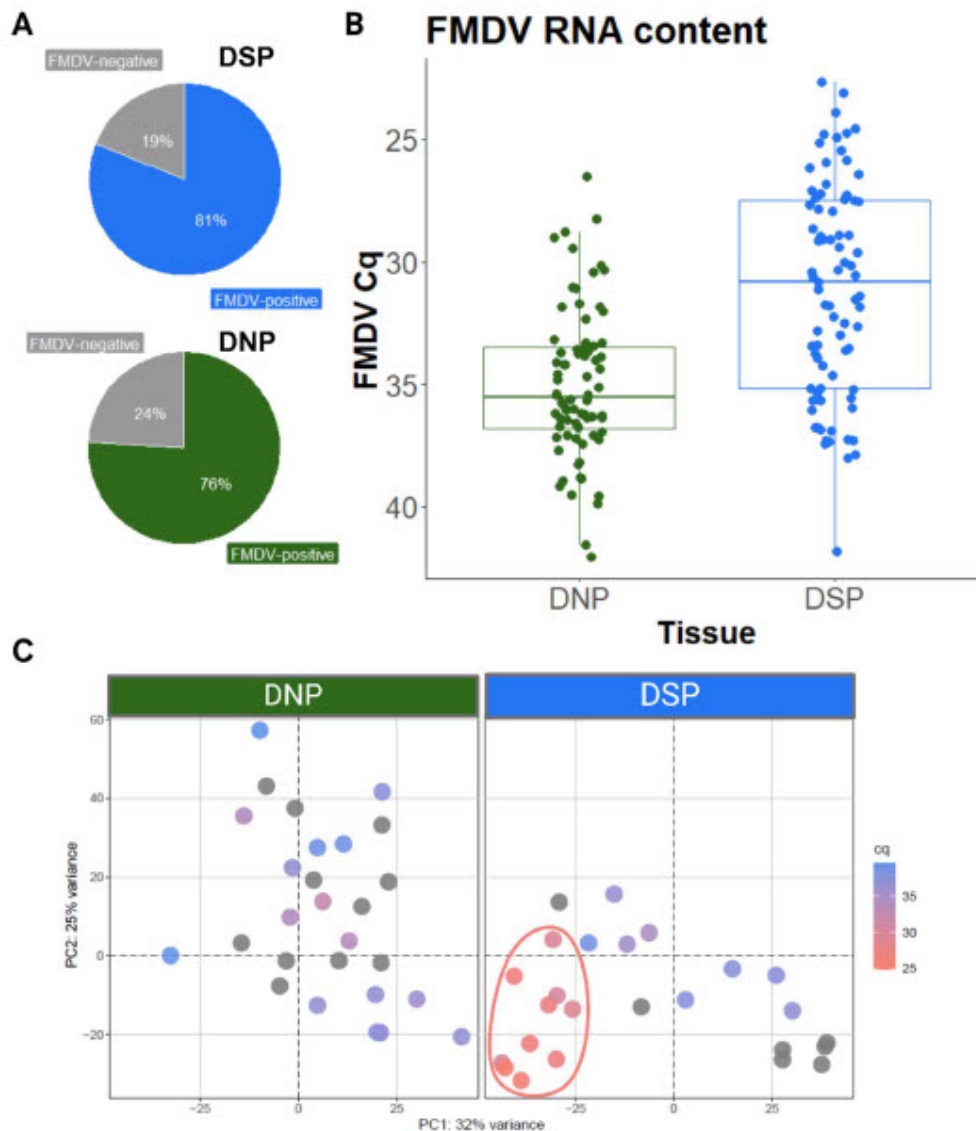
### 197 **Clinical protection and incidence of persistent infection**

198 Animals vaccinated with the experimental vaccine were not protected from challenge and  
199 developed clinical FMD with vesicular lesions similar to those observed in non-vaccinated  
200 animals, while commercially vaccinated cattle did not show any clinical signs. However, the  
201 efficacy of the vaccines and the outcome of the challenge infection is outside of the scope of  
202 the study reported here.

203 Virus isolation from OPF samples was performed to determine the incidence of persistent  
204 infection. Carriers are defined as cattle from which virus can be recovered later than the 28<sup>th</sup>  
205 day of infection [21]. The incidence of persistent FMDV infection was 85% (64–95%), with two  
206 animals (ear tags 506 and 508) positive in the virus isolation on day 28 but not on day 35. OPF  
207 from two animals (426 and 662) remained negative throughout the entire trial.

### 208 **FMDV tissue distribution and overall gene expression**

209 The entire sample set consisted of 200 tissue samples collected from 20 animals, of which 17  
210 were persistently infected at the time of euthanasia. In this sample set, 100 samples were from  
211 the DSP and 100 from the DNP. Among DSP samples, a higher proportion was positive in the  
212 RT-qPCR for FMDV compared to DNP samples (**Figure 1A**). DSP samples also contained  
213 higher loads of FMDV genome than DNP (**Figure 1B**). The median quantification cycle (Cq)  
214 value was 30.8 for positive DSP samples and 35.5 for positive DNP samples. The vaccination  
215 status of the animals had no influence on the quantity of detectable FMDV RNA (data not  
216 shown). Additionally, in a principal component analysis (PCA) that was based on normalized  
217 gene expression data from 27 DNP and 25 DSP tissue samples, a cluster of highly positive  
218 DSP samples (Cq < 30) is visible (**Figure 1C**). In the DNP, on the other hand, no clustering by  
219 Cq value was observed, as these samples contained overall lower viral genome loads than DSP  
220 samples (**Figure 1B, C**). This implies a tissue preference of persistent infection and suggests  
221 that the presence of a high viral genome load modulates host gene expression. In contrast to  
222 the FMDV RNA content of the tissue samples, the vaccination status was not reflected in the  
223 clustering of samples in the PCA (data not shown).



224

225 **Figure 1.** (A) Ratio of FMDV RT-qPCR positive samples for DSP (blue) and DNP (green)  
 226 samples. (n=200) (B) Boxplot showing FMDV-specific RT-qPCR Cq values as correlate for viral load  
 227 in DSP and DNP samples (C) Principal component analysis of gene expression in DNP  
 228 and DSP based on the normalized transcript abundancies of the 1000 transcripts with the  
 229 highest variance within the dataset. FMDV-specific RT-qPCR Cq values are indicated by color.  
 230 A cluster of highly positive DSP samples is highlighted by a red circle. (n=52)

### 231 Overall differential gene expression

232 From the set of tissue samples, 27 DNP and 25 DSP samples were selected for transcriptomic  
 233 analysis using RNA-seq (Table S1). The samples were grouped based on their Cq value in the  
 234 FMDV-specific RT-qPCR and categorized in three groups: highly positive ( $Cq \leq 30$ ), weakly  
 235 positive ( $30 < Cq < 45$ ) and negative (no Cq). As there were only two animals in the trial that were

236 clearly not persistently infected, we were not able to base our comparison on the carrier state  
237 of the animals themselves and had to classify the individual tissue samples instead.

238 Differential gene expression was performed for three contrasts: (1) samples from DSP  
239 compared to samples from DNP: "DSP vs. DNP"; (2) all highly FMDV-positive samples ( $Cq \leq 30$ )  
240 compared to all FMDV-negative (no Cq) samples: "FMDVpos vs. FMDVneg"; (3) highly FMDV-  
241 positive samples ( $Cq \leq 30$ ) from DSP compared to FMDV-negative (no Cq) samples from DSP:  
242 "DSP+FMDVpos vs. DSP+FMDVneg". For further analysis, we focussed on the third contrast,  
243 which resulted in 417 DEGs (**Table 1**).

244 A pathway analysis of these DEGs showed that many of the upregulated genes are related to  
245 immune responses, while many of the downregulated genes are associated with epithelial  
246 differentiation and keratinization. A selection of the most significant differentially expressed  
247 canonical pathways is depicted in **Supplemental Figure S1**. The top up- and downregulated  
248 genes can be found in **Table 2**. In the following chapters, the DEGs from DSP+FMDVpos vs.  
249 DSP+FMDVneg were further analysed in detail. Therefore, we compared only DSP tissues  
250 grouped by their FMDV RNA content, but all samples derive from experimentally infected  
251 animals and the carrier status of the animals themselves was not taken into account.

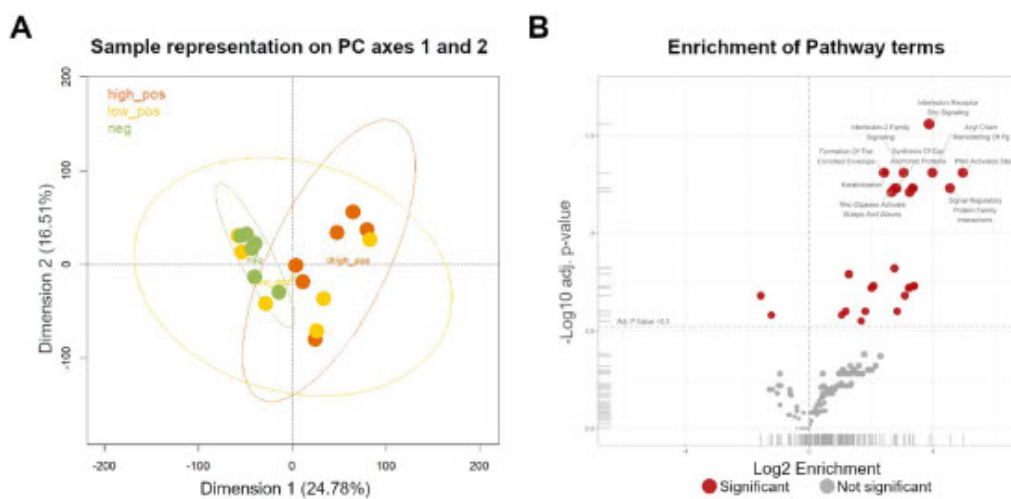
## 252 **Differential protein expression and overlap with transcriptomic analysis**

253 The 18 samples selected for proteomic analysis corresponded to the DSP tissues used for  
254 RNA-seq. After the application of the TMTpro MS2 workflow, 79,888 peptides and 8,937 protein  
255 groups were quantified and assigned to the *Bos taurus* genome. No proteins of FMDV were  
256 identified. Principal component analysis (PCA) of the 18 samples showed a clear separation of  
257 highly positive and negative samples along the 1<sup>st</sup> dimension, accounting for 24.8% of the  
258 variance, while weakly positive samples were scattered between those two groups (**Figure**  
259 **2A**). For samples 180 and 129, the rather low Cq values between 30 and 31 (barely above the  
260 cut-off for a classification as highly positive) may explain their clustering with the strongly  
261 positive samples.

262 Pronounced differences in protein abundance were observed between highly FMDV-positive  
263 ( $Cq \leq 30$ ) and FMDV-negative samples, as it has been also observed in the PCA of the  
264 transcriptomic data of the DSP samples. The following analysis will focus mainly on this  
265 contrast. The thresholds for this contrast were set at a p-value of 0.0001 and a log<sub>2</sub>FC of  $\pm 0.58$ .  
266 In this group, 562 proteins were significantly regulated, of which 322 were downregulated and  
267 240 upregulated. **Table 3** shows the 10 most upregulated and downregulated proteins.

268 A functional analysis indicated the enrichment of pathways associated with interleukin  
 269 signaling, lipid metabolism, and keratinization, as well as Gene Ontology Biological Process  
 270 (GOBP) terms associated with proteolysis, immune response and de-ubiquitylation (**Figure**  
 271 **2B**).

272 Overall, we detected 102 proteins to be significantly regulated in the proteomics analysis,  
 273 which were already differentially expressed in the transcriptomics analysis. Among them, 101  
 274 showed concurring regulation, only one gene, PGLYRP2, was divergently regulated between  
 275 the proteomic and transcriptomic analysis. For 7 of the 20 highest up- or downregulated  
 276 proteins identified in the proteomic analysis, the corresponding gene was found to be regulated  
 277 in the same way by RNA-seq: SBSN, KLK12, FAM25A, A2ML1, LIMD2, SCIMP, and GRAP.



278 **Figure 2.** (A) Principal component analysis (PCA) performed with data from the proteomic  
 279 analysis of DSP samples. Samples are grouped according to their FMDV Cq value: highly  
 280 positive ( $Cq \leq 30$ ) in orange, weakly positive ( $45 > Cq > 30$ ) in yellow and negative (no Cq) in  
 281 green; circle indicates individual sample, square indicates average of positive, weakly positive  
 282 and negative samples. (B) Analysis of enriched Gene Ontology Biological Process (GOBP)  
 283 terms from the proteomic analysis of DSP samples.  
 284

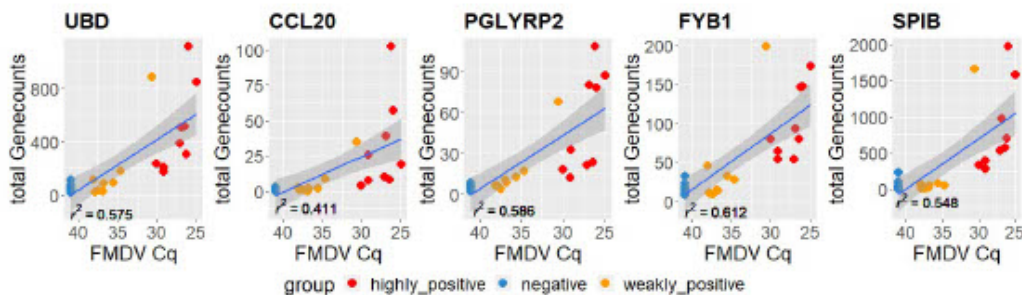
285 **High viral load of persistent FMDV is associated to FAE markers**

286 The FAE has a different cellular phenotype in comparison to surrounding epithelia and can be  
 287 observed microscopically. Gene expression of the specialized FAE tissue has been  
 288 characterized well in Peyer's patches in the intestinal tract [22,23]. Some of the previously  
 289 reported FAE-specific marker genes were significantly upregulated in the highly FMDV-positive  
 290 DSP samples from this study (UB-D, CCL20, PGLYRP2, FYB1 and, not significantly, SpiB; see  
 291 **Figure 3**) [22–24]. This could be interpreted as colocalization of FMDV genome and tissue with

292 high FAE content. This is in accordance with previous immunofluorescence studies that  
293 localized the persistent FMDV infection in the FAE of the bovine nasopharynx, especially in the  
294 region of the caudal DSP.

295 Furthermore, the epithelium overlying the follicular dome has been described as “rarefied and  
296 disorganized” [8]. This could be reflected in our samples by strongly downregulated genes  
297 coding for structural constituents of the cornified epidermis (e.g., LORICRIN, SERPINB12,  
298 KRT1, KRT10, KLK7, KLK6) and components of the extracellular space (e.g., ARG1,  
299 SERPINB12, AHSG, KRTDAP, KLK7, A2ML1, LOC519132, IL36A, IL36G), some of which were  
300 among the 10 most strongly downregulated genes overall as shown in Table 2. This is reflected  
301 by the strong downregulation on the protein level of SBSN, which is involved in keratinization  
302 [25], and A2ML1, a component of the extracellular matrix. Since FAE is not a keratinized  
303 stratified squamous epithelium like most pharyngeal epithelia, its keratinocytes are not highly  
304 differentiated and the epithelial integrity is compromised to allow mononuclear cells to infiltrate  
305 into the epithelium to target invading pathogens. This results in a gene expression pattern like  
306 it was observed in this and previous studies [26].

307 In contrast to analyses with tissues prepared by LCM [5], using whole pieces of tissue provides  
308 a larger amount of higher-quality RNA, but does not allow any control over how much of the  
309 sample is FAE rather than normal nasopharyngeal epithelium. Using the level of detectable  
310 FMDV RNA to group these samples for further analysis will then lead to comparisons of non-  
311 infected normal nasopharyngeal epithelium with FMDV-infected FAE. The differential expres-  
312 sion of genes coding for elements of keratinization or structural components of the extracellu-  
313 lar matrix observed in this and previous studies [26] is likely due to this difference in sample  
314 composition.



315  
316 **Figure 3.** Gene expression of marker genes for the FAE (UB-D, CCL20, PGLYRP2, FYB1 and  
317 SpiB) in DSP samples. Samples are grouped by their FMDV Cq value into highly positive  
318 (Cq≤30), weakly positive (45>Cq>30) and negative (no Cq).

### 319 **Sites of FMDV persistence show impaired desquamation**

320 Desquamation of superficial cells is typical of epithelia and has also been documented in  
321 lymphatic epithelia covering the tonsils [27]. To allow the shedding of cells,  
322 corneodesmosomes are cleaved by a set of different kallikreins [28]. In our FMDV-positive  
323 samples, genes coding for components of the corneodesmosome (e.g., CDSN, DSG1, DSC2,  
324 DSC3) but also several kallikreins (e.g., KLK 6, 7, 8, 12, 14) were significantly downregulated.  
325 Especially the kallikreins 6, 7 and 12 are usually highly expressed in healthy lymphatic tissue  
326 of tonsils [29]. On the protein level, kallikrein-related peptidases (KLK 7, 10, 11, 12, 13, 14)  
327 were among the proteins with the most pronounced change in abundance as well. As additional  
328 evidence of impaired desquamation, several inhibitors that usually control kallikreins, such as  
329 serpins (SERPINB10, SERPINB12) [30],  $\alpha$ 2 macroglobulins (A2ML1) [31], Kazal-type inhibitors  
330 (SPINK5, SPINK7) [32] and AHSG [33] were also downregulated in the FMDV-positive samples.  
331 The downregulation of genes coding for components of tight junctions such as occludin  
332 (OCLN), claudin-1 (CLDN1) and the tight junction protein 1 (TJP1/ZO-1) in FMDV-positive DSP  
333 samples was not statistically significant, but a clear trend in the expression of these proteins  
334 was visible as shown in **Figure 4A**. An absence of tight junctions can enhance paracellular viral  
335 spread in the epithelium and increase the receptor availability for FMDV [26].

### 336 **Apoptosis**

337 A programmed cell death can be triggered in order to eliminate dysfunctional cells or limit viral  
338 replication [34]. In the pathway analysis, 28 genes related to apoptosis were upregulated in  
339 persistently FMDV-infected DSP, but careful consideration of their individual functions shows  
340 a more ambiguous picture. Some of these genes are associated with positive regulation of  
341 apoptosis such as the highly upregulated genes ELL3 [35], MMP9 [36] and IKZF3 [37].  
342 However, ELL3, which is the most strongly upregulated gene (see **Table 2**), has divergent  
343 functions. Its overexpression can promote apoptosis, but ELL3 has also been demonstrated to  
344 degrade p53 and inhibit apoptosis in mouse embryonic stem cells [38]. In our study, the  
345 important regulator of apoptosis p53, however, was not significantly upregulated, neither on  
346 the gene nor on the protein level, on which the degradation by ELL3 occurs. Another important  
347 inhibitor of p53 is BCL2 [39]. The related protein BCL2A1 was highly expressed in FMDV-  
348 infected tissue in our study (log<sub>2</sub>FC 4.9 and p-value 3.7E-07). Viral orthologues of BCL2 were  
349 discovered in several DNA viruses such as African swine fever virus or lumpy skin disease  
350 virus, preventing premature cell death [40]. Together with NAIP, which was significantly  
351 upregulated and belongs to the cellular inhibitor of apoptosis (CIAP) [41], BCL2A1 exerts a  
352 strong influence on the downstream apoptosis signaling, predicted to suppress several

353 mechanisms leading ultimately to cell death as it is depicted in the IPA of apoptosis signaling  
354 in **Supplemental Figure S2**. In addition to this important regulator of programmed cell death,  
355 a few genes associated with anti-apoptotic features were upregulated in FMDV-infected  
356 tissues, including IL-10 [42] and LRRK2 [43]. A tissue-specific aspect of apoptosis is the  
357 aforementioned insignificant upregulation of SpiB, which is necessary for the differentiation of  
358 M-cells and expressed in the FAE of MALT [23], but SpiB also inhibits detachment-induced  
359 apoptosis [44].

## 360 **Adaptive Immunity**

### 361 **B-cell response**

362 The humoral response initiated by B-cells is an adaptive immune response in animals. In the  
363 blood, the primary response with an early onset of IgM followed by IgG is important for the  
364 clearance of viremia. In carrier animals, a prolonged IgA response in saliva can be observed  
365 [45]. In this study, the upregulation of BCL7A, which is restricted to B cells of tonsils and lymph  
366 nodes [46], suggests the presence of B cells and supports the findings from above, that the  
367 infected tissue is the FAE overlying the lymph follicles. Several genes of the B-cell activation  
368 pathway were significantly upregulated in FMDV-infected samples (IL10, CTLA4, CD22,  
369 SH3KBP1, POU2F2, BANK1). Of these, the IL10 gene showed the highest differential  
370 expression ( $\log_2FC$  5.56,  $p = 5.3E-04$ ). In humans, there is a subset of B cells expressing IL10  
371 and exerting regulatory functions on T cells, which is further supported by the observed  
372 upregulation of CD38, a characteristic antigen for this B cell subset [47]. Vice versa, CTLA4,  
373 which is expressed by T regulatory cells ( $T_{reg}$  cells), inhibits B cell responses and decreases  
374 antibody levels [48], which seems contradictory to the higher antibody levels found in carriers.  
375 Furthermore, CD22, which was also upregulated, is mainly restricted to B cells and negatively  
376 regulates B-cell receptor signaling [49], but at the same time it is an adhesion molecule, which  
377 can regulate homing of antibody-producing B cells. The ligand for CD22, St6Gal1, is selectively  
378 expressed in the Peyer patches [50], which are a lymphatic epithelium like FAE, and where B  
379 cells can produce secretory IgA [51]. This further supports the localization of infected tissue in  
380 the FAE, where elevated levels of IgA are produced during persistent infection, even though  
381 we have also observed strong inhibitory signals, which may be due to the prolonged antigen  
382 presence.

### 383 **T-cell response**

384 The cellular immune response by CD3+ and CD8+ T cells has been suggested to be a driving  
385 force for the clearance of persistent FMDV infection in the FAE [52]. The presence of T cells in  
386 FMDV-positive samples is indicated by the upregulated T-cell antigens CD4, CD83, CD84 and

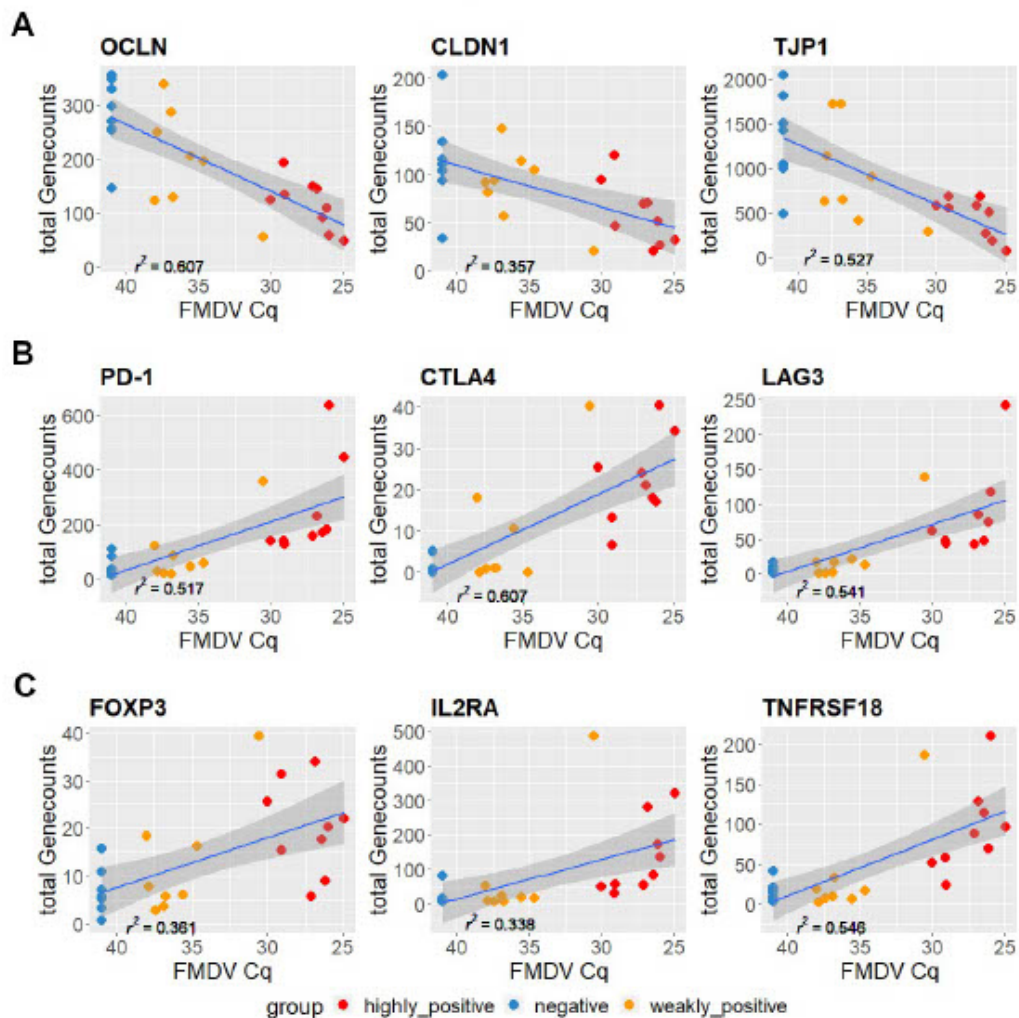
387 CD86. From the 20 most upregulated genes of the T-cell activation pathway, 12 genes are  
388 associated with negatively regulating T-cell responses (NLRC3, CTLA4, CCL19, CCR7, IKZF3,  
389 RHOH, EGR3, LAG3, BOLA-DOB, TOX, BATF, SIT1). The individual functions of several of  
390 these genes are listed in **Table 4**, among them NLRC3, IKZF3, RIPOR2 and GRAP, which were  
391 also upregulated on the protein level.

392 The most upregulated genes that promote T-cell activation, such as CCL19, CCR7 and ITGAL,  
393 are important for chemotaxis. However, CCL19 and its specific receptor CCR7 can play an  
394 ambiguous role by mediating the homing of lymphocytes but also by inducing immune  
395 tolerance and the recruitment of T<sub>reg</sub> cells [53], while ITGAL facilitates adhesion of T cells to  
396 intercellular adhesion molecule-1 and -2 (ICAM-1,-2) on endothelia or other T cells [54]. But  
397 this effect on chemotaxis and cell adhesion can be antagonized by an upregulation of RHOH  
398 [55], which was also observed in our samples.

399 PD-1, CTLA4 and LAG-3 are important immune checkpoints for regulating T-cell proliferation  
400 and their upregulation can occur during chronic viral infections which result in a dysfunctional  
401 population of T cells, so-called exhausted T cells. The presence of exhausted T cells in infected  
402 tissue is indicated by the upregulation of CD83 and CCR7CT [56]. This T-cell exhaustion allows  
403 viruses such as HIV-1 and HCV to persist and is facilitated by inhibitory receptors including  
404 PD-1, CTLA4 and LAG-3 [57,58], from which CTLA4 and LAG-3 were significantly and PD-1  
405 not significantly upregulated in FMDV-positive DSP samples (**Figure 4B**). IL411, which was  
406 upregulated on the protein level, can induce the expression of PD-L1, a PD-1 ligand [59]. BATF,  
407 whose expression is directly upregulated by PD-1 and inhibits T-cell proliferation [60], was  
408 upregulated as well (see **Table 4**). T-cell exhaustion is also associated with an overexpression  
409 of MAP4K1 [61] and the immunosuppressive interleukin IL-10, which were both highly  
410 upregulated with log<sub>2</sub>FC of >4.00 in FMDV infected DSP samples. IL-10 has been shown to  
411 facilitate persistent LCMV infection in rodents [62] and was previously observed to be  
412 upregulated in FMDV carrier animals [5,11].

413 Another well-characterized mechanism of inhibiting the T-cell response is the presence of  
414 FOXP3+ CD4+ T<sub>reg</sub> cells. The presence of this special subset of T cells in FMDV-positive DSP  
415 samples is indicated by the expression of several marker genes for T<sub>reg</sub> cells including FOXP3,  
416 CTLA4, IL2RA and TNFRSF18 [63], of which only CTLA4 was significantly upregulated (**Figure**  
417 **4B**), but FOXP3, IL2RA, and TNFRSF18 show a clear trend of increased expression in FMDV-  
418 infected tissue as depicted in **Figure 4C**. On the protein level, we detected an upregulation of  
419 IL411, which inhibits T-cell proliferation and induces T<sub>reg</sub> cell activation [64]. In accordance with  
420 the association of IL-10 with T-cell exhaustion described above, T<sub>reg</sub> cells are a source for this  
421 immunosuppressive cytokine [65]. T<sub>reg</sub> cells prevent lymphocyte migration into affected tissue

422 by the downregulation of neutral sphingomyelinase 3 (SMPD3) in endothelial cells [66], which  
423 was strongly downregulated in FMDV-positive DSP samples (log2FC -6.33, p = 1.1E-09).  
424 In addition to the overexpression of genes that exert a negative influence on the T-cell response  
425 in FMDV-positive DSP tissues, some genes positively correlated with T-cell activity were  
426 significantly downregulated. Among these, FABP4 with a log2FC of -6.66 was most strongly  
427 affected in its gene expression and showed a strong downregulation in its protein expression  
428 as well. Together with FABP5 (log2FC -3.86), these fatty-acid-binding proteins have been  
429 shown to be required for the survival of tissue-resident memory CD8 T cells after viral infection.  
430 These cells are located in the epithelial barrier tissue and mediate a first-line response against  
431 viral reinfection [67].  
432 For the recognition of pathogens by CD4 T cells, major histocompatibility receptors (MHCII)  
433 are a crucial cross-link between antigen-presenting cells (APCs) and CD4 T cells, ultimately  
434 leading to the activation of cytotoxic CD8 T cells and the proliferation of T memory cells [68].  
435 Several genes associated with bovine MHCII are significantly upregulated in FMDV-positive  
436 DSP samples. Among these the highest differential expression was observed for the DSB gene  
437 (MHC class II antigen DS beta; log2FC 5.71), an ortholog to HLA-DRB1 and a structural  
438 component of the MHCII receptor. On the protein level, structural components of the MHCII  
439 receptor such as BOLA-DRB and SCIMP, which is involved in MHCII signaling [69], were  
440 upregulated as well. The expression of MHCII complexes can be initiated by  $\gamma$ -interferon (IFN-  
441  $\gamma$ ) or by the transcription factor CIITA [68], which was significantly upregulated. The  
442 overexpressed gene BOLA-DMB, an ortholog to HLA-DMB, is responsible for antigen loading  
443 of the MHCII but can be antagonized competitively by HLA-DO [70], an ortholog of BOLA-DO.  
444 Its subunit BOLA-DOB (log2FC 3.43) was upregulated to a higher degree than BOLA-DMB.  
445 Taken together, this gene expression pattern of major parts of the adaptive immune response  
446 shows signs of a prolonged stimulation, which is counteracted by a plethora of differentially  
447 expressed genes inhibiting the migration of active cells into the tissue. At same time, an  
448 immunologically dysfunctional microenvironment with T<sub>reg</sub> cells and exhausted T cells is  
449 established in the infected FAE.



450

451 **Figure 4.** (A) Gene expression of the components of cellular tight junctions occludin (OCLN),  
 452 claudin-1 (CLDN1) and the tight junction protein 1 (TJP1/ZO-1) in DSP samples. (B) Gene  
 453 expression of important immune checkpoints for regulating T-cell proliferation: PD-1, CTLA4  
 454 and LAG-3 in DSP samples. (C) Gene expression of marker genes for T<sub>reg</sub> cells in FMDV RT-  
 455 qPCR in DSP samples. Samples are grouped by their FMDV Cq value into highly positive  
 456 (Cq≤30), weakly positive (45>Cq>30) and negative (no Cq).

#### 457 Innate Immunity

#### 458 IFN response

459 Whether viral infections provoke an antiviral innate immune response depends on the  
 460 recognition of viral components such as viral RNA or proteins. This leads to an interferon (IFN)  
 461 response mediated by several signal transduction pathways. FMDV has evolved several  
 462 inhibitory mechanisms to counteract the IFN response [71]. In this analysis, neither IFN-α nor

463 IFN- $\beta$  were significantly enriched and only a few genes associated with both pathways were  
464 differentially expressed. Only genes responsible for the positive regulation of the IFN- $\gamma$  pathway  
465 were upregulated in FMDV-positive DSP tissue, with overexpression of LTA, TNF, SLAMF6,  
466 SASH3, TLR8, TLR7, IRF8 and RASGRP1. On the other hand, the highly overexpressed genes  
467 IL10 and CCR7 can exert a negative influence on IFN- $\gamma$  and suppress its expression [72,73].  
468 IFN- $\gamma$ -induced genes like STAT1, CXCL10, CXCL16 and IFI16 were not significantly  
469 upregulated. Only the upregulation of STAT1 was also observed on the protein level. IRF9 and  
470 interferon-stimulated genes activated by IRF9 such as ISG15, OAS2, MX1 and MX2 were  
471 neither significantly upregulated (data not shown). Even though we and others observed a  
472 upregulation of TNF- $\alpha$  [52,74], which could induce an IFN- $\gamma$  response [75], we did not detect a  
473 significant upregulation of genes further downstream in the IFN signaling cascade. This could  
474 indicate an inhibition of this pathway, like it was observed by Zhu *et al.* [11], who suggested the  
475 activation of the noncanonical NF- $\kappa$ B pathway in carriers.

#### 476 Toll-like receptor (TLR) pathway

477 One important pathway of pathogen recognition is the Toll-like receptor (TLR) pathway. For  
478 the detection of endosomal viral ssRNA, especially TLR7 and TLR8 are crucial [76]. TLR7  
479 (log<sub>2</sub>FC 3.21) as well as TLR8 (log<sub>2</sub>FC 3.28) were significantly upregulated in FMDV-positive  
480 DSP samples. In contrast to the high expression of TLRs in FMDV-positive samples, MYD88  
481 was expressed to the same extent as in negative samples regardless of the examined tissue.  
482 MYD88 is a central downstream regulator of the TLR pathway and linked directly to TLR7 and  
483 TLR8 [77]. But for further transmission of TLR signaling, MYD88 has to be oligomerized in  
484 interaction with RNF152 to allow the recruitment of downstream signaling mediators. An  
485 RNF152 deficiency has been shown to exert a negative effect on NF- $\kappa$ B activation, which is  
486 downstream of the TLR pathway [78] (see **Figure 5A**). A similar effect could occur in FMDV-  
487 positive DSP samples, where RNF152 was significantly downregulated (log<sub>2</sub>FC -3.49). Another  
488 interesting significantly upregulated gene in the TLR pathway was TLR10, the only known TLR  
489 to exert an anti-inflammatory influence. Fittingly, its expression is induced by FOXOP3 in T<sub>reg</sub>  
490 cells [79,80].

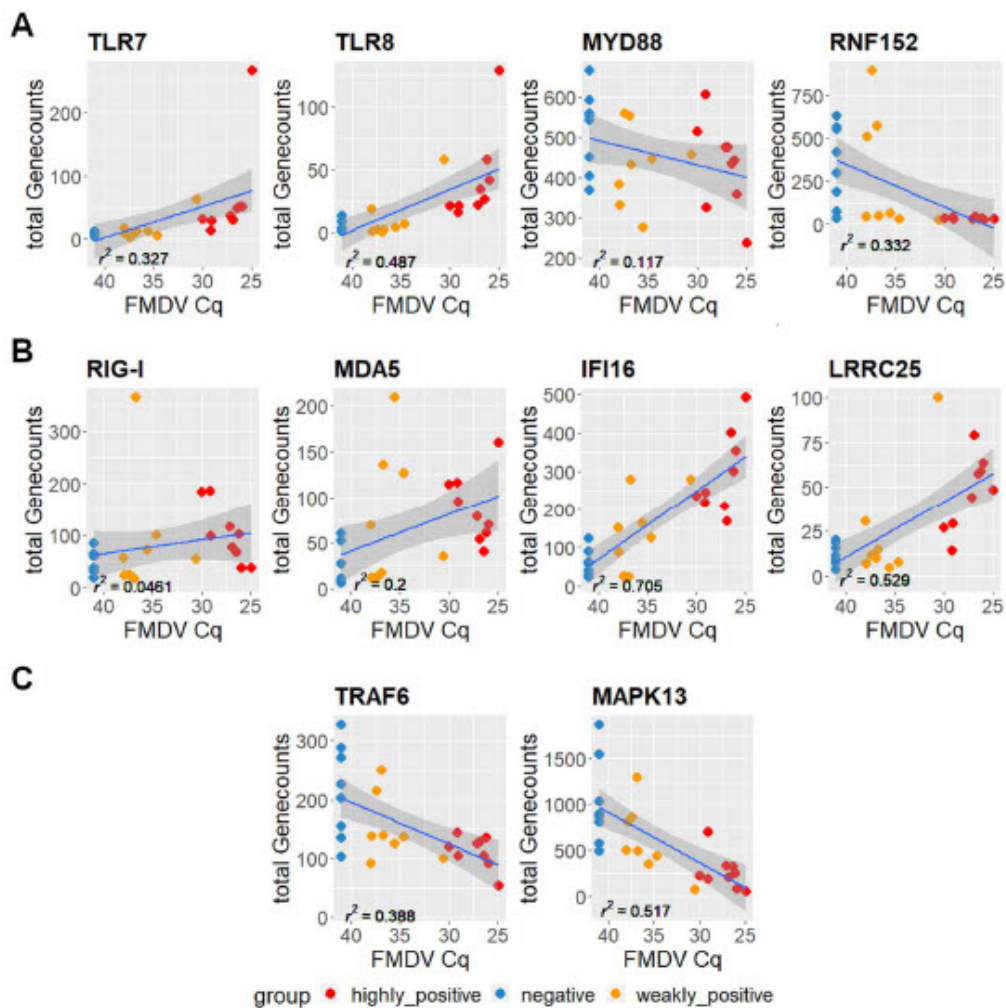
#### 491 RIG-I-like Receptor (RLR) pathway

492 The RIG-I-like Receptor (RLR) pathway is an important component of the innate immune  
493 response. There was only a small difference in the expression of the main receptor for viral  
494 RNA, RIG-I, as well as the expression of MDA5 and other members of the RLR pathway such  
495 as LGP2 and MAVS between FMDV-positive and negative DSP samples (**Figure 5B**).  
496 Especially RIG-I, responsible for the detection of cytoplasmic viral RNA, was expressed at low  
497 levels even in presence of high viral genome loads in the sample and a high expression of

498 IFI16, which has been shown to upregulate RIG-I expression after detection of viral RNA [81].  
499 This observation may be explained by the upregulation of LRCC25. It has been demonstrated  
500 that the FMDV protein 3A upregulates the expression of LRCC25 and, via inhibition of G3BP1,  
501 downregulates the expression of RIG-I and MDA5 [82]. This recently discovered mechanism  
502 may have an important influence during the persistent infection to allow the continued  
503 presence of viral RNA in the cytoplasm in a balance between RIG-I upregulation by IFI16 and  
504 downregulation by LRCC25.

505 **NOD-like receptor (NLR) pathway**

506 TRAF6 is a central signaling component downstream of the TLR, RLR and NOD-like receptor  
507 (NLR) pathways leading to NF- $\kappa$ B activation amongst others [71]. In FMDV-positive DSP  
508 samples, TRAF6 is downregulated but not significantly. It is targeted by the FMDV leader  
509 protease L<sup>pro</sup>, which deubiquitinates and thereby inactivates TRAF6 [83]. A direct regulation of  
510 its expression has not been demonstrated, but deubiquitinating TRAF6 could cause a negative  
511 feedback loop [84]. Downstream of TRAF6, MAPK13, one of the lesser characterized p38  
512 isoforms which is activated by TRAF6 [85], is also clearly, but not significantly, downregulated  
513 in FMDV-positive DSP samples and could contribute to the non-activation of apoptosis through  
514 NF $\kappa$ B (**Figure 5C**). The downregulation of TRAF6 has previously been observed in a microarray  
515 study with tissue samples of persistently FMDV-infected animals [10].



516  
 517 **Figure 5.** Gene expression of selected genes of the innate immune response signalling  
 518 cascade in DSP samples. (A) Genes of the TLR pathway including TLR7, TLR8, MYD88 and  
 519 RNF152. (B) Genes involved in the detection of viral RNA: the RNA-sensing receptors RIG-I  
 520 and MDA5, IFI16, which exerts a positive influence on RIG-I expression, as well as LRRC25,  
 521 possibly upregulated by FMDV 3A and exerting a negative influence on RIG-I and MDA5  
 522 expression. (C) Downregulated genes downstream the TLR, RLR and NLR pathways  
 523 including TRAF6 and MAPK13 expression. Samples are grouped by their FMDV RT-qPCR Cq  
 524 value into highly positive ( $Cq \leq 30$ ), weakly positive ( $45 > Cq > 30$ ) and negative.

525 **Lysozyme**

526 The important antimicrobial protein lysozyme is usually found in lymphoid tissue and lymphoid  
 527 epithelia as an effective agent against invading microbes [86]. Two bovine genes associated  
 528 with lysozyme were significantly downregulated in FMDV-positive samples: LYZ1  
 529 ( $\log_2FC -4.79$ ;  $p = 2.67E-05$ ) and LOC112446693 coding for a tracheal isozyme-like lysozyme  
 530 C ( $\log_2FC -7.38$ ,  $p = 9.0E-04$ ). This is of particular interest since lysozyme is usually secreted  
 531 in epithelia for protection and can exert limited antiviral activity [87].

## 532 **Phospholipases**

533 Phospholipases are a part of the cellular lipid metabolism but exert important immunological  
534 functions beyond that. Several genes coding for phospholipases were differentially expressed  
535 in FMDV-positive DSP samples. These can be categorized into different subfamilies of  
536 phospholipase A2 (PLA<sub>2</sub>) [88]: genes of the cPLA<sub>2</sub> subfamily (PLA2G4B and PLA2G4F) were  
537 significantly downregulated, while a phospholipase of the subfamily sPLA<sub>2</sub> (PLA2G2D4) was  
538 significantly upregulated. PLAG2a of the sPLA<sub>2</sub> subfamily was also upregulated, but only on  
539 the protein level. Genes coding for phospholipase C (PLCG2, PLCL2) were upregulated  
540 significantly as well. cPLA<sub>2</sub>s promote inflammation by hydrolyzing phospholipids and releasing  
541 arachidonic acid and lysophospholipids [89]. They are associated with inflammatory skin  
542 diseases and, especially for PLA2G4B, it has been shown that it promotes the expression of  
543 other inflammatory genes such as IL36A, IL36B, IL36G, and IL17 [90]. Fittingly, in our FMDV-  
544 positive samples, IL36A and IL36G were significantly downregulated. From the sPLA<sub>2</sub>  
545 subfamily, the gene coding for PLA2 group IID (PLA2G2D4) is expressed by dendritic cells and  
546 macrophages and supports the clearance of inflammation [91]. Genes coding for  
547 phospholipase C are also involved in inflammatory pathways [92]. This distribution of PLA<sub>2</sub>s  
548 describes an environment in which inflammation is resolved by the upregulation of anti-  
549 inflammatory sPLA<sub>2</sub>s and a downregulation of proinflammatory cPLA<sub>2</sub>s.

## 550 **Conclusions**

551 The animal experiment that this study is based on resulted in a large number of carrier animals  
552 with a high incidence of persistent infection. This allowed for the first time ever a simultaneous  
553 analysis of the transcriptome and proteome of *in vivo* tissue samples from persistently FMDV-  
554 infected animals. Furthermore, the use of the same samples for transcriptomic and proteomic  
555 analysis allowed us to corroborate our findings within our own study.

556 In our cohort of 18 animals, regardless of their vaccination status, the DSP tissue contained a  
557 higher proportion of FMDV-positive samples and higher viral genome loads than the DNP  
558 tissue, which has often been described as the preferential site of persistent FMDV infection [4].  
559 However, we did confirm that persistent FMDV is likely found in the FAE, as previously  
560 demonstrated with other methods, such as LCM or immunofluorescence [5]. The observed  
561 differences between FAE and adjacent epithelial, uninfected cells in the expression of genes  
562 associated with extracellular matrix, cell-to-cell connections and desquamation, may explain  
563 the enhanced susceptibility of the FAE for persistent infection.

564 Between survival and death, the fate of cells is decided by the balance of differentially  
565 expressed genes with pro- and anti-apoptotic functions. An enhanced resistance to apoptosis  
566 in tissues susceptible to persistent FMDV infection was already suggested by Zhu et al. [26].  
567 Based on our results, the strong expression of BCLA1 is likely to play a decisive role in  
568 regulating apoptosis. This upregulation of BCLA1 has previously been described in FMDV  
569 carriers compared to non-carriers [9]. Additionally, the anti-apoptotic function of SpiB which is  
570 expressed in M-cells of the FAE [23] hints at a tissue-specific advantage of the FAE that  
571 prevents the demise of its epithelial cells.

572 It is well known that there is a strong FMDV-specific IgA response in secretions of carrier  
573 animals and that this can even be exploited for the diagnosis of persistent infection [45]. In our  
574 set of samples, we observed a gene expression pattern, which suggests the presence of IgA-  
575 producing B cells in the FAE, but inhibitory signals were present as well. More revealing of the  
576 virus-host relationship is the gene expression pattern influencing the T-cell response. We  
577 observed both T-cell activation and repression at the same time. However, genes and proteins  
578 exerting a negative influence on T cells seem to be dominating (see **Table 4**). This  
579 transcriptomic and proteomic landscape paints a picture of a microenvironment in the FAE  
580 favoring T-cell exhaustion and the presence of T<sub>reg</sub> cells, while inhibiting efficient clearance of  
581 virus by cytotoxic T cells. This cellular immune response has previously been hypothesized to  
582 be responsible for the inability of carrier animals to clear FMDV from the nasopharynx [9,52].

583 Concerning the innate immune response, we noted an absence of differentially expressed  
584 genes associated with an IFN type I response. The IFN- $\gamma$  pathway was found to be activated,  
585 but ISGs were not significantly overexpressed. Several genes involved in TLR and RLR  
586 pathways were downregulated in FMDV-positive samples, which could be caused by the IFN-  
587 inhibitory functions of FMDV. Of particular interest is the upregulation of LRRC25, indicating an  
588 inhibition of RIG-I and MAPK5 which can be caused by the viral FMDV protein 3A [82], as well  
589 as the downregulation of TRAF6, which is targeted by FMDV L<sup>pro</sup> [83]. The inhibition of innate  
590 immune responses following detection of viral RNA via the TLR, RLR and NLR pathways may  
591 be actively facilitated by FMDV viral proteins targeting central signalling components such as  
592 RIG-I, MDA5 and TRAF6. Major pressure on the type I IFN response is exerted by the FMDV  
593 leader protease L<sup>pro</sup> and this might be a critical factor in the establishment of persistent  
594 infection. Leaderless FMDV are strongly attenuated and unable to persist in cattle [93].

595 Ultimately, the reason for the preferential localisation of persistent FMDV infection in the FAE  
596 remains elusive. This microanatomic compartment, which is also the location of primary  
597 replication of FMDV in cattle, serves as a reservoir of FMDV in an otherwise immune host. We  
598 suspect that the persistent infection of FMDV in the epithelia of the nasopharynx is enabled by

599 an interplay between virally induced inhibition of the innate immune response, suppression of  
600 apoptosis and a permissive microenvironment of T<sub>reg</sub> cells and exhausted T cells in a highly  
601 susceptible epithelium.

## 602 **Author contributions**

603 Writing—Original Draft Preparation, B.L.; Writing—Review and Editing, B.L., F.P., M.B., S.H.,  
604 J.V. and M.E.; Methodology, B.L., F.P. and M.E.; Investigation, B.L., F.P., L.F., S.H., J.V. and  
605 M.E.; Formal Analysis, Visualization, and Data Curation, B.L., F.P., S.H. and J.V.; Supervision,  
606 F.P., M.B. and M.E.; Conceptualization, F.P., M.B. and M.E.; Project Administration, M.E.

## 607 **Conflict of interest**

608 The authors declare no conflict of interest.

## 609 **Funding**

610 This work was funded by the Federal Office for Agriculture and Food (Bundesanstalt für  
611 Landwirtschaft und Ernährung, Germany) and the Swedish Research Council (FORMAS,  
612 Sweden) through the International Coordination of Research on Infectious Animal Diseases  
613 (ICRAD) ERA-Net project FMDV\_PersistOmics, grant number 2821ERA28D and 2020-02741,  
614 respectively.

## 615 **Data availability statement**

616 All Data has been uploded to ArrayExpress.

## 617 **Acknowledgement**

618 We thank Jenny Lorke and Patrick Zitzow for their excellent technical assistance.

## 619 **Tables**

620 **Table 1.** The number of differentially expressed genes (DEG) for different contrasts. “FMDV”  
621 are samples with a Cq≤30 (highly positive) and “FMDVneg” are FMDV-negative samples (no  
622 Cq) in the FMDV-specific RT-qPCR.

Contrast	Number of total DEGs	Number of downregulated DEGs	Number of upregulated DEGs
----------	----------------------	------------------------------	----------------------------

DSP ↔ DNP	294	126	168
FMDVpos ↔ FMDVneg	7	5	2
DSP+FMDVpos ↔ DSP+FMDVneg	416	176	240

623

624 **Table 2.** Top 10 up- and downregulated genes when comparing FMDV-positive to negative  
625 DSP samples. “FMDVpos” are samples with an Cq≤30 (highly positive) and “FMDVneg” are  
626 FMDV-negative samples (no Cq) in the FMDV-specific RT-qPCR. The corresponding Reactome  
627 pathways were listed if possible. Positive log<sub>2</sub> fold change (log<sub>2</sub>FC) indicates upregulation  
628 while negative log<sub>2</sub>FC indicates downregulation.

Gene	Name	Reactome pathways	p-value	log <sub>2</sub> FC
ELL3	elongation factor for RNA polymerase II 3	RNA polymerase II transcribes snRNA genes	4.6E-07	6.41
DSB	MHC class II antigen DS beta		2.6E-04	5.71
CD300LB	CD300 molecule-like family member b	Immunoregulatory interactions between a lymphoid and a non-lymphoid cell	7.5E-04	5.69
IL10	interleukin 10	Signaling by interleukins	9.0E-04	5.56
NLRC3	NLR family CARD domain containing 3	IRF3-mediated induction of type I interferon	3.8E-06	5.50
GPRIN3	GPRIN family member 3	Assembly and cell surface presentation of NMDA receptors	1.3E-06	5.25
CCL20	C-C motif chemokine ligand 20	Signaling by interleukins	8.3E-05	5.12
CEND1	cell cycle exit and neuronal differentiation 1		1.7E-05	4.96

TIMD4	T cell immunoglobulin and mucin domain containing 4		3.0E-07	4.94
CXCL8	C-X-C motif chemokine ligand 8	Signaling by interleukins	9.0E-04	4.93
KPRP	keratinocyte proline rich protein	Keratinization	7.7E-07	-8.77
KRT3	keratin 3	Keratinization	1.3E-13	-8.66
CWH43	cell wall biogenesis 43 C-terminal homolog		6.2E-05	-8.51
CDSN	corneodesmosin	Keratinization	3.3E-06	-8.21
LCE3C	late cornified envelope 3C	Keratinization	3.3E-05	-8.00
UGT1A60	UDP glucuronosyltransferase 1 family, polypeptide A6	Biological oxidations	2.9E-06	-7.95
KRT35	keratin 35	Keratinization	6.0E-07	-7.48
ARG1	arginase 1	Neutrophil degranulation	2.0E-05	-7.41
LORICRIN	loricrin cornified envelope precursor protein	Keratinization	2.5E-08	-7.40
DYNAP	dynactin associated protein		2.1E-04	-7.29

629 **Table 3.** Top 10 list of significantly up- and downregulated characterized proteins when  
630 comparing highly FMDV-positive DSP samples to negative samples. Selected and sorted by  
631 log2FC, filtered for peptide spectral matches (PSM) >1. A positive log2FC indicates  
632 upregulation, a negative log2FC downregulation.

Gene	Name	p-value	Log2FC
LIMD2	LIM domain-containing protein 2	2.8E-04	2.16
SCIMP	SLP adaptor and CSK interacting membrane protein	6.7E-04	2.11

CXCL13	C-X-C motif chemokine	4.9E-06	2.01
PLA2G2A	Phospholipase A2, membrane associated	2.8E-05	1.96
IL4I1	Interleukin 4 induced 1	5.0E-04	1.56
BOLA-DRB2	Ig-like domain-containing protein	2.2E-04	1.56
MS4A1	Membrane spanning 4-domains A1	5.6E-04	1.50
GIMAP7	GTPase, IMAP family member 7	3.6E-04	1.48
FCRLA	Fc receptor like A	3.1E-04	1.47
GRAP	GRB2-related adapter protein	4.4E-04	1.44
LY6D	Lymphocyte antigen 6D	2.1E-05	-3.02
SBSN	Suprabasin	8.7E-06	-2.89
F1N6D1	WAP domain-containing protein	8.0E-05	-2.57
AKAP14	A-kinase anchoring protein 14	5.0E-05	-2.53
SPRR2F	Small proline-rich protein 2f-like	8.5E-07	-2.36
KLK13	Kallikrein related peptidase 13	2.8E-11	-2.35
KLK12	Kallikrein related peptidase 12	3.1E-08	-2.23
FAM25A	Protein FAM25A	6.6E-04	-2.15
SCEL	SCEL protein	1.4E-05	-2.13
A2ML1	Alpha-2-macroglobulin like 1	2.4E-04	-2.11

633 **Table 4.** Overexpressed genes in DSP FMDVpos vs. FMDVneg which can exert negative influ-  
634 ence on T-cell-mediated immune responses, ordered by log2FC.

Gene	p-value	log2FC	Function	Reference
NLRC3	3.79E-06	5.50	Attenuates CD4+ T cell response and auto-immunity	[94]

TIMD4	2.95E-07	4.94	Tim-4+ cavity-resident macrophages impair anti-tumor CD8+ T cell immunity	[95]
CTLA4	1.19E-03	4.67	Suppresses T cell response	[96]
CCL19	3.22E-08	4.51	CCL19/CCR7 drives T <sub>reg</sub> cell migration	[97]
CCR7	4.01E-04	4.12	CCL19/CCR7 drives T <sub>reg</sub> cell migration	[97]
RIPOR2 (FAM65B)	9.52E-05	3.81	Inhibits chemokine-induced T cell response	[98]
IKZF3	4.07E-04	3.76	Deficiency promotes T cell activation	[37]
RHOH	1.04E-03	3.68	Impairing T cell chemotaxis	[55]
EGR3	5.99E-05	3.52	Suppressive activity to CD4+ T cells and regulates the production of inhibitory cytokines such as IL-10 and TGF- $\beta$ 1	[99]
LAG3	1.11E-03	3.51	Inhibits the immune microenvironment	[100]
BOLA-DOB	1.04E-03	3.43	Suppresses antigen loading of MHCII	[70]
TOX	1.45E-04	3.41	Central regulator of T cell exhaustion	[101]
GRAP	1.22E-04	3.39	Negatively regulates TCR induced proliferation	[102]
BATF	7.32E-05	3.31	Positively regulates Treg cell expression	[103]
SIT1	3.54E-04	3.16	Overexpression downmodulates T cell receptor activation	[104]

## 635 References

- 636 1. Stenfeldt, C.; Arzt, J. The Carrier Conundrum; A Review of Recent Advances and Persistent  
637 Gaps Regarding the Carrier State of Foot-and-Mouth Disease Virus. *Pathogens* **2020**,  
638 *9*, doi:10.3390/pathogens9030167.
- 639 2. Jolles, A.; Gorsich, E.; Gubbins, S.; Beechler, B.; Buss, P.; Juleff, N.; Klerk-Lorist, L.-M. de;  
640 Maree, F.; Perez-Martin, E.; van Schalkwyk, O.L.; et al. Endemic persistence of a highly  
641 contagious pathogen: Foot-and-mouth disease in its wildlife host. *Science* **2021**, *374*, 104–  
642 109, doi:10.1126/science.abd2475.

- 643 3. Suttmoller, P.; Cottral, G.E. Improved techniques for the detection of foot-and-mouth dis-  
644 ease virus in carrier cattle. *Arch. Gesamte Virusforsch.* **1967**, *21*, 170–177,  
645 doi:10.1007/BF01241441.
- 646 4. Pacheco, J.M.; Smoliga, G.R.; O'Donnell, V.; Brito, B.P.; Stenfeldt, C.; Rodriguez, L.L.; Arzt,  
647 J. Persistent Foot-and-Mouth Disease Virus Infection in the Nasopharynx of Cattle; Tissue-  
648 Specific Distribution and Local Cytokine Expression. *PLoS One* **2015**, *10*, e0125698,  
649 doi:10.1371/journal.pone.0125698.
- 650 5. Stenfeldt, C.; Eschbaumer, M.; Rekant, S.I.; Pacheco, J.M.; Smoliga, G.R.; Hartwig, E.J.;  
651 Rodriguez, L.L.; Arzt, J. The Foot-and-Mouth Disease Carrier State Divergence in Cattle.  
652 *J. Virol.* **2016**, *90*, 6344–6364, doi:10.1128/JVI.00388-16.
- 653 6. Stanley, A.C.; Huntley, J.F.; Jeffrey, M.; Buxton, D. Characterization of ovine nasal-associ-  
654 ated lymphoid tissue and identification of M cells in the overlying follicle-associated epi-  
655 thelium. *J. Comp. Pathol.* **2001**, *125*, 262–270, doi:10.1053/jcpa.2001.0506.
- 656 7. Saxena, V.K.; Diaz, A.; Scheerlinck, J.-P.Y. Identification and characterization of an M cell  
657 marker in nasopharynx- and oropharynx-associated lymphoid tissue of sheep. *Vet. Immu-  
658 nol. Immunopathol.* **2019**, *208*, 1–5, doi:10.1016/j.vetimm.2018.12.005.
- 659 8. Meek, H.C.; Stenfeldt, C.; Arzt, J. Morphological and Phenotypic Characteristics of the  
660 Bovine Nasopharyngeal Mucosa and Associated Lymphoid Tissue. *J. Comp. Pathol.* **2022**,  
661 *198*, 62–79, doi:10.1016/j.jcpa.2022.07.011.
- 662 9. Eschbaumer, M.; Stenfeldt, C.; Smoliga, G.R.; Pacheco, J.M.; Rodriguez, L.L.; Li, R.W.; Zhu,  
663 J.; Arzt, J. Transcriptomic Analysis of Persistent Infection with Foot-and-Mouth Disease  
664 Virus in Cattle Suggests Impairment of Apoptosis and Cell-Mediated Immunity in the Na-  
665 sopharynx. *PLoS One* **2016**, *11*, e0162750, doi:10.1371/journal.pone.0162750.
- 666 10. Zhu, J.J.; Stenfeldt, C.; Bishop, E.A.; Canter, J.A.; Eschbaumer, M.; Rodriguez, L.L.; Arzt,  
667 J. Mechanisms of Maintenance of Foot-and-Mouth Disease Virus Persistence Inferred  
668 From Genes Differentially Expressed in Nasopharyngeal Epithelia of Virus Carriers and  
669 Non-carriers. *Front. Vet. Sci.* **2020**, *7*, doi:10.3389/fvets.2020.00340.
- 670 11. Zhu, J.J.; Stenfeldt, C.; Bishop, E.A.; Canter, J.A.; Eschbaumer, M.; Rodriguez, L.L.; Arzt,  
671 J. Inferred Causal Mechanisms of Persistent FMDV Infection in Cattle from Differential  
672 Gene Expression in the Nasopharyngeal Mucosa. *Pathogens* **2022**, *11*, doi:10.3390/path-  
673 ogens11080822.
- 674 12. Han, L.; Yuan, Y.; Hu, J.; Li, J.; Zhu, S.; Yang, P.; Cheng, A.; Li, X.; Shen, C. Next-generation  
675 sequencing sheds light on the interaction between virus and cell during foot-and-mouth

- 676 disease virus persistent infection. *Vet. Microbiol.* **2021**, *263*, 109247,  
677 doi:10.1016/j.vetmic.2021.109247.
- 678 13. Mao, R.; Sun, D.; Yang, F.; Tian, H.; Zhu, Z.; Zheng, H.; Liu, X. Establishment and Evaluation  
679 of a Stable Bovine Thyroid Cell Line for Investigating Foot-and-Mouth Disease Virus. *Front.*  
680 *Microbiol.* **2018**, *9*, 2149, doi:10.3389/fmicb.2018.02149.
- 681 14. Pfaff, F.; Häggglund, S.; Zoli, M.; Blaise-Boisseau, S.; Laloy, E.; Koethe, S.; Zühlke, D.; Riedel,  
682 K.; Zientara, S.; Bakkali-Kassimi, L.; et al. Proteogenomics Uncovers Critical Elements of  
683 Host Response in Bovine Soft Palate Epithelial Cells Following In Vitro Infection with Foot-  
684 And-Mouth Disease Virus. *Viruses* **2019**, *11*, doi:10.3390/v11010053.
- 685 15. Pacheco, J.M.; Stenfeldt, C.; Rodriguez, L.L.; Arzt, J. Infection Dynamics of Foot-and-  
686 Mouth Disease Virus in Cattle Following Intranasopharyngeal Inoculation or Contact Ex-  
687 posure. *J. Comp. Pathol.* **2016**, *155*, 314–325, doi:10.1016/j.jcpa.2016.08.005.
- 688 16. Callahan, J.D.; Brown, F.; Osorio, F.A.; Sur, J.H.; Kramer, E.; Long, G.W.; Lubroth, J.; Ellis,  
689 S.J.; Shoulars, K.S.; Gaffney, K.L.; et al. Use of a portable real-time reverse transcriptase-  
690 polymerase chain reaction assay for rapid detection of foot-and-mouth disease virus. *J.*  
691 *Am. Vet. Med. Assoc.* **2002**, *220*, 1636–1642, doi:10.2460/javma.2002.220.1636.
- 692 17. Yu, G.; He, Q.-Y. ReactomePA: an R/Bioconductor package for reactome pathway analysis  
693 and visualization. *Mol. Biosyst.* **2016**, *12*, 477–479, doi:10.1039/C5MB00663E.
- 694 18. Kolberg, L.; Raudvere, U.; Kuzmin, I.; Adler, P.; Vilo, J.; Peterson, H. g:Profiler-interopera-  
695 ble web service for functional enrichment analysis and gene identifier mapping (2023 up-  
696 date). *Nucleic Acids Res.* **2023**, *51*, W207-W212, doi:10.1093/nar/gkad347.
- 697 19. Krämer, A.; Green, J.; Pollard, J.; Tugendreich, S. Causal analysis approaches in Ingenuity  
698 Pathway Analysis. *Bioinformatics* **2014**, *30*, 523–530, doi:10.1093/bioinformatics/btt703.
- 699 20. Wilson, E.B. Probable Inference, the Law of Succession, and Statistical Inference. *Journal*  
700 *of the American Statistical Association* **1927**, *22*, 209–212,  
701 doi:10.1080/01621459.1927.10502953.
- 702 21. Suttmoller, P.; McVicar, J.W.; Cottral, G.E. The epizootiological importance of foot-and-  
703 mouth disease carriers. I. Experimentally produced foot-and-mouth disease carriers in  
704 susceptible and immune cattle. *Arch. Gesamte Virusforsch.* **1968**, *23*, 227–235,  
705 doi:10.1007/BF01241895.
- 706 22. Kobayashi, A.; Donaldson, D.S.; Kanaya, T.; Fukuda, S.; Baillie, J.K.; Freeman, T.C.; Ohno,  
707 H.; Williams, I.R.; Mabbott, N.A. Identification of novel genes selectively expressed in the  
708 follicle-associated epithelium from the meta-analysis of transcriptomics data from multiple

- 709 mouse cell and tissue populations. *DNA Res.* **2012**, *19*, 407–422,  
710 doi:10.1093/dnares/dss022.
- 711 23. Oya, Y.; Kimura, S.; Nakamura, Y.; Ishihara, N.; Takano, S.; Morita, R.; Endo, M.; Hase, K.  
712 Characterization of M Cells in Tear Duct-Associated Lymphoid Tissue of Mice: A Potential  
713 Role in Immunosurveillance on the Ocular Surface. *Front. Immunol.* **2021**, *12*, 779709,  
714 doi:10.3389/fimmu.2021.779709.
- 715 24. Mutoh, M.; Kimura, S.; Takahashi-Iwanaga, H.; Hisamoto, M.; Iwanaga, T.; Iida, J. RANKL  
716 regulates differentiation of microfold cells in mouse nasopharynx-associated lymphoid tis-  
717 sue (NALT). *Cell Tissue Res.* **2016**, *364*, 175–184, doi:10.1007/s00441-015-2309-2.
- 718 25. Pribyl, M.; Hodny, Z.; Kubikova, I. Suprabasin—A Review. *Genes (Basel)* **2021**, *12*,  
719 doi:10.3390/genes12010108.
- 720 26. Zhu, J.J.; Arzt, J.; Puckette, M.C.; Smoliga, G.R.; Pacheco, J.M.; Rodriguez, L.L. Mecha-  
721 nisms of Foot-and-Mouth Disease Virus Tropism Inferred from Differential Tissue Gene  
722 Expression. *PLoS One* **2013**, *8*, doi:10.1371/journal.pone.0064119.
- 723 27. Perry, M.E. The specialised structure of crypt epithelium in the human palatine tonsil and  
724 its functional significance. *J. Anat.* **1994**, *185 (Pt 1)*, 111–127.
- 725 28. Nauroy, P.; Nyström, A. Kallikreins: Essential epidermal messengers for regulation of the  
726 skin microenvironment during homeostasis, repair and disease. *Matrix Biol. Plus* **2020**, *6*-  
727 *7*, 100019, doi:10.1016/j.mbplus.2019.100019.
- 728 29. Filippou, P.S.; Ren, A.H.; Soosaipillai, A.; Safar, R.; Prassas, I.; Diamandis, E.P.; Conner,  
729 J.R. Kallikrein-related peptidases protein expression in lymphoid tissues suggests poten-  
730 tial implications in immune response. *Clin. Biochem.* **2020**, *77*, 41–47, doi:10.1016/j.clinbi-  
731 ochem.2019.12.015.
- 732 30. Ulbricht, D.; Tindall, C.A.; Oertwig, K.; Hanke, S.; Sträter, N.; Heiker, J.T. Kallikrein-related  
733 peptidase 14 is the second KLK protease targeted by the serpin vaspin. *Biol. Chem.* **2018**,  
734 *399*, 1079–1084, doi:10.1515/hsz-2018-0108.
- 735 31. Galliano, M.-F.; Toulza, E.; Gallinaro, H.; Jonca, N.; Ishida-Yamamoto, A.; Serre, G.;  
736 Guerrin, M. A novel protease inhibitor of the alpha2-macroglobulin family expressed in the  
737 human epidermis. *J. Biol. Chem.* **2006**, *281*, 5780–5789, doi:10.1074/jbc.M508017200.
- 738 32. Chavarria-Smith, J.; Chiu, C.P.C.; Jackman, J.K.; Yin, J.; Zhang, J.; Hackney, J.A.; Lin, W.-  
739 Y.; Tyagi, T.; Sun, Y.; Tao, J.; et al. Dual antibody inhibition of KLK5 and KLK7 for Netherton  
740 syndrome and atopic dermatitis. *Sci. Transl. Med.* **2022**, *14*, eabp9159, doi:10.1126/sci-  
741 translmed.abp9159.

- 742 33. Kryza, T.; Bock, N.; Lovell, S.; Rockstroh, A.; Lehman, M.L.; Lesner, A.; Panchadsaram, J.;  
743 Silva, L.M.; Srinivasan, S.; Snell, C.E.; et al. The molecular function of kallikrein-related  
744 peptidase 14 demonstrates a key modulatory role in advanced prostate cancer. *Mol. On-*  
745 *col.* **2020**, *14*, 105–128, doi:10.1002/1878-0261.12587.
- 746 34. Deretic, V.; Levine, B. Autophagy, immunity, and microbial adaptations. *Cell Host Microbe*  
747 **2009**, *5*, 527–549, doi:10.1016/j.chom.2009.05.016.
- 748 35. Lee, J.-Y.; Lee, S.-H.; Kim, K.-S.; Park, K.-H.; Park, K.-S. E13 functions as a critical decision  
749 maker at the crossroad between stem cell senescence and apoptosis. *Stem Cell Res.*  
750 *Ther.* **2019**, *10*, doi:10.1186/s13287-019-1137-9.
- 751 36. Cabral-Pacheco, G.A.; Garza-Veloz, I.; La Castruita-De Rosa, C.; Ramirez-Acuña, J.M.; Pe-  
752 rez-Romero, B.A.; Guerrero-Rodriguez, J.F.; Martinez-Avila, N.; Martinez-Fierro, M.L. The  
753 Roles of Matrix Metalloproteinases and Their Inhibitors in Human Diseases. *Int. J. Mol. Sci.*  
754 **2020**, *21*, doi:10.3390/ijms21249739.
- 755 37. Zou, Y.; Liu, B.; Li, L.; Yin, Q.; Tang, J.; Jing, Z.; Huang, X.; Zhu, X.; Chi, T. IKZF3 deficiency  
756 potentiates chimeric antigen receptor T cells targeting solid tumors. *Cancer Lett.* **2022**,  
757 *524*, 121–130, doi:10.1016/j.canlet.2021.10.016.
- 758 38. Ahn, H.-J.; Cha, Y.; Moon, S.-H.; Jung, J.-E.; Park, K.-S. E13 enhances differentiation of  
759 mouse embryonic stem cells by regulating epithelial-mesenchymal transition and apopto-  
760 sis. *PLoS One* **2012**, *7*, e40293, doi:10.1371/journal.pone.0040293.
- 761 39. Chiou, S.K.; Rao, L.; White, E. Bcl-2 blocks p53-dependent apoptosis. *Mol. Cell. Biol.* **1994**,  
762 *14*, 2556–2563, doi:10.1128/mcb.14.4.2556-2563.1994.
- 763 40. Kvensakul, M.; Caria, S.; Hinds, M.G. The Bcl-2 Family in Host-Virus Interactions. *Viruses*  
764 **2017**, *9*, doi:10.3390/v9100290.
- 765 41. Beug, S.T.; Cheung, H.H.; LaCasse, E.C.; Korneluk, R.G. Modulation of immune signalling  
766 by inhibitors of apoptosis. *Trends Immunol.* **2012**, *33*, 535–545,  
767 doi:10.1016/j.it.2012.06.004.
- 768 42. Dhingra, S.; Sharma, A.K.; Arora, R.C.; Slezak, J.; Singal, P.K. IL-10 attenuates TNF-alpha-  
769 induced NF kappaB pathway activation and cardiomyocyte apoptosis. *Cardiovasc. Res.*  
770 **2009**, *82*, 59–66, doi:10.1093/cvr/cvp040.
- 771 43. Giaime, E.; Tong, Y.; Wagner, L.K.; Yuan, Y.; Huang, G.; Shen, J. Age-dependent dopa-  
772 minergic neurodegeneration and impairment of the autophagy-lysosomal pathway in  
773 LRRK-deficient mice. *Neuron* **2017**, *96*, 796-807.e6, doi:10.1016/j.neuron.2017.09.036.

- 774 44. Zhang, H.; Wang, G.; Zhou, R.; Li, X.; Sun, Y.; Li, Y.; Du, W.; Yan, X.; Yang, J.; Chang, X.;  
775 et al. SPIB promotes anoikis resistance via elevated autolysosomal process in lung cancer  
776 cells. *FEBS J.* **2020**, *287*, 4696–4709, doi:10.1111/febs.15272.
- 777 45. Archetti, I.L.; Amadori, M.; Donn, A.; Salt, J.; Lodetti, E. Detection of foot-and-mouth dis-  
778 ease virus-infected cattle by assessment of antibody response in oropharyngeal fluids. *J.*  
779 *Clin. Microbiol.* **1995**, *33*, 79–84, doi:10.1128/jcm.33.1.79-84.1995.
- 780 46. Ramos-Medina, R.; Montes-Moreno, S.; Maestre, L.; Cañamero, M.; Rodríguez-Pinilla, M.;  
781 Martínez-Torrecuadrada, J.; Piris, M.Á.; Majid, A.; Dyer, M.J.S.; Pulford, K.; et al. BCL7A  
782 protein expression in normal and malignant lymphoid tissues. *Br. J. Haematol.* **2013**, *160*,  
783 106–109, doi:10.1111/bjh.12080.
- 784 47. Clatworthy, M.R. B-cell regulation and its application to transplantation. *Transpl. Int.* **2014**,  
785 *27*, 117–128, doi:10.1111/tri.12160.
- 786 48. Sage, P.T.; Paterson, A.M.; Lovitch, S.B.; Sharpe, A.H. The coinhibitory receptor CTLA-4  
787 controls B cell responses by modulating T follicular helper, T follicular regulatory, and T  
788 regulatory cells. *Immunity* **2014**, *41*, 1026–1039, doi:10.1016/j.immuni.2014.12.005.
- 789 49. Clark, E.A.; Giltiay, N.V. CD22: A Regulator of Innate and Adaptive B Cell Responses and  
790 Autoimmunity. *Front. Immunol.* **2018**, *9*, doi:10.3389/fimmu.2018.02235.
- 791 50. Lee, M.; Kiefel, H.; LaJevic, M.D.; Macauley, M.S.; Kawashima, H.; O'Hara, E.; Pan, J.; Paul-  
792 son, J.C.; Butcher, E.C. Transcriptional programs of lymphoid tissue capillary and high  
793 endothelium reveal control mechanisms for lymphocyte homing. *Nat. Immunol.* **2014**, *15*,  
794 982–995, doi:10.1038/ni.2983.
- 795 51. Park, J. in; Cho, S.W.; Kang, J.H.; Park, T.-E. Intestinal Peyer's Patches: Structure, Func-  
796 tion, and In Vitro Modeling. *Tissue Eng. Regen. Med.* **2023**, *20*, 341–353,  
797 doi:10.1007/s13770-023-00543-y.
- 798 52. Stenfeldt, C.; Eschbaumer, M.; Smoliga, G.R.; Rodriguez, L.L.; Zhu, J.; Arzt, J. Clearance  
799 of a persistent picornavirus infection is associated with enhanced pro-apoptotic and cel-  
800 lular immune responses. *Sci. Rep.* **2017**, *7*, 17800, doi:10.1038/s41598-017-18112-4.
- 801 53. Förster, R.; Davalos-Misnitz, A.C.; Rot, A. CCR7 and its ligands: balancing immunity and  
802 tolerance. *Nat. Rev. Immunol.* **2008**, *8*, 362–371, doi:10.1038/nri2297.
- 803 54. Boscacci, R.T.; Pfeiffer, F.; Gollmer, K.; Sevilla, A.I.C.; Martin, A.M.; Soriano, S.F.; Natale,  
804 D.; Henrickson, S.; Andrian, U.H. von; Fukui, Y.; et al. Comprehensive analysis of lymph  
805 node stroma-expressed Ig superfamily members reveals redundant and nonredundant

- 806 roles for ICAM-1, ICAM-2, and VCAM-1 in lymphocyte homing. *Blood* **2010**, *116*, 915–925,  
807 doi:10.1182/blood-2009-11-254334.
- 808 55. Baker, C.M.; Comrie, W.A.; Hyun, Y.-M.; Chung, H.-L.; Fedorchuk, C.A.; Lim, K.; Brake-  
809 busch, C.; McGrath, J.L.; Waugh, R.E.; Meier-Schellersheim, M.; et al. Opposing roles for  
810 RhoH GTPase during T-cell migration and activation. *Proc. Natl. Acad. Sci. U. S. A.* **2012**,  
811 *109*, 10474–10479, doi:10.1073/pnas.1114214109.
- 812 56. Wu, Z.; Yoshikawa, T.; Inoue, S.; Ito, Y.; Kasuya, H.; Nakashima, T.; Zhang, H.; Kotaka, S.;  
813 Hosoda, W.; Suzuki, S.; et al. CD83 expression characterizes precursor exhausted T cell  
814 population. *Commun. Biol.* **2023**, *6*, doi:10.1038/s42003-023-04631-6.
- 815 57. Blackburn, S.D.; Shin, H.; Haining, W.N.; Zou, T.; Workman, C.J.; Polley, A.; Betts, M.R.;  
816 Freeman, G.J.; Vignali, D.A.A.; Wherry, E.J. Coregulation of CD8+ T cell exhaustion by  
817 multiple inhibitory receptors during chronic viral infection. *Nat. Immunol.* **2009**, *10*, 29–37,  
818 doi:10.1038/ni.1679.
- 819 58. Apol, Á.D.; Winkelmann, A.A.; Duus, R.B.; Bukh, J.; Weis, N. The Role of CTLA-4 in T Cell  
820 Exhaustion in Chronic Hepatitis B Virus Infection. *Viruses* **2023**, *15*,  
821 doi:10.3390/v15051141.
- 822 59. Zhu, J.; Li, Y.; Lv, X. IL411 enhances PD-L1 expression through JAK/STAT signaling path-  
823 way in lung adenocarcinoma. *Immunogenetics* **2023**, *75*, 17–25, doi:10.1007/s00251-022-  
824 01275-4.
- 825 60. Quigley, M.; Pereyra, F.; Nilsson, B.; Porichis, F.; Fonseca, C.; Eichbaum, Q.; Julg, B.;  
826 Jesneck, J.L.; Brosnahan, K.; Imam, S.; et al. Integrative genomic analysis of HIV-specific  
827 CD8+ T cells reveals that PD-1 inhibits T cell function by upregulating BATF. *Nat. Med.*  
828 **2010**, *16*, 1147–1151, doi:10.1038/nm.2232.
- 829 61. Si, J.; Shi, X.; Sun, S.; Zou, B.; Li, Y.; An, D.; Lin, X.; Gao, Y.; Long, F.; Pang, B.; et al.  
830 Hematopoietic Progenitor Kinase1 (HPK1) Mediates T Cell Dysfunction and Is a Druggable  
831 Target for T Cell-Based Immunotherapies. *Cancer Cell* **2020**, *38*, 551-566.e11,  
832 doi:10.1016/j.ccell.2020.08.001.
- 833 62. Brooks, D.G.; Trifilo, M.J.; Edelmann, K.H.; Teyton, L.; McGavern, D.B.; Oldstone, M.B.A.  
834 Interleukin-10 determines viral clearance or persistence in vivo. *Nat. Med.* **2006**, *12*, 1301–  
835 1309, doi:10.1038/nm1492.
- 836 63. Piotrowska, M.; Gliwiński, M.; Trzonkowski, P.; Iwaszkiewicz-Grzes, D. Regulatory T Cells-  
837 Related Genes Are under DNA Methylation Influence. *Int. J. Mol. Sci.* **2021**, *22*,  
838 doi:10.3390/ijms22137144.

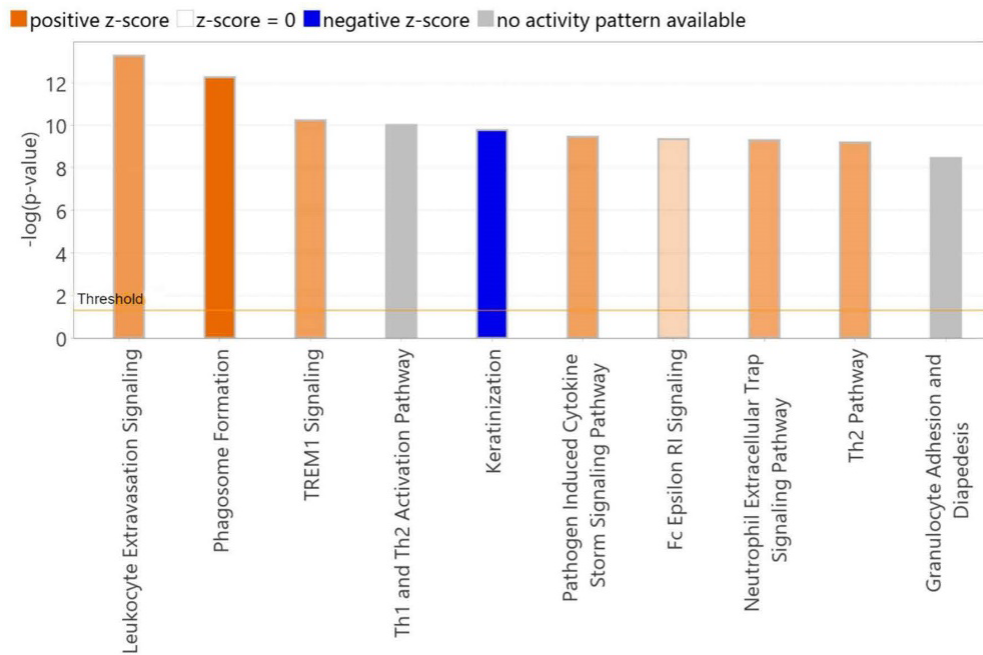
- 839 64. Molinier-Frenkel, V.; Prévost-Blondel, A.; Castellano, F. The IL4I1 Enzyme: A New Player  
840 in the Immunosuppressive Tumor Microenvironment. *Cells* **2019**, *8*,  
841 doi:10.3390/cells8070757.
- 842 65. Veiga-Parga, T.; Sehrawat, S.; Rouse, B.T. Role of Regulatory T Cells during Virus Infec-  
843 tion. *Immunol. Rev.* **2013**, *255*, 182–196, doi:10.1111/imr.12085.
- 844 66. Akeus, P.; Szeponik, L.; Langenes, V.; Karlsson, V.; Sundström, P.; Bexe-Lindskog, E.; Tal-  
845 lon, C.; Slusher, B.S.; Quiding-Järbrink, M. Regulatory T cells reduce endothelial neutral  
846 sphingomyelinase 2 to prevent T-cell migration into tumors. *Eur. J. Immunol.* **2021**, *51*,  
847 2317–2329, doi:10.1002/eji.202149208.
- 848 67. Pan, Y.; Tian, T.; Park, C.O.; Lofftus, S.Y.; Mei, S.; Liu, X.; Luo, C.; O'Malley, J.T.; Gehad,  
849 A.; Teague, J.E.; et al. Survival of tissue-resident memory T cells requires exogenous lipid  
850 uptake and metabolism. *Nature* **2017**, *543*, 252–256, doi:10.1038/nature21379.
- 851 68. Axelrod, M.L.; Cook, R.S.; Johnson, D.B.; Balko, J.M. Biological Consequences of Major  
852 Histocompatibility Class-II Expression by Tumor Cells in Cancer. *Clin. Cancer Res.* **2018**,  
853 *25*, 2392–2402, doi:10.1158/1078-0432.CCR-18-3200.
- 854 69. Draber, P.; Vonkova, I.; Stepanek, O.; Hrdinka, M.; Kucova, M.; Skopцова, T.; Otahal, P.;  
855 Angelisova, P.; Horejsi, V.; Yeung, M.; et al. SCIMP, a transmembrane adaptor protein  
856 involved in major histocompatibility complex class II signaling. *Mol. Cell. Biol.* **2011**, *31*,  
857 4550–4562, doi:10.1128/MCB.05817-11.
- 858 70. Guce, A.I.; Mortimer, S.E.; Yoon, T.; Painter, C.A.; Jiang, W.; Mellins, E.D.; Stern, L.J. HLA-  
859 DO acts as a substrate mimic to inhibit HLA-DM by a competitive mechanism. *Nat. Struct.*  
860 *Mol. Biol.* **2013**, *20*, 90–98, doi:10.1038/nsmb.2460.
- 861 71. Sarry, M.; Vitour, D.; Zientara, S.; Bakkali Kassimi, L.; Blaise-Boisseau, S. Foot-and-Mouth  
862 Disease Virus: Molecular Interplays with IFN Response and the Importance of the Model.  
863 *Viruses* **2022**, *14*, doi:10.3390/v14102129.
- 864 72. Takekoshi, T.; Fang, L.; Paragh, G.; Hwang, S.T. CCR7-expressing B16 melanoma cells  
865 downregulate interferon- $\gamma$ -mediated inflammation and increase lymphangiogenesis in the  
866 tumor microenvironment. *Oncogenesis* **2012**, *1*, e9, doi:10.1038/oncsis.2012.9.
- 867 73. Moore, K.W.; Waal Malefyt, R. de; Coffman, R.L.; O'Garra, A. Interleukin-10 and the inter-  
868 leukin-10 receptor. *Annu. Rev. Immunol.* **2001**, *19*, 683–765, doi:10.1146/annurev.immu-  
869 nol.19.1.683.
- 870 74. Zhang, Z.; Bashiruddin, J.B.; Doel, C.; Horsington, J.; Durand, S.; Alexandersen, S. Cyto-  
871 kine and Toll-like receptor mRNAs in the nasal-associated lymphoid tissues of cattle during

- 872 foot-and-mouth disease virus infection. *J. Comp. Pathol.* **2006**, *134*, 56–62,  
873 doi:10.1016/j.jcpa.2005.06.011.
- 874 75. Boehm, U.; Klamp, T.; Groot, M.; Howard, J.C. Cellular responses to interferon-gamma.  
875 *Annu. Rev. Immunol.* **1997**, *15*, 749–795, doi:10.1146/annurev.immunol.15.1.749.
- 876 76. Heil, F.; Hemmi, H.; Hochrein, H.; Ampenberger, F.; Kirschning, C.; Akira, S.; Lipford, G.;  
877 Wagner, H.; Bauer, S. Species-specific recognition of single-stranded RNA via toll-like re-  
878 ceptor 7 and 8. *Science* **2004**, *303*, 1526–1529, doi:10.1126/science.1093620.
- 879 77. Deguine, J.; Barton, G.M. MyD88: a central player in innate immune signaling. *F1000Prime*  
880 *Rep.* **2014**, *6*, 97, doi:10.12703/p6-97.
- 881 78. Xiong, M.-G.; Xu, Z.-S.; Li, Y.-H.; Wang, S.-Y.; Wang, Y.-Y.; Ran, Y. RNF152 positively reg-  
882 ulates TLR/IL-1R signaling by enhancing MyD88 oligomerization. *EMBO Rep.* **2020**, *21*,  
883 e48860, doi:10.15252/embr.201948860.
- 884 79. Fore, F.; Indriputri, C.; Mamutse, J.; Nugraha, J. TLR10 and Its Unique Anti-Inflammatory  
885 Properties and Potential Use as a Target in Therapeutics. *Immune Netw.* **2020**, *20*, e21,  
886 doi:10.4110/in.2020.20.e21.
- 887 80. Bell, M.P.; Svingen, P.A.; Rahman, M.K.; Xiong, Y.; Faubion, W.A. FOXP3 regulates TLR10  
888 expression in human T regulatory cells. *J. Immunol.* **2007**, *179*, 1893–1900,  
889 doi:10.4049/jimmunol.179.3.1893.
- 890 81. Jiang, Z.; Wei, F.; Zhang, Y.; Wang, T.; Gao, W.; Yu, S.; Sun, H.; Pu, J.; Sun, Y.; Wang, M.;  
891 et al. IFI16 directly senses viral RNA and enhances RIG-I transcription and activation to  
892 restrict influenza virus infection. *Nat. Microbiol.* **2021**, *6*, 932–945, doi:10.1038/s41564-  
893 021-00907-x.
- 894 82. Yang, W.; Li, D.; Ru, Y.; Bai, J.; Ren, J.; Zhang, J.; Li, L.; Liu, X.; Zheng, H. Foot-and-Mouth  
895 Disease Virus 3A Protein Causes Upregulation of Autophagy-Related Protein LRRC25 To  
896 Inhibit the G3BP1-Mediated RIG-Like Helicase-Signaling Pathway. *J Virol* **2020**, *94*,  
897 doi:10.1128/JVI.02086-19.
- 898 83. Wang, D.; Fang, L.; Li, P.; Sun, L.; Fan, J.; Zhang, Q.; Luo, R.; Liu, X.; Li, K.; Chen, H.; et al.  
899 The leader proteinase of foot-and-mouth disease virus negatively regulates the type I in-  
900 terferon pathway by acting as a viral deubiquitinase. *J. Virol.* **2011**, *85*, 3758–3766,  
901 doi:10.1128/JVI.02589-10.
- 902 84. Sun, S.-C. Deubiquitylation and regulation of the immune response. *Nat. Rev. Immunol.*  
903 **2008**, *8*, 501–511, doi:10.1038/nri2337.

- 904 85. Matsuzawa, A.; Saegusa, K.; Noguchi, T.; Sadamitsu, C.; Nishitoh, H.; Nagai, S.; Koyasu,  
905 S.; Matsumoto, K.; Takeda, K.; Ichijo, H. ROS-dependent activation of the TRAF6-ASK1-  
906 p38 pathway is selectively required for TLR4-mediated innate immunity. *Nat. Immunol.*  
907 **2005**, *6*, 587–592, doi:10.1038/ni1200.
- 908 86. Dubin, R.F.; Robinson, S.K.; Widdicombe, J.H. Secretion of lactoferrin and lysozyme by  
909 cultures of human airway epithelium. *Am. J. Physiol. Lung Cell. Mol. Physiol.* **2004**, *286*,  
910 L750-5, doi:10.1152/ajplung.00326.2003.
- 911 87. Moutsopoulos, N.M.; Nares, S.; Nikitakis, N.; Rangel, Z.; Wen, J.; Munson, P.; Sauk, J.;  
912 Wahl, S.M. Tonsil epithelial factors may influence oropharyngeal human immunodeficiency  
913 virus transmission. *Am. J. Pathol.* **2007**, *171*, 571–579, doi:10.2353/aj-  
914 path.2007.061006.
- 915 88. Murakami, M. Novel functions of phospholipase A2s: Overview. *Biochim. Biophys. Acta*  
916 *Mol. Cell Biol. Lipids* **2019**, *1864*, 763–765, doi:10.1016/j.bbalip.2019.02.005.
- 917 89. Khan, S.A.; Ilies, M.A. The Phospholipase A2 Superfamily: Structure, Isozymes, Catalysis,  
918 Physiologic and Pathologic Roles. *Int. J. Mol. Sci.* **2023**, *24*, doi:10.3390/ijms24021353.
- 919 90. Gao, Y.; Lu, J.; Bao, X.; Yi, X.; Peng, C.; Chen, W.; Zhen, T.; Shi, Y.; Xing, K.; Zhu, S.; et al.  
920 Inhibition of phospholipases suppresses progression of psoriasis through modulation of  
921 inflammation. *Exp. Biol. Med. (Maywood)* **2021**, *246*, 1253–1262,  
922 doi:10.1177/1535370221993424.
- 923 91. Miki, Y.; Yamamoto, K.; Taketomi, Y.; Sato, H.; Shimo, K.; Kobayashi, T.; Ishikawa, Y.; Ishii,  
924 T.; Nakanishi, H.; Ikeda, K.; et al. Lymphoid tissue phospholipase A2 group IID resolves  
925 contact hypersensitivity by driving antiinflammatory lipid mediators. *J. Exp. Med.* **2013**,  
926 *210*, 1217–1234, doi:10.1084/jem.20121887.
- 927 92. Tsai, A.P.; Dong, C.; Lin, P.B.-C.; Messenger, E.J.; Casali, B.T.; Moutinho, M.; Liu, Y.; Oblak,  
928 A.L.; Lamb, B.T.; Landreth, G.E.; et al. PLAG2 is associated with the inflammatory response  
929 and is induced by amyloid plaques in Alzheimer's disease. *Genome Med.* **2022**, *14*, 17,  
930 doi:10.1186/s13073-022-01022-0.
- 931 93. Litz, B.; Sehl-Ewert, J.; Breithaupt, A.; Landmesser, A.; Pfaff, F.; Romey, A.; Blaise-Bois-  
932 seau, S.; Beer, M.; Eschbaumer, M. Leaderless foot-and-mouth disease virus serotype O  
933 did not cause clinical disease and failed to establish a persistent infection in cattle. *Emerg.*  
934 *Microbes Infect.* **2024**, 2348526, doi:10.1080/22221751.2024.2348526.

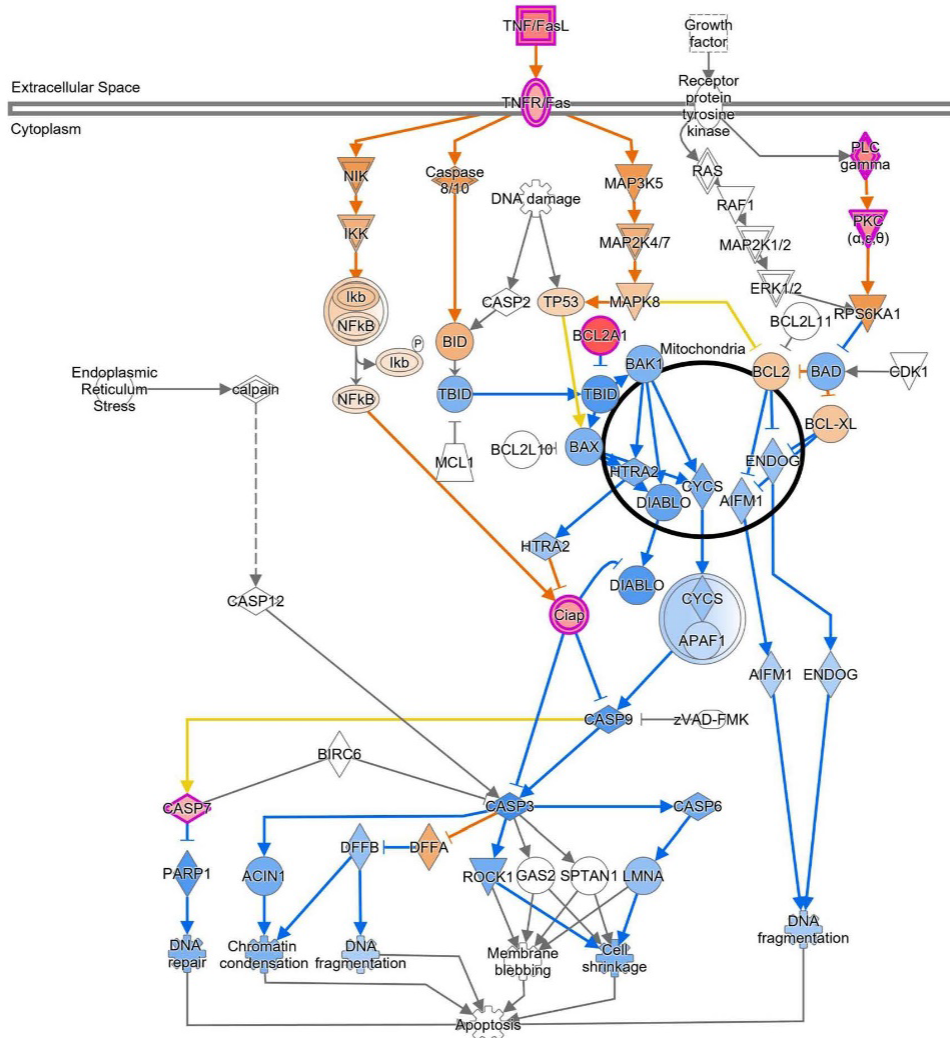
- 935 94. Fu, Y.; Zhan, X.; Wang, Y.; Jiang, X.; Liu, M.; Yang, Y.; Huang, Y.; Du, X.; Zhong, X.-P.; Li,  
936 L.; et al. NLRC3 expression in dendritic cells attenuates CD4+ T cell response and auto-  
937 immunity. *EMBO J.* **2019**, *38*, e101397, doi:10.15252/embj.2018101397.
- 938 95. Chow, A.; Schad, S.; Green, M.D.; Hellmann, M.D.; Allaj, V.; Ceglia, N.; Zago, G.; Shah,  
939 N.S.; Sharma, S.K.; Mattar, M.; et al. Tim-4+ cavity-resident macrophages impair anti-tu-  
940 mor CD8+ T cell immunity. *Cancer Cell* **2021**, *39*, 973-988.e9,  
941 doi:10.1016/j.ccell.2021.05.006.
- 942 96. Hosseini, A.; Gharibi, T.; Marofi, F.; Babaloo, Z.; Baradaran, B. CTLA-4: From mechanism  
943 to autoimmune therapy. *Int. Immunopharmacol.* **2020**, *80*, 106221, doi:10.1016/j.in-  
944 timp.2020.106221.
- 945 97. Xu, D.; Liu, X.; Ke, S.; Guo, Y.; Zhu, C.; Cao, H. CCL19/CCR7 drives regulatory T cell  
946 migration and indicates poor prognosis in gastric cancer. *BMC Cancer* **2023**, *23*, 464,  
947 doi:10.1186/s12885-023-10882-7.
- 948 98. Rougerie, P.; Largeteau, Q.; Megrelis, L.; Carrette, F.; Lejeune, T.; Toffali, L.; Rossi, B.;  
949 Zeghouf, M.; Cherfils, J.; Constantin, G.; et al. Fam65b is a new transcriptional target of  
950 FOXO1 that regulates RhoA signaling for T lymphocyte migration. *J. Immunol.* **2013**, *190*,  
951 748–755, doi:10.4049/jimmunol.1201174.
- 952 99. Morita, K.; Okamura, T.; Sumitomo, S.; Iwasaki, Y.; Fujio, K.; Yamamoto, K. Emerging roles  
953 of Egr2 and Egr3 in the control of systemic autoimmunity. *Rheumatology (Oxford)* **2016**,  
954 *55*, ii76-ii81, doi:10.1093/rheumatology/kew342.
- 955 100. Shi, A.-P.; Tang, X.-Y.; Xiong, Y.-L.; Zheng, K.-F.; Liu, Y.-J.; Shi, X.-G.; Lv, Y.; Jiang, T.; Ma,  
956 N.; Zhao, J.-B. Immune Checkpoint LAG3 and Its Ligand FGL1 in Cancer. *Front. Immunol.*  
957 **2021**, *12*, 785091, doi:10.3389/fimmu.2021.785091.
- 958 101. Khan, O.; Giles, J.R.; McDonald, S.; Manne, S.; Ngiow, S.F.; Patel, K.P.; Werner, M.T.;  
959 Huang, A.C.; Alexander, K.A.; Wu, J.E.; et al. TOX transcriptionally and epigenetically pro-  
960 grams CD8+ T cell exhaustion. *Nature* **2019**, *571*, 211–218, doi:10.1038/s41586-019-  
961 1325-x.
- 962 102. Shen, R.; Ouyang, Y.-B.; Qu, C.-K.; Alonso, A.; Sperzel, L.; Mustelin, T.; Kaplan, M.H.; Feng,  
963 G.-S. Grap negatively regulates T-cell receptor-elicited lymphocyte proliferation and inter-  
964 leukin-2 induction. *Mol. Cell. Biol.* **2002**, *22*, 3230–3236, doi:10.1128/MCB.22.10.3230-  
965 3236.2002.

- 966 103. Itahashi, K.; Irie, T.; Yuda, J.; Kumagai, S.; Tanegashima, T.; Lin, Y.-T.; Watanabe, S.; Goto,  
967 Y.; Suzuki, J.; Aokage, K.; et al. BATF epigenetically and transcriptionally controls the ac-  
968 tivation program of regulatory T cells in human tumors. *Sci. Immunol.* **2022**, *7*, eabk0957,  
969 doi:10.1126/sciimmunol.abk0957.
- 970 104. Marie-Cardine, A.; Kirchgessner, H.; Bruyns, E.; Shevchenko, A.; Mann, M.; Autschbach,  
971 F.; Ratnofsky, S.; Meuer, S.; Schraven, B. SHP2-interacting transmembrane adaptor pro-  
972 tein (SIT), a novel disulfide-linked dimer regulating human T cell activation. *J. Exp. Med.*  
973 **1999**, *189*, 1181–1194, doi:10.1084/jem.189.8.1181.
- 974
- 975



© 2000-2024 QIAGEN. All rights reserved.

**Supplemental Figure S1.** Top 10 canonical pathways sorted by p-value. A right-tailed Fisher's Exact Test was used to calculate a p-value determining the probability that the association between the genes in the dataset and the canonical pathway is explained by chance alone. Z-score indicates the likelihood of activation or inhibition of that pathway.



© 2000-2024 QIAGEN. All rights reserved.

**S2 Fig. Integrated pathway analysis of the apoptosis canonical pathway.** Solid lines are direct relationships and dashed lines are indirect. Purple outline = measured as differentially expressed - intensity of colored infill indicating the level of up (red) or down (green) regulation, Blue color = predicted inhibition, Orange = predicted activation (Molecular Activity Predictor function), Yellow lines = inconsistency with the state of the downstream molecule. Functional classes: Nested Circle/Square = Group/Complex, Horizontal ellipse = Transcriptional Regulator, Vertical Ellipse = transmembrane receptor, Vertical Rhombus = enzyme, Square = Cytokine/Growth Factor, Triangle = Kinase, Vertical Ellipse = Transmembrane Receptor, Circle = other

**S1 Table.** Tissue Samples (n=52) collected during necropsy submitted for RNAseq 951 transcriptomic analysis

Sample	Tissue	Animal	Subsample	Group	Virusisolation Probang 35dpi	mean Cq FMD-3D-OIE-Mix (n=2)
61	DNP	190	1	CAV-2-MKS i.n.	pos	35,38
65	DNP	190	5	CAV-2-MKS i.n.	pos	36,33
70	DSP	190	5	CAV-2-MKS i.n.	pos	27,09
181	DNP	191	1	PBS i.n.	pos	31,84
184	DNP	191	4	PBS i.n.	pos	33,72
71	DNP	425	1	CAV-2-MKS i.n.	pos	36,72
121	DNP	426	1	Merial O-675 i.m.	neg	N/A
122	DNP	426	2	Merial O-675 i.m.	neg	N/A
123	DNP	426	3	Merial O-675 i.m.	neg	N/A
129	DSP	426	4	Merial O-675 i.m.	neg	30,57
130	DSP	426	5	Merial O-675 i.m.	neg	N/A
172	DNP	507	2	PBS i.n.	pos	33,73
179	DSP	507	4	PBS i.n.	pos	29,09
180	DSP	507	5	PBS i.n.	pos	30,00
91	DNP	509	1	CAV-2-MKS i.n.	pos	N/A
97	DSP	509	2	CAV-2-MKS i.n.	pos	26,40
11	DNP	510	1	CAV-2-MKS i.m.	pos	39,49
15	DNP	510	5	CAV-2-MKS i.m.	pos	38,82
20	DSP	510	5	CAV-2-MKS i.m.	pos	29,07
111	DNP	647	1	Merial O-675 i.m.	pos	36,38
115	DNP	647	5	Merial O-675 i.m.	pos	N/A
119	DSP	647	4	Merial O-675 i.m.	pos	26,16
120	DSP	647	5	Merial O-675 i.m.	pos	26,84
101	DNP	649	1	Merial O-675 i.m.	pos	36,95
108	DSP	649	2	Merial O-675 i.m.	pos	N/A
191	DNP	662	1	CAV-2-MKS i.n.	neg	37,25
193	DNP	662	3	CAV-2-MKS i.n.	neg	N/A
196	DSP	662	1	CAV-2-MKS i.n.	neg	37,42
198	DSP	662	3	CAV-2-MKS i.n.	neg	N/A
41	DNP	663	1	CAV-2-MKS i.m.	pos	N/A
45	DNP	663	5	CAV-2-MKS i.m.	pos	N/A
46	DSP	663	1	CAV-2-MKS i.m.	pos	N/A
47	DSP	663	2	CAV-2-MKS i.m.	pos	37,87
31	DNP	669	1	CAV-2-MKS i.m.	pos	39,17
32	DNP	669	2	CAV-2-MKS i.m.	pos	N/A
37	DSP	669	2	CAV-2-MKS i.m.	pos	25,95
39	DSP	669	4	CAV-2-MKS i.m.	pos	24,93
1	DNP	940	1	Merial O-675 i.m.	neg	39,88
6	DSP	940	1	Merial O-675 i.m.	neg	N/A

7	DSP	940	2	Merial O-675 i.m.	neg	38,02
141	DNP	943	1	Merial O-675 i.m.	pos	38,20
149	DSP	943	4	Merial O-675 i.m.	pos	34,65
150	DSP	943	5	Merial O-675 i.m.	pos	N/A
151	DNP	945	1	PBS i.n.	pos	37,05
153	DNP	945	3	PBS i.n.	pos	33,82
155	DNP	945	5	PBS i.n.	pos	N/A
158	DSP	945	3	PBS i.n.	pos	N/A
159	DSP	945	4	PBS i.n.	pos	36,88
160	DSP	945	5	PBS i.n.	pos	N/A
83	DNP	946	3	CAV-2-MKS i.n.	pos	N/A
87	DSP	946	2	CAV-2-MKS i.n.	pos	35,57
90	DSP	946	5	CAV-2-MKS i.n.	pos	36,75



3. Publication III: Distinct mutations emerge in the genome of serotype O foot-and-mouth disease virus during persistence in cattle

Publication III

**Distinct mutations emerge in the genome of serotype O foot-and-mouth disease virus during persistence in cattle**

Benedikt Litz, Leonie Forth, Florian Pfaff, Martin Beer, Michael Eschbaumer

Journal of Virology

2025

<https://doi.org/10.1128/jvi.01422-2>

# Distinct mutations emerge in the genome of serotype O foot-and-mouth disease virus during persistence in cattle

Benedikt Litz,<sup>1</sup> Leonie F. Forth,<sup>1</sup> Florian Pfaff,<sup>1</sup> Martin Beer,<sup>1</sup> Michael Eschbaumer<sup>1</sup>

**AUTHOR AFFILIATION** See affiliation list on p. 23.

**ABSTRACT** Like other RNA viruses, foot-and-mouth disease virus (FMDV) has a high mutation rate. After the acute phase of infection, about half of infected cattle develop a persistent FMDV infection that can last for weeks or months. During this persistent phase, the virus continues to replicate, resulting in the emergence of genomic heterogeneity. We have documented the pattern of mutations in the persistent phase by obtaining consensus-level sequences directly from oropharyngeal fluid (OPF) without prior virus isolation in culture. OPF samples were repeatedly collected from 22 experimentally infected cattle, 20 of which were virus positive in the OPF on day 21 after infection or later. We observed that during the persistent phase, the amount of non-synonymous mutations causing an amino acid change increased over time. Two amino acid changes that showed a striking increase during the persistent phase, VP3 A75T and VP2 Y79H, were present neither in the inoculum nor during the acute phase. Another amino acid change in VP3, R56C, which was previously implicated in FMDV pathogenicity, was already present in the inoculum and dominated toward the end of the trial in most samples. Several other amino acid changes occurred, particularly on the surface of VP2 around residue VP2 79. By functional analysis, we show that the persistent isolates evolve distinctly compared with cell culture adaptation but do not show signs of antigenic escape from neutralizing antibodies. In agreement with previous observations, we conclude that these amino acid changes are indeed associated with persistent infection of cattle with FMDV serotype O.

**IMPORTANCE** Our research article describes the genetic changes that occur during the acute and persistent foot-and-mouth disease (FMDV) infection. This is of particular interest to understand viral dynamics within an infected population from which new viral strains could emerge. Especially FMDV, with its high antigenic diversity and very limited cross-reactivity between strains and serotypes, has already demonstrated in the past that new variants can quickly emerge and evade vaccine responses. In our study, we have observed that this dynamic evolution continues during the persistent phase. Persistently infected animals, which are clinically indistinguishable from healthy animals, also pose a reservoir for recombination. A better understanding of viral dynamics is essential for improved vaccines to prevent the emergence of antigenic variants.

**KEYWORDS** FMDV, persistence, carrier, sequencing, mutation, SNP

RNA viruses have developed a distinct evolutionary strategy by maintaining a high error rate of their RNA-dependent RNA polymerase. The naturally occurring virus population is therefore, in some cases, composed of a viral swarm or quasispecies, which supports rapid adaptation to changing environments (1). For foot-and-mouth disease virus (FMDV, species *Aphthovirus vesiculae*), which belongs to the genus *Aphthovirus* in the family *Picornaviridae*, the high mutation rate has resulted in a diverse set of seven serotypes with many subtypes. The mutation rate is estimated to be  $7.8 \times 10^{-4}$

**Editor** Anice C. Lowen, Emory University School of Medicine, Atlanta, Georgia, USA

Address correspondence to Michael Eschbaumer, Michael.Eschbaumer@fli.de

The authors declare no conflict of interest.

See the funding table on p. 23.

**Received** 15 August 2024

**Accepted** 21 December 2024

**Published** 7 February 2025

Copyright © 2025 Litz et al. This is an open-access article distributed under the terms of the Creative Commons Attribution 4.0 International license.

per nucleotide and transcription event, which equals approximately one mutation per genome per replication cycle (2). In comparison, severe acute respiratory syndrome coronavirus 2 (SARS-CoV-2) has a mutation rate of  $1.3 \times 10^{-6}$  per nucleotide and infection cycle (3). Eradication measures against FMD, a highly infectious transboundary disease of livestock, are impeded by the limited cross-reactivity between newly emerging strains and available vaccines, due to the high genetic and antigenic diversity of FMDV (4).

The FMDV genome codes for one large open reading frame (ORF), which is translated into a single polyprotein. This polyprotein contains the precursor of four structural proteins (VP1, VP2, VP3, and VP4) and eight non-structural proteins ( $L^{pro}$ , 2A, 2B, 2C, 3A, 3B<sup>1-3</sup>, 3C, and 3D). The structural proteins form the capsid, with VP1, VP2, and VP3 exposed on the outer surface, while VP4 is located on the inside of the capsid (5). Therefore, the structural proteins on the outside are major targets of neutralizing antibodies, while VP4 is hidden from the humoral response. The capsid surface features five antigenic sites, which influence the serotype and cross-reactivity. The “antigenic site 1” on VP1 has long been considered to be immunodominant and stood in the focus of research, but following vaccination against serotype O, the strongest antibody response was directed against “antigenic site 2” on the surface of VP2 (6). A peculiarity of “site 1,” however, is the G-H loop of VP1 with an RGD-binding motif, which facilitates the binding to integrin receptors as a first step in viral cell entry. Apart from its antigenicity and the receptor-binding domain, the G-H loop of VP1 is motile and its orientation can influence its antigenicity (7).

FMDV causes a highly infectious disease in cloven-hoofed animals characterized by vesicular lesions in the mouth, on the muzzle, and in the interdigital cleft. In about 50% of FMDV-infected cattle, the virus remains in the cattle after the acute phase and persistently infects the epithelia of the nasopharynx. These persistently infected animals are called “virus carriers.” The persistent phase of infection follows the acute phase characterized by clinical signs of FMD and usually resolves after 10 days postinfection (dpi). The animal then enters a transitional stage in which virus is either cleared from the nasopharynx or remains persistent (8). An infection that lasts longer than 28 dpi is conventionally defined as a persistent infection, while the earliest time point for identifying persistently infected cattle is as early as 21 dpi (9). Even though infectious virus can be recovered from persistently infected cattle by sampling oropharyngeal fluid (OPF) with a probang cup, which collects superficial cells and saliva from the pharynx (10), it is still debated whether persistently infected cattle are contagious at all (8, 11).

The preferred sites of persistent infection are the epithelia of the nasopharynx, namely the dorsal nasopharynx (DNP) and the opposing dorsal soft palate (DSP). Here, the follicle-associated epithelia (FAE), which covers the mucosa-associated lymphoid tissue (MALT), are infected (9). The patchy distribution of the MALT in the pharynx results in a very focal occurrence of persistent infection (12). Because this remote location is not easily accessible by standard sampling techniques, use of the probang cup was established early in FMDV research. Using this metal cup, saliva and epithelial cell scrapings are collected from the pharynx, the so-called oropharyngeal fluid (OPF), from which virus can be recovered if the animal is persistently infected (13).

In Theiler's virus (species *Cardiovirus theileri*), a picornavirus causing infection of the central nervous system in mice, a single amino acid change is responsible for the persistent virus phenotype (14); hence, studies of virus isolates from the persistent phase of FMDV were focused on finding similar mutations. Historically, sequencing was focused on VP1, as performed by Gebauer et al., who claimed that the number of amino acid substitutions fixed in VP1 during the persistent phase was similar to that after several years of acute-phase transmission (15). Other studies found certain amino acid changes to be associated with persistent infection (16, 17), but these were observed to also occur during acute transmission and were not considered unique to persistent replication (18). More recent investigations using whole-genome sequencing focused on the mechanisms of virus evolution during the persistent phase (19, 20). They showed that early during the acute phase, several haplotypes, which were acquired in the infection, can

coexist, but over time haplotypes with new mutations become increasingly dominant. During the persistent phase, multiple viral subpopulations within an animal could still be distinguished, reflecting the focal nature of infection.

We sequenced the entire ORF of FMDV from 20 persistently infected animals directly from OPF without prior amplification in cell culture. To our knowledge, this is the largest set of native whole-ORF sequences from experimentally infected carriers collected so far. Samples were collected in the acute, transitional, and persistent phases. This allowed us to document the evolution of FMDV and its adaptation to the host.

## RESULTS

### Animal trials

In the vaccination study, animals vaccinated with the experimental vaccine were not protected from challenge infection and developed clinical signs with vesicular lesions similar to those observed in non-vaccinated animals. The commercially vaccinated cattle did not develop clinical signs. However, the efficacy of the vaccines and the outcome of the challenge infection are outside of the scope of this paper. An overview of clinical data collected in the vaccination study is shown in Fig. S1. In the infection study, all animals developed clinical signs consistent with FMDV.

### Variation in the inoculum

For the vaccination trial, the plaque-purified clone of FMDV O/FRA/1/2001 was passaged once in a heifer. Lesion material from the tongue was collected and deep sequenced to examine the consensus sequence and minor variants. The consensus sequence remained unchanged in comparison with the plaque-purified clone (GenBank accession [OV121130](#)); however, 50 minor variants were detected with a frequency between 0.5% and 22% (Table S1). Of the 50 minor variants, 33 were in the coding region, of which 25 were non-synonymous variants. Of the 33 variants in the ORF, 25 variants were in the P1 region, with three variants in VP4, six variants in VP2, 10 variants in VP3, and six variants in VP1. In some cases, two variants were found at the same position (e.g., positions 2352 and 2354 corresponding to residue 134 of VP2, positions 2772 and 2773 corresponding to residue 56 of VP3; Table S1). Neighboring variants were not present on the same read and are therefore likely to represent independent genomic variants. From the non-synonymous variants, seven variants rose to consensus level at a later time point of the trial. Majority of these are located in the capsid-coding region. The minor variant with the highest frequency in the inoculum, VP3 R56C (22.1%), later became dominant in the vast majority of consensus sequences recovered throughout the whole study, from the acute phase as well as from the persistent phase of infection. Not all variants were detected throughout the study. Missense variants like VP3 R56L, VP1 H195L, and VP1 H195Q were detected at the consensus level in samples from the acute phase but were absent in OPF samples from 10 dpi onward. VP3 G60D was present in the inoculum at 2% and detectable at the consensus level in samples from the acute phase. It then disappeared from the consensus sequences, only to reappear at 35 dpi in animal 509. Another missense variant was absent in the acute phase but emerged during persistent infection: 3A S140F, which was found in the consensus sequences of two animals (ID 943 and 946) from 14 and 17 dpi, respectively, onward until the end of the study as well as a polymorphic variant in animal 506 at 28 dpi. VP1 A199D was also present in the inoculum and re-appeared in animal 649 during persistence at 28 and 35 dpi. The variants VP3 56, VP1 195, and 199 are known to be associated with heparan sulfate (HS)-binding sites (21, 22).

In a comparison with field isolates from a large outbreak caused by a closely related virus in the United Kingdom in 2001 (23), six amino acids were different in our inoculum: L<sup>Pro</sup> I104V, VP3 H56R, VP1 E198G, 3A I3S, 3D A94T, and 3D F294I.

### Variation in vesicular lesions from the acute phase

Deep sequencing of vesicular material from six animals collected during the acute phase revealed changes in the consensus sequence in each sample, including one to three variants fixed in the consensus sequence and four to nine minor variants in the coding region compared with the inoculum. In animal 191, variants at nucleotide positions 2772 and 2773 were present at frequencies of 50.2% and 49.3%, respectively, encoding VP3 R56C and R56H, with only the first represented in the consensus sequence. These two variants were not found on the same reads, likely representing uncorrelated mutations.

Four minor variants from the inoculum were also found in these samples: VP3 R56C, VP3 R56H, VP3 G60D, and VP1 H195Q. Of these, VP3 R56C was dominant in three animals and was present as a minor variant in two others but was not detectable in the sample from one animal (ID 509). Additionally, three minor variants from the vesicular material were detected at the consensus level in other samples from the acute phase of the same animal but not during the persistent phase (2A F4S, 2C P220L, 3D H378T). Interestingly, 2A F4S and 3D H378T were detected in samples from the acute phase of one other animal.

### Incidence of persistent infection and probang samples

Persistently infected animals were defined by positive virus isolation from the OPF collected by probang cup after 28 dpi (24). In the vaccination trial, virus was isolated from 17 of 20 infected animals after 28 dpi, and in one additional animal (ID 940), virus was recovered from the OPF at 24 dpi but not at 28 or 35 dpi. In vaccinated animals, the carrier state can be reliably determined as early as 10 dpi (8); therefore, we included animal 940 in the group of persistently infected animals in further studies. With this animal included, the incidence of persistent infection is 90% (with a confidence interval of 70%–97%). From the two animals, 426 and 662, no virus was recovered from the OPF at any time. Animal 426 had received the commercial vaccine and was clinically protected, but animal 662 had received the experimental vaccine intranasally and developed clinical FMD.

The virus isolation results are consistent with the FMDV RT-qPCR data for the OPF as shown in Fig. 1. There is no definite C<sub>q</sub> (quantification cycle) threshold above which virus isolation from the OPF is not possible, but above a C<sub>q</sub> value of 35, the rate of positive virus isolations decreases and few positive results are obtained for such samples. Overall, the amount of detectable FMDV RNA often fluctuates between sample days. The overall mean C<sub>q</sub> value was 31.8. This is significantly lower than the amount of FMDV RNA detected in nasal fluid during the acute phase (data not shown). The highest FMDV RNA content in the OPF, corresponding to a C<sub>q</sub> of 24, was detected in a sample from animal 190 collected at 35 dpi.

### Nucleotide sequence data from the acute and persistent phases

For this study, we analyzed 130 consensus-level sequences spanning the FMDV ORF from 21 animals. A complete sequence of the ORF was obtained for 97 persistent-phase samples from 18 animals. From the acute phase of infection, one serum and one nasal fluid sample collected between 3 and 6 dpi from 16 animals were sequenced. From animals 758 and 773, an additional saliva sample was sequenced. In the clinically protected animals, low levels of viral RNA were detectable in some acute-phase samples by RT-qPCR, but it was too low to be sequenced. For probang samples, the threshold for recovering a full-length ORF sequence was estimated to be around a C<sub>q</sub> of 35, which is similar to the viral load necessary for successful virus isolation mentioned above.

### Virus phylogeny

For a phylogenetic analysis to assess the evolution of FMDV over the course of the infection, the sequences were categorized into three phases: the acute phase for samples collected between 3 to 6 dpi, the transitional phase for OPF collected between 10 and 21

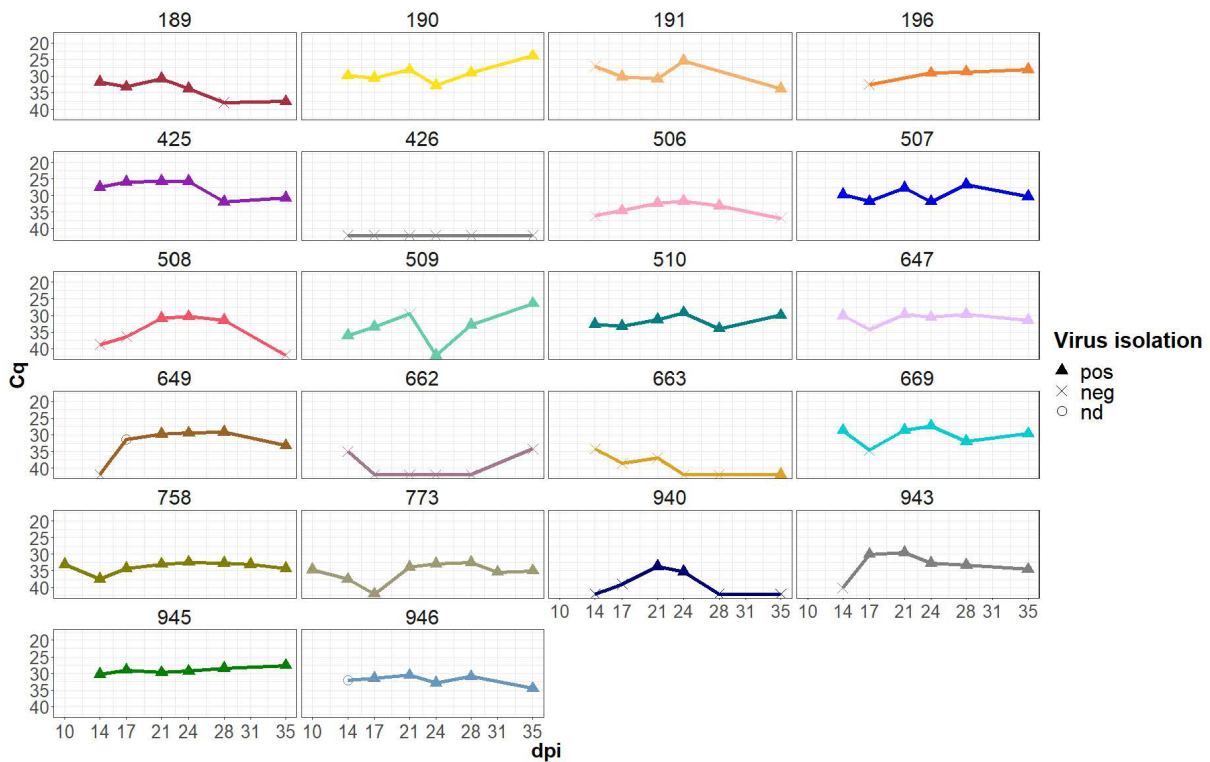


FIG 1 FMDV RT-qPCR results for OPF collected by probang cup starting at 10 or 14 dpi. The results of the virus isolation from the same sample are indicated by the shape of each data point (pos, positive virus isolation/CPE; neg, negative virus isolation/no CPE; nd, not done).

dpi, and the persistent phase for OPF collected later than 21 dpi. In the phylogenetic tree, samples appeared to cluster based on the phase of infection. Samples from the acute phase formed two separate clusters. Also, sequences from the transient and persistent phases clustered closely together (Fig. 2). Transient- and persistent-phase samples within the same animal tended to group together. In terms of infection progression, we did not observe a clear phylogenetic trend for OPF samples from later phases of infection to segregate from samples from earlier phases. In some animals, such as ear tags 758 and 773, this seemed to be the case and suggests an accumulation of mutations during infection, but in others (e.g., ear tags 196 and 669), no definite clusters differentiating OPF sequences from the transient and persistent phase can be distinguished.

However, in terms of infection progression, they are based on only a few or even single mutations in the sequences, and the construction of a phylogenetic tree may be compromised by this. Therefore, a classical multidimensional scaling was performed based on the sequence alignment. Distances between each sample were calculated based on the number of different nucleotides between each sequence, and the distances were calculated between them in two dimensions by multidimensional scaling. The distances between the samples were illustrated in a scaled interpretation of this distance matrix (Fig. 3). The findings therein support the results from the phylogenetic tree, which show a close relationship of acute-phase samples to the inoculum and clustered probang samples from the persistent phase of each animal, but still there are some outliers. We did not observe a distinct cluster of samples from the late phase of persistent infection separated from earlier samples from the transitional phase.

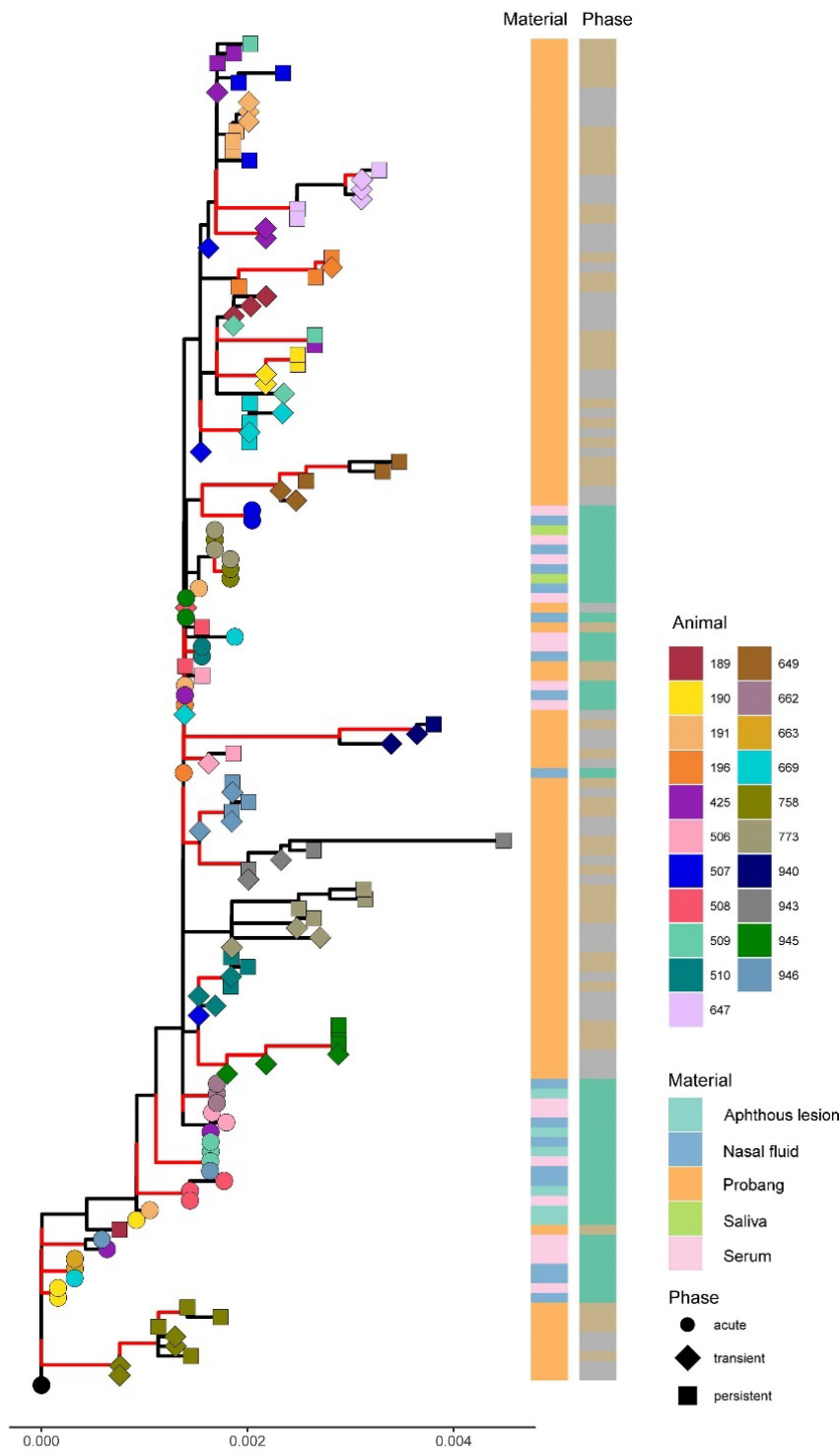
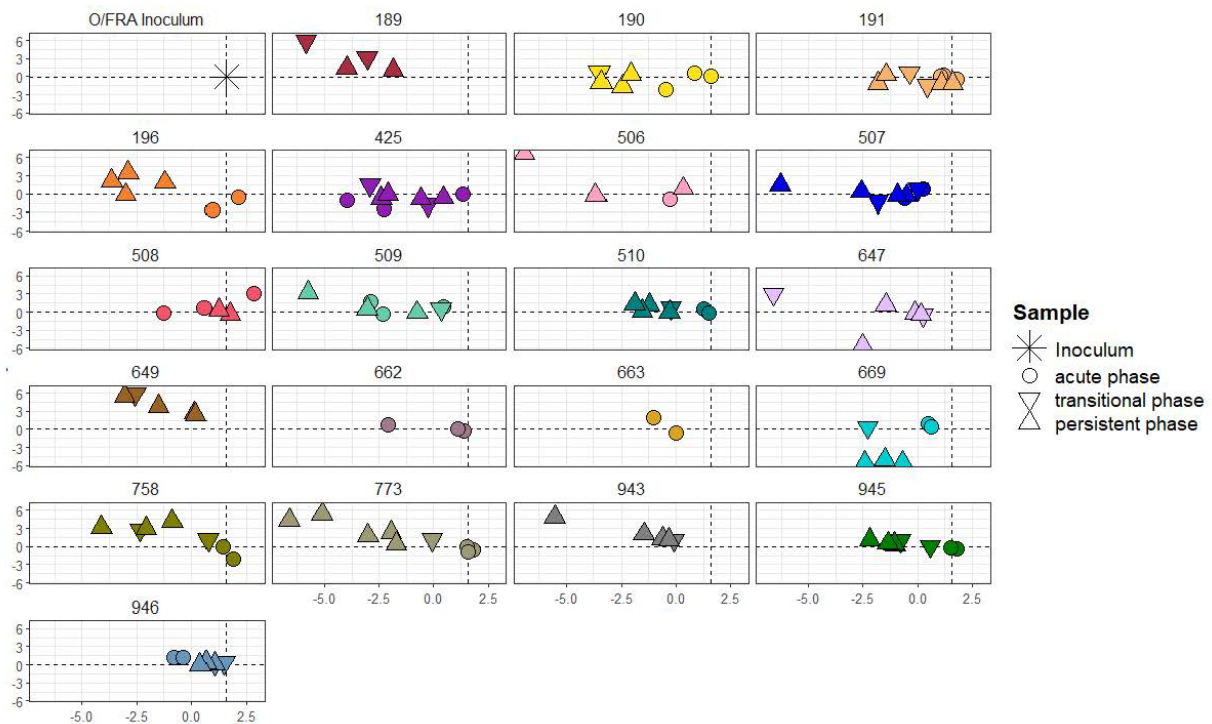


FIG 2 Inoculum-rooted phylogenetic tree of the sequences obtained from cattle persistently infected with FMDV, categorized by animal, sampling material, and phase (acute-phase samples were collected from 3 to 6 dpi, transient-phase samples were collected from 10 to 21 dpi, and persistent-phase samples were collected after 21 dpi). All samples from the same animal are displayed in the same color in the tree. Branches are color coded according to their bootstrap support: ≥95% red; <95% black.



**FIG 3** Scaled interpretation of a distance matrix based on the sequences obtained from cattle persistently infected with FMDV (acute-phase samples were collected from 3 to 6 dpi, transient-phase samples were collected from 10 to 21 dpi, and persistent-phase samples were collected after 21 dpi). The inoculum as the origin is indicated in each panel by the intersection of a vertical and a horizontal dashed line. Thirteen samples were excluded from the detailed view.

### Cell culture passage influences FMDV sequences

We compared persistent-phase sequences that were obtained directly from the *ex vivo* OPF sample (probang) with sequences obtained from the same OPF samples after one passage in LFBK- $\alpha$ V $\beta$ 6 cells, as sequencing of persistent FMDV is usually performed after a cell culture passage because of low viral loads in the OPF (15, 19). The sequences obtained from the virus isolates were in two parts and did not cover the complete ORF; therefore, the comparison only includes Lpro to VP3 and the 3' half of 2C, 3A, and 3B1-3. The phylogenetic tree for the culture-passaged samples showed a higher degree of sample diversification (data not shown). Some samples from the same animal still clustered together, but more samples from the same individual were scattered across the tree, clustering with sequences from other animals. A side-by-side comparison of the sequences from the culture-passaged samples with directly sequenced samples shows that the mutations found in them were different (see Fig. 4). Generally, more mutations in comparison with the inoculum were present in sequences from the culture-passaged samples (in this set: 76 variants in sequences from the native OPF and 151 variants in the sequences after cell culture passage). New mutations appeared after the passage, and in a few samples, mutations that were present in directly sequenced samples could no longer be detected after passaging. This included the variation at nucleotide position 2040 (amino acid VP2 31), which was present in seven sequences from the native OPF as heterozygotes (ambiguous base call in the Sanger sequencing; counted as 0.5 for the y-axis of Fig. 4) but not detectable in the corresponding cell culture samples. Most of the mutations that were introduced by a single cell culture passage were unique and only detected in one sequence. In general, most mutations found in sequences from the native OPF samples were preserved in the corresponding culture sequences but to a varying degree. The highest difference between mutations observed in the native and

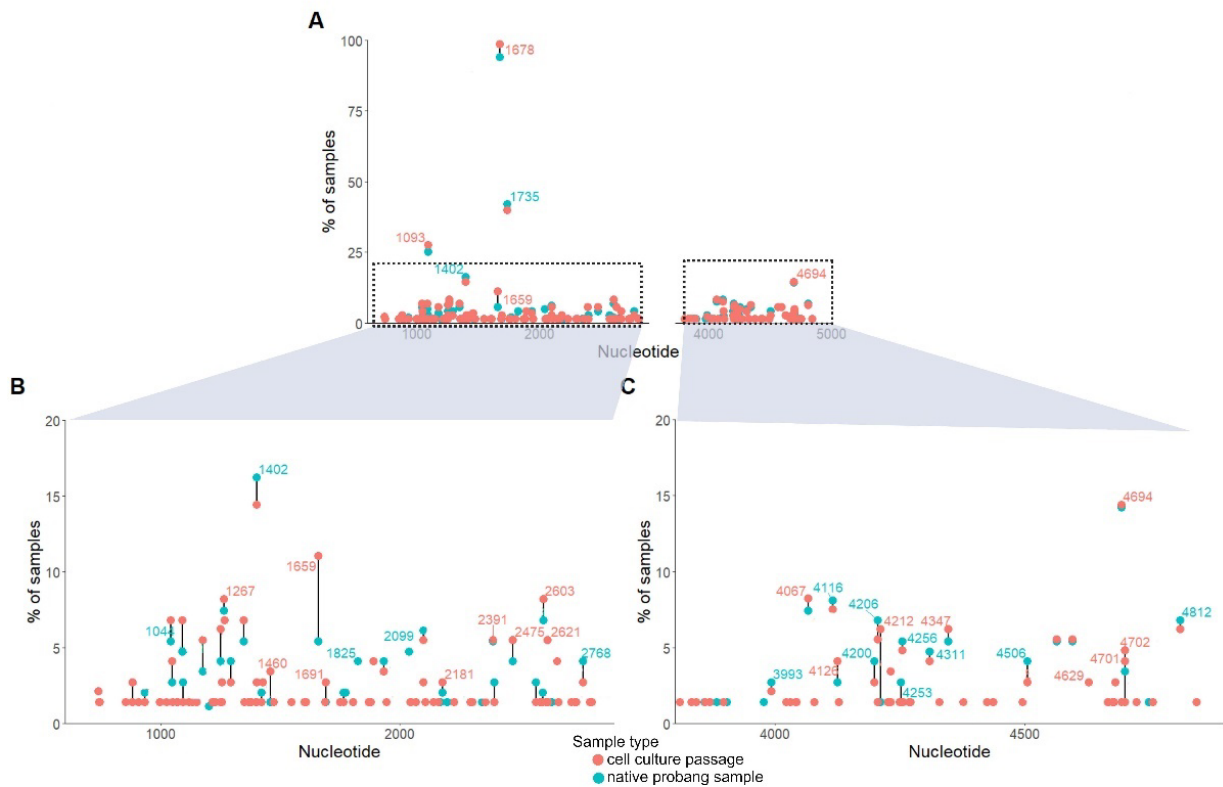


**FIG 4** Comparison of mutation frequencies in sequences obtained directly from native OPF collected by probang (blue) and after one cell culture passage (red). Two parts of the genome were included in the comparison, from Lpro to VP3 (nucleotides 600–2900, left) and from 2C to 3B3 (3800–4900, right). (A) Overview of all mutations in the compared regions; the gap on the x-axis indicates where no sequencing was performed. (B and C) Detailed view of the data from panel A. (B) Only shows mutations between nucleotides 600 and 2900 and with a frequency of less than 20%. (C) Shows only mutations between nucleotides 3800 and 4900 and with a frequency of less than 20%. The comparison only includes samples for which a pair of corresponding sequences (cell culture and native probang) was available.

cell-culture-passaged virus was found at nucleotide position 1659 (amino acid L<sup>190</sup>). Only in half of the samples that contained a variation at this site in the native OPF was the variation preserved in the cell culture passage.

### Mutations during the acute phase

The consensus sequences of the six vesicular samples and 33 Sanger-sequenced samples from the acute phase (serum, nasal fluid, and saliva) were mapped against the consensus sequence of the inoculum. Herein, we observed 27 mutations, of which 10 were missense mutations. In more than half of the samples (59%) from 11 animals, VP3 R56C was dominant in the consensus sequence. Only three of the acute-phase mutations were later seen in samples from the persistent phase: VP3 R56C, VP3 G60D, and a synonymous mutation at nucleotide 3971 corresponding to amino acid residue 7 of 2B. A detailed breakdown of amino acid changes by animal and sample is given in Table S2.

### Mutations during the persistent phase

In the consensus sequences ( $n = 97$ ) recovered from the OPF in the transitional and persistent phases, 142 mutations were detected. Thereof, 46 mutations coded for an amino acid change. A detailed list of non-synonymous nucleotide mutations by day and animal is shown in Fig. 5. The mutations that were present in most samples are three non-synonymous mutations VP3 R56C (found in 84 samples), VP3 A75T (in 36 samples),

animal ID	vaccine	clinical FMD	carrier animal	dpi	Lpro				VP2							VP3				VP1				2C			3A			3B	3C		3D			
					72	92	64	71	78	79	132	133	137	182	56	60	75	105	134	196	133	144	199	494	249	269	311	312	24	97	140	143	6	28	40	72
O/FRA/1/2001					Y	E	T	T	C	Y	D	L	M	R	C	G	A	K	G	N	V	A	K	K	L	S	S	E	A	S	A	P	V	A	A	T
189	inact FMDV O i.m.		+	14	Y	E	T	T	C	Y	D	L	M	R/C	G	A	K	G	N	V	A	K	K	L	S	S	E	A	S	A	P	V	A	A	T	
				17	Y	E	T	T	C	Y	D	L	M	R/C	G	A	K	G	N	V	A	K	K	L	S	S	E	A	S	A	P	V	A	A	T	
				21	Y	E	T	T	C	Y	D	L	M	R	G	A	K	G	N	V	A	K	K	L	S	S	E	A	S	A	P	V	A	A	T	
				24	Y	E	T	T	C	Y	D	L	M	C	G	A	K	G	N	V	A	K	K	L	S	S	E	A	S	A	P	V	A	A	T	
190	CAV-2-FMD i.n.	+	+	14	Y	E	T	T	C	Y	D	L	M	C	G	A	K	G	N	V	A	K	K	L	S	S	E	A	S	A	P	V	A	A	T	
				21	Y	E	T	T	C	Y	D	L	M	C	G	A	K	G	N	V	A	K	K	L	S	S	E	A	S	A	P	V	A	A	T	
				24	Y	E	T	T	C	Y	D	L	M	C	G	A	K	G	N	V	A	K	K	L	S	S	E	A	S	A	P	V	A	A	T	
				28	Y	E	T	T	C	Y	D	L	M	C	G	A	K	G	N	V	A	K	K	L	S	S	E	A	S	A	P	V	A	A	T	
191	PBS i.n.	+	+	14	Y	E	T	T	C	Y	D	L	M	C	G	A	K	G	N	V	A	K	K	L	S	S	E	A	S	A	P	V	A	A	T	
				17	Y	E	T	T	C	Y	D	L	M	R/C	G	A	K	G	N	V	A	K	K	L	S	S	E	A	S	A	P	V	A	A	T	
				21	Y	E	T	T	C	Y	D	L	M	C	G	A	K	G	N	V	A	K	K	L	S	S	E	A	S	A	P	V	A	A	T	
				24	Y	E	T	T	C	Y	D	L	M	C	G	A	K	G	N	V	A	K	K	L	S	S	E	A	S	A	P	V	A	A	T	
196	PBS i.n.	+	+	14	Y	E	T	T	C	Y	D	L	M	C	G	A	K	G	N	V	A	K	K	L	S	S	E	A	S	A	P	V	A	A	T	
				17	Y	E	T	T	C	Y	D	L	M	C	G	A	K	G	N	V	A	K	K	L	S	S	E	A	S	A	P	V	A	A	T	
				21	Y	E	T	T	C	Y	D	L	M	C	G	A	K	G	N	V	A	K	K	L	S	S	E	A	S	A	P	V	A	A	T	
				24	Y	E	T	T	C	Y	D	L	M	C	G	A	K	G	N	V	A	K	K	L	S	S	E	A	S	A	P	V	A	A	T	
425	CAV-2-FMD i.n.	+	+	14	Y	E	T	T	C	Y	D	L	M	C	G	A	K	G	N	V	A	K	K	L	S	S	E	A	S	A	P	V	A	A	T	
				17	Y	E	T	T	C	Y	D	L	M	C	G	A	K	G	N	V	A	K	K	L	S	S	E	A	S	A	P	V	A	A	T	
				21	Y	E	T	T	C	Y	D	L	M	C	G	A	K	G	N	V	A	K	K	L	S	S	E	A	S	A	P	V	A	A	T	
				24	Y	E	T	T	C	Y	D	L	M	C	G	A	K	G	N	V	A	K	K	L	S	S	E	A	S	A	P	V	A	A	T	
506	CAV-2-FMD i.n.	+	+	14	Y	E	T	T	C	Y	D	L	M	C	G	A	K	G	N	V	A	K	K	L	S	S	E	A	S	A	P	V	A	A	T	
				17	Y	E	T	T	C	Y	D	L	M	C	G	A	K	G	N	V	A	K	K	L	S	S	E	A	S	A	P	V	A	A	T	
				21	Y	E	T	T	C	Y	D	L	M	C	G	A	K	G	N	V	A	K	K	L	S	S	E	A	S	A	P	V	A	A	T	
				24	Y	E	T	T	C	Y	D	L	M	C	G	A	K	G	N	V	A	K	K	L	S	S	E	A	S	A	P	V	A	A	T	
507	PBS i.n.	+	+	14	Y	E	T	T	C	H	D	L	M	R/C	G	A	K	G	N	V	A	K	K	L	S	S	E	A	S	A	P	V	A	A	T	
				17	Y	E	T	T	C	Y	D	L	M	C	G	A	K	G	N	V	A	K	K	L	S	S	E	A	S	A	P	V	A	A	T	
				21	Y	E	T	T	C	Y/H	D	L	M	C	G	A	K	G	N	V	A	K	K	L	S	S	E	A	S	A	P	V	A	A	T	
				24	Y	E	T	T	C	Y	D	L	M	C	G	A	K	G	N	V	A	K	K	L	S	S	E	A	S	A	P	V	A	A	T	
508	CAV-2-FMD i.m.	+	+	14	Y	E	T	T	C	Y	D	L	M	C	G	A	K	G	N	V	A	K	K	L	S	S	E	A	S	A	P	V	A	A	T	
				17	Y	E	T	T	C	Y	D	L	M	C	G	A	K	G	N	V	A	K	K	L	S	S	E	A	S	A	P	V	A	A	T	
				21	Y	E	T	T	C	Y/H	D	L	M	C	G	A	K	G	N	V	A	K	K	L	S	S	E	A	S	A	P	V	A	A	T	
				24	Y	E	T	T	C	Y	D	L	M	C	G	A	K	G	N	V	A	K	K	L	S	S	E	A	S	A	P	V	A	A	T	
509	CAV-2-FMD i.n.	+	+	17	Y	E	T	T	C	Y	D	L	M	C	G	A	K	G	N	V	A	K	K	L	S	S	E	A	S	A	P	V	A	A	T	
				21	Y	E	T	T	C	Y	D	L	M	C	G	A	K	G	N	V	A	K	K	L	S	S	E	A	S	A	P	V	A	A	T	
				24	Y	E	T	T	C	Y	D	L	M	C	G	A	K	G	N	V	A	K	K	L	S	S	E	A	S	A	P	V	A	A	T	
				28	Y	E	T	T	C	Y/H	D	L	M	C	G	A	K	G	N	V	A	K	K	L	S	S	E	A	S	A	P	V	A	A	T	
510	CAV-2-FMD i.m.	+	+	14	Y	E	T	T	C	H	D	L	M	C	G	A	K	G	N	V	A	K	K	L	S	S	E	A	S	A	P	V	A	A	T	
				17	Y	E	T	T	C	H	D	L	M	C	G	A	K	G	N	V	A	K	K	L	S	S	E	A	S	A	P	V	A	A	T	
				21	Y	E	T	T	C	H	D	L	M	C	G	A	K	G	N	V	A	K	K	L	S	S	E	A	S	A	P	V	A	A	T	
				24	Y	E	T	T	C	H	D	L	M	C	G	A	K	G	N	V	A	K	K	L	S	S	E	A	S	A	P	V	A	A	T	
647	inact FMDV O i.m.	+	+	14	Y	E	T	T	C	Y	D	L	M	R/C	G	A	K	G	N	V	A	K	K	L	S	S	E	A	S	A	P	V	A	A	T	
				17	Y	E	T	T	C	Y	D	L	M	C	G	A	K	G	N	V	A	K	K	L	S	S	E	A	S	A	P	V	A	A	T	
				21	Y	E	T	T	C	Y	D	L	M	C	G	A	K	G	N	V	A	K	K	L	S	S	E	A	S	A	P	V	A	A	T	
				24	Y	E	T	T	C	Y	D	L	M	C	G	A	K	G	N	V	A	K	K	L	S	S	E	A	S	A	P	V	A	A	T	
649	inact FMDV O i.m.	+	+	17	Y	E	T	T	C	Y	D	L	M	C	G	A	K	G	N	V	A	K	K	L	S	S	E	A	S	A	P	V	A	A	T	
				21	Y	E	T	T	C	Y	D	L	M	C	G	A	K	G	N	V	A	K	K	L	S	S	E	A	S	A	P	V	A	A	T	
				24	Y	E	T	T	C	Y	D	L	M	C	G	A	K	G	N	V	A	K	K	L	S	S	E	A	S	A	P	V	A	A	T	
				28	Y	E	T	T	C	H	D	L	M	C	G	A	K	G	N	V	A	K	K	L	S	S	E	A	S	A	P	V	A	A	T	
669	CAV-2-FMD i.m.	+	+	14	Y	E	T	T	C	Y	D	L	M	C	G	A	K	G	N	V	A	K	K	L	S	S	E	A	S	A	P	V	A	A	T	
				17	Y	E	T	T	C	Y	D	L	M	C	G	A	K	G	N	V	A	K	K	L	S	S	E	A	S	A	P	V	A	A	T	
				21	Y	E	T	T	C	Y	D	L	M	C	G	A	K	G	N	V	A	K	K	L	S	S	E	A	S	A	P	V	A	A	T	
				24	Y	E	T	T	C	Y	D	L	M	C	G	A	K	G	N	V	A	K	K	L	S	S	E	A	S	A	P	V	A	A	T	
940	inact FMDV O i.m.			17	Y	E	T	T	C	Y	D	L	M	C	G	A	K	G	N	V	A	K	K	L	S	S	E	A	S	A	P	V	A	A	T	
				21	H	E	T	T	C	Y	D	L	M	C	G	A	K	G	N	V	A	K	K	L	S	S	E	A	S	A	P	V	A	A	T	
				24	H	E	T	T	C	Y	D	L	M	C	G	A	K	G	N	V	A	K	K	L	S	S	E	A	S	A	P	V	A	A	T	
				28	Y	E	T	T	C	Y	D	L	M	C	G	A	K	G	N	V	A	K	K	L	S	S	E	A	S	A	P	V	A	A	T	
943	inact FMDV O i.m.	+	+	17	Y	E	T	T	C	Y	D	L	M	C	G	A	K	G	N	V	A	K	K	L	S	S	E	A	S	A	P	V	A	A	T	
				21	Y	E	T	T	C	Y	D	L	M	C	G	A	K	G	N	V	A	K	K	L	S	S	E	A	S	A	P	V	A	A	T	
				24	Y	E	T	T	C	Y	D	L	M	C	G	A	K	G	N	V	A	K	K	L	S	S	E	A	S	A	P	V	A	A	T	
				28	Y	E	T	T	C	Y	D	L	M	C	G	A	K	G	N	V	A	K	K	L	S	S	E	A	S	A	P	V	A	A	T	
945	PBS i.n.	+	+	14	Y	E	T	T	C	H	D	L	M	C	G	A	K	G	N	V	A	K	K	L	S	S	E	A	S	A	P	V	A	A	T	
				17	Y	E	T	T	C	H	D	L	M	C	G	A	K	G	N	V	A	K	K	L	S	S	E	A	S	A	P	V	A	A	T	
				21	Y	E	T	T	C	H	D	L	M	C	G	A	K	G	N	V	A	K	K	L	S	S	E	A	S	A	P	V	A	A	T	

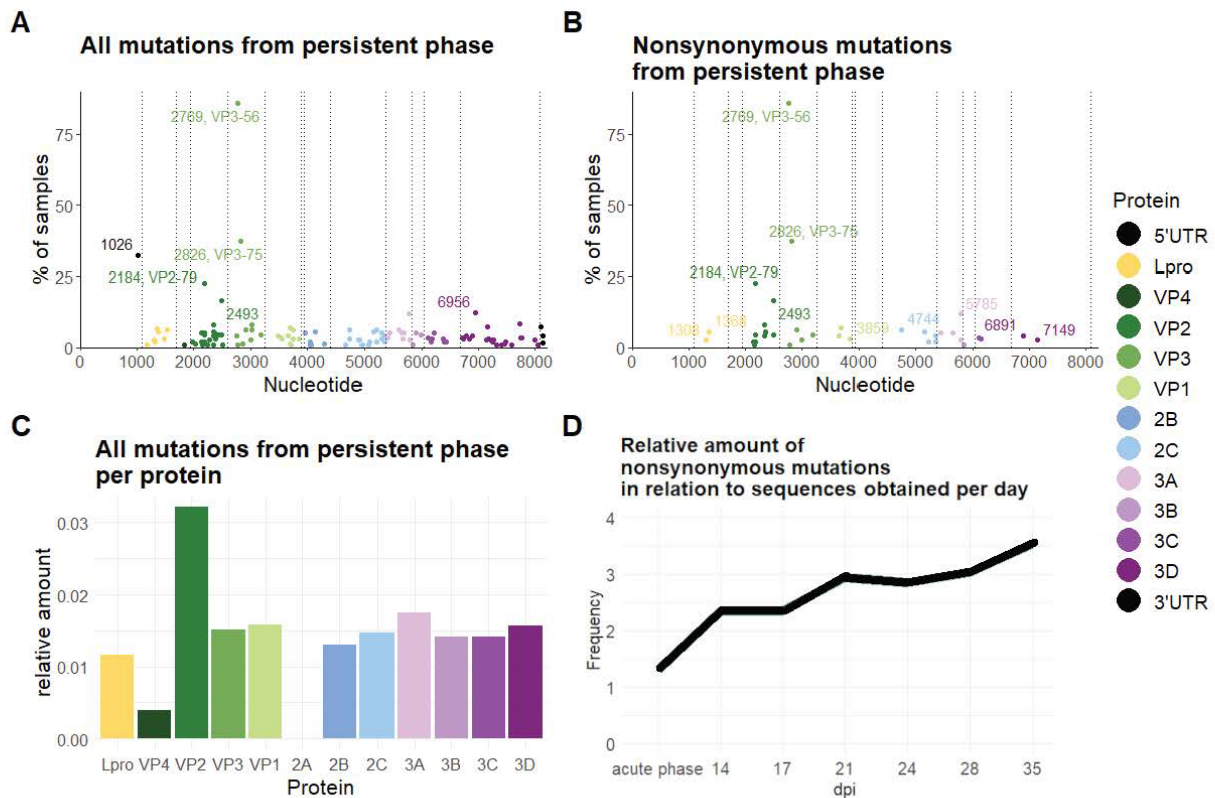


**FIG 6** Persistent-phase mutations. Mutations detected in the transitional and persistent-phase OPF samples. Mutations are shown with their position in the genome and the occurrence of each mutation in percent of all samples, for all mutations (A) or only non-synonymous mutations (B). The affected amino acid is annotated for the three most frequent non-synonymous mutations. The counts of all non-synonymous mutations were summarized by virus protein, and the amount of mutations was divided by the length of the protein (C). The amount of mutations per day was divided by the number of sequences obtained for each day to calculate the relative occurrence of mutations (D).

and VP2 Y79H (in 22 samples), together with a silent mutation at nucleotide 1026 in the 5' UTR (in 28 samples) as shown in Fig. 6A and B. After grouping the mutations by protein, the highest number of mutations was detected in the polymerase 3D with 22 mutations, followed by VP2 with 21 mutations. Divided by the length of each coding region, the largest protein of FMDV 3D has a low frequency of mutations, while VP2 still has the highest number of mutations relative to the length of its coding region (not shown). This is further emphasized when only non-synonymous mutations are considered: the capsid proteins VP2 and VP3 had the most non-synonymous mutations, in absolute numbers (not shown) and relative to the length of their coding regions (Fig. 6C).

### Mutations over time

To quantify the occurrence of non-synonymous mutations over time, all samples with mutations compared with the inoculum were counted for each sampling day following 14 dpi. All mutations found in samples from the acute phase were grouped together irrespective of the sampling day. In absolute terms, the frequency of non-synonymous mutations declined after the acute phase to reach the lowest point on day 14 with 22 non-synonymous mutations found in samples collected on this day. Relative to the number of whole-ORF consensus sequences recovered on each day, a steady increase in the frequency of mutations was observed over the course of infection, reaching a peak

at 35 dpi with a frequency of 3.5 (Fig. 5D), meaning that on average, in every sequence recovered from this day, more than three mutations were found relative to the inoculum.

There were distinct sets of mutations occurring only during the acute phase or during the transitional and persistent phase. Only a few mutations that were already present in sequences from the acute phase remained detectable in the consensus sequences recovered from OPF samples (including VP3 R56C and VP3 G60D), while the majority of non-synonymous mutations disappeared after the acute phase. Interestingly, we saw an increase in the emergence of non-synonymous mutations over time at nucleotides 2826 and 2184, coding for amino acid exchanges in VP3 (A75T) and VP2 (Y79H) (Fig. 7A). While the non-synonymous mutation at position 2769 coding for VP3 R56C was already present in more than half of the samples collected during the acute phase and was subsequently found in almost all OPF samples, VP3 A75T and VP2 Y79H were not detected in any consensus sequence from the acute phase nor as a minor variant in the deep-sequenced vesicular samples. They were also not present as minor variants in the deep-sequenced inoculum but appear in the consensus sequences from 14 dpi onward, with VP3 A75T present in 41% and VP2 Y79H in 27% of samples from this day. At 35 dpi, VP3 A75T occurs in more than half of the samples (53%) and VP2 Y79H almost in every second sample (47%). They were found in several animals regardless of the vaccination group, and VP2 Y79H occurred independently in both animal trials. VP3 A75T was detected at the consensus level in eight animals from the vaccination trial (ear tags 190, 191, 196, 425, 507, 509, 647, and 669) but was not found in the two persistently infected animals from the infection study. In contrast, VP2 Y79H was present in five cattle from the vaccination study at the consensus level (ear tag numbers 507, 510, 649, 943, and 945) as well as in one animal from the infection study (773). Additionally, VP2 Y79H was observed as a heterozygous base in the Sanger consensus sequence of four animals (191, 196, 506, and 507), adding up to 10 of 20 persistently infected animals in this study in which this non-synonymous mutation was found.

### Structural analysis

The localization of the non-synonymous mutations in the capsid proteins was hypothesized to have functional implications. After mapping the amino acid changes on the capsid, the first observation was that the majority of amino acid changes lies on the outer surface of the capsid (Fig. 8A) and none on the inner surface. Important structures on the surface are the five major antigenic sites and the receptor-binding sites.

The following amino acid changes have been observed to constitute immunologically relevant major antigenic sites or lie in close proximity to these: VP1 residue 144, VP2 residues 64, 78, 79, 132, 133, 137, and 182, and VP3 residue 56 (6). VP1 144 is a central amino acid of the antigenic site 1 in the GH loop (25). The mentioned amino acids of VP2 (except 182) lie close to the “antigenic site 2” on VP2 (26). The exchanged amino acid VP2 182 (found in six animals) is not exposed on the surface in our AlphaFold prediction of VP2 of O/FRA/1/2001 but lies in the  $\beta$ -strand H directly beneath the amino acid residue 79 located in  $\beta$ -strand C. VP3 56 is a critical residue of the “antigenic site 4,” enabling escape mutants (27).

Using an X-ray crystallography model in the “down” position, we observed an accumulation of amino acid changes on the surface of VP2 in direct vicinity of the RGD motif of the GH loop of VP1. In addition to forming the “antigenic site 2,” VP2 residues 64, 78, and 79 are located right beneath the RGD motif (Fig. 7B). The motility of the GH loop allows a change between an “up” and a “down” constitution, simultaneously altering its own antigenicity (7, 28).

An amino acid change in residue VP3 79, which lies outside the canonical antigenic sites, was previously linked with mutation pressure in the presence of antibody (29).

Apart from the antigenic sites, some residues constitute receptor-binding sites as well, such as VP3 56 and VP2 residues 78, 79, 132, and 133, which form the canonical HS-binding sites. Arginine at VP3 56 can interact with sulfide groups on heparin, while the

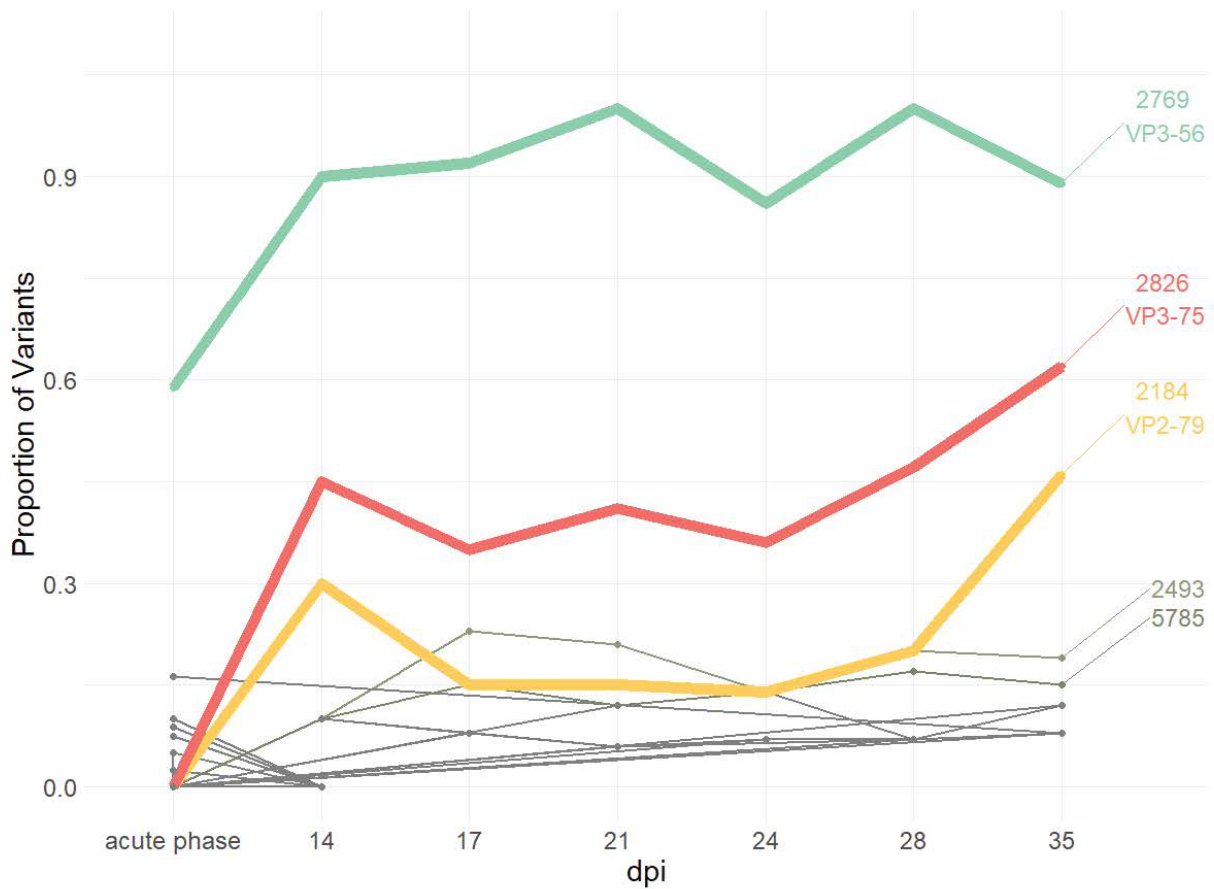


FIG 7 Non-synonymous mutations by sampling day. Observed frequency of specific non-synonymous mutations over time during the acute phase (3–6 dpi) and on each sampling day in the transitional and persistent phases.

other residues support interactions through local charges (30, 31). A detailed description of which mutation occurred in what animals is shown in Fig. 7C.

Furthermore, both amino acid changes that were observed to emerge during FMDV persistence, VP3 A75T and VP2 Y79H, are located in regions associated with T-cell epitopes (32).

### Viral dynamics within one animal

The diversity of the viral population within one animal was examined using different samples collected from animal 758. We used three samples from the acute phase (serum, nasal fluid, and saliva), eight OPF samples, and three tissue samples collected at necropsy at 35 dpi (dorsal soft palate, dorsal nasopharynx, and larynx epithelium from the bottom of the epiglottis; all were positive in the virus isolation). The tissue samples are the only samples included in this study in which sequencing was performed after one passage on LFBK- $\alpha$ V $\beta$ 6. The tissues used here are also the preferential localization for persistent FMDV (33). In samples from the acute phase, we detected two to three mutations in each consensus sequence. During the persistent phase, this number rose from two mutations in OPF from 10 dpi to six mutations at the consensus level in OPF samples from 28 and 31 dpi. In the virus isolates from the tissue samples from the end of the trial, 10 to 17 mutations were found. The consensus sequences from the DSP and DNP were highly similar with nine shared mutations compared with the inoculum, while the larynx sample

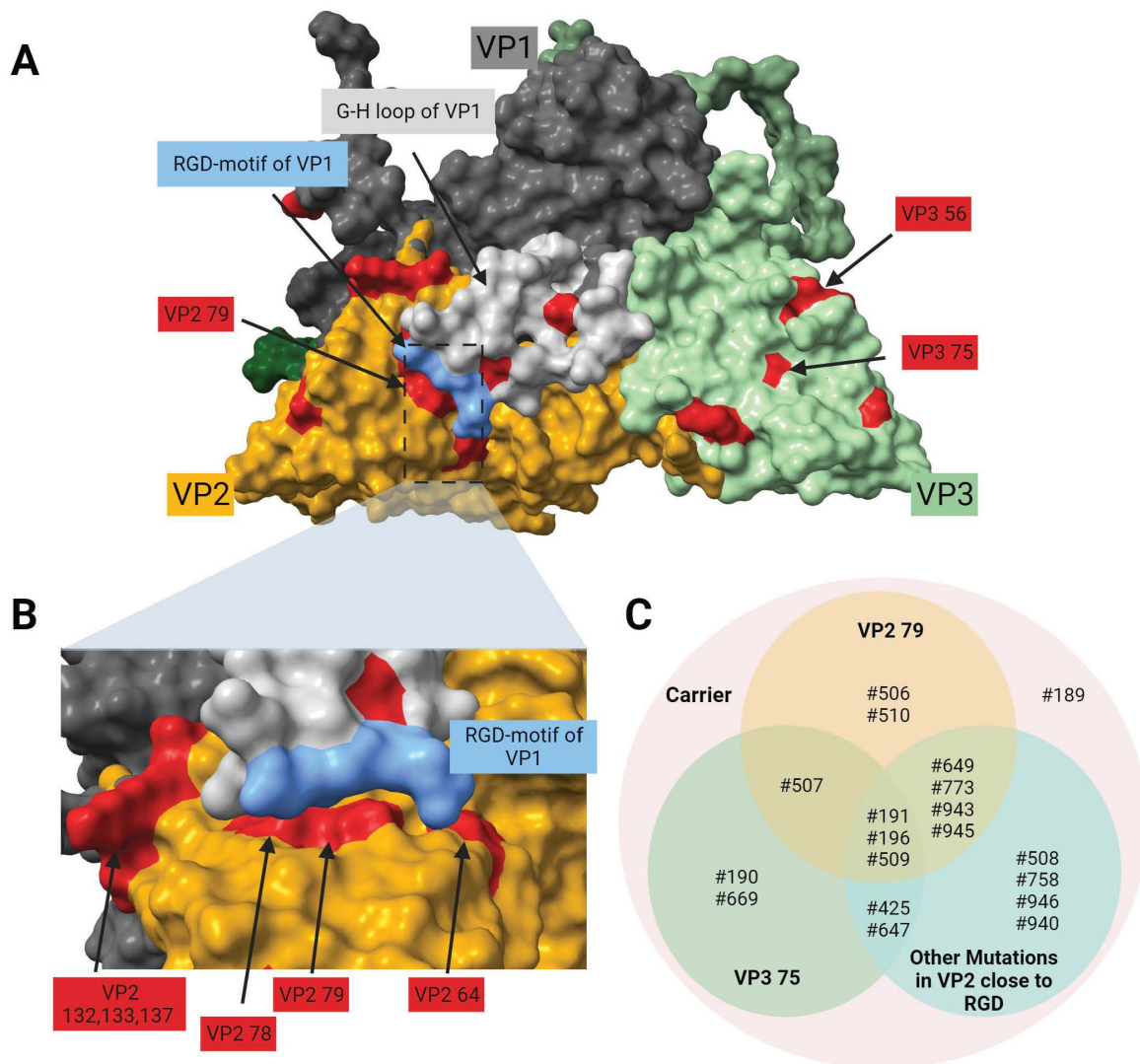


**FIG 8** Localization of amino acid changes in the virus capsid. (A) Amino acid changes (colored red) on the capsid surface; the G-H loop of VP1 in the “down” position is colored in light gray, including the RGD residues 145–147 shown in blue. (B) Detailed view of the vicinity of the G-H loop with the RGD motif in the “down” position, with the amino acid changes in VP2 again shown in red. (C) Venn diagram of persistently infected animals in which certain amino acid changes on the capsid surface were observed; “other mutations in VP2 close to RGD” include the residues at positions 64, 78, 79, 132, 133, 137, and 182.

shared only 3 of its 17 mutations with the other tissues. In a phylogenetic analysis, DNP and DSP samples were closely related to each other and to the OPF samples, while the sequence from the larynx sample had no close relation with any other sample from the persistent phase (Fig. 9). The larynx sample is the only sample from this animal in which the amino acid change VP2 Y79H was detected.

One non-synonymous mutation shared by all OPF samples and tissues codes for an amino acid change in VP2 (D133G), which is located on the capsid surface. Interestingly, animal 758 is also the only animal in both trials in which the VP3 R56C variant was dominant during the acute phase but disappeared from the consensus sequences in OPF

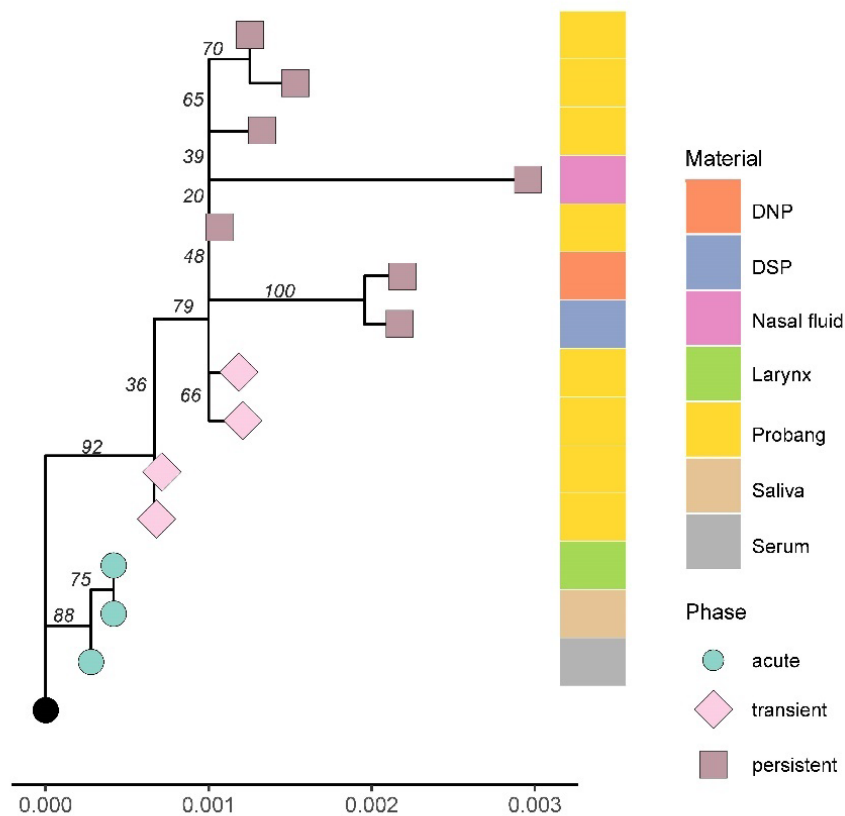


**FIG 9** Inoculum-rooted phylogenetic analysis of all sequences recovered from animal 758 categorized by phase of infection and sampling material. Samples from the acute phase were taken from 3 to 6 dpi, from the transient phase from 10 to 21 dpi, and from the persistent phase after 21 dpi; tissue samples including DNP, DSP, and larynx epithelium were collected during necropsy at 35 dpi.

samples. Overall, we observed a disparity between the high amount of mutations found in persistently infected epithelia in the nasopharynx and the reduced presence of mutations in the consensus sequences of OPF samples.

### Functional analyses

The selection of isolates that met our requirements for a functional analysis was confounded by the diversity of isolates obtained by plaque purification. This broad diversity of sequences from the plaques reflects the nature of the viral quasispecies in the persistently infected animals. VP3 R56C was fixed in all sampled plaques. Several plaques shared mutations, among them amino acid changes, which were also observed in other OPF isolates, such as VP1 144 (found in 5 of 25 plaques of the isolate obtained from animal 510 at 14 dpi) and VP2 182 (found in 12 of 27 plaques of the 508/24 dpi isolate; this variant becomes the consensus of this animal at 28 dpi). We selected plaque-purified isolates corresponding to the consensus sequence of the inoculum (plaque #2) and two isolates from the persistent phase, one with the VP3 R56C mutation (plaque #65) and one with VP3 R56C and VP2 Y79H (plaque #57). These mutations were the only non-synonymous mutations in the P1 of both isolates.

To test the ability of each variant to infect different receptor-deficient cells, the isolates were used to infect five cell lines. All isolates were able to productively infect integrin-expressing cells (BHK-21, LFBK- $\alpha$ V $\beta$ 6, and IB-RS-2) and reached high titers. In integrin-deficient but HS-expressing CHO-K1 cells, only the plaque isolate with the

inoculum sequence (#2) was able to reproduce, albeit at decreased titers. In contrast to this, no isolate could productively infect the integrin- and HS-deficient cell line pgsD-677. The isolates from the persistent phase were unable to infect cells using HS alone (Fig. 10A).

The differences between the two integrin-expressing cell lines were further evaluated using growth kinetics on LFBK- $\alpha$ V $\beta$ 6 and IB-RS-2 cells. In the LFBK- $\alpha$ V $\beta$ 6 cells, which express the bovine  $\alpha$ V $\beta$ 6 integrin (34), all three isolates showed very similar growth with slightly lower titers for the inoculum isolate. In IB-RS-2 cells, which express  $\alpha$ V $\beta$ 8 integrin but not  $\alpha$ V $\beta$ 6 (35), the inoculum isolate grew unimpeded, similar to LFBK- $\alpha$ V $\beta$ 6 cells. Both isolates of persistent viruses seem to exhibit retarded growth but not to a statistically significant extent (Fig. 10B).

In the virus neutralization assay, we observed no difference in the neutralizing activity of serum collected from persistently infected animals (ear tags 508 and 510) at 35 dpi against the plaque-purified inoculum and the isolates from persistently infected animals (data not shown).

## DISCUSSION

Understanding the replication of FMDV in the acutely and persistently infected host is of great importance. Heterologous superinfection of persistently infected cattle gives rise to inter-serotype recombinants that can evade the host immune response by replacing the capsid-coding region of their genome (36, 37). However, in addition to this sudden antigenic shift caused by recombination between serotypes, FMDV continuously evolves over the course of infection in persistently infected carriers. What we observed in this study constitutes a genetic drift with a steadily increasing amount of mutations accumulating in the viral genome. In addition to this accumulation of mutations, another piece of evidence for the ongoing viral replication in the persistent phase is the presence of negative-strand viral RNA in tonsils and DSP of persistently infected sheep (38).

We avoided culture passages of virus recovered from the animals prior to sequencing to avoid culture-induced mutations. Sequencing FMDV directly from the *ex vivo* samples may have reduced our sample set slightly but supplied sequences as close to the natural infection as possible. The importance of this approach is emphasized by a comparison with the same samples after one culture passage, which revealed different consensus-level mutations in several corresponding sequences. Although many mutations were preserved through a cell culture passage, even a single passage can introduce many unique mutations, which seem to be randomly distributed over the genome. However, amplification of viral RNA through PCR may alter the relative frequencies of quasispecies variants, potentially skewing the consensus sequence away from the true population diversity.

Our phylogenetic analysis has shown that in the same animal, many samples are highly homologous with only single mutations occurring between sampling timepoints, but single clade-shifted samples were found to cluster with samples from a different animal rather than with others from the same animal. Similar patterns of phylogenetic relation have been observed before (19). The original hypothesis of Fish et al., (20) that this presence of viral quasispecies within the same animal can be explained by a multitude of infection foci with independent replication, is supported further by our finding of divergent sequences of FMDV in different tissues collected from the same animal at necropsy. Even in our limited sample set of virus-isolation positive tissues of animal 758, a distinct set of viral subpopulations was present in each of the tissues. The subpopulations in DSP and DNP differed only in a few nucleotides, which may be associated with their close anatomic localization, while FMDV recovered from laryngeal epithelium was clearly different from the two others with several mutations that were not detected in the OPF of animal 758 but were present in the consensus sequence of OPF from other animals, including amino acid change VP2 Y79H. The disparity between the number of mutations observed in tissue isolates and in OPF might not be fully attributable to the cell culture passage, as many of the single nucleotide polymorphisms

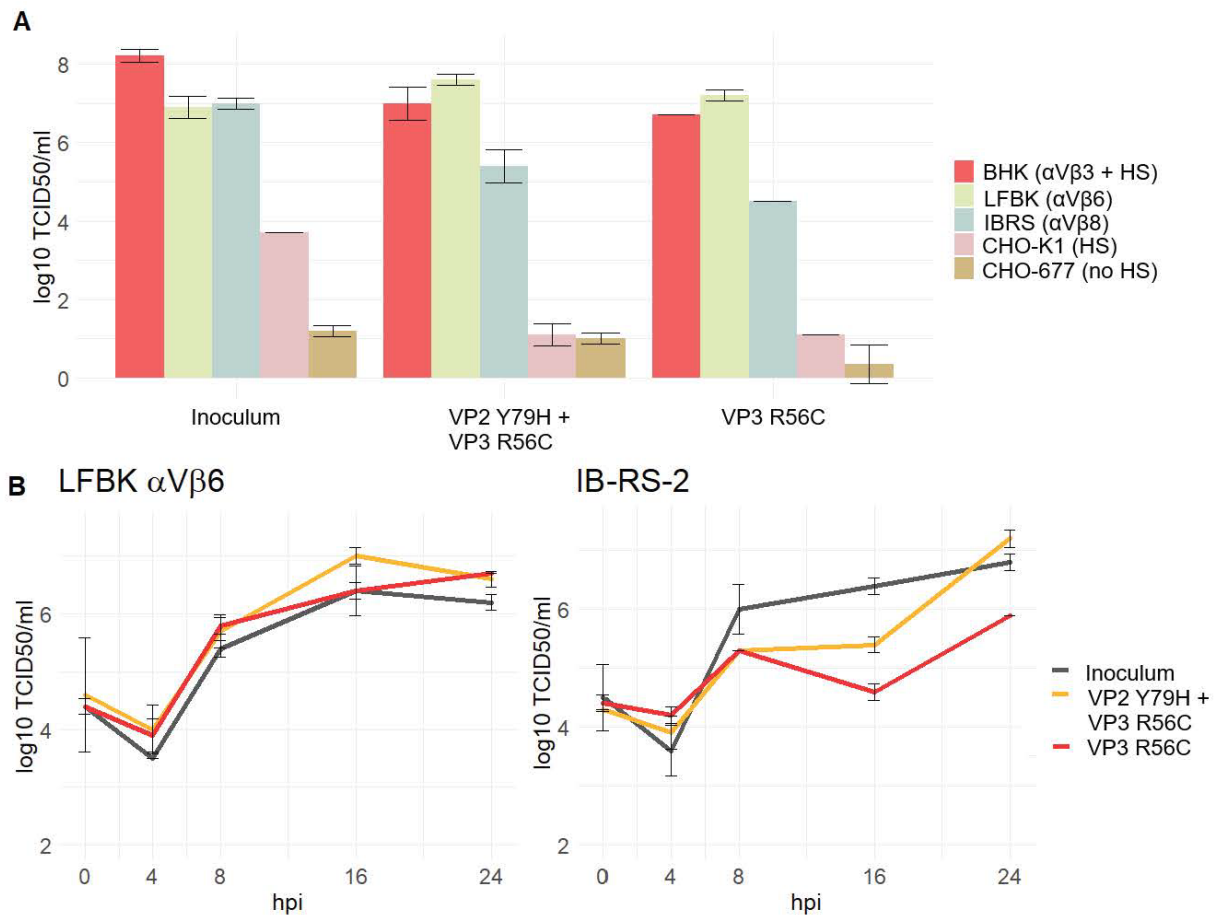


**FIG 10** Characterization of the plaque isolates. Plaque identical to the inoculum consensus, plaque with VP2 Y79H and VP3 R56C, and plaque containing VP3 R56C only. (A) Infectivity assay with receptor-deficient cell lines; the main receptors are indicated in the brackets: integrins  $\alpha V\beta 3$ ,  $\alpha V\beta 6$  or  $\alpha V\beta 8$ , and HS. (B) Comparison of viral growth kinetics of the plaque isolates on LFBK- $\alpha V\beta 6$  and IB-RS-2 cells over 24 hpi.

(SNPs) were shared between DNP and DSP tissue isolates. Vice versa, the consensus sequence of the OPF of this animal mostly contained mutations that were found in the tissues as well. This suggests that OPF encompasses a broad variety of subspecies, and its sequence is drawn from a set of individual subpopulations. This may be explained by the technique of probang sampling to collect OPF. The metal probang cup is inserted through the mouth and swallowed by the animal, then saliva and superficial scrapes of epithelium are collected by retracting the cup (8, 39). Therefore, the probang cup samples viral subpopulations from this entire region, but it will not always be exactly the same foci of infection that are sampled on different days.

Another interesting finding of this study was the emergence of three non-synonymous mutations, coming to dominate the consensus sequence in several animals. Among these, the non-synonymous mutation coding for VP3 R56C was the variant with the highest prevalence across samples, being detected in over 90% of all samples from the persistent phase. However, this variant was already present in the inoculum at a frequency of 22% and already constituted the consensus in over half of the samples from the acute phase (3–6 dpi). It was found in all persistently infected animals except animal 758, from which it disappeared after the acute phase. Residue 56 of VP3 is well characterized, and arginine at this position is associated with attenuation *in vivo* and increased HS binding (40). Especially the substitution of arginine (R) with cysteine (C)

was associated with a reversion to pathogenicity (21) and was quickly introduced by serial passages in cattle (41). Remarkably, most of the field strains for which sequence information is available in online databases have a histidine at this position (93% of 479 sequences), in contrast to only very few sequences with a cysteine at residue 56, which all come from the aforementioned passage experiment. Juleff et al. (41) used intradermolingual inoculation of cattle to obtain vesicular material for further passage, like we did for our inoculum. In our study, this mutation was likely induced by the animal passage of the previously plaque-purified inoculum before the infection of animals in the vaccination trial, as a comparison with closely related field strains from the 2001 outbreak implies as well. The inoculum of the infection trial, on the other hand, does not have a history of animal passage, and the emergence of VP3 R56C was associated only with the acute phase. After the acute phase, it was no longer detected at the consensus level in animal 758. In animal 507, arginine similarly reappears at residue 56 on days 24 and 35. The dynamic of the occurrence and shortly thereafter the disappearance of VP3 R56C in these animals, as well as the distinct mutations acquired during the acute and the persistent phases, may reflect the viral subpopulation that initially infects the FAE of the nasopharynx then spreads from this microanatomic compartment throughout the body, where it acquires several mutations during rapid replication and is cleared with the onset of the antibody response. In the FAE, however, the viral subpopulation from the primary infection may remain and replicate slowly but steadily, thus “conserving” its genetic makeup.

In contrast to the VP3 R56C variant, which is tied to the acute phase of infection, two other non-synonymous mutations were associated with the persistent phase: VP2 Y79H and VP3 A75T. These were detectable neither in the deep-sequenced inoculum or vesicular lesions nor in any consensus sequence of other samples from the acute phase. They first appear in our samples at 14 dpi, increasing in prevalence toward the end of the trial, whereupon they appear in the consensus of half of the samples. Especially for VP2 Y79H, there is an astonishing presence of ambiguous base calls. VP2 Y79H has previously been found to be associated with FMDV persistence in an animal trial with FMDV O UKG/34/2001 (a very close relative of O FRA/1/2001), where it was present in six of six carrier animals (16). In another experimental study with FMDV O UKG/34/2001, VP2 Y79H was detected in four of six samples from three carrier animals, while in the same study, VP3 A75T was found in five of the sequences (18). Parthiban et al. (18) did not assert an association of these samples with persistent infection because the same substitutions were also found in samples collected from acutely infected animals in the field. In a comparison of 479 FMDV serotype O sequences available in online databases, histidine is indeed the dominant amino acid at residue 79 of VP2 (occurring in 70.5% of samples). However, in our view, this does not necessarily contradict the association of VP2 Y79H with the persistence of FMDV O/ME-SA/PanAsia (i.e., O FRA and O UKG 2001), because most of the field viruses in the database are not of this toptotype. In a comparison of PanAsia strains, only an isolate of O/JPN/2000 that had been obtained from OPF (42) had a histidine at residue 79 (43). What is more, in the FMD epizootic in the United Kingdom in 2001, where the transmission of O UKG between acutely infected animals took place over the course of nearly 7 months, VP2 Y97H was not observed in any of the field samples taken over the whole period, and neither was VP3 A75T (23). The commonness of histidine at residue 79 of VP2 in other strains, however, may limit our findings to PanAsia strains. While similar associations with FMDV persistence could be assumed for neighboring residues of VP2 79 on the capsid surface, these would require a more detailed analysis.

For VP3 residue 75, an analysis of the publicly available sequences of FMDV serotype O ( $n = 479$ ) revealed threonine to be the least abundant amino acid at this position with an occurrence of 14%, while alanine was dominant with 84%. In an infection experiment with O<sub>1</sub> Manisa in cattle, VP3 A75T was found in samples taken from one persistently infected animal but only after the 21st day after infection (accession

numbers [MT431591–MT431613](#) (36, 44). In general, information about this amino acid is scarce, but it could potentially be associated with FMDV persistence as well.

We observed no antigenic differences when testing the neutralizing capacity of serum from the persistent phase against the inoculum and a late isolate from a carrier animal. This is in agreement with the findings of the previous study of VP2 Y79H (16) and with neutralization tests performed with serum and virus recovered from persistently infected African buffalo (45). Testing the neutralizing capacity of monoclonal antibodies against our plaque-purified isolates would allow a more detailed study of their antigenic character, especially considering the antigenic site 1 in the G-H loop, whose antigenicity may be influenced by the closely located amino acid changes on the surface of VP2. The accumulation of amino acid changes in critical residues of antigenic sites and receptor-binding motifs suggests a fitness advantage conferred by these changes during viral persistence. Gebauer et al. found differences in the neutralizing capacity of two of her persistent-phase isolates with monoclonal antibodies (15), while Salt could not corroborate this in his experiments (46). However, the possibility that the mutations influence the T-cell epitope should not be disregarded, but testing this hypothesis lies outside of the scope of this study.

We further investigated the functional differences between VP2 Y79H and VP3 R56C. We chose an isolate with both mutations, VP2 Y79H and VP3 R56C, because the variant VP2 Y79H was detected independently in sequences from both trials, but no plaque isolate had VP2 Y79H as the only amino acid change without VP3 R56C. As suggested by previous studies of the VP3 R56C mutation, both persistent isolates (one containing VP2 Y79H and VP3 R56C, and one containing only VP3 R56C) lost their ability to infect integrin-deficient but HS-expressing cells. This may demonstrate the evolution of animal-passaged viruses away from the cell-culture-adapted original isolate; however, using hamster-derived cells is quite artificial, and the growth of certain virus isolates may be inhibited by unknown other factors in these cell lines. Based on the growth kinetics, VP2 Y79H may pose an advantage over VP3 R56C alone by enabling an infection of cells via the integrin receptor  $\alpha V\beta 8$ , but in our case, this trend was not significant and may also be influenced by other factors. This receptor binding is facilitated as well by the RGD motif in VP1 (47) and would thus be influenced by VP2 79, which is in close vicinity to the G-H loop in its “down” position. In contrast to  $\alpha V\beta 6$ , the integrin receptor  $\alpha V\beta 8$  is not only expressed on epithelial cells, but also on  $T_{reg}$  cells and dendritic cells, which are present in the FAE (48, 49), and at least dendritic cells can be infected by FMDV under certain circumstances (50).

Our results show that in FMDV serotype O infections, there are indeed unique mutations associated with the persistent phase of infection. In addition, the VP2 Y79H variant may confer a functional change in receptor usage. However, the broader implications of both findings currently remain unclear.

## MATERIALS AND METHODS

### Cells

BHK-21 cells (Collection of Cell Lines in Veterinary Medicine [CCLV]-RIE 164, FLI, Greifswald, Germany) and IB-RS-2 (CCLV-RIE 103) (51) were cultured in minimum essential medium (MEM) with Hanks' and Earle's salts and non-essential amino acids. LFBK- $\alpha V\beta 6$  (CCLV-RIE 1419) (34), CHO-K1 (CCLV-RIE 134) (52) and CHO-677 cells (pgsD-677, CCLV-RIE 1524) (53) were cultured in medium containing Ham's F12 Nutrient Mixture and Iscove's modified Dulbecco's medium (IMDM) with sodium bicarbonate. For routine propagation, 10% fetal bovine serum (FBS) was added.

### Viruses

All experiments were performed with FMDV O/FRA/1/2001. For the two animal trials, two differently prepared inocula with the same consensus sequence (GenBank accession no. [OV121130.1](#)) were used. For the first trial, a vaccination trial, virus was provided by the

Animal Health Laboratory, ANSES, Maisons-Alfort, France. It had been plaque-purified twice on BHK-21 cells and was then passaged once in a heifer that was infected by intraepidermolingual inoculation. The inoculum was prepared from a vesicular lesion on the tongue of this animal collected at 1 dpi. For the second trial, an infection study, the inoculum was recombinantly produced O/FRA/1/2001 and passaged twice on BHK-21 cells.

### Animal trial

The samples used in this study were collected in two separate animal trials. Both were carried out under BSL4vet conditions at the Riems site of the Friedrich-Loeffler-Institut (Germany). The majority of samples stem from a vaccination trial in which 20 Holstein-Frisian cattle (*Bos taurus*) were challenged by intranasopharyngeal instillation with the animal-passaged inoculum. Prior to challenge infection, six animals had been vaccinated twice intramuscularly (i.m.) with a commercially available inactivated FMDV O<sub>1</sub> Manisa vaccine, six animals had been vaccinated three times intranasally with an experimental canine adenovirus vector vaccine expressing P1 and 3C of FMDV O/FRA/1/2001, four animals had been vaccinated three times i.m. with the same vector vaccine, and one control group of four animals had been injected with sterile phosphate-buffered saline (PBS). All animals remained in the trial until the 35th day after the challenge, at which point they were euthanized.

The samples from animals 758 and 773 were obtained from an infection experiment previously described in Litz et al. (54). Here, the intranasopharyngeal inoculation was performed with recombinant O/FRA/1/2001, which had the same consensus sequence as the inoculum of the experiment described above. All animals remained in the trial until 35 dpi.

### Sample collection

Serum, nasal fluid, and saliva were collected daily from 0 to 10 dpi and on days 14, 17, 21, 24, 28, 31, and 35 postinfection. Serum was collected from the jugular vein into tubes containing clotting activators. Saliva samples and nasal fluid were obtained by swabbing the oral or nasal cavity with a human vaginal tampon as previously described (55). Probang samples were collected on days 0, 14, 17, 21, 24, 28, and 35. In the infection study, additional probang samples were performed at 10 and 31 dpi, as described by Suttmoller and Cottral (13). In the infection study, tissue samples from the nasopharynx were collected at the time of necropsy. To address the focal nature of persistent FMDV, five biological replicates of each of the preferred epithelia, the dorsal nasopharynx, and the dorsal soft palate, and one sample of epithelium at the base of the epiglottis were taken from each animal. These tissue samples were used for viral genome detection and virus isolation. All samples were frozen at  $-80^{\circ}\text{C}$  on the day of collection pending further analysis.

### Virus isolation from probang samples

To determine the carrier status of FMDV-infected cattle, virus isolation was attempted from the OPF collected with the probang cup (13). An equal amount of approximately 4 mL of cell culture medium was added to the sample and then it was homogenized through repeated aspiration using a 1.7 mm blunt cannula. The homogenate was aliquoted, and one part was stored at  $-80^{\circ}\text{C}$  untreated while approximately 2 mL was mixed with an equal amount of 1,1,2-trichloro-1,2,2-trifluoroethane (TTE) (56). The OPF with TTE was then vigorously shaken for 5 minutes and centrifuged at  $1,000 \times g$  at  $4^{\circ}\text{C}$  for 10 minutes. The supernatant was removed and aliquoted for virus isolation, which was performed with 250  $\mu\text{L}$  of the TTE-treated OPF on a confluent monolayer of LFBK- $\alpha\text{V}\beta 6$  cells.

### FMDV genome detection

For FMDV genome detection, RNA was extracted from 100  $\mu$ L of serum, nasal fluid, saliva, and untreated OPF using the NucleoMag Vet kit (Macherey-Nagel) and a King Fisher Flex magnetic particle processor (Thermo Scientific). As an internal control, 10  $\mu$ L of IC2 RNA was added to each sample (57). An RT-qPCR using AgPath-ID One-Step RT-PCR reagents (Thermo Fisher Scientific) with a primer/probe set targeting the 3D-coding region (58) was performed to detect FMDV RNA.

### RNA extraction and sequencing

For the sequencing of FMDV genomes, the untreated OPF, as well as samples of serum, nasal fluid, and saliva collected during the acute phase, was used. RNA extraction was performed with 250  $\mu$ L of the original sample (without prior amplification of virus in culture) and 750  $\mu$ L TRIzol LS Reagent (Thermo Fisher Scientific) as described by the manufacturer. To obtain a sequence of the entire ORF, a set of 10 primer pairs was chosen, each spanning 900 to 1,000 nucleotides with overlapping ends, as described in Table S3. Apart from the FMD Mix 3 of Dill et al. (59), all primer pairs were specifically designed for FMDV O/FRA/1/2001 using Primer3web version 4.1.0 (<https://primer3.ut.ee/>) (60). The genome was amplified using the qScript XLT One-Step RT-qPCR ToughMix (Quantabio) on a SimpliAmp Thermocycler (Thermo Fisher Scientific) with the following temperature profile: 20 minutes at 48°C for reverse transcription, 3 minutes of activation at 94°C, 45 cycles of 15 seconds at 94°C, 30 seconds at 60°C, 60 seconds at 68°C, and a final elongation of 5 minutes at 68°C. Afterward, the DNA amplicon was purified by gel electrophoresis. Bands of the expected lengths were excised, and a clean-up was performed with the QIAquick Gel Extraction Kit (Qiagen). The purified DNA was sent to Eurofins Genomics (Ebersberg, Germany) for Sanger sequencing.

For comparison, supernatants of virus isolations from the same OPF samples on LFBK- $\alpha$ V $\beta$ 6 cells were partially sequenced using the primer sets of Dill et al. (59), covering the region coding for the polyprotein P1 and a region spanning from 2C to 3B.

A selected set of samples was used for deep sequencing, including the homogenized vesicular material used as the inoculum of the vaccination trial and vesicular fluid collected from the interdigital cleft of six animals during the acute phase (animals 190, 191, 425, 508, 509, and 662). Total RNA was extracted, converted into cDNA libraries, and sequenced as previously described (61). In short, RNA was extracted with TRIzol LS (Thermo Fisher Scientific) and RNeasy Mini spin columns (Qiagen) with on-column DNase I digestion. Subsequently, 500 ng of total RNA was reverse transcribed using SuperScript IV First-Strand cDNA Synthesis System (Thermo Fisher Scientific) in combination with the NEBNext Ultra II Non-Directional RNA Second Strand Synthesis Module (New England Biolabs), according to the manufacturers' instructions. The cDNA was sheared on a Covaris M220 Focused-ultrasonicator with a target size of 400 bp. Sheared DNA was concentrated by adding 1.8 volumes Agencourt AMPure XP beads (Beckman Coulter), washed twice with 80% (vol/vol) ethanol, eluted in 25  $\mu$ L nuclease-free water, and used for library preparation with the GeneRead DNA Library L Core kit (Qiagen). After end repair and adapter ligation, the library was purified using 1.8 volumes AMPure XP beads, followed by a size selection aiming at a target size of around 350 to 550 bp. Quality control was performed with an Agilent High Sensitivity DNA kit, and the molarity was determined with a KAPA Library Quantification kit. Sequencing was performed in a pooled run on an Ion Torrent S5 XL instrument with an Ion 530 Chip Kit.

### Sequence analysis

Sanger sequencing reads were mapped to the consensus sequence of the inoculum, and a consensus sequence of the ORF of each sample was generated with Geneious Prime 2021.0.1 (<https://www.geneious.com>). Sanger reads with low-quality chromatograms (e.g., high background or no discernable peaks) were excluded. For most of the ORF, this consensus sequence was created from two overlapping, quality- and

primer-trimmed Sanger reads of 900–1,000 nucleotides in length. In Geneious Prime, the consensus threshold was set at 75% and heterozygotes were called at 50%. The “Find Variations/SNPs” tool in Geneious was used to detect discrepancies between the mapped sequences and the consensus sequence of the inoculum.

For deep-sequenced samples, data sets of 1.6 to 4.4 million reads were quality trimmed with Trimmomatic version 0.39 (<https://github.com/usadellab/Trimmomatic>) using an average quality of 22 in a sliding window of 5-mers. Additionally, reads shorter than 50 bp were discarded. In general, during quality trimming, around one-third of the input reads was dropped, leaving two-thirds of the data set as high-quality data for further analysis. The trimmed reads were mapped against the full genome sequence of the twice plaque-purified cell culture isolate (GenBank accession no. [OV121130](https://www.ncbi.nlm.nih.gov/nuccore/OV121130)) using Bowtie2 (<https://github.com/BenLangmead/bowtie2>; version 2.3.4.3) in the --sensitive mode (end-to-end alignment), with 34% of the data set aligned (inoculum) or >95% (vesicular fluid), respectively. Variants were called using LoFreq (<https://github.com/CSB5/lofreq>; version 2.1.3.1) with default filter settings. Variants with <0.5% frequency were excluded from further analysis and interpretation. Consensus-level mutations were defined as variants that appeared in more than 50% of the reads with respect to the original inoculum.

Detailed analysis and graphical representation of mutations were performed using R (<https://www.r-project.org/>). Visualization of mutations in the capsid was conducted with ChimeraX (62, 63) based on the X-ray crystal structure of 1FOD, an FMDV O1K strain including the G-H loop in a “down” position (7). The VP2 capsid protein structure of O/FRA/1/2001 was predicted using AlphaFold (64) in ChimeraX.

### Phylogenetic analysis

An alignment of all sequences including the inoculum was prepared using MUSCLE (version 3.8.425 [65]) in Geneious. From this alignment, a distance matrix based on the differences in the alignment was constructed in R (<https://www.r-project.org/>) and calculated using classical multidimensional scaling (66). A phylogenetic tree was constructed with IQ-TREE2 (version 2.3.6) using automatic model selection and 10,000 ultrafast bootstrap replicates.

### Functional analyses

Functional analyses were performed comparing the inoculum and two isolates from the persistent phase of infection, one containing only one amino acid exchange in VP3 (R56C) and one isolate containing VP3 R56C as well as an amino acid exchange in VP2 (Y79H).

### Plaque purification

To obtain virus isolates with the appropriate genotypes, plaque purification was performed with the inoculum, TTE-treated OPF from animal 508 collected at 24 dpi, and TTE-treated OPF from animal 510 collected at 14 dpi, which was passaged once on LFBK- $\alpha$ V $\beta$ 6 cells. The plaque purification was carried out on a 90% confluent LFBK- $\alpha$ V $\beta$ 6 monolayer with an overlay of 1.5% methyl cellulose (Sigma-Aldrich) in cell culture medium. Plaques were picked after 24 to 48 hours with a pipette tip, transferred to culture medium, incubated overnight, and passaged once on LFBK- $\alpha$ V $\beta$ 6 cells until a cytopathic effect was apparent. The desired mutations were confirmed by sequencing the P1-coding region with the primer pairs described above.

### Virus titration

Endpoint titration was conducted on LFBK- $\alpha$ V $\beta$ 6 cells. Viral titers were calculated as 50% tissue culture infectious doses (TCID<sub>50</sub>) per 100  $\mu$ L using the Spearman-Kärber method (67, 68).

### ***Infectivity assay on receptor-deficient cells***

The infectivity assay was adapted from Jackson et al. (69), without washing the cell monolayers with citric acid buffer. The receptor-binding capacity of the plaque-purified viruses was evaluated by infecting cells expressing different receptors FMDV can utilize for cell entry. This included LFBK- $\alpha$ V $\beta$ 6 cells expressing the preferred integrin receptor  $\alpha$ V $\beta$ 6; IB-RS-2 cells expressing only integrin  $\alpha$ V $\beta$ 8 but not  $\alpha$ V $\beta$ 6 (35); BHK-21 cells expressing the integrin  $\alpha$ V $\beta$ 3 and HS, but for efficient FMDV infection, HS is required (70); CHO-K1 cells expressing only HS but no integrins (71); and CHO-677 cells expressing neither integrins nor HS (53). These experiments were performed in duplicate. Confluent monolayers of cells were infected, incubated for 1 hour at 37°C, and then washed with culture medium. Supernatant from the cultures was harvested 16 hours postinfection.

### ***Growth kinetics***

Viral growth on LFBK- $\alpha$ V $\beta$ 6 and IB-RS-2 cells was characterized and compared between the three isolates. Cell monolayers in 12-well plates were infected at a multiplicity of infection of 0.1. Samples were taken at 0, 4, 8, 16, and 24 hours postinfection and were titrated on LFBK- $\alpha$ V $\beta$ 6 cells (72). These experiments were performed in duplicate.

### ***Virus neutralization test (VNT)***

A neutralization test to compare the inoculum and plaque-purified virus from the persistent phase was performed using the serum collected from the same animal. The VNT was performed as described by the World Organisation for Animal Health (WOAH) (73). Briefly, a twofold serial dilution of serum was prepared in a 96-well plate in duplicate. To each well, 50  $\mu$ L of virus suspension containing 100 TCID<sub>50</sub> was added. After an incubation of 2 hours at 37°C, 50  $\mu$ L of a BHK-21 cell suspension was added. The plates were read after 3 days at 37°C with 5% CO<sub>2</sub>. Titers are expressed as the final dilution of serum where 50% of wells were protected from cytopathic effect.

### ***Statistical analysis***

The binomial proportion confidence interval for the incidence of persistent FMDV infection was calculated by the Wilson method (74) using R (<https://www.r-project.org/>).

### **ACKNOWLEDGMENTS**

We thank Anja Landmesser and Anja Schulz for their excellent technical assistance; Christian Loth, Ralf Henkel, and Andreas Bath for their valuable support during necropsies; Matthias Jahn, Steffen Brenz, Dominique Lux, and Patrice Mary for their diligent animal care; and Patrick Zitzow for excellent technical assistance in deep sequencing.

Molecular analyses and visualizations were performed with UCSF ChimeraX, developed by the Resource for Biocomputing, Visualization, and Informatics at the University of California, San Francisco, with support from the National Institutes of Health R01-GM129325 and the Office of Cyber Infrastructure and Computational Biology, National Institute of Allergy and Infectious Diseases.

Figures 4 and 8 were created using BioRender.com under the agreement numbers CI274PK8H0 and AG274PJ8LT.

This work was funded by the Federal Office for Agriculture and Food (BLE, Germany) through the ICRAD ERA-Net project FMDV\_PersistOmics, grant number 2821ERA28D.

Writing—original draft: B.L., F.P., and M.E.; methodology: B.L., F.P., and M.E.; investigation: B.L., F.P., L.F., and M.E.; formal analysis, visualization, and data curation: B.L. and F.P.; supervision: F.P., M.B., and M.E.; conceptualization: F.P., M.B., and M.E.; project administration: M.E.

**AUTHOR AFFILIATION**

<sup>1</sup>Institute of Diagnostic Virology, Friedrich-Loeffler-Institut, Greifswald-Insel Riems, Germany

**PRESENT ADDRESS**

Leonie F. Forth, Department of Biological Safety, German Federal Institute for Risk Assessment, Berlin, Germany

**AUTHOR ORCIDs**

Benedikt Litz  <http://orcid.org/0000-0003-2263-7048>

Florian Pfaff  <http://orcid.org/0000-0003-0178-6183>

Martin Beer  <http://orcid.org/0000-0002-0598-5254>

Michael Eschbaumer  <http://orcid.org/0000-0002-1104-0695>

**FUNDING**

Funder	Grant(s)	Author(s)
ICRAD ERA-net	2821ERA28D	Benedikt Litz

**AUTHOR CONTRIBUTIONS**

Benedikt Litz, Data curation, Formal analysis, Investigation, Methodology, Visualization, Writing – original draft | Leonie F. Forth, Data curation, Investigation, Writing – review and editing | Florian Pfaff, Conceptualization, Data curation, Formal analysis, Investigation, Methodology, Supervision, Visualization, Writing – original draft, Writing – review and editing | Martin Beer, Conceptualization, Resources, Supervision, Writing – review and editing | Michael Eschbaumer, Conceptualization, Funding acquisition, Investigation, Methodology, Project administration, Resources, Supervision, Writing – original draft, Writing – review and editing

**DATA AVAILABILITY**

The deep sequencing data used in this study were uploaded to SRA under accession no. [SRR31675832–SRR31675838](https://www.ncbi.nlm.nih.gov/sra/SRR31675832-SRR31675838). The consensus-level sequences spanning the FMDV ORF from 21 animals along with metadata were published in Zenodo project [10.5281/zenodo.14384049](https://zenodo.org/record/14384049).

**ETHICS APPROVAL**

Animal trials were approved by the State Office for Agriculture, Food and Fisheries of Mecklenburg-Vorpommern under the file numbers 7221.3-1-019/18 and 7221.3-1-052/21.

**ADDITIONAL FILES**

The following material is available [online](#).

**Supplemental Material**

**Figure S1** (JVI01422-24-S0001.docx). Body temperature and vesicular lesions of the animals in the vaccination study.

**Table S1** (JVI01422-24-S0002.xlsx). Detected single nucleotide variants (SNVs) in inoculum and vesicular material from different animals.

**Table S2** (JVI01422-24-S0003.xlsx). Non-synonymous consensus-level amino acid variants detected during the acute phase of FMDV infection.

**Table S3** (JVI01422-24-S0004.xlsx). Primers.

## REFERENCES

- Mandary MB, Masomian M, Poh CL. 2019. Impact of RNA virus evolution on quasispecies formation and virulence. *Int J Mol Sci* 20:18. <https://doi.org/10.3390/ijms20184657>
- Wright CF, Morelli MJ, Thébaud G, Knowles NJ, Herzyk P, Paton DJ, Haydon DT, King DP. 2011. Beyond the consensus: dissecting within-host viral population diversity of foot-and-mouth disease virus by using next-generation genome sequencing. *J Virol* 85:2266–2275. <https://doi.org/10.1128/JVI.01396-10>
- Amicone M, Borges V, Alves MJ, Isidro J, Zé-Zé L, Duarte S, Vieira L, Guiomar R, Gomes JP, Gordo I. 2022. Mutation rate of SARS-CoV-2 and emergence of mutators during experimental evolution. *Evol Med Public Health* 10:142–155. <https://doi.org/10.1093/emph/eoac010>
- Diaz-San Segundo F, Medina GN, Stenfeldt C, Arzt J, de Los Santos T. 2017. Foot-and-mouth disease vaccines. *Vet Microbiol* 206:102–112. <https://doi.org/10.1016/j.vetmic.2016.12.018>
- Belsham GJ. 2005. Translation and replication of FMDV RNA. *Curr Top Microbiol Immunol* 288:43–70. [https://doi.org/10.1007/3-540-27109-0\\_3](https://doi.org/10.1007/3-540-27109-0_3)
- Mahapatra M, Hamblin P, Paton DJ. 2012. Foot-and-mouth disease virus epitope dominance in the antibody response of vaccinated animals. *J Gen Virol* 93:488–493. <https://doi.org/10.1099/vir.0.037952-0>
- Logan D, Abu-Ghazaleh R, Blakemore W, Curry S, Jackson T, King A, Lea S, Lewis R, Newman J, Parry N, Rowlands D, Stuart D, Fry E. 1993. Structure of a major immunogenic site on foot-and-mouth disease virus. *Nature* 362:566–568. <https://doi.org/10.1038/362566a0>
- Stenfeldt C, Arzt J. 2020. The carrier conundrum: a review of recent advances and persistent gaps regarding the carrier state of foot-and-mouth disease virus. *Pathogens* 9:167. <https://doi.org/10.3390/pathogens9030167>
- Stenfeldt C, Eschbaumer M, Rekant SI, Pacheco JM, Smoliga GR, Hartwig EJ, Rodriguez LL, Arzt J. 2016. The foot-and-mouth disease carrier state divergence in cattle. *J Virol* 90:6344–6364. <https://doi.org/10.1128/JVI.00388-16>
- Arzt J, Belsham GJ, Lohse L, Bøtner A, Stenfeldt C. 2018. Transmission of foot-and-mouth disease from persistently infected carrier cattle to naive cattle via transfer of oropharyngeal fluid. *mSphere* 3:e00365-18. <https://doi.org/10.1128/mSphere.00365-18>
- Tenzin DA, Vernooij H, Bouma A, Stegeman A. 2008. Rate of foot-and-mouth disease virus transmission by carriers quantified from experimental data. *Risk Anal* 28:303–309. <https://doi.org/10.1111/j.1539-6924.2008.01020.x>
- Meek HC, Stenfeldt C, Arzt J. 2022. Morphological and phenotypic characteristics of the bovine nasopharyngeal mucosa and associated lymphoid tissue. *J Comp Pathol* 198:62–79. <https://doi.org/10.1016/j.jcpa.2022.07.011>
- Sutmoller P, Cottral GE. 1967. Improved techniques for the detection of foot-and-mouth disease virus in carrier cattle. *Archiv f Virusforsch* 21:170–177. <https://doi.org/10.1007/BF01241441>
- Jarousse N, Grant RA, Hogle JM, Zhang L, Senkowski A, Roos RP, Michiels T, Brahm M, McAllister A. 1994. A single amino acid change determines persistence of a chimeric theiler's virus. *J Virol* 68:3364–3368. <https://doi.org/10.1128/JVI.68.5.3364-3368.1994>
- Gebauer F, de la Torre JC, Gomes I, Mateu MG, Barahona H, Tiraboschi B, Bergmann I, de Mello PA, Domingo E. 1988. Rapid selection of genetic and antigenic variants of foot-and-mouth disease virus during persistence in cattle. *J Virol* 62:2041–2049. <https://doi.org/10.1128/JVI.62.6.2041-2049.1988>
- Horsington J, Zhang Z. 2007. Consistent change in the B–C loop of VP2 observed in foot-and-mouth disease virus from persistently infected cattle: implications for association with persistence. *Virus Res* 125:114–118. <https://doi.org/10.1016/j.virusres.2006.12.008>
- Pauszek SJ, Eschbaumer M, Brito B, de Carvalho Ferreira HC, Vu LT, Phuong NT, Hoang BH, Tho ND, Dong PV, Minh PQ, Long NT, Dung DH, Rodriguez LL, Arzt J. 2016. Site-specific substitution (Q172R) in the VP1 protein of FMDV isolates collected from asymptomatic carrier ruminants in Vietnam. *Viral Rep* 6:90–96. <https://doi.org/10.1016/j.virep.2016.10.001>
- Parthiban ABR, Mahapatra M, Gubbins S, Parida S. 2015. Virus excretion from foot-and-mouth disease virus carrier cattle and their potential role in causing new outbreaks. *PLoS ONE* 10:e0128815. <https://doi.org/10.1371/journal.pone.0128815>
- Arzt J, Fish I, Pauszek SJ, Johnson SL, Chain PS, Rai DK, Rieder E, Goldberg TL, Rodriguez LL, Stenfeldt C. 2019. The evolution of a super-swarm of foot-and-mouth disease virus in cattle. *PLoS ONE* 14:e0210847. <https://doi.org/10.1371/journal.pone.0210847>
- Fish I, Stenfeldt C, Palinski RM, Pauszek SJ, Arzt J. 2020. Into the deep (Sequence) of the foot-and-mouth disease virus gene pool: bottlenecks and adaptation during infection in naive and vaccinated cattle. *Pathogens* 9:208. <https://doi.org/10.3390/pathogens9030208>
- Borca MV, Pacheco JM, Holinka LG, Carrillo C, Hartwig E, Garriga D, Kramer E, Rodriguez L, Piccone ME. 2012. Role of arginine-56 within the structural protein VP3 of foot-and-mouth disease virus (FMDV) O1 campos in virus virulence. *Virology (Auckl)* 422:37–45. <https://doi.org/10.1016/j.virol.2011.09.031>
- Dill V, Eschbaumer M. 2020. Cell culture propagation of foot-and-mouth disease virus: adaptive amino acid substitutions in structural proteins and their functional implications. *Virus Genes* 56:1–15. <https://doi.org/10.1007/s11262-019-01714-7>
- Cottam EM, Haydon DT, Paton DJ, Gloster J, Wilesmith JW, Ferris NP, Hutchings GH, King DP. 2006. Molecular epidemiology of the foot-and-mouth disease virus outbreak in the United Kingdom in 2001. *J Virol* 80:11274–11282. <https://doi.org/10.1128/JVI.01236-06>
- Sutmoller P, McVicar JW, Cottral GE. 1968. The epizootiological importance of foot-and-mouth disease carriers. I. Experimentally produced foot-and-mouth disease carriers in susceptible and immune cattle. In *Archiv fur die gesamte Virusforschung* 23:227–235. <https://doi.org/10.1007/BF01241895>
- Aktas S, Samuel AR. 2000. Identification of antigenic epitopes on the foot and mouth disease virus isolate O1/Manisa/Turkey/69 using monoclonal antibodies. *Rev Sci Tech OIE* 19:744–753. <https://doi.org/10.20506/rst.19.3.1244>
- Barnett PV, Samuel AR, Pullen L, Ansell D, Butcher RN, Parkhouse RM. 1998. Monoclonal antibodies, against O1 serotype foot-and-mouth disease virus, from a natural bovine host, recognize similar antigenic features to those defined by the mouse. *J Gen Virol* 79 ( Pt 7):1687–1697. <https://doi.org/10.1099/0022-1317-79-7-1687>
- Kitson JDA, McCahon D, Belsham GJ. 1990. Sequence analysis of monoclonal antibody resistant mutants of type O foot and mouth disease virus: evidence for the involvement of the three surface exposed capsid proteins in four antigenic sites. *Virology (Auckl)* 179:26–34. [https://doi.org/10.1016/0042-6822\(90\)90269-W](https://doi.org/10.1016/0042-6822(90)90269-W)
- Parry N, Fox G, Rowlands D, Brown F, Fry E, Acharya R, Logan D, Stuart D. 1990. Structural and serological evidence for a novel mechanism of antigenic variation in foot-and-mouth disease virus. *Nature* 347:569–572. <https://doi.org/10.1038/347569a0>
- Sarangi LN, Mahapatra JK, Subramaniam S, Sanyal A, Pattnaik B. 2013. Antigenic site variation in foot-and-mouth disease virus serotype O grown under vaccinal serum antibodies *in vitro*. *Virus Res* 176:273–279. <https://doi.org/10.1016/j.virusres.2013.07.003>
- Chamberlain K, Fowler VL, Barnett PV, Gold S, Wadsworth J, Knowles NJ, Jackson T. 2015. Identification of a novel cell culture adaptation site on the capsid of foot-and-mouth disease virus. *J Gen Virol* 96:2684–2692. <https://doi.org/10.1099/jgv.0.000222>
- Fry EE, Newman JW, Curry S, Najjam S, Jackson T, Blakemore W, Lea SM, Miller L, Burman A, King AMQ, Stuart DI. 2005. Structure of foot-and-mouth disease virus serotype A10 61 alone and complexed with oligosaccharide receptor: receptor conservation in the face of antigenic variation. *J Gen Virol* 86:1909–1920. <https://doi.org/10.1099/vir.0.80730-0>
- Haghparast A, Wauben MHM, Grosfeld-Stulemeyer MC, van Kooten P, Hensen EJ. 2000. Selection of T-cell epitopes from foot-and-mouth disease virus reflects the binding affinity to different cattle MHC class II molecules. *Immunogenetics* 51:733–742. <https://doi.org/10.1007/s002510000205>
- Pacheco JM, Smoliga GR, O'Donnell V, Brito BP, Stenfeldt C, Rodriguez LL, Arzt J. 2015. Persistent foot-and-mouth disease virus infection in the nasopharynx of cattle; tissue-specific distribution and local cytokine expression. *PLoS ONE* 10:e0125698. <https://doi.org/10.1371/journal.pone.0125698>
- LaRocco M, Krug PW, Kramer E, Ahmed Z, Pacheco JM, Duque H, Baxt B, Rodriguez LL. 2013. A continuous bovine kidney cell line constitutively expressing bovine  $\alpha\beta 6$  integrin has increased susceptibility to foot-and-mouth disease virus. *J Clin Microbiol* 51:1714–1720. <https://doi.org/10.1128/JCM.03370-12>

35. King DP, Burman A, Gold S, Shaw AE, Jackson T, Ferris NP. 2011. Integrin sub-unit expression in cell cultures used for the diagnosis of foot-and-mouth disease. *Vet Immunol Immunopathol* 140:259–265. <https://doi.org/10.1016/j.vetimm.2011.01.008>
36. Arzt J, Fish IH, Bertram MR, Smoliga GR, Hartwig EJ, Pauszek SJ, Holinka-Patterson L, Diaz-San Segundo FC, Sitt T, Rieder E, Stenfeldt C. 2021. Simultaneous and staggered foot-and-mouth disease virus coinfection of cattle. *J Virol* 95:e0165021. <https://doi.org/10.1128/JVI.01650-21>
37. Fish I, Stenfeldt C, Spinard E, Medina GN, Azzinaro PA, Bertram MR, Holinka L, Smoliga GR, Hartwig EJ, de Los Santos T, Arzt J. 2022. Foot-and-mouth disease virus interserotypic recombination in superinfected carrier cattle. *Pathogens* 11:644. <https://doi.org/10.3390/pathogens11060644>
38. Horsington J, Zhang Z. 2007. Analysis of foot-and-mouth disease virus replication using strand-specific quantitative RT-PCR. *J Virol Methods* 144:149–155. <https://doi.org/10.1016/j.jviromet.2007.05.002>
39. Suttmoller P, Gaggero A. 1965. Foot-and mouth diseases carriers. *Vet Rec* 77:968–969. <https://doi.org/10.1136/vr.77.33.968>
40. Sa-Carvalho D, Rieder E, Baxt B, Rodarte R, Tanuri A, Mason PW. 1997. Tissue culture adaptation of foot-and-mouth disease virus selects viruses that bind to heparin and are attenuated in cattle. *J Virol* 71:5115–5123. <https://doi.org/10.1128/JVI.71.7.5115-5123.1997>
41. Juleff N, Valdazo-González B, Wadsworth J, Wright CF, Charleston B, Paton DJ, King DP, Knowles NJ. 2013. Accumulation of nucleotide substitutions occurring during experimental transmission of foot-and-mouth disease virus. *J Gen Virol* 94:108–119. <https://doi.org/10.1099/vir.0.046029-0>
42. Kanno T, Yamakawa M, Yoshida K, Sakamoto K. 2002. The complete nucleotide sequence of the PanAsia strain of foot-and-mouth disease virus isolated in Japan. *Virus Genes* 25:119–125. <https://doi.org/10.1023/a:1020103700108>
43. Mason PW, Pacheco JM, Zhao Q-Z, Knowles NJ. 2003. Comparisons of the complete genomes of Asian, African and European isolates of a recent foot-and-mouth disease virus type O pandemic strain (PanAsia). *J Gen Virol* 84:1583–1593. <https://doi.org/10.1099/vir.0.18669-0>
44. Stenfeldt C, Fish I, Meek HC, Arzt J. 2023. Heterogeneity and recombination of foot-and-mouth disease virus during multi-strain coinfection of cattle. *mSphere* 8:e0064322. <https://doi.org/10.1128/msphere.00643-22>
45. Cortey M, Ferretti L, Pérez-Martín E, Zhang F, de Klerk-Lorist L-M, Scott K, Freimanis G, Seago J, Ribeca P, van Schalkwyk L, Juleff ND, Maree FF, Charleston B. 2019. Persistent infection of african buffalo (*Syncerus caffer*) with foot-and-mouth disease virus: limited viral evolution and no evidence of antibody neutralization escape. *J Virol* 93:15. <https://doi.org/10.1128/JVI.00563-19>
46. Salt JS. 1993. The carrier state in foot and mouth disease—an immunological review. *Br Vet J* 149:207–223. [https://doi.org/10.1016/S0007-1935\(05\)80168-X](https://doi.org/10.1016/S0007-1935(05)80168-X)
47. Burman A, Clark S, Abrescia NGA, Fry EE, Stuart DI, Jackson T. 2006. Specificity of the VP1 GH loop of foot-and-mouth disease virus for alphav integrins. *J Virol* 80:9798–9810. <https://doi.org/10.1128/JVI.00577-06>
48. Koivisto L, Bi J, Häkkinen L, Larjava H. 2018. Integrin  $\alpha\beta 6$ : structure, function and role in health and disease. *Int J Biochem Cell Biol* 99:186–196. <https://doi.org/10.1016/j.biocel.2018.04.013>
49. McCarty JH. 2020.  $\text{Av}\beta 8$  integrin adhesion and signaling pathways in development, physiology and disease. *J Cell Sci* 133:12. <https://doi.org/10.1242/jcs.239434>
50. Robinson L, Windsor M, McLaughlin K, Hope J, Jackson T, Charleston B. 2011. Foot-and-mouth disease virus exhibits an altered tropism in the presence of specific immunoglobulins, enabling productive infection and killing of dendritic cells. *J Virol* 85:2212–2223. <https://doi.org/10.1128/JVI.02180-10>
51. Castro M de. 1964. Comportamento do vírus aftoso em cultura de células: susceptibilidade da linhagem de células suínas IB-RS-2, p 63–78. In *Archivos do Instituto Biológico, São Paulo* (31)
52. Puck TT, Cieciura SJ, Robinson A. 1958. Genetics of somatic mammalian cells. III. Long-term cultivation of euploid cells from human and animal subjects. *J Exp Med* 108:945–956. <https://doi.org/10.1084/jem.108.6.945>
53. Lidholt K, Weinke JL, Kiser CS, Lugemwa FN, Bame KJ, Cheifetz S, Massagué J, Lindahl U, Esko JD. 1992. A single mutation affects both N-acetylglucosaminyltransferase and glucuronosyltransferase activities in a Chinese hamster ovary cell mutant defective in heparan sulfate biosynthesis. *Proc Natl Acad Sci U S A* 89:2267–2271. <https://doi.org/10.1073/pnas.89.6.2267>
54. Litz B, Sehl-Ewert J, Breithaupt A, Landmesser A, Pfaff F, Romey A, Blaise-Boisseau S, Beer M, Eschbaumer M. 2024. Leaderless foot-and-mouth disease virus serotype O did not cause clinical disease and failed to establish a persistent infection in cattle. *Emerg Microbes Infect* 13:2348526. <https://doi.org/10.1080/22221751.2024.2348526>
55. Keck H, Litz B, Hoffmann B, Sehl-Ewert J, Beer M, Eschbaumer M. 2022. Full-length genomic RNA of foot-and-mouth disease virus is infectious for cattle by injection. *Viruses* 14:1924. <https://doi.org/10.3390/v14091924>
56. Brown F, Cartwright B. 1960. Purification of the virus of foot-and-mouth disease by fluorocarbon treatment and its dissociation from neutralizing antibody. *J Immunol* 85:309–313. <https://doi.org/10.4049/jimmunol.85.3.309>
57. Hoffmann B, Depner K, Schirmer H, Beer M. 2006. A universal heterologous internal control system for duplex real-time RT-PCR assays used in a detection system for pestiviruses. *J Virol Methods* 136:200–209. <https://doi.org/10.1016/j.jviromet.2006.05.020>
58. Callahan JD, Brown F, Osorio FA, Sur JH, Kramer E, Long GW, Lubroth J, Ellis SJ, Shoulars KS, Gaffney KL, Rock DL, Nelson WM. 2002. Use of a portable real-time reverse transcriptase-polymerase chain reaction assay for rapid detection of foot-and-mouth disease virus. *J Am Vet Med Assoc* 220:1636–1642. <https://doi.org/10.2460/javma.2002.220.1636>
59. Dill V, Beer M, Hoffmann B. 2017. Simple, quick and cost-efficient: a universal RT-PCR and sequencing strategy for genomic characterisation of foot-and-mouth disease viruses. *J Virol Methods* 246:58–64. <https://doi.org/10.1016/j.jviromet.2017.04.007>
60. Untergrasser A, Cutcutache I, Koresaar T, Ye J, Faircloth BC, Remm M, Rozen SG. 2012. Primer3—new capabilities and interfaces. *Nucleic Acids Res* 40:e115. <https://doi.org/10.1093/nar/gks596>
61. Forth LF, Höper D, Beer M, Eschbaumer M. 2020. High-resolution composition analysis of an inactivated polyvalent foot-and-mouth disease vaccine. *Pathogens* 9:63. <https://doi.org/10.3390/pathogens9010063>
62. Meng EC, Goddard TD, Pettersen EF, Couch GS, Pearson ZJ, Morris JH, Ferrin TE. 2023. UCSF chimeraX: tools for structure building and analysis. *Protein Sci* 32:e4792. <https://doi.org/10.1002/pro.4792>
63. Pettersen EF, Goddard TD, Huang CC, Meng EC, Couch GS, Croll TI, Morris JH, Ferrin TE. 2021. UCSF ChimeraX: structure visualization for researchers, educators, and developers. *Protein Sci* 30:70–82. <https://doi.org/10.1002/pro.3943>
64. Jumper J, Evans R, Pritzel A, Green T, Figurnov M, Ronneberger O, Tunyasuvunakool K, Bates R, Židek A, Potapenko A, et al. 2021. Highly accurate protein structure prediction with alphafold. *Nature* 596:583–589. <https://doi.org/10.1038/s41586-021-03819-2>
65. Edgar RC. 2021. High-accuracy alignment ensembles enable unbiased assessments of sequence homology and phylogeny. <https://doi.org/10.1101/2021.06.20.449169>
66. Mardia KV. 1978. Some properties of classical multi-dimensional scaling. *Commun Stat Theory Methods* 7:1233–1241. <https://doi.org/10.1080/03610927808827707>
67. Kärber G. 1931. Beitrag zur kollektiven behandlung pharmakologischer reihenversuche. *Archiv f experiment Pathol u Pharmakol* 162:480–483. <https://doi.org/10.1007/BF01863914>
68. Spearman C. 1908. THE method of “right and wrong cases” (“constant stimuli”) without Gauss’s formulae. *British J Psychol* 2:227–242. <https://doi.org/10.1111/j.2044-8295.1908.tb00176.x>
69. Jackson T, Sheppard D, Denyer M, Blakemore W, King AMQ. 2000. The epithelial integrin  $\alpha\beta 6$  is a receptor for foot-and-mouth disease virus. *J Virol* 74:4949–4956. <https://doi.org/10.1128/JVI.74.11.4949-4956.2000>
70. Jackson T, Ellard FM, Ghazaleh RA, Brookes SM, Blakemore WE, Corteyn AH, Stuart DI, Newman JW, King AM. 1996. Efficient infection of cells in culture by type O foot-and-mouth disease virus requires binding to cell surface heparan sulfate. *J Virol* 70:5282–5287. <https://doi.org/10.1128/JVI.70.8.5282-5287.1996>
71. Baranowski E, Sevilla N, Verdaguer N, Ruiz-Jarabo CM, Beck E, Domingo E. 1998. Multiple virulence determinants of foot-and-mouth disease virus in cell culture. *J Virol* 72:6362–6372. <https://doi.org/10.1128/JVI.72.8.6362-6372.1998>
72. Dill V, Zimmer A, Beer M, Eschbaumer M. 2020. Targeted modification of the foot-and-mouth disease virus genome for quick cell culture adaptation. *Vaccines (Basel)* 8:583. <https://doi.org/10.3390/vacines8040583>
73. Chapter 3.1.8. Foot and Mouth Disease (Infection with Foot and Mouth Disease Virus). 2022 In *World Organisation for Animal Health: Manual of*

Diagnostic Tests and Vaccines for Terrestrial Animals 2022. [https://www.oie.int/fileadmin/Home/eng/Health\\_standards/tahm/3.01.08\\_FMD.pdf](https://www.oie.int/fileadmin/Home/eng/Health_standards/tahm/3.01.08_FMD.pdf).

74. Wilson EB. 1927. Probable inference, the law of succession, and statistical Inference. *J Am Stat Assoc* 22:209–212. <https://doi.org/10.1080/01621459.1927.10502953>



## CHAPTER V: DISCUSSION



## V. Discussion

Acute FMD with its fulminant clinical signs and highly infectious lesions is caused by the (fleeting) triumph of the virus over the host's innate immune system. Only the onset of the adaptive immune response, particularly the appearance of neutralizing antibodies, is able to resolve the acute phase of the infection. During the persistent phase, however, virus is still present despite an immune reaction which was capable of clearing the infection from the rest of the body, but is unable to remove FMDV from the epithelia of the nasopharynx.

Many viruses have found ways to maintain a productive viral replication even after they have been recognized by the host's immune defenses. However, the mechanisms they are using are as diverse as the viruses itself. For persistent FMDV infection, a conclusive mechanism has not yet been postulated. This thesis aims to uncover the virus-host interactions that allow FMDV to sustain a productive infection in the nasopharynx of cattle. Herein, I describe the influence of the virus on the host and the infected tissues with a focus on the role of the Leader proteinase L<sup>pro</sup> and the adaptation of FMDV to the host environment through genomic evolution.

### ***Objective I: Influence of FMDV on the host***

#### Publications I & II

The twelve proteins encoded by the genomic RNA of FMDV utilize a plethora of mechanisms counteracting the triggered innate immune response and inhibiting the IFN activation (Sarry et al. 2022). In the present publications I & II, we aimed to characterize the viral properties that are essential for the establishment of a persistent infection. Publication I focused on the non-structural Leader protein L<sup>pro</sup>. Our results showed that FMDV lacking L<sup>pro</sup> can actively replicate in cell culture with a noticeable growth inhibition relative to wildtype virus in IFN-competent cell lines. But *in vivo*, leaderless FMDV is even more strongly attenuated and could establish neither an acute nor a persistent infection. The Leader protein is therefore an essential protein for FMDV to productively infect animals. Whether the deletion of L<sup>pro</sup> prevented the primary infection completely or just suppressed the acute phase and in consequence thereof blocked the development of a persistent infection could not be determined in detail

in our study. An acute clinical phase, however, is not necessary for persistence as vaccinated animals which are clinically protected from FMD can develop a persistent infection as well. This is shown in publication II, where four of six vaccinated and challenged animals, which were all clinically protected nevertheless, remained persistently infected until the end of the study. The primary infection of the nasopharynx, on the other hand, is probably required for persistence since inoculation methods such as the intraepidermolingual or intramuscular infection, which bypass primary infection in the nasopharynx, do not recreate natural infection properly and the incidence of persistence is decreased (Sutmoller et al. 1968; Stenfeldt and Arzt 2020). But as described in publication I, in contrast to the wildtype-infected group, we did not detect viral RNA or infectious virus in animals infected with the leaderless FMDV and euthanized 24 hours later. Even *in vitro*, the ability of leaderless FMDV to productively infect a cell line decreases the closer the cellular phenotype is to the natural host, as it was previously demonstrated with a leaderless mutant of FMDV strain O<sub>1</sub> Kaufbeuren. It showed good replication in highly altered BHK-21 cells, but infection was blocked in primary bovine thyroid cells (Belsham 2013). The Leader protein L<sup>pro</sup> is a potent inhibitor of the type I IFN response and is involved early on in the host cell shut-off (Chinsangaram et al. 2001; Belsham et al. 2000). The severe impairment of the virus caused by its deletion suggests that even though other proteins of FMDV can also counteract the innate immune response, these mechanisms by themselves are insufficient or too slow to allow effective replication and the establishment of infection. In the case of leaderless FMDV, the innate immune response outweighs the viral counter mechanisms and prevents viral replication.

We documented some of the effects exerted by L<sup>pro</sup> *in vivo* on the transcriptome level, where L<sup>pro</sup> targets IFN-regulating factors as well as important IFN signaling transmitters of which some are downregulated in FMDV-infected tissue, suppressing an effective type I IFN response (see publication II). Targeting the receptors sensing viral RNA and their signaling pathways is a widely used strategy to antagonize the type I IFN response also employed by hepatitis C virus, another RNA virus with a single-stranded positive RNA genome that can cause chronic hepatitis (Chigbu et al. 2019). Meanwhile, IFN- $\gamma$  expression is less affected by FMDV, a bias that is also observed in chronic infections with human or simian immunodeficiency viruses (HIV/SIV). During the acute phase of HIV/SIV infection, both IFN- $\alpha/\beta$  and IFN- $\gamma$  responses are activated, but during chronic infection the IFN- $\alpha/\beta$  activity is often below the limit of detection

while IFN- $\gamma$  is still expressed by activated T cells and NK cells (Echebli et al. 2018). An activated IFN- $\gamma$  response in persistently BVDV-infected fetuses can limit viremia independently from the adaptive immune response. The increased IFN- $\gamma$  response usually functions as a bridge between innate and adaptive immune responses, but due to the early infection timepoint BVDV encounters an undeveloped immune system and infected fetuses are unable to mount an efficient adaptive immune response (Smirnova et al. 2014). Similar to BVDV, only inhibiting the IFN response is not enough to sustain a persistent FMDV infection, the adaptive immune system has to be suppressed as well.

A closer look at the progression of persistent BVDV infections leads to another important aspect of viral persistence. BVDV occurs in two biotypes: cytopathic and non-cytopathic. Only non-cytopathic strains are capable of producing persistently infected calves when infecting pregnant cows between the second and fourth month of gestation (Peterhans et al. 2010). The non-cytolytic phenotype is a pivotal requirement for the establishment of viral persistence. While some persistent viruses, such as lymphocytic choriomeningitis virus, are inherently non-cytopathic, other viruses can switch from cytopathic to non-cytopathic replication like Epstein-Barr virus (Flint et al. 2020). For FMDV, this would also mean a change in phenotype, from a cytolytic virus in the acute phase to a non-cytolytic infection during persistence. In immunofluorescence analyses of tissues from persistently FMDV-infected cattle, which were superinfected with a heterologous virus, Stenfeldt et al. (2023) showed that the localization of FMDV infection at 48 hpi and during the persistent phase is similar. But virus from the acute phase was colocalized more often with epithelial erosions while persistent virus was found in the superficial layer of intact epithelia. Whether the erosions from the acute phase were caused by the virus or preexisting lesions have enhanced the susceptibility of the epithelia for infection could not be determined, but nevertheless this suggests a change in the phenotype of FMDV, limiting its cytopathogenicity during persistent infection. *In vitro* experiments aiming to produce persistently FMDV-infected cell lines demonstrated that in MDBK cells, a bovine epithelial cell line, a subset of cells is infected but no cell lysis occurs, in contrast to the surrounding cells. The remaining MDBK cells are then again able to regrow into a confluent monolayer, creating a stable persistently FMDV-infected cell line (Kopliku et al. 2015). Similarly, in a primary culture of epithelial dorsal soft palate cells, which are the preferential localization of FMDV persistence, maintained at an air-liquid interface (DSP-ALI), epithelial

cells expressing integrin  $\alpha V\beta 6$  were susceptible to cell lysis, while the remaining cells, which were infected but did not show cytopathic effect, expressed vimentin but not integrin  $\alpha V\beta 6$  (Hägglund et al. 2020). This is corroborated by findings of O'Donnell et al. (2014) who showed that the epithelial character of persistently FMDV infected cells derived from the bovine pharynx decreases with increasing passage number and that a majority of cells in the persistently FMDV-infected culture are of non-epithelial origin, expressing vimentin but not cytokeratin or integrin  $\alpha V\beta 6$ . The increasing expression of vimentin can be caused by repeated cell passage inducing an epithelial-mesenchymal transition in epithelial cells (Hägglund et al. 2020). However, in epithelia, especially in lymphatic epithelia like the FAE of the MALT in the nasopharynx, the expression of vimentin is indicative of microfold cells (M-cells) (Tahoun et al. 2011). M-cells constitute a minor proportion of the cells of the FAE, but play an important role by sampling antigens from the lumen and transmitting them to the immune cells of the MALT beneath (Oya et al. 2021). The presence of M-cells in the FAE of the bovine nasopharynx may also be relevant for changes of host cell tropism since the FAE is the preferred micro-localization for persistent FMDV infection (Stenfeldt et al. 2018). Overall, this suggests a higher resistance against virus-induced cell lysis in a subset of cells in the FAE, which is constituted of cells of non-epithelial origin, including M-cells.

Normally, in FMDV-infected cells, virus-induced cell death can be prevented by an inhibition of apoptosis which has been observed *in vitro* and *in vivo*. One viral protein which can directly inhibit apoptosis is the Leader proteinase L<sup>PRO</sup>. It suppresses apoptosis by targeting RNase L, whose expression is triggered by viral dsRNA and leads to the degradation of host RNA and ultimately cell death (Sui et al. 2021). The tissue susceptible to persistent FMDV infection itself may also be a determining factor in reducing cell death, as it shows a higher expression of anti-apoptotic survivin and fewer death receptor signaling genes, suggesting a physiologically impeded apoptosis in uninfected tissue (Zhu et al. 2013). *In vitro* in the persistently FMDV-infected DSP-ALI model described above, the pro-apoptotic response of the acute phase was reduced during the persistent phase of FMDV infection (Pfaff et al. 2019). *In vivo*, Eschbaumer et al. could show by a microarray analysis of differentially expressed genes that fewer death receptors were expressed in carriers compared to non-carriers, and anti-apoptotic genes, such as BIRC3 and BCL2, were upregulated in persistently infected animals. This was corroborated in part by our transcriptomic study using RNA-seq, especially by the observed overexpression

of the anti-apoptotic genes SpiB and BCL2. Here, SpiB is of special interest since its overexpression has been demonstrated to enhance resistance against anoikis or detachment-induced cell death (Zhang et al. 2020a). Anoikis likely occurs in FMDV-infected tissue, where the majority of cells undergoes lysis and only a subset of cells remains intact but loses connections to surrounding cells, as described above for the persistently infected cell lines. And to pick up the hypothesis from before, SpiB is expressed in M-cells and encodes proteins involved in the uptake of antigens (Oya et al. 2021). M-cells would probably be susceptible to FMDV infection, since they express at least the integrin subunits  $\alpha V$  and  $\beta 3$  (Secott et al. 2004) but it is unknown if they are permissive. To our knowledge, no study has shown an FMDV infection of M-cells yet. During primary and acute infection of pigs, Stenfeldt et al. (2014b) did observe M-cells not to colocalize with FMDV antigen in porcine tonsils. Another interesting aspect of the possibly suppressed apoptosis in persistently FMDV-infected cattle is the upregulation of BCL2 found in our study as well in the microarray study of Eschbaumer et al. (2016b). BCL2 has been associated with persistence of Epstein-Barr virus (Astorga-Gamaza et al. 2022) (EBV; Lymphocryptovirus humangamma4) and with Sindbis virus infection. In persistent EBV infection, a viral homologue of BCL2, called BHRF1, suppresses apoptosis in infected B cells and enables EBV to persist in these cells (Henderson et al. 1993). Sindbis virus is even able to increase BCL2 expression in persistently infected cell lines, but here the virulence of the strain is pivotal as only the non-virulent strains induce persistence while the virulent strains provoke apoptosis (Appel et al. 2000).

That the virulence of a virus strain is correlated to the ability to establish persistent infection was also suggested for FMDV in its wildlife reservoir the African buffalo, but with an inverse relationship. In a coinfection study in which buffalo were simultaneously co-infected with strains of the three SAT serotypes, all strains were able to persistently infect animals, but SAT1 outcompeted the other two serotypes in terms of carrier incidence and duration of persistence. This phenotype was correlated with a higher cell killing capacity in an *in vitro* coinfection of ZZ-R cells (Maree et al. 2016). Using the same FMDV strains in single-serotype infections of buffalo, it was demonstrated that this SAT1 strain had a higher probability of persistently infecting animals and in addition there was a higher chance of viral transmission during the persistent phase of infection. This enables SAT1 to remain endemic in buffalo populations, where it would go extinct if only acute-phase transmission were to occur (Jolles et al. 2021).

Whether this is serotype-specific or strain-specific cannot be determined by these studies, but it shows a correlation between virulence and the ability to cause persistent FMDV infection. The high cell-killing capacity of SAT1, which can persist at higher rates in buffalo, is diametrically opposed to the described suppression of apoptosis in tissues persistently infected with the nonvirulent Sindbis virus strain. The cell killing assays for SAT1 have been performed with an immortalized culture of ZZ-R cells, stemming from goat tongue epithelium. It is a highly FMDV-sensitive cell line (Fukai et al. 2015), but originates from a tissue which is strongly affected by FMD lesions caused by cytolytic replication during the acute phase. The cultivation of virus on a cell line highly susceptible to cell lysis may explain the apparent contradiction. A repetition of the cell killing assay with primary cells from pharyngeal epithelia or an *in vivo* comparison of the infection kinetics in the pharynx between these strains would be insightful. It could be hypothesized that more virulent FMDV strains are more capable to induce persistence due to a higher expression of immunomodulatory viral proteins.

If there is no cell lysis during the persistent phase of FMDV infection, how can replicative virus be recovered from animals *ex vivo*? This is explained by the sampling methods used for the detection of carriers, which collect saliva and mucus as well as superficial tissue. The probang cup with its sharp metal edges scrapes off superficial epithelial cells from a region spanning from the esophagus to the pharynx (Sutmoller and Gaggero 1965). In buffalo, cytology brushes capture more cellular material yielding higher viral RNA amounts than the probang, especially from the palatine tonsils (Maree et al. 2016). Both sampling methods can recover cell-associated persistent virus, but whether natural transmission from carrier buffalo is cell-associated as well remains unknown. Non-enveloped viruses like FMDV usually depend on cell lysis for the release of viral particles. But in related picornaviruses non-cytolytic spread has been observed as well. Poliovirus can be released from the apical surface of epithelial cells in the intestine into the lumen and hepatitis A virus is released from intact cells in exosomes (Bird and Kirkegaard 2015).

A reshaping of the infected tissue itself favoring viral replication is another method exploited by viruses to extend an infection. During papillomavirus infection, viral DNA is maintained at low levels in the basal layers of infected keratinizing epithelium. With progressing differentiation of infected keratinocytes, the translation of viral proteins is enhanced until the newly

assembled viral particles are released with desquamated keratinocytes of the superficial layer. This creates a sequestered compartment containing the antigenic proteins. Papillomavirus promotes this process by accelerating epithelial differentiation and inhibiting apoptosis at the same time, resulting in hyperproliferative epithelia (Kajitani et al. 2012). A similar distribution of viral genome in basal layers of the epithelium was also observed in persistently FMDV infected tissues as described in publication I and others (Alexandersen et al. 2002; Prato Murphy et al. 1999), while antigenic viral structural proteins are most commonly found in superficial layers (Stenfeldt et al. 2018). But in contrast to papillomavirus, the preferential microanatomic localization of persistent FMDV, the FAE, is a non-keratinizing epithelium, in which cuboidal epithelial cells are disorganized and interspersed with immune cells (Meek et al. 2022). This phenotype of epithelial tissue of the FAE is also described in our transcriptomic analysis in publication II, where we saw a reduction of components of the extracellular matrix and a reduced cell-to-cell interaction. Even though FMDV might not actively reshape its infected tissue like papillomavirus, it can benefit from the loose epithelial structure of the FAE, as integrin receptors, which allow cell entry of FMDV and cell-to-cell attachment at the same time, are increasingly available in detached epithelial cells (Zhu et al. 2013).

The mucosal epithelia of the FAE could further support FMDV infection by a physiologically reduced immune response, like in tissues persistently infected with Ebola virus. After the acute hemorrhagic phase of Ebola virus disease, the virus retreats into tissues that are sequestered from the blood and thus from the immune response by a blood-tissue barrier like the brain, eye or testes. In these tissues, Ebola virus can persist and in the case of infected testes even be transmitted via seminal fluid (Schindell et al. 2018). These sites with limited accessibility for the immune response have historically been regarded as immunoprivileged sites. More recently, tissues such as hair follicles or mucosa have been included in this circle as well (Forrester et al. 2008). In mucosal immunity, a crucial role in tolerating foreign pathogens is likely conferred on a subset of T cells with a suppressive function, which showed the highest change in cell count after the exposition of MALT to antigen (Gormley et al. 1998). This is in accordance with our findings from the transcriptomic study, which suggest activation of regulatory T cells and an immunosuppressive milieu promoting T-cell exhaustion and rendering cytotoxic T cells unable to clear infected cells. This is further supported by other studies of differential gene expression using microarrays (Eschbaumer et al. 2016b; Zhu et al. 2020,

2022). In physiological, i.e. uninfected, mucosal epithelium from the bovine pharynx, the distribution of different subsets of T cells could prime the FAE for a non-functional T-cell response. While cytotoxic CD8<sup>+</sup> T cells are more common in the surrounding epithelium than in the lymphatic FAE itself, the majority of  $\gamma/\delta$  T cells in the MALT of the nasopharynx are located in the epithelium (Meek et al. 2022). In ruminants, this subset of  $\gamma/\delta$  T cells constitutes a large proportion of mononuclear lymphocytes and can exert regulatory functions on CD4<sup>+</sup> and CD8<sup>+</sup> T cells (Guzman et al. 2014). Especially for FMDV, the presence of  $\gamma/\delta$  T cells can be an advantage as the depletion of  $\gamma/\delta$  T cells resulted in shorter viremia than the depletion of CD4<sup>+</sup> and CD8<sup>+</sup> T cells (Juleff et al. 2009). T-cell exhaustion can be induced by a prolonged viral presence in the FAE of persistently FMDV-infected animals, but infected tissue itself can enhance this immunosuppressive milieu by the strong physiological presence of suppressive regulatory T cells.

The susceptibility of epithelia of the nasopharynx to persistent FMDV infection is likely determined by two crucial factors. On the one hand, viral influence, mainly facilitated by L<sup>pro</sup>, counteracts the innate immune system and induces an anti-apoptotic state, at least in a subset of infected cells. On the other hand, the virus encounters a mucosal epithelium specialized in the sampling and presentation of antigens, a process which would be hindered by an overshooting immune reaction. Therefore, the lymphatic mucosa of the nasopharynx can be characterized as an immunoprivileged site, whose immunosuppressive and anti-apoptotic character is then enhanced by the viral mechanisms.

### ***Objective II: Influences of the host on the viral evolution***

#### Publication III

The evolution of FMDV does not stop during the persistent phase of infection. We detected a clear correlation between the progression of infection and the emergence of two virus variants, VP2 Y79C and VP3 A75T. These amino acid changes on the surface of the capsid have already been described in persistently infected animals in two other studies using a closely related FMDV strain (Horsington and Zhang 2007b; Parthiban et al. 2015) and they did not occur during acute-phase transmission during the FMD epizootic in the UK in 2001, from which

our strain originated (Cottam et al. 2006). However, the functional implications of these amino acid changes could not be determined in our study.

Another amino acid change which rose to dominance in our data set was VP3 R56C. An arginine at this well-characterized residue facilitates heparan sulfate binding and is an indication of virus adaptation to cell culture. The change back to cysteine was previously found to be associated with a reversion to pathogenicity *in vivo* (Borca et al. 2012). In our study, this amino acid change was likely induced by the prior animal passage of the inoculum and its dominance was manifested early in the acute phase. Thus, this variant is more relevant for the early stage of infection than for the establishment of persistence. Nevertheless, as already mentioned above, the virulence of SAT strains of FMDV was associated with a higher prevalence of persistently infected African buffalo and a higher likelihood for transmission of virus during persistence (Jolles et al. 2021; Maree et al. 2016). This hypothesis of higher carrier incidence caused by more virulent strains may explain the different incidence of persistent infection observed in the two animal trials included in this work. The virus used in the vaccination trial had been adapted to cattle. It had originally been plaque purified-twice, but then passaged once in a cow infected by intradermolingual inoculation. The inoculum for the vaccination trial was then prepared from vesicular material from this animal and it already contained VP3 R56C at over 20% frequency. This cattle-adapted virus caused a carrier incidence of 85%, i.e. 18 out of 20 cattle. The virus used in the infection study, on the other hand, had been rescued from an infectious clone built using the consensus sequence of the other inoculum, which has an arginine at position 56 of VP3. It was then passaged twice on BHK-21 cells and its consensus sequence was verified by Sanger sequencing. No deep-sequence data for this inoculum is available, but it can be assumed that it is virtually 100% VP3 56R. Using this culture-adapted virus, a carrier incidence of only 33%, i.e. 2 out of 6 cattle, was achieved. Even though the confidence intervals of both estimates are overlapping at the margin, this difference should not be neglected. In similar studies, where a bovine-derived FMDV strain was used as an inoculum, high carrier incidences (78% and 80%) were achieved as well (Stenfeldt et al. 2016a). This is further supported by findings of the initial study that validated the intranasopharyngeal inoculation route for cattle with three different serotypes. The greatest difference between needle, contact and intranasopharyngeal infection was observed in animals infected with an infectious clone of FMDV A<sub>24</sub>. After intranasopharyngeal inoculation, the culture-adapted

virus showed milder clinical disease and less synchronous infection dynamics compared to the two other methods. The two other virus strains used in the study, O1 Manisa and Asia-1 Shamir, were animal-derived and did not show such disparities between the inoculation methods (Pacheco et al. 2016). Thus, intranasopharyngeal inoculation with a culture-adapted strain might not be an adequate inoculation method, therefore the infection trial included in publication I could be repeated with two animal-adapted strains to obtain results that are more applicable to natural infection.

Regarding the less well-characterized amino acid changes, which we assume to be associated with FMDV persistence, the functional properties conferred by them could not be fully elucidated in our study. Even though the changed amino acids are located on the capsid surface, constituting antigenic sites or at least in close vicinity to such, we did not observe a difference in susceptibility to neutralizing antibodies compared to the inoculum. This corroborates findings in persistently infected buffalo (Cortey et al. 2019). Using a set of monoclonal antibodies, Gebauer et al. (1988) did observe a decreased reactivity of two isolates from the persistent phase, but Salt (1993) could not reproduce their findings. While the neutralizing antibody response is the driving factor in the clearance of acute-phase virus from the body, increased presence of cytotoxic CD8<sup>+</sup> T cell in infected epithelia of the pharynx has been associated with the clearance of virus in the transitional phase (Stenfeldt et al. 2017). The hypothesized immune evasion conferred by these single nucleotide mutations could therefore also be based on bypassing the cytotoxic T cell response by altering T cell epitopes like it has been documented for HIV and persistent hepatitis C virus infection (Dazert et al. 2009). Interestingly, both amino acid changes observed in our study are located in or close to known cytotoxic T cell epitopes and show binding affinity to bovine MHC II molecules (Haghparast et al. 2000). However, it is unknown whether an amino acid change in this epitope is sufficient to evade the cytotoxic T cell response or if a distinct genomic haplotype of MHC II is responsible for some animals to become carriers.

Alternatively, instead of an immune evasion by altering antigenic epitopes, persistent virus could have undergone a change in host cell tropism caused by a different receptor binding capacity. This is supported by the findings of Hägglund et al. (2020) and O'Donnell et al. (2014), as already mentioned above, who showed that persistently infected cells *in vitro*, which are

resistant to virus-induced lysis, are not of epithelial origin and do not express  $\alpha V\beta 6$  integrin. In our study, we could not find any evidence for an extended receptor binding capacity of viruses isolated from persistently infected animals, but persistent virus isolates were no longer able to bind to heparan sulfate, unlike the inoculum. We furthermore observed the amino acid change VP2 Y79C to confer an advantage in infecting IB-RS-2 cells predominantly expressing  $\alpha V\beta 8$  integrin (King et al. 2011). The integrins  $\alpha V\beta 6$  and  $\alpha V\beta 8$  are both expressed by epithelial cells, but only  $\alpha V\beta 8$  is also expressed in several immune cells which can be found in the FAE, such as regulatory T cells, dendritic cells and macrophages (McCarty 2020). Even though some of these cells may be susceptible due to their expression of FMDV receptors (Salt 1993; Robinson et al. 2011), during FMDV persistence *in vivo* these immune cells are found adjacent to cells positive for FMDV antigens but are not positive themselves (Stenfeldt et al. 2016a). Another non-epithelial cell expressing integrins that FMDV can utilize for cell entry which is present in the FAE is the M-cell, as already discussed above.

The findings of our and similar studies are limited to a retrospective analysis of mutational changes in the genome of FMDV. The prospective approach by generating a virus containing an amino acid change hypothetically associated with persistence, for example VP2 Y79C, which may achieve a higher carrier incidence, has not been performed yet. To achieve statistical significance such a study would require high animal numbers, which is not just a matter of resources but also a question of animal welfare.



## CHAPTER VI: SUMMARY



## VI. Summary

As foot-and-mouth disease is one of the most feared diseases of livestock, stringent restrictions are imposed on free countries after outbreaks of the virus. Rigorous culling of susceptible animals and huge economic losses in the agricultural sector are the consequence. The reliable prevention of persistent FMDV infection, which can occur even in vaccinated animals, would support the quick recovery of FMDV-free status granted by the WOAHP without the indiscriminate culling of vaccinated animals. Still, our knowledge of the mechanisms which allow FMDV to remain in otherwise immune hosts is scarce. This thesis aims to better characterize the fine balance between the virus and the infected tissue, their influence on each other and which viral properties are required for the establishment of a persistent infection.

We could demonstrate the essential role of the Leader protein L<sup>pro</sup> for the acute and persistent infection *in vivo*. Cattle that were inoculated with a FMDV strain lacking the L<sup>pro</sup> coding sequence did not show any clinical signs of FMD, supporting the strongly attenuated nature of leaderless FMDV. Furthermore, no virus was detected in the animals during the presumed phase of persistent infection, neither in oropharyngeal fluid nor in tissues collected at necropsy. This effective clearance of leaderless FMDV demonstrates that the virus is not able to outcompete the host immune response without L<sup>pro</sup>.

Besides L<sup>pro</sup>, other viral proteins also exert functions counteracting the innate immune response. In our study, which assessed the transcriptome and proteome of tissues from persistently infected animals, we documented some of these effects for the first time *in vivo*. With state-of-the-art analytical approaches, which have never before been applied to tissues from persistently FMDV-infected animals, we could observe a downregulation of receptors sensing viral RNA and an inhibition of interferon signaling, which we attributed to the immune inhibitory functions of FMDV mainly exerted by L<sup>pro</sup> and 3A. Overall, infected tissue showed a different cellular phenotype which we could ascribe to the predominance of follicle-associated epithelium (FAE) and its gene expression patterns indicate a suppression of apoptosis and an insufficient T-cell response.

Our collection of whole-ORF FMDV sequences from persistently infected animals is the biggest set of samples ever analysed in this context. This large dataset revealed an emergence of

amino acid changes at the residues VP3 75 and VP2 79 with ongoing infection. Both have been previously associated with persistent FMDV infection in serotype O. The functional analysis we performed showed no evidence for a different susceptibility of persistent isolates to neutralizing antibodies, but indicated an enhancement of their binding capacity for integrin  $\alpha V\beta 8$ . Overall, our findings support the hypothesis that at least in serotype O FMDV there is a persistence-associated genotype with point mutations that are unique to the persistent infection.

Conclusively, when FMDV first invades the host, it encounters the FAE in the nasopharynx, where primary infection takes place and from where it spreads systemically. FMDV can remain here over months as a persistent infection. In this specialized tissue, an impaired innate immune response and restricted apoptosis is observed after prolonged FMDV infection, which is partly promoted by the virus, but to which this specific epithelium also seems to be particularly susceptible. The persistent FMDV infection of this tissue likely benefits from both factors, virally induced immunosuppression and host-specific physiological immune tolerance.

## VII. Zusammenfassung

Da die Maul- und Klauenseuche (MKS) zu den gefürchtetsten Erkrankungen landwirtschaftlicher Nutztiere gehört, werden MKS-freien Ländern nach Wiedereinschleppung der Seuche strenge Beschränkungen auferlegt. Das rigorose Keulen empfänglicher Tiere und enorme wirtschaftliche Verluste im Agrarsektor sind die Folge. Das zuverlässige Verhindern der persistenten MKSV-Infektion, die selbst nach einer Impfung gegen MKS auftreten kann, würde ein rasches Wiedererlangen des von der WOAH gewährten Status der MKS-Freiheit ohne die massenhafte Keulung geimpfter Tiere erleichtern. Dennoch ist unser Wissen über die Mechanismen, die es MKSV ermöglichen, in ansonst immunen Wirtstieren zu verbleiben, bis heute eingeschränkt. Die vorliegende kumulative Doktorarbeit befasst sich mit der feinen Balance zwischen dem Virus und seinem Wirt. Sie zielt darauf ab, den gegenseitigen Einfluss zu beschreiben und die viralen Eigenschaften zu benennen, die für die Etablierung einer persistenten Infektion essentiell sind.

Wir konnten die wesentliche Rolle des Leader-Proteins L<sup>pro</sup> für die akute und persistente Infektion *in vivo* nachweisen. Rinder, die mit einem MKS-Virus infiziert wurden, dem die kodierende Sequenz für L<sup>pro</sup> fehlte, zeigten keine klinischen Anzeichen von MKS. Dies bestätigt den stark attenuierten Charakter eines *leaderless* MKSV. Auch nach der akuten Phase der Infektion konnte bei den Tieren kein Virus nachgewiesen werden, weder im mit Hilfe des Probangbechers beprobten Rachenschleim noch in den bei der Sektion entnommenen Geweben des Nasopharynx. Dies verdeutlicht, dass MKSV ohne das Leader-Protein nicht in der Lage ist, die Immunantwort des Wirts zu überwinden.

Neben L<sup>pro</sup> üben auch etliche andere virale Proteine Funktionen aus, die der angeborenen Immunantwort entgegenwirken. In unserer Studie, die sich mit dem Transkriptom und Proteom infizierter Gewebe befasste, konnten wir einige dieser Mechanismen erstmals *in vivo* beobachten. Mit modernen analytischen Ansätzen, die bisher noch keine Anwendung bei persistent MKSV-infiziertem Gewebe fanden, konnten wir einen direkten Einfluss des viralen Nicht-Struktur-Proteins 3A auf die Expression von Rezeptoren für virale RNA und von L<sup>pro</sup> auf die Interferon-Signalkaskade durch eine Interaktion mit TRAF6 feststellen. Insgesamt zeigte infiziertes Gewebe einen veränderten zellulären Phänotyp, den wir dem follikelassoziierten

Epithel (FAE) zuschreiben konnten. Die Genexpressionsmuster des persistent infizierten Epithels deuteten darüber hinaus auf eine gehemmte Apoptose und eine ineffektive T-Zell Antwort hin.

Unsere aus persistent infizierten Tieren gesammelten Virussequenzen, die den gesamten offenen Leserahmen von MKSV abdecken, sind der größte Datensatz, der jemals in diesem Zusammenhang analysiert wurde. Diese umfangreiche Bibliothek an Sequenzen veranschaulichte ein zunehmendes Auftreten von Mutationen bei persistierender Infektion. Zwei Mutationen, die eine Änderung der Aminosäuresequenz an den Positionen VP3 75 und VP2 79 verursachen, waren von besonderem Augenmerk, da beide Mutationen bereits zuvor mit der persistenten Infektion von MKSV des Serotyps O in Zusammenhang gebracht worden waren. Die von uns durchgeführten funktionelle Analysen konnten keine geänderte Empfindlichkeit der persistierenden Virusisolate gegenüber neutralisierenden Antikörpern nachweisen, deuteten aber auf eine Verbesserung der Bindungskapazität für den Integrin  $\alpha V\beta 8$  Rezeptor hin. Insgesamt stützen unsere Ergebnisse die Hypothese, dass zumindest bei MKSV vom Serotyp O diese Mutationen spezifisch für die persistente Infektion sind und einen persistenzassoziierten Genotyp darstellen.

Zusammenfassend lässt sich sagen, dass MKSV beim ersten Eindringen in den Wirt auf das FAE im Nasenrachenraum trifft. Dort findet die primäre Infektion statt und von dort breitet sich das Virus systemisch aus. MKSV kann hier monatelang als persistente Infektion verbleiben. In diesem Gewebe ist während der persistenten Infektion eine Störung der angeborenen Immunantwort und eine Hemmung der Apoptose zu beobachten, was teilweise durch das Virus befördert wird, wofür dieses spezielle Epithel aber auch besonders anfällig ist. Die persistente MKSV-Infektion scheint durch ein Zusammenspiel beider Faktoren erst ermöglicht zu werden, zum einen durch die viral bedingte Hemmung der Immunantwort und zum andern durch die wirtsgegebene Immuntoleranz in diesem Gewebe.

## CHAPTER VIII: REFERENCES



## VIII. REFERENCES

- Aiewsakun, P.; Pamornchainavakul, N.; Inchaisri, C. (2020): Early origin and global colonisation of foot-and-mouth disease virus. In *Scientific reports* 10 (1). DOI: 10.1038/s41598-020-72246-6.
- Alexandersen, S.; Mowat, N. (2005): Foot-and-mouth disease: host range and pathogenesis. In *Current topics in microbiology and immunology* 288, pp. 9–42. DOI: 10.1007/3-540-27109-0\_2.
- Alexandersen, S.; Zhang, Z.; Donaldson, A. I. (2002): Aspects of the persistence of foot-and-mouth disease virus in animals—the carrier problem. In *Microbes and Infection* 4 (10), pp. 1099–1110. DOI: 10.1016/S1286-4579(02)01634-9.
- Alexandersen, S.; Zhang, Z.; Donaldson, A. I.; Garland, A. J. M. (2003): The pathogenesis and diagnosis of foot-and-mouth disease. In *Journal of comparative pathology* 129 (1), pp. 1–36. DOI: 10.1016/S0021-9975(03)00041-0.
- Anderson, E. C.; Doughty, W. J.; Anderson, J.; Paling, R. (1979): The pathogenesis of foot-and-mouth disease in the African buffalo (*Syncerus caffer*) and the role of this species in the epidemiology of the disease in Kenya. In *Journal of comparative pathology* 89 (4), pp. 541–549. DOI: 10.1016/0021-9975(79)90045-8.
- Appel, E.; Katzoff, A.; Ben-Moshe, T.; Kazimirsky, G.; Kobiler, D.; Lustig, S.; Brodie, C. (2000): Differential regulation of Bcl-2 and Bax expression in cells infected with virulent and nonvirulent strains of sindbis virus. In *Virology* 276 (2), pp. 238–242. DOI: 10.1006/viro.2000.0458.
- Arzt, J.; Belsham, G. J.; Lohse, L.; Bøtner, A.; Stenfeldt, C. (2018): Transmission of Foot-and-Mouth Disease from Persistently Infected Carrier Cattle to Naive Cattle via Transfer of Oropharyngeal Fluid. In *mSphere* 3 (5). DOI: 10.1128/mSphere.00365-18.
- Arzt, J.; Fish, I.; Pauszek, S. J.; Johnson, S. L.; Chain, P. S.; Rai, D. K. et al. (2019): The evolution of a super-swarm of foot-and-mouth disease virus in cattle. In *PloS one* 14 (4). DOI: 10.1371/journal.pone.0210847.
- Arzt, J.; Fish, I. H.; Bertram, M. R.; Smoliga, G. R.; Hartwig, E. J.; Pauszek, S. J. et al. (2021): Simultaneous and Staggered Foot-and-Mouth Disease Virus Coinfection of Cattle. In *J Virol* 95 (24), Article e01650-21. DOI: 10.1128/JVI.01650-21.

- Arzt, J.; Pacheco, J. M.; Rodriguez, L. L. (2010): The early pathogenesis of foot-and-mouth disease in cattle after aerosol inoculation. Identification of the nasopharynx as the primary site of infection. In *Veterinary pathology* 47 (6), pp. 1048–1063. DOI: 10.1177/0300985810372509.
- Astorga-Gamaza, A.; Grau-Expósito, J.; Burgos, J.; Navarro, J.; Curran, A.; Planas, B. et al. (2022): Identification of HIV-reservoir cells with reduced susceptibility to antibody-dependent immune response. In *eLife* 11. DOI: 10.7554/elife.78294.
- Bablanian, G. M.; Grubman, M. J. (1993): Characterization of the foot-and-mouth disease virus 3C protease expressed in *Escherichia coli*. In *Virology* 197 (1), pp. 320–327. DOI: 10.1006/viro.1993.1593.
- Bauer, K. (1997): Foot- and-mouth disease as zoonosis. In *Archives of virology. Supplementum* 13, pp. 95–97. DOI: 10.1007/978-3-7091-6534-8\_9.
- Beard, C. W.; Mason, P. W. (2000): Genetic Determinants of Altered Virulence of Taiwanese Foot-and-Mouth Disease Virus. In *J Virol* 74 (2), pp. 987–991.
- Belsham, G. J. (2005): Translation and replication of FMDV RNA. In *Current topics in microbiology and immunology* 288, pp. 43–70. DOI: 10.1007/3-540-27109-0\_3.
- Belsham, G. J. (2013): Influence of the Leader protein coding region of foot-and-mouth disease virus on virus replication. In *The Journal of general virology* 94 (Pt 7), pp. 1486–1495. DOI: 10.1099/vir.0.052126-0.
- Belsham, G. J.; McInerney, G. M.; Ross-Smith, N. (2000): Foot-and-Mouth Disease Virus 3C Protease Induces Cleavage of Translation Initiation Factors eIF4A and eIF4G within Infected Cells. In *J Virol* 74 (1), pp. 272–280.
- Berryman, S.; Clark, S.; Monaghan, P.; Jackson, T. (2005): Early events in integrin  $\alpha$ -phavbeta6-mediated cell entry of foot-and-mouth disease virus. In *J Virol* 79 (13), pp. 8519–8534. DOI: 10.1128/jvi.79.13.8519-8534.2005.
- Bird, S. W.; Kirkegaard, K. (2015): Escape of non-enveloped virus from intact cells. In *Virology* 0, pp. 444–449. DOI: 10.1016/j.virol.2015.03.044.
- Birtley, J. R.; Knox, S. R.; Jaulent, A. M.; Brick, P.; Leatherbarrow, R. J.; Curry, S. (2005): Crystal structure of foot-and-mouth disease virus 3C protease. New insights into catalytic mechanism and cleavage specificity. In *The Journal of biological chemistry* 280 (12), pp. 11520–11527. DOI: 10.1074/jbc.M413254200.

- Biswal, J. K.; Di Nardo, A.; Taylor, G.; Paton, D. J.; Parida, S. (2021): Development and Validation of a Mucosal Antibody (IgA) Test to Identify Persistent Infection with Foot-and-Mouth Disease Virus. In *Viruses* 13 (5). DOI: 10.3390/v13050814.
- Bittle, J. L.; Houghten, R. A.; Alexander, H.; Shinnick, T. M.; Sutcliffe, J. G.; Lerner, R. A. et al. (1982): Protection against foot-and-mouth disease by immunization with a chemically synthesized peptide predicted from the viral nucleotide sequence. In *Nature* 298 (5869), pp. 30–33. DOI: 10.1038/298030a0.
- Borca, M. V.; Fernández, F. M.; Sadir, A. M.; Braun, M.; Schudel, A. A. (1986): Immune response to foot-and-mouth disease virus in a murine experimental model: effective thymus-independent primary and secondary reaction. In *Immunology* 59 (2), pp. 261–267.
- Borca, M. V.; Pacheco, J. M.; Holinka, L. G.; Carrillo, C.; Hartwig, E.; Garriga, D. et al. (2012): Role of arginine-56 within the structural protein VP3 of foot-and-mouth disease virus (FMDV) O1 Campos in virus virulence. In *Virology* 422 (1), pp. 37–45. DOI: 10.1016/j.virol.2011.09.031.
- Breithaupt, A.; Depner, K.; Haas, B.; Alexandrov, T.; Polihronova, L.; Georgiev, G. et al. (2012): Experimental infection of wild boar and domestic pigs with a foot and mouth disease virus strain detected in the southeast of Bulgaria in December of 2010. In *Veterinary microbiology* 159 (1-2), pp. 33–39. DOI: 10.1016/j.vetmic.2012.03.021.
- Brooksby, J. B.; Rogers J. (1957): Methods used in typing the virus of foot-and-mouth disease at Pirbright. 1950-55. In *Methods of typing and cultivation of foot-and-mouth disease virus* (208), p. 31.
- Brown, F.; Cartwright, B. (1960): Purification of the Virus of Foot-and-Mouth Disease by Fluorocarbon Treatment and Its Dissociation from Neutralizing Antibody. In *Journal of immunology (Baltimore, Md.: 1950)* 85 (3), pp. 309–313. DOI: 10.4049/jimmunol.85.3.309.
- Brown, V. R.; Bevins, S. N. (2019): Potential role of wildlife in the USA in the event of a foot-and-mouth disease virus incursion. In *The Veterinary record* 184 (24), p. 741. DOI: 10.1136/vr.104895.
- Chen, P.; Li, Z.; Cui, S. (2021): Picornaviral 2C proteins: A unique ATPase family critical in virus replication. In *The Enzymes* 49, pp. 235–264. DOI: 10.1016/bs.enz.2021.06.008.

- Chigbu, D. I.; Loonawat, R.; Sehgal, M.; Patel, D.; Jain, P. (2019): Hepatitis C Virus Infection: Host–Virus Interaction and Mechanisms of Viral Persistence. In *Cells* 8 (4). DOI: 10.3390/cells8040376.
- Chinsangaram, J.; Koster, M.; Grubman, M. J. (2001): Inhibition of L-Deleted Foot-and-Mouth Disease Virus Replication by Alpha/Beta Interferon Involves Double-Stranded RNA-Dependent Protein Kinase. In *J Virol* 75 (12), pp. 5498–5503. DOI: 10.1128/JVI.75.12.5498-5503.2001.
- Chow, M.; Newman, J. F.; Filman, D.; Hogle, J. M.; Rowlands, D. J.; Brown, F. (1987): Myristylation of picornavirus capsid protein VP4 and its structural significance. In *Nature* 327 (6122), pp. 482–486. DOI: 10.1038/327482a0.
- Cortey, M.; Ferretti, L.; Pérez-Martín, E.; Zhang, F.; Klerk-Lorist, L.-M. de; Scott, K. et al. (2019): Persistent Infection of African Buffalo (*Syncerus caffer*) with Foot-and-Mouth Disease Virus: Limited Viral Evolution and No Evidence of Antibody Neutralization Escape. In *Journal of virology* 93 (15). DOI: 10.1128/JVI.00563-19.
- Cottam, E. M.; Haydon, D. T.; Paton, D. J.; Gloster, J.; Wilesmith, J. W.; Ferris, N. P. et al. (2006): Molecular epidemiology of the foot-and-mouth disease virus outbreak in the United Kingdom in 2001. In *J Virol* 80 (22), pp. 11274–11282. DOI: 10.1128/JVI.01236-06.
- Da Ao; Sun, S.-Q.; Guo, H.-C. (2014): Topology and biological function of enterovirus non-structural protein 2B as a member of the viroporin family. In *Veterinary Research* 45 (1), p. 87. DOI: 10.1186/s13567-014-0087-6#Sec12.
- Dawe, P. S.; Flanagan, F. O.; Madekurozwa, R. L.; Sorensen, K. J.; Anderson, E. C.; Foggin, C. M. et al. (1994a): Natural transmission of foot-and-mouth disease virus from African buffalo (*Syncerus caffer*) to cattle in a wildlife area of Zimbabwe. In *The Veterinary record* 134 (10), pp. 230–232. DOI: 10.1136/vr.134.10.230.
- Dawe, P. S.; Sorensen, K.; Ferris, N. P.; Barnett, I. T.; Armstrong, R. M.; Knowles, N. J. (1994b): Experimental transmission of foot-and-mouth disease virus from carrier African buffalo (*Syncerus caffer*) to cattle in Zimbabwe. In *The Veterinary record* 134 (9), pp. 211–215. DOI: 10.1136/vr.134.9.211.
- Dazert, E.; Neumann-Haefelin, C.; Bressanelli, S.; Fitzmaurice, K.; Kort, J.; Timm, J. et al. (2009): Loss of viral fitness and cross-recognition by CD8+ T cells limit HCV escape from a protective HLA-B27-restricted human immune response. In *The Journal of clinical investigation* 119 (2), pp. 376–386. DOI: 10.1172/JCI36587.

- Denison, M. R.; Graham, R. L.; Donaldson, E. F.; Eckerle, L. D.; Baric, R. S. (2011): Coronavirus: an RNA proofreading machine regulates replication fidelity and diversity. In *RNA biology* 8 (2), pp. 270–279. DOI: 10.4161/rna.8.2.15013.
- Devaney, M. A.; Vakharia, V. N.; Lloyd, R. E.; Ehrenfeld, E.; Grubman, M. J. (1988): Leader protein of foot-and-mouth disease virus is required for cleavage of the p220 component of the cap-binding protein complex. In *J Virol* 62 (11), pp. 4407–4409. DOI: 10.1128/jvi.62.11.4407-4409.1988.
- Dias, C. C. A.; Moraes, M. P.; Segundo, F. D.-S.; Los Santos, T. de; Grubman, M. J. (2011): Porcine type I interferon rapidly protects swine against challenge with multiple serotypes of foot-and-mouth disease virus. In *Journal of interferon & cytokine research: the official journal of the International Society for Interferon and Cytokine Research* 31 (2), pp. 227–236. DOI: 10.1089/jir.2010.0055.
- Díaz-San Segundo, F.; Rodríguez-Calvo, T.; Avila, A. de; Sevilla, N. (2009): Immunosuppression during acute infection with foot-and-mouth disease virus in swine is mediated by IL-10. In *PloS one* 4 (5), e5659. DOI: 10.1371/journal.pone.0005659.
- Donnelly, M. L. L.; Luke, G.; Mehrotra, A.; Li, X.; Hughes, L. E.; Gani, D.; Ryan, M. D. (2001): Analysis of the aphthovirus 2A/2B polyprotein 'cleavage' mechanism indicates not a proteolytic reaction, but a novel translational effect: a putative ribosomal 'skip'. In *The Journal of general virology* 82 (Pt 5), pp. 1013–1025. DOI: 10.1099/0022-1317-82-5-1013.
- Du, Y.; Bi, J.; Liu, J.; Liu, X.; Wu, X.; Jiang, P. et al. (2014): 3Cpro of Foot-and-Mouth Disease Virus Antagonizes the Interferon Signaling Pathway by Blocking STAT1/STAT2 Nuclear Translocation. In *J Virol* 88 (9), pp. 4908–4920. DOI: 10.1128/JVI.03668-13.
- Echebli, N.; Tchitchek, N.; Dupuy, S.; Bruel, T.; Peireira Bittencourt Passaes, C.; Bosquet, N. et al. (2018): Stage-specific IFN-induced and IFN gene expression reveal convergence of type I and type II IFN and highlight their role in both acute and chronic stage of pathogenic SIV infection. In *PloS one* 13 (1), e0190334. DOI: 10.1371/journal.pone.0190334.
- Eschbaumer, M.; Stenfeldt, C.; Rekant, S. I.; Pacheco, J. M.; Hartwig, E. J.; Smoliga, G. R. et al. (2016a): Systemic immune response and virus persistence after foot-and-mouth disease virus infection of naïve cattle and cattle vaccinated with a homologous adenovirus-vectored vaccine. In *BMC veterinary research* 12, p. 205. DOI: 10.1186/s12917-016-0838-x.

- Eschbaumer, M.; Stenfeldt, C.; Smoliga, G. R.; Pacheco, J. M.; Rodriguez, L. L.; Li, R. W. et al. (2016b): Transcriptomic Analysis of Persistent Infection with Foot-and-Mouth Disease Virus in Cattle Suggests Impairment of Apoptosis and Cell-Mediated Immunity in the Nasopharynx. In *PloS one* 11 (9), e0162750. DOI: 10.1371/journal.pone.0162750.
- Falk, M. M.; Grigera, P. R.; Bergmann, I. E.; Zibert, A.; Multhaup, G.; Beck, E. (1990): Foot-and-mouth disease virus protease 3C induces specific proteolytic cleavage of host cell histone H3. In *J Virol* 64 (2), pp. 748–756. DOI: 10.1128/jvi.64.2.748-756.1990.
- Falk, M. M.; Sobrino, F.; Beck, E. (1992): VPg gene amplification correlates with infective particle formation in foot-and-mouth disease virus. In *J Virol* 66 (4), pp. 2251–2260.
- Fish, I.; Stenfeldt, C.; Palinski, R. M.; Pauszek, S. J.; Arzt, J. (2020): Into the Deep (Sequence) of the Foot-and-Mouth Disease Virus Gene Pool: Bottlenecks and Adaptation during Infection in Naïve and Vaccinated Cattle. In *Pathogens (Basel, Switzerland)* 9 (3). DOI: 10.3390/pathogens9030208.
- Flint, S. J.; Racaniello, V. R.; Rall, G. F.; Hatzioannou, T.; Skalka, A. M. (2020): Principles of virology. Fifth edition. Hoboken, NJ: Wiley/ASM Press.
- Forrester, J. V.; Xu, H.; Lambe, T.; Cornall, R. (2008): Immune privilege or privileged immunity? In *Mucosal immunology* 1 (5), pp. 372–381. DOI: 10.1038/mi.2008.27.
- Forss, S.; Schaller, H. (1982): A tandem repeat gene in a picornavirus. In *Nucleic Acids Research* 10 (20), pp. 6441–6450. DOI: 10.1093/nar/10.20.6441.
- Freimanis, G. L.; Di Nardo, A.; Bankowska, K.; King, D. J.; Wadsworth, J.; Knowles, N. J.; King, D. P. (2016): Genomics and outbreaks: foot and mouth disease. In *Revue scientifique et technique (International Office of Epizootics)* 35 (1), pp. 175–189. DOI: 10.20506/rst.35.1.2426.
- Fry, E. E.; Stuart, D. I.; Rowlands, D. J. (2005): The structure of foot-and-mouth disease virus. In *Current topics in microbiology and immunology* 288, pp. 71–101. DOI: 10.1007/3-540-27109-0\_4.

- Fukai, K.; Morioka, K.; Yamada, M.; Nishi, T.; Yoshida, K.; Kitano, R. et al. (2015): Comparative performance of fetal goat tongue cell line ZZ-R 127 and fetal porcine kidney cell line LFBK- $\alpha\beta 6$  for Foot-and-mouth disease virus isolation. In *Journal of veterinary diagnostic investigation : official publication of the American Association of Veterinary Laboratory Diagnosticians, Inc* 27 (4), pp. 516–521. DOI: 10.1177/1040638715584156.
- Gamarnik, A. V.; Andino, R. (1998): Switch from translation to RNA replication in a positive-stranded RNA virus. In *Genes & development* 12 (15), pp. 2293–2304. DOI: 10.1101/gad.12.15.2293.
- García-Briones, M.; Rosas, M. F.; González-Magaldi, M.; Martín-Acebes, M. A.; Sobrino, F.; Armas-Portela, R. (2006): Differential distribution of non-structural proteins of foot-and-mouth disease virus in BHK-21 cells. In *Virology* 349 (2), pp. 409–421. DOI: 10.1016/j.virol.2006.02.042.
- Gebauer, F.; La Torre, J. C. de; Gomes, I.; Mateu, M. G.; Barahona, H.; Tiraboschi, B. et al. (1988): Rapid selection of genetic and antigenic variants of foot-and-mouth disease virus during persistence in cattle. In *J Virol* 62 (6), pp. 2041–2049. DOI: 10.1128/JVI.62.6.2041-2049.1988.
- George, M.; Venkataramanan, R.; Pattnaik, B.; Sanyal, A.; Gurumurthy, C. B.; Hemadri, D.; Tosh, C. (2001): Sequence analysis of the RNA polymerase gene of foot-and-mouth disease virus serotype Asia1. In *Virus genes* 22 (1), pp. 21–26. DOI: 10.1023/a:1008174100886.
- Gormley, P. D.; Powell-Richards, A. O.; Azuara-Blanco, A.; Donoso, L. A.; Dua, H. S. (1998): Lymphocyte subsets in conjunctival mucosa-associated-lymphoid-tissue after exposure to retinal-S-antigen. In *International ophthalmology* 22 (2), pp. 77–80. DOI: 10.1023/a:1006191022900.
- Gosert, R.; Egger, D.; Bienz, K. (2000): A cytopathic and a cell culture adapted hepatitis A virus strain differ in cell killing but not in intracellular membrane rearrangements. In *Virology* 266 (1), pp. 157–169. DOI: 10.1006/viro.1999.0070.
- Guzman, E.; Hope, J.; Taylor, G.; Smith, A. L.; Cubillos-Zapata, C.; Charleston, B. (2014): Bovine  $\gamma\delta$  T Cells Are a Major Regulatory T Cell Subset. In *Journal of immunology (Baltimore, Md. : 1950)* 193 (1), pp. 208–222. DOI: 10.4049/jimmunol.1303398.
- Hägglund, S.; Laloy, E.; Näslund, K.; Pfaff, F.; Eschbaumer, M.; Romey, A. et al. (2020): Model of persistent foot-and-mouth disease virus infection in multilayered cells derived from bovine dorsal soft palate. In *Transboundary and emerging diseases* 67 (1), pp. 133–148. DOI: 10.1111/tbed.13332.

- Haghparast, A.; Wauben, M. H.; Grosfeld-Stulemeyer, M. C.; van Kooten, P.; Hensen, E. J. (2000): Selection of T-cell epitopes from foot-and-mouth disease virus reflects the binding affinity to different cattle MHC class II molecules. In *Immunogenetics* 51 (8-9), pp. 733–742. DOI: 10.1007/s002510000205.
- Henderson, S.; Huen, D.; Rowe, M.; Dawson, C.; Johnson, G.; Rickinson, A. (1993): Epstein-Barr virus-coded BHRF1 protein, a viral homologue of Bcl-2, protects human B cells from programmed cell death. In *Proceedings of the National Academy of Sciences of the United States of America* 90 (18), pp. 8479–8483.
- Hogle, J. M. (2002): Poliovirus cell entry: common structural themes in viral cell entry pathways. In *Annual review of microbiology* 56, pp. 677–702. DOI: 10.1146/annurev.micro.56.012302.160757.
- Horsington, J.; Zhang, Z. (2007a): Analysis of foot-and-mouth disease virus replication using strand-specific quantitative RT-PCR. In *Journal of virological methods* 144 (1-2), pp. 149–155. DOI: 10.1016/j.jviromet.2007.05.002.
- Horsington, J.; Zhang, Z. (2007b): Consistent change in the B-C loop of VP2 observed in foot-and-mouth disease virus from persistently infected cattle: implications for association with persistence. In *Virus research* 125 (1), pp. 114–118. DOI: 10.1016/j.virusres.2006.12.008.
- Ito, M.; Yanagi, Y.; Ichinohe, T. (2012): Encephalomyocarditis virus viroporin 2B activates NLRP3 inflammasome. In *PLoS pathogens* 8 (8), e1002857. DOI: 10.1371/journal.ppat.1002857.
- Jacob, S. T.; Crozier, I.; Fischer, W. A.; Hewlett, A.; Kraft, C. S.; La Vega, M.-A. d. et al. (2020): Ebola virus disease. In *Nature Reviews. Disease Primers* 6 (1). DOI: 10.1038/s41572-020-0147-3.
- Jamal, S. M.; Nazem Shirazi, M. H.; Ozyoruk, F.; Parlak, U.; Normann, P.; Belsham, G. J. (2020): Evidence for multiple recombination events within foot-and-mouth disease viruses circulating in West Eurasia. In *Transboundary and emerging diseases* 67 (2), pp. 979–993. DOI: 10.1111/tbed.13433.
- James, C.; Harfouche, M.; Welton, N. J.; Turner, K. M. E.; Abu-Raddad, L. J.; Gottlieb, S. L.; Looker, K. J. (2020): Herpes simplex virus: global infection prevalence and incidence estimates, 2016. In *Bulletin of the World Health Organization* 98 (5), pp. 315–329. DOI: 10.2471/BLT.19.237149.

- Jarousse, N.; Grant, R. A.; Hogle, J. M.; Zhang, L.; Senkowski, A.; Roos, R. P. et al. (1994): A single amino acid change determines persistence of a chimeric Theiler's virus. In *J Virol* 68 (5), pp. 3364–3368. DOI: 10.1128/jvi.68.5.3364-3368.1994.
- Jolles, A.; Gorsich, E.; Gubbins, S.; Beechler, B.; Buss, P.; Juleff, N. et al. (2021): Endemic persistence of a highly contagious pathogen: Foot-and-mouth disease in its wild-life host. In *Science (New York, N.Y.)* 374 (6563), pp. 104–109. DOI: 10.1126/science.abd2475.
- Juleff, N.; Windsor, M.; Lefevre, E. A.; Gubbins, S.; Hamblin, P.; Reid, E. et al. (2009): Foot-and-mouth disease virus can induce a specific and rapid CD4+ T-cell-independent neutralizing and isotype class-switched antibody response in naïve cattle. In *J Virol* 83 (8), pp. 3626–3636. DOI: 10.1128/jvi.02613-08.
- Kajitani, N.; Satsuka, A.; Kawate, A.; Sakai, H. (2012): Productive Lifecycle of Human Papillomaviruses that Depends Upon Squamous Epithelial Differentiation. In *Frontiers in microbiology* 3. DOI: 10.3389/fmicb.2012.00152.
- Kar, P.; Kumar, D.; Gumma, P. K.; Chowdhury, S. J.; Karra, V. K. (2017): Down regulation of TRIF, TLR3, and MAVS in HCV infected liver correlates with the outcome of infection. In *Journal of medical virology* 89 (12), pp. 2165–2172. DOI: 10.1002/jmv.24849.
- King, D. P.; Burman, A.; Gold, S.; Shaw, A. E.; Jackson, T.; Ferris, N. P. (2011): Integrin subunit expression in cell cultures used for the diagnosis of foot-and-mouth disease. In *Veterinary immunology and immunopathology* 140 (3-4), pp. 259–265. DOI: 10.1016/j.vetimm.2011.01.008.
- Knight-Jones, T. J. D.; Rushton, J. (2013): The economic impacts of foot and mouth disease - what are they, how big are they and where do they occur? In *Preventive veterinary medicine* 112 (3-4), pp. 161–173. DOI: 10.1016/j.prevet-med.2013.07.013.
- Knowles, N. J.; Samuel, A. R. (2003): Molecular epidemiology of foot-and-mouth disease virus. In *Virus research* 91 (1), pp. 65–80. DOI: 10.1016/S0168-1702(02)00260-5.
- Kopliku, L.; Relmy, A.; Romey, A.; Gorna, K.; Zientara, S.; Bakkali-Kassimi, L.; Blaise-Boisseau, S. (2015): Establishment of persistent foot-and-mouth disease virus (FMDV) infection in MDBK cells. In *Archives of virology* 160 (10), pp. 2503–2516. DOI: 10.1007/s00705-015-2526-8.

- Lanyon, S. R.; Hill, F. I.; Reichel, M. P.; Brownlie, J. (2014): Bovine viral diarrhoea: pathogenesis and diagnosis. In *Veterinary journal (London, England: 1997)* 199 (2), pp. 201–209. DOI: 10.1016/j.tvjl.2013.07.024.
- Li, D.; Lei, C.; Xu, Z.; Yang, F.; Liu, H.; Zhu, Z. et al. (2016a): Foot-and-mouth disease virus non-structural protein 3A inhibits the interferon- $\beta$  signaling pathway. In *Scientific reports* 6. DOI: 10.1038/srep21888.
- Li, D.; Wei, J.; Yang, F.; Liu, H.-N.; Zhu, Z.-X.; Cao, W.-J. et al. (2016b): Foot-and-mouth disease virus structural protein VP3 degrades Janus kinase 1 to inhibit IFN- $\gamma$  signal transduction pathways. In *Cell Cycle* 15 (6), pp. 850–860. DOI: 10.1080/15384101.2016.1151584.
- Li, M.; Xin, T.; Gao, X.; Wu, J.; Wang, X.; Fang, L. et al. (2018): Foot-and-mouth disease virus non-structural protein 2B negatively regulates the RLR-mediated IFN- $\beta$  induction. In *Biochemical and biophysical research communications* 504 (1), pp. 238–244. DOI: 10.1016/j.bbrc.2018.08.161.
- Li, Z.; Zou, Z.; Jiang, Z.; Huang, X.; Liu, Q. (2019): Biological Function and Application of Picornaviral 2B Protein: A New Target for Antiviral Drug Development. In *Viruses* 11 (6). DOI: 10.3390/v11060510.
- Liang, Y.; Cao, X.; Ding, Q.; Zhao, Y.; He, Z.; Zhong, J. (2018): Hepatitis C virus NS4B induces the degradation of TRIF to inhibit TLR3-mediated interferon signaling pathway. In *PLoS pathogens* 14 (5), e1007075. DOI: 10.1371/journal.ppat.1007075.
- Liu, H.; Xue, Q.; Cao, W.; Yang, F.; Ma, L.; Liu, W. et al. (2018): Foot-and-mouth disease virus nonstructural protein 2B interacts with cyclophilin A, modulating virus replication. In *FASEB journal: official publication of the Federation of American Societies for Experimental Biology*, fj201701351. DOI: 10.1096/fj.201701351.
- Liu, H.; Zhu, Z.; Xue, Q.; Yang, F.; Cao, W.; Zhang, K. et al. (2019): Foot-and-Mouth Disease Virus Antagonizes NOD2-Mediated Antiviral Effects by Inhibiting NOD2 Protein Expression. In *J Virol* 93 (11). DOI: 10.1128/JVI.00124-19.
- Logan, D.; Abu-Ghazaleh, R.; Blakemore, W.; Curry, S.; Jackson, T.; King, A. et al. (1993): Structure of a major immunogenic site on foot-and-mouth disease virus. In *Nature* 362 (6420), pp. 566–568. DOI: 10.1038/362566a0.
- López de Quinto, S.; Lafuente, E.; Martínez-Salas, E. (2001): IRES interaction with translation initiation factors: functional characterization of novel RNA contacts with eIF3, eIF4B, and eIF4GII. In *RNA* 7 (9), pp. 1213–1226. DOI: 10.1017/S1355838201010433.

- Los Santos, T. de; Avila Botton, S. de; Weiblen, R.; Grubman, M. J. (2006): The leader proteinase of foot-and-mouth disease virus inhibits the induction of beta interferon mRNA and blocks the host innate immune response. In *J Virol* 80 (4), pp. 1906–1914. DOI: 10.1128/JVI.80.4.1906-1914.2006.
- Los Santos, T. de; Diaz-San Segundo, F.; Grubman, M. J. (2007): Degradation of nuclear factor kappa B during foot-and-mouth disease virus infection. In *J Virol* 81 (23), pp. 12803–12815. DOI: 10.1128/jvi.01467-07.
- Los Santos, T. de; Segundo, F. D.-S.; Zhu, J.; Koster, M.; Dias, C. C. A.; Grubman, M. J. (2009): A conserved domain in the leader proteinase of foot-and-mouth disease virus is required for proper subcellular localization and function. In *J Virol* 83 (4), pp. 1800–1810. DOI: 10.1128/JVI.02112-08.
- Ma, Y. B.; Hao, C. X.; Chang, H. Y. (2013): Nucleotide mismatches of foot-and-mouth disease virus during replication. In *Genetics and molecular research : GMR* 12 (2), pp. 1022–1027. DOI: 10.4238/2013.april.2.18.
- Mahapatra, M.; Hamblin, P.; Paton, D. J. (2012): Foot-and-mouth disease virus epitope dominance in the antibody response of vaccinated animals. In *The Journal of general virology* 93 (Pt 3), pp. 488–493. DOI: 10.1099/vir.0.037952-0.
- Mahy, B. W. J. (2005): Introduction and history of foot-and-mouth disease virus. In *Current topics in microbiology and immunology* 288, pp. 1–8. DOI: 10.1007/3-540-27109-0\_1.
- Maree, F.; Klerk-Lorist, L.-M. de; Gubbins, S.; Zhang, F.; Seago, J.; Pérez-Martín, E. et al. (2016): Differential Persistence of Foot-and-Mouth Disease Virus in African Buffalo Is Related to Virus Virulence. In *J Virol* 90 (10), pp. 5132–5140. DOI: 10.1128/JVI.00166-16.
- Mateu, M. G. (1995): Antibody recognition of picornaviruses and escape from neutralization: a structural view. In *Virus research* 38 (1), pp. 1–24. DOI: 10.1016/0168-1702(95)00048-u.
- Mateu, M. G.; Hernández, J.; Martínez, M. A.; Feigelstock, D.; Lea, S.; Pérez, J. J. et al. (1994): Antigenic heterogeneity of a foot-and-mouth disease virus serotype in the field is mediated by very limited sequence variation at several antigenic sites. In *J Virol* 68 (3), pp. 1407–1417. DOI: 10.1128/jvi.68.3.1407-1417.1994.

- Mathieu, C.; Bovier, F. T.; Ferren, M.; Lieberman, N. A. P.; Predella, C.; Lalande, A. et al. (2021): Molecular Features of the Measles Virus Viral Fusion Complex That Favor Infection and Spread in the Brain. In *mBio* 12 (3), e0079921. DOI: 10.1128/mbio.00799-21.
- McCarty, J. H. (2020):  $\alpha\beta 8$  integrin adhesion and signaling pathways in development, physiology and disease. In *Journal of Cell Science* 133 (12). DOI: 10.1242/jcs.239434.
- McVicar, J. W.; Suttmoller, P. (1976): Growth of foot-and-mouth disease virus in the upper respiratory tract of non-immunized, vaccinated, and recovered cattle after intranasal inoculation. In *The Journal of hygiene* 76 (3), pp. 467–481. DOI: 10.1017/s0022172400055406.
- Medina, M.; Domingo, E.; Brangwyn, J. K.; Belsham, G. J. (1993): The two species of the foot-and-mouth disease virus leader protein, expressed individually, exhibit the same activities. In *Virology* 194 (1), pp. 355–359. DOI: 10.1006/viro.1993.1267.
- Meek, H. C.; Stenfeldt, C.; Arzt, J. (2022): Morphological and Phenotypic Characteristics of the Bovine Nasopharyngeal Mucosa and Associated Lymphoid Tissue. In *Journal of comparative pathology* 198, pp. 62–79. DOI: 10.1016/j.jcpa.2022.07.011.
- Monaghan, P.; Cook, H.; Jackson, T.; Ryan, M.; Wileman, T. (2004): The ultrastructure of the developing replication site in foot-and-mouth disease virus-infected BHK-38 cells. In *The Journal of general virology* 85 (Pt 4), pp. 933–946. DOI: 10.1099/vir.0.19408-0.
- Moonen, P.; Schrijver, R. (2000): Carriers of foot-and-mouth disease virus: a review. In *The veterinary quarterly* 22 (4), pp. 193–197. DOI: 10.1080/01652176.2000.9695056.
- Negishi, H.; Taniguchi, T.; Yanai, H. (2018): The Interferon (IFN) Class of Cytokines and the IFN Regulatory Factor (IRF) Transcription Factor Family. In *Cold Spring Harbor perspectives in biology* 10 (11). DOI: 10.1101/cshperspect.a028423.
- Nfon, C. K.; Toka, F. N.; Kenney, M.; Pacheco, J. M.; Golde, W. T. (2010): Loss of plasmacytoid dendritic cell function coincides with lymphopenia and viremia during foot-and-mouth disease virus infection. In *Viral immunology* 23 (1), pp. 29–41. DOI: 10.1089/vim.2009.0078.

- Núñez, J. I.; Baranowski, E.; Molina, N.; Ruiz-Jarabo, C. M.; Sánchez, C.; Domingo, E.; Sobrino, F. (2001): A single amino acid substitution in nonstructural protein 3A can mediate adaptation of foot-and-mouth disease virus to the guinea pig. In *J Virol* 75 (8), pp. 3977–3983. DOI: 10.1128/jvi.75.8.3977-3983.2001.
- O'Donnell, V.; Pacheco, J. M.; Gregg, D.; Baxt, B. (2009): Analysis of foot-and-mouth disease virus integrin receptor expression in tissues from naïve and infected cattle. In *Journal of comparative pathology* 141 (2-3), pp. 98–112. DOI: 10.1016/j.jcpa.2008.09.008.
- O'Donnell, V.; Pacheco, J. M.; Larocco, M.; Gladue, D. P.; Pauszek, S. J.; Smoliga, G. et al. (2014): Virus-host interactions in persistently FMDV-infected cells derived from bovine pharynx. In *Virology* 468-470, pp. 185–196. DOI: 10.1016/j.virol.2014.08.004.
- Oya, Y.; Kimura, S.; Nakamura, Y.; Ishihara, N.; Takano, S.; Morita, R. et al. (2021): Characterization of M Cells in Tear Duct-Associated Lymphoid Tissue of Mice: A Potential Role in Immunosurveillance on the Ocular Surface. In *Frontiers in immunology* 12, p. 779709. DOI: 10.3389/fimmu.2021.779709.
- Pacheco, J. M.; Henry, T. M.; O'Donnell, V.; Gregory, J. B.; Mason, P. W. (2003): Role of Nonstructural Proteins 3A and 3B in Host Range and Pathogenicity of Foot-and-Mouth Disease Virus. In *J Virol* 77 (24), pp. 13017–13027. DOI: 10.1128/JVI.77.24.13017-13027.2003.
- Pacheco, J. M.; Smoliga, G. R.; O'Donnell, V.; Brito, B. P.; Stenfeldt, C.; Rodriguez, L. L.; Arzt, J. (2015): Persistent Foot-and-Mouth Disease Virus Infection in the Nasopharynx of Cattle; Tissue-Specific Distribution and Local Cytokine Expression. In *PloS one* 10 (5), e0125698. DOI: 10.1371/journal.pone.0125698.
- Pacheco, J. M.; Stenfeldt, C.; Rodriguez, L. L.; Arzt, J. (2016): Infection Dynamics of Foot-and-Mouth Disease Virus in Cattle Following Intranasopharyngeal Inoculation or Contact Exposure. In *Journal of comparative pathology* 155 (4), pp. 314–325. DOI: 10.1016/j.jcpa.2016.08.005.
- Parida, S. (2009): Vaccination against foot-and-mouth disease virus: strategies and effectiveness. In *Expert review of vaccines* 8 (3), pp. 347–365. DOI: 10.1586/14760584.8.3.347.
- Parry, N.; Fox, G.; Rowlands, D.; Brown, F.; Fry, E.; Acharya, R. et al. (1990): Structural and serological evidence for a novel mechanism of antigenic variation in foot-and-mouth disease virus. In *Nature* 347 (6293), pp. 569–572. DOI: 10.1038/347569a0.

- Parthiban, A. B. R.; Mahapatra, M.; Gubbins, S.; Parida, S. (2015): Virus Excretion from Foot-And-Mouth Disease Virus Carrier Cattle and Their Potential Role in Causing New Outbreaks. In *PloS one* 10 (6), e0128815. DOI: 10.1371/journal.pone.0128815.
- Patch, J. R.; Dar, P. A.; Waters, R.; Toka, F. N.; Barrera, J.; Schutta, C. et al. (2014): Infection with foot-and-mouth disease virus (FMDV) induces a natural killer (NK) cell response in cattle that is lacking following vaccination. In *Comparative immunology, microbiology and infectious diseases* 37 (4), pp. 249–257. DOI: 10.1016/j.cimid.2014.07.004.
- Paton, D. J.; Di Nardo, A.; Knowles, N. J.; Wadsworth, J.; Pituco, E. M.; Cosivi, O. et al. (2021): The history of foot-and-mouth disease virus serotype C: the first known extinct serotype? In *Virus Evolution* 7 (1), Article veab009. DOI: 10.1093/ve/veab009.
- Paton, D. J.; Sumption, K. J.; Charleston, B. (2009): Options for control of foot-and-mouth disease: knowledge, capability and policy. In *Philosophical Transactions of the Royal Society B: Biological Sciences* 364 (1530), pp. 2657–2667. DOI: 10.1098/rstb.2009.0100.
- Paul, A. V.; Wimmer, E. (2015): Initiation of protein-primed picornavirus RNA synthesis. In *Virus research* 206, pp. 12–26. DOI: 10.1016/j.virusres.2014.12.028.
- Pauszek, S. J.; Eschbaumer, M.; Brito, B.; Carvalho Ferreira, H. C. de; Le Vu, T.; Phuong, N. T. et al. (2016): Site-specific substitution (Q172R) in the VP1 protein of FMDV isolates collected from asymptomatic carrier ruminants in Vietnam. In *Virology Reports* 6, pp. 90–96. DOI: 10.1016/j.virep.2016.10.001.
- Peterhans, E.; Bachofen, C.; Stalder, H.; Schweizer, M. (2010): Cytopathic bovine viral diarrhoea viruses (BVDV): emerging pestiviruses doomed to extinction. In *Veterinary Research* 41 (6), p. 44. DOI: 10.1051/vetres/2010016.
- Peterhans, E.; Schweizer, M. (2010): Pestiviruses: how to outmaneuver your hosts. In *Veterinary microbiology* 142 (1-2), pp. 18–25. DOI: 10.1016/j.vetmic.2009.09.038.
- Pfaff, F.; Hägglund, S.; Zoli, M.; Blaise-Boisseau, S.; Laloy, E.; Koethe, S. et al. (2019): Proteogenomics Uncovers Critical Elements of Host Response in Bovine Soft Palate Epithelial Cells Following In Vitro Infection with Foot-And-Mouth Disease Virus. In *Viruses* 11 (1). DOI: 10.3390/v11010053.

- Prato Murphy, M. L.; Forsyth, M. A.; Belsham, G. J.; Salt, J. S. (1999): Localization of foot-and-mouth disease virus RNA by in situ hybridization within bovine tissues. In *Virus research* 62 (1), pp. 67–76. DOI: 10.1016/s0168-1702(99)00050-7.
- Regge, N. de; van Opdenbosch, N.; Nauwynck, H. J.; Efstathiou, S.; Favoreel, H. W. (2010): Interferon Alpha Induces Establishment of Alphaherpesvirus Latency in Sensory Neurons In Vitro. In *PLoS one* 5 (9). DOI: 10.1371/journal.pone.0013076.
- Robinson, L.; Windsor, M.; McLaughlin, K.; Hope, J.; Jackson, T.; Charleston, B. (2011): Foot-and-mouth disease virus exhibits an altered tropism in the presence of specific immunoglobulins, enabling productive infection and killing of dendritic cells. In *J Virol* 85 (5), pp. 2212–2223. DOI: 10.1128/jvi.02180-10.
- Rodríguez Pulido, M.; Sánchez-Aparicio, M. T.; Martínez-Salas, E.; García-Sastre, A.; Sobrino, F.; Sáiz, M. (2018): Innate immune sensor LGP2 is cleaved by the Leader protease of foot-and-mouth disease virus. In *PLoS pathogens* 14 (6). DOI: 10.1371/journal.ppat.1007135.
- Rodríguez Pulido, M.; Serrano, P.; Sáiz, M.; Martínez-Salas, E. (2007): Foot-and-mouth disease virus infection induces proteolytic cleavage of PTB, eIF3a,b, and PABP RNA-binding proteins. In *Virology* 364 (2), pp. 466–474. DOI: 10.1016/j.virol.2007.03.013.
- Roizman, B.; Whitley, R. J. (2013): An inquiry into the molecular basis of HSV latency and reactivation. In *Annual review of microbiology* 67, pp. 355–374. DOI: 10.1146/annurev-micro-092412-155654.
- Ryan, E.; Horsington, J.; Durand, S.; Brooks, H.; Alexandersen, S.; Brownlie, J.; Zhang, Z. (2008): Foot-and-mouth disease virus infection in young lambs: pathogenesis and tissue tropism. In *Veterinary microbiology* 127 (3-4), pp. 258–274. DOI: 10.1016/j.vetmic.2007.08.029.
- Sahoo, M.; Singh, R.; Kumar, P.; Kumar Mariappan, A.; Munnuswamy, P.; Singh, K. et al. (2023): Novel pathologic findings and viral antigen distribution in cattle and buffalo calves naturally infected with Foot-and-Mouth disease virus. In *The veterinary quarterly* 43 (1), pp. 1–13. DOI: 10.1080/01652176.2023.2260435.
- Salt, J. S. (1993): The carrier state in foot and mouth disease—an immunological review. In *British Veterinary Journal* 149 (3), pp. 207–223. DOI: 10.1016/s0007-1935(05)80168-x.

- Sarry, M.; Vitour, D.; Zientara, S.; Bakkali Kassimi, L.; Blaise-Boisseau, S. (2022): Foot-and-Mouth Disease Virus: Molecular Interplays with IFN Response and the Importance of the Model. In *Viruses* 14 (10). DOI: 10.3390/v14102129.
- Schindell, B. G.; Webb, A. L.; Kindrachuk, J. (2018): Persistence and Sexual Transmission of Filoviruses. In *Viruses* 10 (12). DOI: 10.3390/v10120683.
- Schoggins, J. W. (2019): Interferon-Stimulated Genes: What Do They All Do? In *Annual review of virology* 6 (1), pp. 567–584. DOI: 10.1146/annurev-virology-092818-015756.
- Secott, T. E.; Lin, T. L.; Wu, C. C. (2004): Mycobacterium avium subsp. paratuberculosis Fibronectin Attachment Protein Facilitates M-Cell Targeting and Invasion through a Fibronectin Bridge with Host Integrins. In *Infection and immunity* 72 (7), pp. 3724–3732. DOI: 10.1128/IAI.72.7.3724-3732.2004.
- Sei, J. J.; Waters, R. A.; Kenney, M.; Barlow, J. W.; Golde, W. T. (2016): Effect of Foot-and-Mouth Disease Virus Infection on the Frequency, Phenotype and Function of Circulating Dendritic Cells in Cattle. In *PloS one* 11 (3). DOI: 10.1371/journal.pone.0152192.
- Sellers, R.; Gloster, J. (2008): Foot-and-mouth disease: a review of intranasal infection of cattle, sheep and pigs. In *Veterinary journal (London, England: 1997)* 177 (2), pp. 159–168. DOI: 10.1016/j.tvjl.2007.03.009.
- Smirnova, N. P.; Webb, B. T.; McGill, J. L.; Schaut, R. G.; Bielefeldt-Ohmann, H.; van Campen, H. et al. (2014): Induction of interferon-gamma and downstream pathways during establishment of fetal persistent infection with bovine viral diarrhoea virus. In *Virus research* 183, pp. 95–106. DOI: 10.1016/j.virusres.2014.02.002.
- Snell, L. M.; McGaha, T. L.; Brooks, D. G. (2017): Type I Interferon in Chronic Virus Infection and Cancer. In *Trends in immunology* 38 (8), pp. 542–557. DOI: 10.1016/j.it.2017.05.005.
- St Leger, A. J.; Hendricks, R. L. (2011): CD8+ T cells patrol HSV-1-infected trigeminal ganglia and prevent viral reactivation. In *Journal of neurovirology* 17 (6), pp. 528–534. DOI: 10.1007/s13365-011-0062-1.
- Stenfeldt, C.; Arzt, J. (2020): The Carrier Conundrum; A Review of Recent Advances and Persistent Gaps Regarding the Carrier State of Foot-and-Mouth Disease Virus. In *Pathogens (Basel, Switzerland)* 9 (3). DOI: 10.3390/pathogens9030167.

- Stenfeldt, C.; Eschbaumer, M.; Pacheco, J. M.; Rekant, S. I.; Rodriguez, L. L.; Arzt, J. (2015): Pathogenesis of Primary Foot-and-Mouth Disease Virus Infection in the Nasopharynx of Vaccinated and Non-Vaccinated Cattle. In *PloS one* 10 (11), e0143666. DOI: 10.1371/journal.pone.0143666.
- Stenfeldt, C.; Eschbaumer, M.; Rekant, S. I.; Pacheco, J. M.; Smoliga, G. R.; Hartwig, E. J. et al. (2016a): The Foot-and-Mouth Disease Carrier State Divergence in Cattle. In *Journal of virology* 90 (14), pp. 6344–6364. DOI: 10.1128/JVI.00388-16.
- Stenfeldt, C.; Eschbaumer, M.; Smoliga, G. R.; Rodriguez, L. L.; Zhu, J.; Arzt, J. (2017): Clearance of a persistent picornavirus infection is associated with enhanced proapoptotic and cellular immune responses. In *Scientific reports* 7 (1), p. 17800. DOI: 10.1038/s41598-017-18112-4.
- Stenfeldt, C.; Fish, I.; Meek, H. C.; Arzt, J. (2023): Heterogeneity and Recombination of Foot-and-Mouth Disease Virus during Multi-Strain Coinfection of Cattle. In *mSphere*, e0064322. DOI: 10.1128/msphere.00643-22.
- Stenfeldt, C.; Hartwig, E. J.; Smoliga, G. R.; Palinski, R.; Silva, E. B.; Bertram, M. R. et al. (2018): Contact Challenge of Cattle with Foot-and-Mouth Disease Virus Validates the Role of the Nasopharyngeal Epithelium as the Site of Primary and Persistent Infection. In *mSphere* 3 (6). DOI: 10.1128/mSphere.00493-18.
- Stenfeldt, C.; Pacheco, J. M.; Borca, M. V.; Rodriguez, L. L.; Arzt, J. (2014a): Morphologic and phenotypic characteristics of myocarditis in two pigs infected by foot-and mouth disease virus strains of serotypes O or A. In *Acta Veterinaria Scandinavica* 56 (1), p. 42. DOI: 10.1186/s13028-014-0042-6.
- Stenfeldt, C.; Pacheco, J. M.; Rodriguez, L. L.; Arzt, J. (2014b): Early events in the pathogenesis of foot-and-mouth disease in pigs; identification of oropharyngeal tonsils as sites of primary and sustained viral replication. In *PloS one* 9 (9), e106859. DOI: 10.1371/journal.pone.0106859.
- Stenfeldt, C.; Pacheco, J. M.; Smoliga, G. R.; Bishop, E.; Pauszek, S. J.; Hartwig, E. J. et al. (2016b): Detection of Foot-and-mouth Disease Virus RNA and Capsid Protein in Lymphoid Tissues of Convalescent Pigs Does Not Indicate Existence of a Carrier State. In *Transboundary and emerging diseases* 63 (2), pp. 152–164. DOI: 10.1111/tbed.12235.
- Sui, C.; Jiang, D.; Wu, X.; Liu, S.; Li, F.; Pan, L. et al. (2021): Inhibition of Antiviral Innate Immunity by Foot-and-Mouth Disease Virus Lpro through Interaction with the N-Terminal Domain of Swine RNase L. In *J Virol* 95 (15), e0036121. DOI: 10.1128/JVI.00361-21.

- Sutmoller, P.; Cottral, G. E. (1967): Improved techniques for the detection of foot-and-mouth disease virus in carrier cattle. In *Archiv fur die gesamte Virusforschung* 21 (2), pp. 170–177. DOI: 10.1007/BF01241441.
- Sutmoller, P.; Gaggero, A. (1965): Foot-and mouth diseases carriers. In *The Veterinary record* 77 (33), pp. 968–969. DOI: 10.1136/vr.77.33.968.
- Sutmoller, P.; McVicar, J. W.; Cottral, G. E. (1968): The epizootiological importance of foot-and-mouth disease carriers. I. Experimentally produced foot-and-mouth disease carriers in susceptible and immune cattle. In *Archiv fur die gesamte Virusforschung* 23 (3), pp. 227–235. DOI: 10.1007/BF01241895.
- Suzuki, K.; Kawamoto, S.; Maruya, M.; Fagarasan, S. (2010): GALT: organization and dynamics leading to IgA synthesis. In *Advances in immunology* 107, pp. 153–185. DOI: 10.1016/B978-0-12-381300-8.00006-X.
- Sweeney, T. R.; Cisnetto, V.; Bose, D.; Bailey, M.; Wilson, J. R.; Zhang, X. et al. (2010): Foot-and-Mouth Disease Virus 2C Is a Hexameric AAA+ Protein with a Coordinated ATP Hydrolysis Mechanism. In *The Journal of biological chemistry* 285 (32), pp. 24347–24359. DOI: 10.1074/jbc.M110.129940.
- Tahoun, A.; Siszler, G.; Spears, K.; McAteer, S.; Tree, J.; Paxton, E. et al. (2011): Comparative analysis of EspF variants in inhibition of Escherichia coli phagocytosis by macrophages and inhibition of E. coli translocation through human- and bovine-derived M cells. In *Infection and immunity* 79 (11), pp. 4716–4729. DOI: 10.1128/IAI.00023-11.
- Tenzin; Dekker, A.; Vernooij, H.; Bouma, A.; Stegeman, A. (2008): Rate of foot-and-mouth disease virus transmission by carriers quantified from experimental data. In *Risk analysis: an official publication of the Society for Risk Analysis* 28 (2), pp. 303–309. DOI: 10.1111/j.1539-6924.2008.01020.x.
- Thomson, G. R. (1995): Overview of foot and mouth disease in southern Africa. In *Revue scientifique et technique (International Office of Epizootics)* 14 (3), pp. 503–520. DOI: 10.20506/rst.14.3.855.
- Toka, F. N.; Nfon, C.; Dawson, H.; Golde, W. T. (2009): Natural killer cell dysfunction during acute infection with foot-and-mouth disease virus. In *Clinical and vaccine immunology: CVI* 16 (12), pp. 1738–1749. DOI: 10.1128/cvi.00280-09.

- Tuthill, T. J.; Harlos, K.; Walter, T. S.; Knowles, N. J.; Gropelli, E.; Rowlands, D. J. et al. (2009): Equine Rhinitis A Virus and Its Low pH Empty Particle: Clues Towards an Aphthovirus Entry Mechanism? In *PLoS pathogens* 5 (10). DOI: 10.1371/journal.ppat.1000620.
- Uddowla, S.; Hollister, J.; Pacheco, J. M.; Rodriguez, L. L.; Rieder, E. (2012): A Safe Foot-and-Mouth Disease Vaccine Platform with Two Negative Markers for Differentiating Infected from Vaccinated Animals. In *Journal of virology* 86 (21), pp. 11675–11685. DOI: 10.1128/JVI.01254-12.
- Vallée, H.; Carré, H. (1922): Sur la pluralité du virus aphteux. In *Comptes rendus de l'Académie des sciences Paris* 174, pp. 1498–1500.
- van Bekkum, J. G.; Frenkel, H. S.; Frederiks, H. H.; Frenkel, S. (1959): Observations on the carrier state of cattle exposed to foot-and-mouth disease virus. In *Tijdschr. Diergeneeskde* 84, pp. 1159–1164.
- van Lierop, M. J.; Wagenaar, J. P.; van Noort, J. M.; Hensen, E. J. (1995): Sequences derived from the highly antigenic VP1 region 140 to 160 of foot-and-mouth disease virus do not prime for a bovine T-cell response against intact virus. In *J Virol* 69 (7), pp. 4511–4514. DOI: 10.1128/jvi.69.7.4511-4514.1995.
- Visser, L. J.; Aloise, C.; Swatek, K. N.; Medina, G. N.; Olek, K. M.; Rabouw, H. H. et al. (2020): Dissecting distinct proteolytic activities of FMDV Lpro implicates cleavage and degradation of RLR signaling proteins, not its delSGylase/DUB activity, in type I interferon suppression. In *PLoS pathogens* 16 (7). DOI: 10.1371/journal.ppat.1008702.
- Vleeschauwer, A. R. de; Lefebvre, D. J.; Willems, T.; Paul, G.; Billiet, A.; Murao, L. E. et al. (2016): A Refined Guinea Pig Model of Foot-and-Mouth Disease Virus Infection for Assessing the Efficacy of Antiviral Compounds. In *Transboundary and emerging diseases* 63 (2), e205-12. DOI: 10.1111/tbed.12255.
- Vosloo, W.; Bastos, A. D.; Kirkbride, E.; Esterhuysen, J. J.; van Rensburg, D. J.; Bengis, R. G. et al. (1996): Persistent infection of African buffalo (*Syncerus caffer*) with SAT-type foot-and-mouth disease viruses: rate of fixation of mutations, antigenic change and interspecies transmission. In *The Journal of general virology* 77 (Pt 7), pp. 1457–1467. DOI: 10.1099/0022-1317-77-7-1457.

- Waldmann, O.; Trautwein, K. (1926): Experimentelle Untersuchungen über die Pluralität des Maul-und Klauenseuchevirus. In *Berliner tierärztliche Wochenschrift* 42, pp. 569–571.
- Wang, D.; Fang, L.; Li, P.; Sun, L.; Fan, J.; Zhang, Q. et al. (2011): The leader proteinase of foot-and-mouth disease virus negatively regulates the type I interferon pathway by acting as a viral deubiquitinase. In *Journal of virology* 85 (8), pp. 3758–3766. DOI: 10.1128/JVI.02589-10.
- Wang, D.; Fang, L.; Luo, R.; Ye, R.; Fang, Y.; Xie, L. et al. (2010): Foot-and-mouth disease virus leader proteinase inhibits dsRNA-induced type I interferon transcription by decreasing interferon regulatory factor 3/7 in protein levels. In *Biochemical and biophysical research communications* 399 (1), pp. 72–78. DOI: 10.1016/j.bbrc.2010.07.044.
- Wang, G.; Wang, Y.; Shang, Y.; Zhang, Z.; Liu, X. (2015): How foot-and-mouth disease virus receptor mediates foot-and-mouth disease virus infection. In *Virology Journal* 12. DOI: 10.1186/s12985-015-0246-z.
- Wernery, U.; Kaaden, O.-R. (2004): Foot-and-mouth disease in camelids: a review. In *Veterinary journal (London, England: 1997)* 168 (2), pp. 134–142. DOI: 10.1016/j.tvjl.2003.10.005.
- Windsor, M. A.; Carr, B. V.; Bankowski, B.; Gibson, D.; Reid, E.; Hamblin, P. et al. (2011): Cattle remain immunocompetent during the acute phase of foot-and-mouth disease virus infection. In *Veterinary Research* 42 (1), p. 108. DOI: 10.1186/1297-9716-42-108.
- Witz, J. (1998): A reappraisal of the contribution of Friedrich Loeffler to the development of the modern concept of virus. In *Archives of virology* 143 (11), pp. 2261–2263. DOI: 10.1007/s007050050458.
- WOAH (2024): Foot and mouth disease. Official Disease Status. Edited by WOAH. Available online at <https://www.woah.org/en/disease/foot-and-mouth-disease/#ui-id-2>, updated on 01.02.2024, checked on 02.03.24.
- WRLFMD (2023): Turkey: livestock, serotype SAT-2, 1st report, spread. Archive Number: 20230310.8708855. Edited by World Reference Laboratory for Foot-and-Mouth Disease. The Pirbright Institute. Available online at <https://www.wrlfmd.org/news/2023/03/turkey-livestock-serotype-sat-2-1st-report-spread>, updated on 10.03.2023, checked on 05.01.24.

- Yadav, S.; Stenfeldt, C.; Branan, M. A.; Moreno-Torres, K. I.; Holmstrom, L. K.; Delgado, A. H.; Arzt, J. (2019): Parameterization of the Durations of Phases of Foot-And-Mouth Disease in Cattle. In *Frontiers in veterinary science* 6, p. 263. DOI: 10.3389/fvets.2019.00263.
- Zhang, H.; Wang, G.; Zhou, R.; Li, X.; Sun, Y.; Li, Y. et al. (2020a): SPIB promotes anoikis resistance via elevated autolysosomal process in lung cancer cells. In *The FEBS journal* 287 (21), pp. 4696–4709. DOI: 10.1111/febs.15272.
- Zhang, X.; Zhu, Z.; Wang, C.; Yang, F.; Cao, W.; Li, P. et al. (2020b): Foot-and-Mouth Disease Virus 3B Protein Interacts with Pattern Recognition Receptor RIG-I to Block RIG-I–Mediated Immune Signaling and Inhibit Host Antiviral Response. In *Journal of immunology (Baltimore, Md.: 1950)* 205 (8), pp. 2207–2221. DOI: 10.4049/jimmunol.1901333.
- Zhang, Z.; Alexandersen, S. (2004): Quantitative analysis of foot-and-mouth disease virus RNA loads in bovine tissues: implications for the site of viral persistence. In *The Journal of general virology* 85 (Pt 9), pp. 2567–2575. DOI: 10.1099/vir.0.80011-0.
- Zheng, W.; Li, X.; Wang, J.; Li, X.; Cao, H.; Wang, Y. et al. (2014): A critical role of interferon-induced protein IFP35 in the type I interferon response in cells induced by foot-and-mouth disease virus (FMDV) protein 2C. In *Archives of virology* 159 (11), pp. 2925–2935. DOI: 10.1007/s00705-014-2147-7.
- Zhu, J. J.; Arzt, J.; Puckette, M. C.; Smoliga, G. R.; Pacheco, J. M.; Rodriguez, L. L. (2013): Mechanisms of Foot-and-Mouth Disease Virus Tropism Inferred from Differential Tissue Gene Expression. In *PloS one* 8 (5). DOI: 10.1371/journal.pone.0064119.
- Zhu, J. J.; Stenfeldt, C.; Bishop, E. A.; Canter, J. A.; Eschbaumer, M.; Rodriguez, L. L.; Arzt, J. (2020): Mechanisms of Maintenance of Foot-and-Mouth Disease Virus Persistence Inferred From Genes Differentially Expressed in Nasopharyngeal Epithelia of Virus Carriers and Non-carriers. In *Frontiers in veterinary science* 7. DOI: 10.3389/fvets.2020.00340.
- Zhu, J. J.; Stenfeldt, C.; Bishop, E. A.; Canter, J. A.; Eschbaumer, M.; Rodriguez, L. L.; Arzt, J. (2022): Inferred Causal Mechanisms of Persistent FMDV Infection in Cattle from Differential Gene Expression in the Nasopharyngeal Mucosa. In *Pathogens (Basel, Switzerland)* 11 (8). DOI: 10.3390/pathogens11080822.
- Zhu, S.; Viejo-Borbolla, A. (2021): Pathogenesis and virulence of herpes simplex virus. In *Virulence* 12 (1), pp. 2670–2702. DOI: 10.1080/21505594.2021.1982373.

Zhu, Z.; Li, C.; Du, X.; Wang, G.; Cao, W.; Yang, F. et al. (2017): Foot-and-mouth disease virus infection inhibits LGP2 protein expression to exaggerate inflammatory response and promote viral replication. In *Cell Death & Disease* 8 (4), e2747-. DOI: 10.1038/cddis.2017.170.

## CHAPTER IX: APPENDIX



# IX. Appendix

## 1. List of Figures

Figure 1. Structure of the virion and genome organization of FMDV (created with BioRender)

Figure 2. Global FMDV distribution, adapted from (Freimanis et al. 2016) using the official FMD status recognized by WOAHA as of February 2024 (WOAHA 2024). Created with map-chart.net

Figure 3. (Left) Sampling of cattle with a probang cup in the BSL4vet facility on the Isle of Riems, (Right) OPF collected in the probang cup.

Figure 4. Progression of FMDV infection in naive cattle from primary infection in the nasopharynx, to a systemic infection with lesions on hairless epithelia and shedding of virus, to the persistent infection with limited replication in the nasopharynx and disputed potential of shedding (Created with BioRender.com)

## 2. Legal Permissions

Figure 1: Created with BioRender.com. (Agreement number: HN26JL7MS4)

Figure 2: This work is licensed under a Creative Commons Attribution-ShareAlike 4.0 International License (CC BY-SA 4.0).

Figure 4: Created with BioRender.com. (Agreement number: BA26JL82QN)

Publication I: The publication reproduced in this thesis is taken from Taylor & Francis Group (<https://www.tandfonline.com/doi/full/10.1080/22221751.2024.2348526>). It is subject to the Creative Commons Attribution CC BY Licence 4.0 (<https://creativecommons.org/licenses/by/4.0/deed.de>), which permits unrestricted use, distribution, and reproduction in any medium, provided the original work is properly cited.

Publication II: The publication reproduced in this thesis is currently submitted to PLOS ONE. The author retains the copyright and PLOS applies the Creative Commons Attribution 4.0 International (CC BY) license that allows free and unrestricted use, to articles and other works published. Anyone may copy, redistribute, reuse, or modify the content as long as the author and original source are properly cited.

Publication III: The publication reproduced in this thesis is currently submitted to Journal of Virology (<https://journals.asm.org/doi/epub/10.1128/jvi.01422-24>). JVI applies the Creative Commons Attribution 4.0 International (CC BY) license that allows free and unrestricted use, to articles and other works published. Anyone may copy, redistribute, reuse, or modify the content as long as the author and original source are properly cited.

### 3. List of abbreviations

ALI	air-liquid interface
BVDV	bovine viral diarrhea virus
DNA	Deoxyribonucleic acid
DSP	dorsal soft palate
dsRNA	double stranded RNA
EBV	Epstein-Barr virus
eIF	eukaryotic translation initiation factor
et al.	et alii / et aliae
FAE	follicle-associated epithelium
FMD	Foot-and-Mouth disease
FMDV	Foot-and-Mouth disease virus
HIV	human immunodeficiency virus
HSV	herpes simplex virus
IFN	interferon

Ig	immunoglobulin
IL	interleukin
IRES	internal ribosome entry site
ISG	interferon stimulated genes
M-cells	microfold cells
MALT	mucosa-associated epithelium
MHC	major histocompatibility complex
mRNA	messenger RNA
NK-cells	natural killer cells
nt	nucleotides
LGP2	Laboratory of Genetics and Physiology 2
L <sup>pro</sup>	Leader protein
OPF	oropharyngeal fluid
ORF	open reading frame
PCR	polymerase chain reaction
RdRp	RNA-dependent RNA polymerase
RNA	ribonucleic acid
SARS-CoV 2	severe acute respiratory syndrome coronavirus 2
SAT	Southern African Territories
SAP	SAF-A/B, Acinus, and PIAS
TTE	1,1,2-trichloro-1,2,2-trifluoroethane
UK	United Kingdom
UTR	untranslated region
VPg	viral protein, genome-linked
WOAH	World Organization for Animal Health
WRLFMD	World Reference Laboratory for Foot-and-Mouth Disease



## CHAPTER X: ACKNOWLEDGEMENTS



## X. Acknowledgements

Vorab gilt mein Dank Herrn Prof. Dr. Markus Meissner für die spontane Übernahme und Beurteilung meiner Arbeit, sowie allen beteiligten Gutachtern.

Des Weiteren möchte ich meinem Mentor Herrn Prof. Dr. Martin Beer für seine Unterstützung bei der Erstellung dieser Arbeit und der Möglichkeit meine Dissertation hier am Institut für Virusdiagnostik des Friedrich-Loeffler-Institutes verfassen zu dürfen, danken. Die Arbeit hier war eine lehrreiche Zeit und eine Bereicherung für meine persönliche und berufliche Zukunft.

Besonders danken möchte ich auch meinen beiden Betreuern Dr. Michael Eschbaumer und Dr. Florian Pfaff, für ihre hilfreiche Unterstützung bei der Arbeit und das produktive Brainstorming. Vor allem die große Hilfsbereitschaft und das schier endlose Wissen von Michael haben mir die Erstellung dieser Dissertation erleichtert. Nicht nur virologisch konnte ich viel von ihm lernen, sondern auch durch Diskussionen beim Mittagessen meine historischen Fun Facts erweitern.

Vielen Dank auch an alle die mich in der täglichen Arbeit im Labor unterstützt haben und durch deren gute Stimmung und Unterhaltung die Arbeit gleich viel leichter lief: Anja Landmesser, Anja Schulz, Jenny Lorke, Hanna Keck, Kira Wisnewski und Constantin Lorenz. Darüber hinaus geht auch mein Dank an alle Tierpfleger, Sektionshelfer und alle Kollegen und Kolleginnen in der 48, die dieses Gebäude zu etwas Besonderem machen.

Meinen Freunden, die mich motiviert haben ans FLI zu gehen und mich immer wieder aufmuntern haben.

Der größte Dank gilt meiner Familie: meinen Eltern, meiner Schwester und Carlos, die mich bedingungslos lieben und unterstützen in allem, was ich vorhabe.